



Dottorato di Ricerca  
in Ingegneria delle Strutture e del Recupero Edilizio ed Urbano

Università degli Studi di Salerno

Elide Nastri THEORY OF PLASTIC MECHANISM CONTROL FOR ECCENTRICALLY BRACED FRAMES: CLOSED FORM SOLUTION

Elide Nastri

***THEORY OF PLASTIC MECHANISM CONTROL FOR  
ECCENTRICALLY BRACED FRAMES:  
CLOSED FORM SOLUTION***

XIII Ciclo Nuova Serie (a.a. 2012 - 2014)





**DIPARTIMENTO DI INGEGNERIA CIVILE**

***Dottorato di Ricerca in Ingegneria delle Strutture e del  
Recupero Edilizio e Urbano***

**XIII Ciclo N.S. (2012-2014)**

**THEORY OF PLASTIC MECHANISM CONTROL FOR  
ECCENTRICALLY BRACED FRAMES:  
CLOSED FORM SOLUTION**

***Elide Nastri***

**Il Tutor**  
***Prof. Ing. Vincenzo Piluso***

**Il Coordinatore**  
***Prof. Ing. Ciro Faella***

**Il Co-Tutor**  
***Dott. Ing. Rosario Montuori***





Nowadays having an employment is a real privilege and it is more than a privilege working for something you really like. In these three years, I had the opportunity to meet with many people with their cultural background and their experiences. There have been dark moments and exciting moments, the research does not always goes smoothly and surprises are always around the corner. This is why I feel compelled to thank Professor Vincenzo Piluso for his continued support, his ideas and his genius in solving issues. Thanks to Professor Rosario Montuori for the constant willingness to discuss, without our reasoning much of the content of the dissertation there would be. Thanks to Professor Gianvittorio Rizzano for the confidence entrusted in me from the day one. Thanks also to PhD Alessandra Longo, more than a friend for me for its moral and material support and to PhD Marina Troisi with whom I shared unforgettable moments.

Thanks to my friends / colleagues for having lightened my daily life of study and research and to everyone who helped me complete this dissertation. Without their continued efforts and support, I would have not been able to bring my work to a successful completion.

Thanks also to my family, believe in me far more than I do.

Finally, thanks to You. Thanks for giving me the wisdom and intelligence to complete this journey. Please make me always able to confront with the other in humility and give me the joy of sharing what I have learned with those who have the desire for understanding.



*Et aedificabunt deserta a saeculo  
et ruinas antiquas erigent  
et instaurabunt civitates desertas  
dissipatas in generatione et generatione*

*(Liber Isaiae 61, 4)*



*Illustration depicts damage to towns, people falling, trees breaking and unusual phenomena in sky  
Lausanne Earthquake, Switzerland. 16th c.– NISEE database*









# TABLE OF CONTENTS

<b>CHAPTER 1</b>	<b>5</b>
1.1 Background	5
1.2 Investigated structural typology	8
1.3 Motivation of the work	11
1.4 Organization of the work	13
<b>CHAPTER 2</b>	<b>15</b>
2.1 Introduction	15
2.2 Plastic Domain for Moment-Shear Interaction	17
2.3 Plastic Mechanism Control of one-storey EBFs	20
2.4 Link Moment-Shear Interaction	23
2.4.1 A-Type Mechanism	23

2.4.2	B-Type Mechanism	26
2.4.3	C-Type Mechanism	30
2.4.4	D-Type Mechanism	30
<b>2.5</b>	<b>Hierarchy Criteria</b>	<b>31</b>
2.5.1	Hierarchy Criteria for Intermediate links	31
2.5.2	Hierarchy Criteria for Long links	35
2.5.3	Hierarchy Criteria for Short Links	38
<b>2.6</b>	<b>Validation and numerical examples</b>	<b>40</b>
<b>2.7</b>	<b>Summary notes</b>	<b>46</b>
<b>CHAPTER 3</b>		<b>49</b>
<b>3.1</b>	<b>Introduction</b>	<b>49</b>
<b>3.2</b>	<b>Theory of Plastic Mechanism Control</b>	<b>51</b>
<b>3.3</b>	<b>Closed Form Solution</b>	<b>58</b>
<b>3.4</b>	<b>Worked example</b>	<b>63</b>
<b>3.5</b>	<b>Validation of the design procedure for MR-Frames</b>	<b>72</b>
<b>3.6</b>	<b>The influence of geometry, loads and steel grade for the development of a specific collapse type</b>	<b>77</b>
<b>3.7</b>	<b>Summary notes</b>	<b>80</b>
<b>CHAPTER 4</b>		<b>81</b>
<b>4.1</b>	<b>Introduction</b>	<b>81</b>

---

<b>4.2</b>	<b>Plastic mechanism typologies</b>	<b>82</b>
<b>4.3</b>	<b>Design of links</b>	<b>84</b>
<b>4.4</b>	<b>Design of beams and diagonals</b>	<b>86</b>
<b>4.5</b>	<b>Column Axial Forces at Collapse</b>	<b>89</b>
4.5.1	EBFs with horizontal link	89
4.5.2	EBFs with vertical link	90
<b>4.6</b>	<b>Equilibrium Curves of the Analysed Plastic Mechanisms</b>	<b>91</b>
4.6.1	Mechanism equilibrium curve for MRF-EBF dual system with horizontal link	96
4.6.2	Mechanism equilibrium curve for MRF-EBF dual system with vertical link (Inverted Y-scheme)	97
<b>4.7</b>	<b>Column design requirements to prevent undesired collapse mechanisms</b>	<b>99</b>
<b>4.8</b>	<b>Closed form solution</b>	<b>100</b>
4.8.1	Closed form solution for MRF-EBF dual system with horizontal link	100
4.8.2	Closed form solution for MRF-EBF dual system with vertical link (Inverted Y-scheme)	104
<b>4.9</b>	<b>Eurocode 8 design provisions for MRF-EBF dual systems</b>	<b>105</b>
<b>CHAPTER 5</b>		<b>107</b>
<b>5.1</b>	<b>Introduction</b>	<b>107</b>

5.2	Study cases	110
5.3	Validation by means of push-over analyses	121
<b>CHAPTER 6</b>		127
6.1	Introduction	127
6.2	Incremental Dynamic Analyses Results	130
6.3	Considerations on economic issues	137
6.4	Summary notes	140
<b>CONCLUSIONS</b>		143
<b>REFERENCES</b>		147
<b>APPENDIX A</b>		155
<b>APPENDIX B</b>		173



# CHAPTER 1

## INTRODUCTION

### 1.1 Background

Collapse mechanism control is universally recognized as one of the primary goals of the structural design process. The aim is to avoid partial collapse mechanisms, such as soft storey mechanisms, which are unsatisfactory in terms of energy dissipation capacity.

The optimization of the seismic structural response is, conversely, obtained when a collapse mechanism of global type is developed [1-3], because, in such case, all the dissipative zones are involved in the corresponding pattern of yielding, leaving all the other structural parts in elastic range.

These are the basis of the so called “capacity design” principles, which state that dissipative zones have to be designed according to the internal actions arising from the design seismic forces, while the non-dissipative zones have to be proportioned on the basis of the maximum internal actions which dissipative ones are able to transmit in the fully yielded and strain-hardened state.

In order to decrease the probability of plastic hinge formation in columns, MR-Frames must be designed to have strong columns and weak beams. To this scope, different simplified design criteria have been proposed [4-10] and the so-called beam-column hierarchy criterion has been introduced in Eurocode 8 [11].

Even though studies on this topic started several decades ago mainly with reference to reinforced concrete structures [9, 12-14] and, in particular, in New Zealand where the capacity design procedure found its codification since 1982 [15], codified design rules included in Eurocode 8 as well as similar procedures adopted by other codes cannot achieve the design goal, i.e. the development of a global type mechanism.

There are a number of reasons why the beam-column hierarchy criterion cannot achieve the above mentioned design goal and these have been widely discussed both with reference to reinforced concrete frames [16] and to steel frames [17]. In fact, it is well known that such hierarchy criterion is able to prevent soft-storey mechanisms, but is not adequate to assure a collapse mechanism of global type [5, 7-10].

Among the different reasons leading the beam-column hierarchy criterion to fail in the achievement of the design goal, probably the most important, and difficult to be accounted for in a simplified design approach, is the shifting of the contraflexure point in columns during the seismic excitation. This considerable shifting leads to a bending moment distribution substantially different from that resulting from code-prescribed design rules [18-19]. The shift of the contraflexure point is caused by the formation of hinges in beams adjacent to the column and even in part of the columns. All these factors alter the stiffness of beam-column subassembly, hence the moment distribution.

The main reason why the above issue cannot be accounted for by means of a simplified design rules, such as the beam-column hierarchy criterion, is that the second principle of capacity design [20] cannot be easily applied in case of multiple resisting mechanisms not located in series. In fact, according to the second principle of capacity design, non-dissipative zones (i.e. the columns in case of MR-Frames) need to be designed considering the maximum internal actions which the dissipative zones (i.e. the beam ends in case of MR-Frames) are able to transmit at their ultimate conditions. The beam-column hierarchy criterion is based on the possibility to accurately evaluate, at any beam-to-column joint, the sum of the bending moments which the beams are able to transmit when ultimate conditions occur, but, conversely, because of the shifting of contraflexure point in columns during the seismic excitation, it is practically impossible to predict how the above sum is shared between the end sections of the top and bottom column converging in the joint [2-10]. For this reason, it is

well known that the beam-column hierarchy criterion, based on simple joint equilibrium, is only able to prevent “soft storey” mechanisms, but it does not allow the development of a collapse mechanism of global type.

For this reason, a rigorous design procedure, based on the kinematic theorem of plastic collapse, has been presented in 1997 by Mazzolani and Piluso [17], aiming to guarantee a collapse mechanism of global type where plastic hinges develop at the beam ends only, while all the columns remain in elastic range. Obviously, exception is made for base section of first storey columns, leading to a kinematic mechanism. Starting from this first work, the “Theory of Plastic Mechanism Control” (TPCM) has been outlined as a useful tool for the seismic design of steel structures. It consists on the extension of the kinematic theorem of plastic collapse to the concept of mechanism equilibrium curve. In fact, for any given structural typology, the design conditions to be applied in order to prevent undesired collapse mechanisms can be derived by imposing that the mechanism equilibrium curve corresponding to the global mechanism has to be located below those corresponding to all the other undesired mechanisms up to a top sway displacement level compatible with the local ductility supply of dissipative zones. For this reason, in case of complex resisting mechanisms, a rigorous application of capacity design principles requires more sophisticated design procedures. This is the case of the column design aiming to assure a collapse mechanism of global type, i.e. a collapse mechanism assuring the dissipation of the earthquake input energy by the participation of all the dissipative zones while all the non-dissipative zones remain in elastic range.

This design approach was successively extended to MRFs with semi-rigid connections [21], MRFs with RBS connections [22], EB-Frames with horizontal links (i.e. split-K scheme and D-scheme) [23-24] or with inverted Y scheme [25-26], knee-braced frames [27], dissipative truss-moment frames DTMFs [28-29] MRF-CBF dual systems.

The problem of failure mode control aiming to assure a strong column-weak beam seismic behaviour has been also faced by Lee and Goel [31] with reference to moment-resisting frames but by means of a static approach.

Starting from the above background, recent important improvement to the original Theory of Plastic Mechanism Control have been achieved [32]. In particular, by means of new considerations regarding collapse mechanism typologies, a closed form solution has been found [32]. The design conditions to

be satisfied to prevent undesired collapse mechanisms can now be solved without any iterative procedure, so that the unknown of the design problem, i.e. column sections at each storey, can now be directly derived.

In this work the new advances in the “Theory of Plastic Mechanism Control” in closed form solution are reported and pointed out. In addition, particular reference is made to the closed form TPMC applied to Moment Resisting Frame-Eccentrically Braced Frames dual systems (MRF-EBFs dual systems).

## 1.2 Investigated structural typology

In the framework of seismic resistant structure, Eccentrically Braced Frames (EBFs) constitute a quite recent structural typology (Figure 1.1, Figure 1.2, Figure 1.3). They gained prominence thanks to the study of Popov and Kasai [33-35]. This structural typology is well suited for tall buildings located in areas of high seismic intensity. For this reason, EBFs are especially widespread in USA and New Zealand where the recent Christchurch earthquake of the February 11<sup>th</sup> 2011 put to the test a great number of structures. In particular, this unfortunate event allowed testing on real scale the damage a high intensity earthquake is able to bring on EBF steel frames (Figure 1.4). Since this earthquake, New Zealand Heavy Engineering Research Association launched rules to the Seismic Design of Eccentrically Braced Frames [36]. As regards their working under seismic actions, EBFs constitute a suitable compromise between seismic resistant MR-frames and concentrically braced frames because they exhibit both adequate lateral stiffness [37-38], due to the high contribution coming from the diagonal braces, and ductile behaviour, due to the ability of the links, constituting the dissipative zones of this structural typology, in developing wide and stable hysteresis loops [33-39]. Therefore, the coupling of MRF and EBF constitute an excellent dual system where the primary structural system is constituted by the EBF part, and a secondary fail-safe system is constituted by the MRF part. This secondary one can be considered as an additional dissipative system where plastic hinges are concentrated at the beam ends. However, the main dissipative system is constituted by the link members located in the braced bay of MRF-EBF dual systems which can be horizontal (K-scheme, D-scheme and V-scheme) or vertical (inverted Y-scheme) [11]. In this framework particular attentions needs to be applied to the connections of diagonals constituting the bracing system. In fact, the practice is divided between those who privilege pinned connection and those

who privilege fixed connection at the brace bases. This second solution is undoubtedly stiffer but shows many problems in term of constructive details. In addition, being the braces able to transmit not only the axial force but also the bending moment, they have to be considered, as same as columns in the framework of the design procedure which assure a collapse mechanism of global type [23], [40]. This problem has been faced by Mastranderea and Piluso [39], who developed the TPMC design procedure for simple EBFs with fixed base brace sections. Conversely, in this work diagonals constituting the bracing system are considered as pinned at their bases; it means that they are assumed unable to transmit the bending moments and, therefore, are modelled with actual hinges in the structural scheme with some relevant advantages also in the design procedure.



**Figure 1.1** – EBFs with D-scheme made by square hollow sections





**Figure 1.2** – EBFs with D-scheme made by double-T sections and removable link



**Figure 1.3** – EBFs with K-scheme made by double-T sections



**Figure 1.4** – EBFs with K-scheme damaged during Christchurch Earthquake (2011)

### 1.3 Motivations of the work

The first aim of this work is to provide a complete procedure to design Moment Resisting Frame-Eccentrically Braced Frames dual systems (MRF-EBFs dual systems) finalized to the development of a collapse mechanism of global type. To this scope, the procedure starts from the design of dissipative zones, called links, switch to the definition of local hierarchy criteria needed to assure that yielding is concentrated only in the link while the other members remain in elastic range and leads to the design of column sections needed to assure the development of a collapse mechanism of global type by means of TPMC.

From its side, Eurocode 8, which is the standard reference to the design of structures in Europe, does not provide specific hierarchy criteria for MRF-EBF dual systems, so that the design procedure is based on simplified hierarchy criteria following the same principle also applied in case of MRFs. In particular, the application rule to design the columns is based on the use of an amplifying factor whose aim is the prevention of yielding or buckling of non-dissipative elements, when the most stressed dissipative zone is yielded and strain-hardened up to its ultimate condition. Regarding non-dissipative elements, i.e. columns,

beams and diagonal braces have to be designed with the most unfavourable combination of the axial force and bending moments.

As preliminarily discussed, Eurocode proposal are able to avoid soft storey mechanisms but are not able to design structures showing a collapse mechanism of global type. For this reason, a number of MRF-EBFs dual systems have been designed with both the procedures, i.e. TPMC and Eurocode 8, with the scope to point out, on one hand, the accuracy of the proposed design procedure (TPMC) which always allow the development of a global mechanism and on the other hand, to compare the structural performance of the designed structures against destructive seismic events. In particular, the validation of the proposed design procedure and the comparison in terms of seismic performance between the structure designed by TPMC and Eurocode 8 have been carried out by means of both push-over analyses and Incremental Dynamic Analyses.

It is useful to underline that this thesis work initially started with the aim of analysing only MRF-EBF dual systems with vertical links (Inverted Y-scheme) which has already led to the publication of some research papers [25], [26], and, only at a later time, moved also to the study of MRF-EBFs dual system with horizontal links (K-scheme, D-scheme and V-scheme).

Inverted Y-scheme is an EBF typology still not sufficiently investigated and not largely widespread despite having many advantages both in term of performance and construction. Its main characteristic is that the link, i.e. the dissipative zone, does not belong to the beam member. In fact, one of the primary benefits in using such structural typology regards the chance to substitute easily the damaged link after a destructive seismic event, and, in addition, the possibility to conceive the scheme within the framework of supplementary energy dissipation strategy, by substituting the vertical link member with a dissipative device, such as a friction damper [41] or hysteretic damper, which is able to exhibit a highly dissipative behaviour if compared with traditional link members. As damaged links can be easily removed and substituted after earthquake, such structural scheme exhibits the greatest advantages provided that the other structural members as beams, diagonals and columns, have been not damaged during the seismic event, i.e. have remained in elastic range. This is precisely why a proper design is of paramount importance. In fact, only with collapse mechanism of global type it is possible to assure that damage is concentrated only in dissipative zones while the other non-dissipative ones

remain in elastic range. This important scope is, out of doubts, the strength of the Theory of Plastic Mechanism Control.

## 1.4 Organization of the work

The dissertation is comprised of six chapters, a conclusive section and two appendices:

**CHAPTER 1** provides the background and motivation, objective and scope, and organization of the work.

**CHAPTER 2** faces the problem of moment-shear interaction within the framework of rigid-plastic analysis. In addition, operative relationships aimed at the development of hierarchy criteria to control the pattern of yielding for single storey EB-Frames are reported. This local hierarchy criterion is able to assure that only the link members are yielded while other members converging in the link remains in elastic range.

**CHAPTER 3** provides the state of the art and the important innovation occurred to the Theory of Plastic Mechanism Control (TPMC), which have led to the closed form solution.

**CHAPTER 4** provides the application of the Theory of Plastic Mechanism control to MRF-EBF dual systems with either horizontal links or vertical links.

**CHAPTER 5** provides the validation of the proposed design procedure (TPMC). In addition, a wide the comparison between structures designed by TPMC and Eurocode 8 is addressed by means of push-over analyses.

**CHAPTER 6** provides the performance evaluation by means of IDA Analyses of the structures designed by the proposed design procedure (TPMC) and Eurocode 8 (EC8). In addition, economic considerations are also reported.

**CONCLUSIONS** present the summary of the work with some suggestions for future research.

**APPENDIX A** are reported the push-over plastic hinge distribution snapshot from SAP2000 for the study cases described in Chapter 5.

**APPENDIX B** the IDA Analyses plastic hinge distribution snapshot from SAP2000 for the study cases described in Chapter 6 are reported.





# CHAPTER 2

## MOMENT-SHEAR INTERACTION IN RIGID-PLASTIC ANALYSIS OF EBFs

### 2.1 Introduction

The basic principles of Capacity Design state that dissipative zones have to be designed according to the internal actions arising from the load combinations provided by seismic codes, whereas non-dissipative zones have to be proportioned on the basis of the maximum internal actions transmitted by dissipative zones in the fully yielded and strain-hardened state [1-3].

This condition need to be fulfilled also in the case of eccentrically braced frames (EBFs) where dissipative zones are constituted by the so-called link elements, whose yielding is significantly affected by moment-shear interaction [35], [37], [38].

Even though the use, as dissipative zones, of members yielding in shear was originally proposed for EBFs, such issue has also been the starting point for the birth of new structural typologies such as knee braced frames [41], aluminium shear links [43] and shear links made of low yield point steel [44], [45]. However, this kind of behaviour is rarely separated from dissipation due to moment yielding, so that the problem of interaction between moment and shear cannot be neglected.

In this work, the problem of moment-shear interaction is considered within the framework of rigid-plastic analysis and the solution is provided with

reference to eccentrically braced frames. In fact, the solution of the interaction problem is affected by the compatibility requirements which depend on the geometrical configuration of the structural scheme. Such issue has already been studied with reference to EB-Frames with D-scheme, K-scheme and V-scheme by Mastrandrea and Piluso [11] and is herein taken up and deepened in order to provide a more complete discussion which includes also EBFs with inverted Y-scheme. The main characteristic of EBFs with inverted Y-scheme is that the dissipative zone, does not belong to the beam member, so that it can be easily substituted after the occurrence of earthquakes.

Aiming at the development of hierarchy criteria able to assure the control of the pattern of yielding, the attention is focused on one-storey EB-Frames to determine how to assure the yielding of predefined dissipative zones only, i.e. the links and the base sections of columns when they are not pinned. Conversely, yielding of diagonals has to be prevented. Regarding the beam member, its yielding can be prevented providing that beam-to-column connections are designed to transmit the shear forces only.

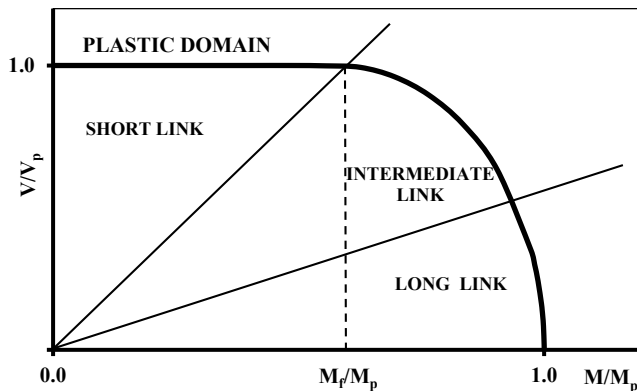


Figure 2.1 –  $M$ - $V$  interaction domain

Conversely, in case of moment resistant connections, yielding of beam ends close to the beam-to-column connections can occur in case of severe seismic events. In fact, generally, by increasing the spectral acceleration yielding occurs at link ends before the involvement of the beam ends. In other words, yielding of

beam ends occurs only in case of very high values of the spectral acceleration. As a consequence the main advantage of the inverted Y-scheme is appreciated after seismic events not involving the beam yielding, so that only the link substitution is required.

The obtained results, herein presented, will constitute the starting point for the development of the Theory of Plastic Mechanism Control (TPMC) not only for MRF-EBF dual systems (which is the typology mainly considered in this work) but also for simple EBFs. The development of TPMC is reported and discussed in the forthcoming chapters.

However, in this chapter, the attention is focused on the study of moment-shear interaction in EB-Frames and on the development of hierarchy criteria at the “storey level”. The validation of the developed hierarchy criteria is carried out by means of push-over analyses aimed to check the actual collapse mechanism developed by the designed structures.

## 2.2 Plastic Domain for Moment-Shear Interaction

Eccentrically braced frames (EBFs) are characterized by dissipative elements which can be either horizontal (D-scheme, K-scheme and V-scheme) or vertical (inverted Y-scheme), called links. Independently of the typology, the main feature of links is due to the interaction between shear force and bending moment which is not negligible in the prediction of the ultimate behaviour of the structural system. In particular, link classification depends on the length of the member. The following classification was originally proposed [3], [33], [37], [38]:

- *Short links* for  $e \leq 1.6M_p/V_p$ ,
- *Intermediate links* for  $1.6M_p/V_p \leq e \leq 3M_p/V_p$ ,
- *Long links* for  $e \geq 3M_p/V_p$ ,

being  $V_p$  and  $M_p$  the plastic shear resistance and the plastic moment resistance of the link cross section, respectively. The long link limit has been successively revised to  $2.6M_p/V_p$  [46], [47], [48]. Unless the link section can be whatever shaped in the following reference is made to double T shaped links.

The link plastic behaviour (Figure 2.1) can be assumed in pure shear, when the bending moment is less than the moment  $M_p = f_y b t_f (d - t_f)$  where  $f_y$  is the yield stress,  $d$  is the link section depth,  $b$  is the base of the flange,  $t_f$  and  $t_w$  are the thicknesses of flange and web, respectively. In this case,  $M_p$  owns the

meaning of  $M_f$  which is the contribution of the flanges to the plastic moment of the cross section [11]. Conversely, for a bending moment exceeding  $M_f$ , the shear resistance of the member is reduced due to the interaction between bending moment and shear. According to Neal [49], the plastic domain can be expressed by means of the following relationships:

$$\left(\frac{|M| - M_f}{M_p - M_f}\right)^2 + \left(\frac{V}{V_p}\right)^2 = 1 \quad \text{for } M_f \leq |M| \leq M_p \quad (2.1)$$

$$V = V_p \quad \text{for } |M| \leq M_f \quad (2.2)$$

Within capacity design an important issue, reported since earlier tests by Hjelmstad and Popov [50] and Malley and Popov [51], is the overstrength developed by the link. Link overstrength is the ratio between the maximum shear force developed by the link and its plastic shear strength. The interpretation of testing results is usually based on the evaluation of the plastic shear resistance as  $V_p = 0.6 f_y (d - 2t_f)t_w$  as reported in [47] (for EC8 [11]  $V_p = \frac{1}{\sqrt{3}} f_y (d - t_f)t_w$ ) where  $f_y$  is the yield stress,  $d$  is the link section depth,  $t_f$  and  $t_w$  are the thicknesses of flange and web, respectively.

According to capacity design, link overstrength has to be accounted for in evaluating the maximum internal actions transferred to non-dissipative zones. A link overstrength factor of 1.50 has been generally recommended on the basis of past experimental researches [53]. Currently, 2005 AISC Seismic Provisions [47] specify a link overstrength factor of 1.25 (double T shaped links) for the design of the diagonal brace and an overstrength factor of 1.10 for the design of the beam segment outside the link and for column design.

Recently some doubts have risen regarding the overstrength factor to be suggested for capacity design purposes. These doubts are related to recent experimental tests showing factors exceeding the code suggested values. In fact, overstrength factors of nearly 2.0 have been obtained in recent tests on large built-up shear links to be used in bridge applications [54], [55], but this is mainly the case of shapes with heavy flanges where a significant contribution of flanges to the shear resistance occurs. Similar results have been obtained by Dusicka et al. [45] who, in addition, obtained an overstrength factor of about 4 for a built-up shape with heavy flanges and webs, made of low yield point steel.

However, it should also be recognized that the amount of overstrength to be considered in design is also dependent on the expected plastic deformation

demands. In fact, with reference to standard European rolled profiles, by means of finite element analyses, Barecchia et al. [56] have found overstrength factors ranging between 2.00 and 2.50 for a link shear deformation equal to 0.10 rad. Notwithstanding, some caution should be adopted in using the above results, because they come from finite element analyses where the influence of stiffeners cannot be accurately accounted for.

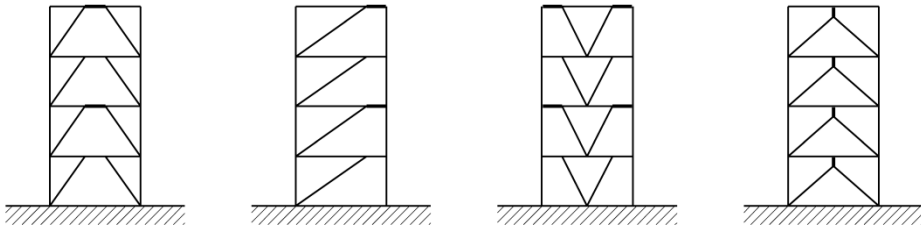


**Figure 2.2** – EBFs typologies proposed by Eurocode 8

In fact, recently Okazaki et al. [48] have pointed out that the failure process of shear links with properly detailed web stiffeners, i.e. according to modern seismic provisions, develops from fractures that arise at the vertical fillet welds connecting the link stiffeners to the link web. On the basis of 23 experimental tests, they have found an overstrength factor ranging from 1.34 to 1.48 in case of short links, and ranging from 1.12 to 1.28 in the case of longer links. These overstrength factors have been computed considering the measured values of the material properties. Therefore, they concluded that an overstrength factor of 1.5, which forms worldwide the basis of capacity design provisions for EBFs, appears reasonable for links constructed by means of typical rolled profiles.

A simple procedure to account for overstrength in hierarchy criteria derived by rigid-plastic analysis was proposed by Mastrandrea et al. [24] based on the use of an interaction domain referring to the ultimate conditions obtained by means of a simple homothetic expansion of the plastic domain.

A more systematic approach is herein developed for EB-Frames with reference to all the link configuration proposed by Eurocode 8 [11], i.e. inverted split K-scheme, D-scheme, V-scheme and inverted Y-scheme (Figure 2.2).

### 2.3 Plastic Mechanism Control of one-storey EBFs

The typologies of plastic collapse mechanisms of one-storey EB-Frames are depicted in Figure 2.3. In particular, in the desired kinematic mechanism (A-type in Figure 2.3) both the ends of the link are yielded. In addition also the base of the columns are yielded while the braces remain in elastic range because they are pinned at their bases. Also beams remain in elastic range for all the horizontal link scheme (K-scheme, D-scheme and V-scheme) while for inverted Y-scheme plastic hinges develop at beam ends as for MR-Frames, if they take into account also the transmission of bending moment.

	DESIRED MECHANISM	UNDESIRED MECHANISMS		
	A-Type	B-Type	C-Type	D-Type
K-Scheme		NOT DEVELOPS	NOT DEVELOPS	
D-Scheme			NOT DEVELOPS	NOT DEVELOPS
V-Scheme			NOT DEVELOPS	NOT DEVELOPS
Inverted Y-Scheme				

Figure 2.3 – Mechanism typologies for one-storey EB-Frames with long links

When only one end of the link yields, the development of a kinematic mechanism requires plastic hinges also at the beam ends adjacent to the link (B-type in Figure 2.3) or at the diagonal ends adjacent to the link (C-type in Figure 2.3). When the link remains in elastic range, the development of a kinematic mechanism involves only the diagonal and beam sections adjacent to the link (D-type in Figure 2.3). In any case, the yielding of column base sections is required unless they are pinned (Figure 2.3).

	DESIRED MECHANISM	UNDESIRED MECHANISMS			
	A-Type	B-Type	C-Type	D-Type	
K-Scheme		NOT DEVELOPS	NOT DEVELOPS		
D-Scheme			NOT DEVELOPS	NOT DEVELOPS	
V-Scheme			NOT DEVELOPS	NOT DEVELOPS	
Inverted Y-Scheme					

**Figure 2.4** – Mechanism typologies for one-storey EB-Frames considering the interaction between moment and shear

B-type, C-type and D-type mechanisms have to be avoided, because they involve non dissipative zones such as the beam and diagonal sections close to the

link, conversely, the diagonal brace and beam segment outside of the link are intended to remain essentially elastic under the forces generated by the fully yielded and strain hardened link as required by the second principle of Capacity Design.

	DESIRED MECHANISM	UNDESIRED MECHANISMS		
	A-Type	B-Type	C-Type	D-Type
K-Scheme		NOT DEVELOPS	NOT DEVELOPS	
D-Scheme		NOT DEVELOPS	NOT DEVELOPS	NOT DEVELOPS
Inverted V-Scheme		NOT DEVELOPS	NOT DEVELOPS	NOT DEVELOPS
Inverted Y-Scheme		NOT DEVELOPS	NOT DEVELOPS	

Figure 2.5 – Mechanism typologies for one-storey EB-Frames with short links

For this reason one of the primary goal for the proper seismic design of the EBFs starts from the definition of simple hierarchy criteria at “storey level”, including also the influence of moment-shear interaction, which assure the development of the desired mechanism. Obviously, in case of beam-to-column connections designed to transmit the shear forces only, A-type mechanism does not require any beam hinging.



In order to account for moment-shear interaction rigid-plastic analysis is applied. In particular, the yielding of the link ends is modelled by a combination of a plastic double pendulum and a plastic hinge, which are able to account for both plastic shear deformation,  $v_p$ , and plastic moment rotation,  $\phi_p$ , respectively (Figure 2.4).

The use of rigid-plastic analysis to compute the plastic resistance of the possible mechanisms requires the evaluation, for a given value of the kinematic parameter  $\theta$ , of the link plastic deformations  $v_p$  and  $\phi_p$  and of the corresponding shear  $V$  and bending moment  $M$ . The solution can be obtained by minimizing the internal work of the link and by imposing the fulfilment of the yielding conditions and the respect of normal plastic flow rule. In addition, also compatibility requirements need to be satisfied. Five overall equations are obtained where the unknown quantities are constituted by the internal actions  $V$  and  $M$ , the plastic deformations  $v_p$  and  $\phi_p$  and, finally, by the parameter  $\lambda$  governing the plastic deformation magnitude in the normal flow rule.

## 2.4 Link Moment-Shear Interaction

### 2.4.1 A-Type Mechanism

As already stated, within the framework of rigid-plastic analysis, moment-shear interaction occurring in link of EB-Frames is governed by five equations which with reference to the desired mechanism (A-type), and for K-scheme, D-scheme, V-scheme and inverted Y-scheme are given by:

- a. Minimisation of the internal work with reference to the collapse configuration for a given plastic rotation  $\theta$  at the base of columns:

$$W_{K.i}^{(A)} = W_{D.i}^{(A)} = 2M^{(A)}\phi_p^{(A)} + 2V^{(A)}v_p^{(A)} + 2M_c\theta = \text{minimum} \quad (2.3)$$

$$W_{V.i}^{(A)} = 4M^{(A)}\phi_p^{(A)} + 4V^{(A)}v_p^{(A)} + 2M_c\theta = \text{minimum} \quad (2.4)$$

$$W_{Y.i}^{(A)} = 2M^{(A)}\phi_p^{(A)} + 2V^{(A)}v_p^{(A)} + 2M_b\theta + 2M_c\theta = \text{minimum} \quad (2.5)$$

- b. Kinematic compatibility condition:

$$\text{K-scheme and D-scheme} \quad 2v_p^{(A)} + \phi_p^{(A)}e = \theta L = \gamma e \quad (2.6)$$

$$\text{V-scheme} \quad 4v_p^{(A)} + 2\phi_p^{(A)}e = \theta L = 2\gamma e \quad (2.7)$$

$$\text{Inverted Y-scheme} \quad 2v_p^{(A)} + \phi_p^{(A)}e = \theta h = \gamma e \quad (2.8)$$

c. Yielding condition of the link sections:

$$F(M^{(A)}, V^{(A)}) = \left( \frac{|M^{(A)}| - M_f}{M_p - M_f} \right)^2 + \left( \frac{V^{(A)}}{V_p} \right)^2 - 1 = 0 \quad (2.9)$$

d. Normal plastic flow rule:

$$v_p^{(A)} = \lambda \frac{\partial F}{\partial V^{(A)}} \quad \phi_p^{(A)} = \lambda \frac{\partial F}{\partial M^{(A)}} \quad (2.10)$$

where  $M^{(A)}$  and  $V^{(A)}$  are the moment and the shear occurring at the link ends in the A-type mechanism, respectively,  $\phi_p^{(A)}$  and  $v_p^{(A)}$  are the plastic rotation and the plastic shear deformations occurring in the A-type mechanism, respectively,  $e$  is the length of the link,  $h$  is the interstorey height and  $\theta$  is the plastic rotation at the beam ends and at the base section of columns. Finally,  $M_b$  and  $M_c$  are the plastic moment of the beam and of the column, respectively.

By substituting Eq. (2.6) into Eq. (2.3), (2.7) into (2.4) and (2.8) into (2.5) the following relations are obtained:

$$W_{K.i}^{(A)} = W_{D.i}^{(A)} = 2M^{(A)}\phi_p^{(A)} + V^{(A)}L\theta - V^{(A)}\phi_p^{(A)}e + 2M_c\theta \quad (2.11)$$

$$W_{V.i}^{(A)} = 4M^{(A)}\phi_p^{(A)} + 2V^{(A)}L\theta - 2V^{(A)}\phi_p^{(A)}e + 2M_c\theta \quad (2.12)$$

$$W_{Y.i}^{(A)} = 2M^{(A)}\phi_p^{(A)} + V^{(A)}h\theta - V^{(A)}\phi_p^{(A)}e + 2M_b\theta + 2M_c\theta \quad (2.13)$$

For a given  $\theta$  value, Eqs. (2.11), (2.12) and (2.13) provide the internal work as a function of the parameter  $\phi_p^{(A)}$  only, so that the minimization of the internal work (i.e. Eqs. (2.3), (2.4) and (2.5)) can be generally expressed as:

$$\frac{dW_i^{(A)}}{d\phi_p^{(A)}} = 0 \quad (2.14)$$

which gives:

$$V^{(A)} = \frac{2M^{(A)}}{e} \quad (2.15)$$

By introducing  $M_w = M_p - M_f$  (where  $M_p$  is the plastic moment of whole section), i.e. the part of the plastic moment due to the web and web-to-flange

connection zone, and by combining Eqs. (2.9) and (2.15) the values of  $M^{(A)}$  and  $V^{(A)}$  can be obtained in closed form as follows:

$$M^{(A)} = \frac{M_f + M_w \sqrt{1 - 4 \frac{M_f^2 - M_w^2}{V_p^2 e^2}}}{1 + 4 \frac{M_w^2}{V_p^2 e^2}} \quad (2.16)$$

$$V^{(A)} = 2 \frac{M_f + M_w \sqrt{1 - 4 \frac{M_f^2 - M_w^2}{V_p^2 e^2}}}{e \left(1 + 4 \frac{M_w^2}{V_p^2 e^2}\right)} \quad (2.17)$$

It is useful to note that, for  $e \rightarrow \infty$ , Eq. (2.16) provides  $M^{(A)} = M_f + M_w = M_p$  and Eq. (2.17) provides  $V^{(A)} = 2M_p/e$ , which represents the limit case of long links in pure bending. Furthermore, it is also interesting to observe that Eq. (2.17) can be simply obtained by considering the link equilibrium providing the shear as the ratio between the sum of the end bending moments and the link length. Therefore, it can be concluded that the solution for  $V^{(A)}$  and  $M^{(A)}$  can also be obtained by simply combining the link equilibrium condition with the yielding condition. In other words, it means that the obtained solution is also valid within the framework of the “static approach”, so that it provides the actual internal actions under yielding conditions in moment-shear interaction. However, even though the “kinematic approach” could seem more complicated, because of the increased number of equations to be considered, its main advantage is constituted by the possibility of evaluating not only the plastic internal actions  $V^{(A)}$  and  $M^{(A)}$ , but also the corresponding plastic shear deformation  $v_p^{(A)}$  and plastic rotation  $\phi_p^{(A)}$ . Therefore, it provides additional information absolutely needed for the following developments. In particular, the internal work,  $W_i^{(A)}$ , is obtained by substituting Eq. (2.15) into Eqs. (2.11), (2.12) and (2.13):

$$W_{K.i}^{(A)} = W_{D.i}^{(A)} = \frac{2M^{(A)}}{e} \theta L + 2M_c \theta \quad (2.18)$$

$$W_{V.i}^{(A)} = \frac{4M^{(A)}}{e} \theta L + 2M_c \theta \quad (2.19)$$

$$W_{Y.i}^{(A)} = \frac{2M^{(A)}}{e} \theta h + 2M_b \theta + 2M_c \theta \quad (2.20)$$

It is useful to note that, being  $\gamma = \theta L/e$  for EBFs with horizontal link and  $\gamma = \theta h/e$  for EBFs with vertical link, the parameter usually adopted to measure

the plastic deformation of links, Eqs. (2.18), (2.19) and (2.20) show that, in case of A-type mechanism, the internal work due to an intermediate link can be simply expressed as the product of the whole plastic moment of the link and the plastic deformation of the link. It also means that  $M^{(A)}$  can be interpreted as an equivalent plastic moment allowing to write the internal work simply as the product between the equivalent plastic moment and the equivalent plastic rotation, even in the case of moment-shear interaction, as already underlined in [24].

In addition, by considering the normal plastic flow rule (Eq. (2.10)) the values of shear deformation  $v_p^{(A)}$  and plastic rotation  $\phi_p^{(A)}$  can be obtained as follows:

$$v_p^{(A)} = 2\lambda \frac{V^{(A)}}{V_p^2} \qquad \phi_p^{(A)} = 2\lambda \frac{M^{(A)} - M_f}{M_w^2} \quad (2.21)$$

where the parameter  $\lambda$  governing the magnitude of the plastic flow can be properly eliminated by evaluating the ratio between  $\phi_p^{(A)}$  and  $v_p^{(A)}$ :

$$\frac{\phi_p^{(A)}}{v_p^{(A)}} = \frac{M^{(A)} - M_f}{M_w^2} \frac{V_p^2}{V^{(A)}} \quad (2.22)$$

In addition, by combining the above equation with the kinematic compatibility condition (Eqs. (2.6), (2.7) and (2.8)), the link plastic shear deformation  $v_p^{(A)}$  and the link plastic rotation  $\phi_p^{(A)}$  are as follows:

$$v_p^{(A)} = \gamma \frac{1}{2 + \frac{M^{(A)} - M_f}{M_w^2} \frac{V_p^2}{V^{(A)}} e} \quad (2.23)$$

and:

$$\phi_p^{(A)} = \gamma \frac{1}{1 + \frac{2M_w^2}{M^{(A)} - M_f} \frac{V^{(A)}}{V_p^2} e} \quad (2.24)$$

## 2.4.2 B-Type Mechanism

B-Type mechanism is characterized by the yielding of one link end while, at the other end, the plastic hinges are concentrated in the beam and diagonal sections adjacent to the link. Such mechanism typology develops in the case of EBF with D-scheme, V-scheme and inverted Y-scheme with the only exception of K-scheme. In particular, for inverted Y-scheme, B-Type mechanism involves the

bottom section of the link (adjacent to diagonal braces) and the beam sections adjacent to the top section of the link (Figure 2.3).

The five relations needed to solve the problem of the interaction between shear and bending moment occurring in intermediate links, with reference to B-type mechanism, are:

- a. Condition of minimisation of the internal work with reference to the collapse configuration for a given rotation  $\theta$ :

$$W_{D.i}^{(B)} = M^{(B)}\phi_p^{(B)} + M_b\phi_p^{(B)} + M_d\phi_p^{(B)} + V^{(B)}v_p^{(B)} + 2M_c\theta = \text{minimum} \quad (2.25)$$

$$W_{V.i}^{(B)} = 2M^{(B)}\phi_p^{(B)} + 2V^{(B)}v_p^{(B)} + 2M_b\phi_p^{(B)} + 2M_d\phi_p^{(B)} + 2M_c\theta = \text{minimum} \quad (2.26)$$

$$W_{Y.i}^{(B)} = M^{(B)}\phi_p^{(B)} + 2M_b\phi_p^{(B)} + V^{(B)}v_p^{(B)} + 2M_b\theta + 2M_c\theta = \text{minimum} \quad (2.27)$$

- b. Kinematic compatibility condition:

$$\text{D-scheme} \quad v_p^{(B)} + \phi_p^{(B)}e = \theta L = \gamma e \quad (2.28)$$

$$\text{V-scheme} \quad 2v_p^{(B)} + 2\phi_p^{(B)}e = \theta L = 2\gamma e \quad (2.29)$$

$$\text{Inverted Y-scheme} \quad v_p^{(B)} + \phi_p^{(B)}e = \theta h = \gamma e \quad (2.30)$$

- c. Yielding condition of the bottom link section:

$$F(M^{(B)}, V^{(B)}) = \left( \frac{|M^{(B)}| - M_f}{M_p - M_f} \right)^2 + \left( \frac{V^{(B)}}{V_p} \right)^2 - 1 = 0 \quad (2.31)$$

- d. Normal plastic flow rule:

$$v_p^{(B)} = \lambda \frac{\partial F}{\partial V^{(B)}} \quad \phi_p^{(B)} = \lambda \frac{\partial F}{\partial M^{(B)}} \quad (2.32)$$

where  $M^{(B)}$  and  $V^{(B)}$  are the bending moment and the shear, respectively, occurring at the yielded end of the link,  $\phi_p^{(B)}$  and  $v_p^{(B)}$  are the plastic rotation and the plastic shear deformation, respectively, occurring at the yielded end of the link.

Regarding Eqs. (2.28), (2.29) and (2.30) it is useful to note that the plastic rotation of the hinges occurring in the beam and in the diagonal at the link-to-beam connection is equal to  $\phi_p^{(B)}$ . By substituting Eq. (2.28) into Eq. (2.25), Eq. (2.29) into Eq. (2.26) and Eq. (2.30) and (2.27) the following relations are obtained:

$$W_{D.i}^{(B)} = M^{(B)}\phi_p^{(B)} + M_b\phi_p^{(B)} + M_d\phi_p^{(B)} + V^{(B)}\theta L - V^{(B)}\phi_p^{(B)}e + 2M_c\theta \quad (2.33)$$

$$W_{V.i}^{(B)} = 2M^{(B)}\phi_p^{(B)} + 2M_b\phi_p^{(B)} + 2M_d\phi_p^{(B)} + 2V^{(B)}\theta L - 2V^{(B)}\phi_p^{(B)}e + 2M_c\theta \quad (2.34)$$

$$W_{Y.i}^{(B)} = M^{(B)}\phi_p^{(B)} + 2M_b\phi_p^{(B)} + V^{(B)}\theta h - V^{(B)}\phi_p^{(B)}e + 2M_b\theta + 2M_c\theta \quad (2.35)$$

which, for a given value of  $\theta$ , expresses the internal work as a function of the plastic rotation  $\phi_p^{(B)}$  of the link bottom end, so that the minimization of the internal work is given by the following relationship:

$$\frac{dW_i^{(B)}}{d\phi_p^{(B)}} = 0 \quad (2.36)$$

which provides:

$$\text{D-scheme} \quad V^{(B)} = \frac{M^{(B)} + (M_b + M_d)}{e} \quad (2.37)$$

$$\text{V-scheme} \quad V^{(B)} = \frac{M^{(B)} + (M_b + M_d)}{e} \quad (2.38)$$

$$\text{Inverted Y-scheme} \quad V^{(B)} = \frac{M^{(B)} + 2M_b}{e} \quad (2.39)$$

By combining Eq. (2.31) with Eqs. (2.37), (2.38) and (2.39), respectively, the values of the internal actions,  $M^{(B)}$  and  $V^{(B)}$ , occurring at the link yielded can be found as follows:

$$M^{(B)} = \frac{M_f \left(1 - \frac{M_b + M_d}{M_f} \frac{M_w^2}{V_p^2 e^2}\right) + M_w \sqrt{1 - \frac{(M_f + M_b + M_d)^2}{V_p^2 e^2}} + \frac{M_w^2}{V_p^2 e^2}}{1 + \frac{M_w^2}{V_p^2 e^2}} \quad (2.40)$$

D-scheme

$$V^{(B)} = \frac{1}{e} \left( \frac{M_f \left(1 - \frac{M_b + M_d}{M_f} \frac{M_w^2}{V_p^2 e^2}\right) + M_w \sqrt{1 - \frac{(M_f + M_b + M_d)^2}{V_p^2 e^2}} + \frac{M_w^2}{V_p^2 e^2}}{1 + \frac{M_w^2}{V_p^2 e^2}} + M_b + M_d \right) \quad (2.41)$$

$$M^{(B)} = \frac{M_f \left(1 - \frac{M_b + M_d}{M_f} \frac{M_w^2}{V_p^2 e^2}\right) + M_w \sqrt{1 - \frac{(M_f + M_b + M_d)^2}{V_p^2 e^2}} + \frac{M_w^2}{V_p^2 e^2}}{1 + \frac{M_w^2}{V_p^2 e^2}} \quad (2.42)$$

V-scheme

$$V^{(B)} = \frac{1}{e} \left( \frac{M_f \left(1 - \frac{M_b + M_d}{M_f} \frac{M_w^2}{V_p^2 e^2}\right) + M_w \sqrt{1 - \frac{(M_f + M_b + M_d)^2}{V_p^2 e^2}} + \frac{M_w^2}{V_p^2 e^2}}{1 + \frac{M_w^2}{V_p^2 e^2}} + M_b + M_d \right) \quad (2.43)$$

$$M^{(B)} = \frac{M_f \left(1 - 2 \frac{M_b}{M_f} \frac{M_w^2}{V_p^2 e^2}\right) + M_w \sqrt{1 - \frac{(M_f + 2M_b)^2}{V_p^2 e^2} + \frac{M_w^2}{V_p^2 e^2}}}{1 + \frac{M_w^2}{V_p^2 e^2}} \quad (2.44)$$

Inverted  
Y-scheme

$$V^{(B)} = \frac{1}{e} \left( \frac{M_f \left(1 - 2 \frac{M_b}{M_f} \frac{M_w^2}{V_p^2 e^2}\right) + M_w \sqrt{1 - \frac{(M_f + 2M_b)^2}{V_p^2 e^2} + \frac{M_w^2}{V_p^2 e^2}}}{1 + \frac{M_w^2}{V_p^2 e^2}} + 2M_b \right) \quad (2.45)$$

In this case, it is also useful to note that, for  $e \rightarrow \infty$ , Eqs. (2.40), (2.42) and (2.44) provide  $M^{(A)} = M_f + M_w = M_p$ . Furthermore, it is also interesting to observe that Eqs. (2.37), (2.38) and (2.39) can be still obtained by simply considering the link equilibrium condition. As a consequence, it means that the solution obtained for  $M^{(B)}$  and  $V^{(B)}$  is also provided by the “static approach”. However, as already underlined with reference to the previous considered case, i.e. A-type mechanism, the “kinematic approach” has to be preferred, because it allows the computation of the plastic deformations,  $v_p^{(B)}$  and  $\phi_p^{(B)}$ , of the link yielded end. Therefore, following the same method already applied for A-type mechanism, by exploiting the normal plastic flow rule, the parameter  $\lambda$  governing the magnitude of the plastic flow can be properly eliminated by evaluating the ratio between  $\phi_p^{(B)}$  and  $v_p^{(B)}$ :

$$\frac{\phi_p^{(B)}}{v_p^{(B)}} = \frac{M^{(B)} - M_f}{M_w^2} \frac{V_p^2}{V^{(B)}} \quad (2.46)$$

By combining Eq. (2.46) with the kinematic compatibility condition for B-type mechanism, i.e. Eqs. (2.28), (2.29) and (2.30) the following relations are obtained:

$$\phi_p^{(B)} = \gamma \frac{1}{1 + \frac{M_w^2}{M^{(B)} - M_f} \frac{V^{(B)}}{V_p^2 e}} \quad (2.47)$$

$$v_p^{(B)} = \gamma e \left( 1 - \frac{1}{1 + \frac{M_w^2}{M^{(B)} - M_f} \frac{V^{(B)}}{V_p^2 e}} \right) \quad (2.48)$$

### 2.4.3 C-Type Mechanism

Regarding C-type mechanism, it is preliminarily useful to observe that occurs only in the case of EBFs with inverted Y-scheme where the link end involved in the kinematic mechanism is now the top one and, in addition, the top ends of the diagonal braces are yielded while the beam at the link-to-beam connection remains in elastic range. As regards EBFs with D-scheme and inverted V-scheme, C-type mechanism is coincident with B-type mechanism. In addition, for EBFs with K-scheme the C-type mechanism and the B-type mechanism do not develop.

As preliminarily stated only EBFs with inverted Y-scheme develop C-type mechanism. In particular, the plastic hinges developed at the top end of diagonal braces are subjected to a plastic rotation equal to the one occurring at the link top end,  $\phi_p^{(C)}$ . Therefore, the problem of the interaction between shear and bending moment in C-type mechanism can be easily solved like in case of B-type mechanism. In particular, Eqs. (2.27), (2.35), (2.39), (2.44) and (2.45) are valid also for C-type mechanism provided that  $M_b$  is substituted with  $M_d$  which represents the plastic moment of the diagonals. As soon as such substitution is made, equations (2.44), (2.45), (2.47) and (2.48) will provide  $M^{(C)}$ ,  $V^{(C)}$ ,  $\phi_p^{(C)}$  and  $v_p^{(C)}$ , respectively, where  $M^{(C)}$  and  $V^{(C)}$  are the bending moment and shear force occurring at the link top end in the yielding condition while,  $\phi_p^{(C)}$  and  $v_p^{(C)}$  are the corresponding plastic rotation and plastic shear.

### 2.4.4 D-Type Mechanism

D-type mechanism occurs only for EBFs with K-scheme and inverted Y-scheme. The peculiarity of this mechanism is that it does not involve the link, so that there is no need to study the problem of moment-shear interaction. In this case, the compatibility equation is given by:

$$\text{K-scheme} \quad \gamma e = \theta L \quad (2.49)$$

$$\text{Inverted Y-scheme} \quad \gamma e = \theta h \quad (2.50)$$



Therefore, the expression of the internal work, required for the following developments aimed at the control of the pattern of yielding, for this kind of mechanism is provided by the following relations:

$$W_{K.i}^{(D)} = 2M_b\theta + 2M_c\theta + 2M_b\theta\frac{L}{e} + 2M_d\theta\frac{L}{e} \quad (2.51)$$

$$W_{Y.i}^{(D)} = 2M_b\theta + 2M_c\theta + 2M_b\theta\frac{h}{e} + 2M_d\theta\frac{h}{e} \quad (2.52)$$

## 2.5 Hierarchy Criteria

### 2.5.1 Hierarchy Criteria for Intermediate links

In this paragraph, the attention is primarily focused on the determination of operative relationships aimed at the development of hierarchy criteria to control the pattern of yielding for single storey of EB-Frames. In particular, A-type mechanism is the desired pattern of yielding, being the only kinematic mechanism leading to the yielding of the two link ends, i.e. the dissipative zones of the structural typology under examination. According to the kinematic theorem of plastic collapse, the requirements to be fulfilled to avoid undesired collapse mechanisms are obtained by imposing that the kinematically admissible horizontal force multiplier corresponding to A-Type mechanism is less than those corresponding to B-type, C-type and D-type mechanisms in the case they develop.

The internal virtual work for the scheme illustrated in Figure 2.4 is expressed by means of Eqs. (2.18), (2.19) and (2.20) in case of A-type mechanism, by means of Eqs. (2.25), (2.26) and (2.27) in case of B-type mechanism. In the case of C-type mechanism, the internal work is given only for the EBFs with inverted Y-scheme and it is equal to:

$$\begin{matrix} \text{C-type} \\ \text{mechanism} \end{matrix} W_{Y.i}^{(C)} = 2M_c\theta + 2M_b\theta + M^{(C)}\phi_p^{(C)} + 2M_d\phi_p^{(C)} + V^{(C)}v_p^{(C)} \quad (2.53)$$

Finally, in case of D-type mechanism, Eqs. (2.51) and (2.52) have to be considered.

The virtual external work is developed by external loads such as vertical loads and seismic horizontal forces. The rate provided by the vertical distributed loads is equal to zero for EBFs with K-scheme, V-scheme and inverted Y-scheme

due to the symmetry of the structural scheme while for D-scheme is expressed as:

$$W_{e,q} = q \frac{L(L-e)}{2} \theta \quad (2.54)$$

The external virtual work is expressed by the following relation for all the structural configurations:

$$W_{e,F} = \alpha F \theta h \quad (2.55)$$

for the four investigated EBFs typologies. The kinematically admissible horizontal force multipliers are obtained by imposing that the internal work has to be equal to the external work. Therefore, equations (2.18) to (2.20), (2.33) to (2.35) and (2.51) to (2.55) provide for:

- A-type mechanism:

$$\text{K-scheme} \quad \alpha_K^{(A)} = \frac{2 M_c + 2 M^{(A)} \frac{L}{e}}{Fh} \quad (2.56)$$

$$\text{D-scheme} \quad \alpha_D^{(A)} = \frac{2 M_c + 2 M^{(A)} \frac{L}{e} - q \frac{L(L-e)}{2}}{Fh} \quad (2.57)$$

$$\text{V-scheme} \quad \alpha_V^{(A)} = \frac{2 M_c + 4 M^{(A)} \frac{L}{e}}{Fh} \quad (2.58)$$

$$\text{Inverted Y-scheme} \quad \alpha_Y^{(A)} = \frac{2 M_c + 2 M_b + 2 M^{(A)} \frac{h}{e}}{Fh} \quad (2.59)$$

- B-type mechanism:

$$\text{D-scheme} \quad \alpha_D^{(B)} = \frac{2 M_c + \frac{M_b \phi_p^{(B)}}{\theta} + \frac{M_d \phi_p^{(B)}}{\theta} + \frac{M^{(B)} \phi_p^{(B)}}{\theta} + \frac{V^{(B)} v_p^{(B)}}{\theta} - q \frac{L(L-e)}{2}}{Fh} \quad (2.60)$$

$$\text{V-scheme} \quad \alpha_V^{(B)} = \frac{2 M_c + 2 \frac{M_b \phi_p^{(B)}}{\theta} + 2 \frac{M_d \phi_p^{(B)}}{\theta} + 2 \frac{M^{(B)} \phi_p^{(B)}}{\theta} + 2 \frac{V^{(B)} v_p^{(B)}}{\theta}}{Fh} \quad (2.61)$$

$$\text{Inverted Y-scheme} \quad \alpha_Y^{(B)} = \frac{2 M_c + 2 M_b + \frac{2 M_b \phi_p^{(B)}}{\theta} + \frac{M^{(B)} \phi_p^{(B)}}{\theta} + \frac{V^{(B)} v_p^{(B)}}{\theta}}{Fh} \quad (2.62)$$

- C-type mechanism:

$$\text{Inverted Y-scheme} \quad \alpha_Y^{(C)} = \frac{2 M_c + 2 M_b + \frac{M^{(C)} \phi_p^{(C)}}{\theta} + \frac{2 M_d \phi_p^{(C)}}{\theta} + \frac{V^{(C)} v_p^{(C)}}{\theta}}{Fh} \quad (2.63)$$

- D-type mechanism:

$$\text{K-scheme} \quad \alpha_K^{(D)} = \frac{2 M_c + 2 M_b \frac{L}{e} + 2 M_d \frac{L}{e}}{Fh} \quad (2.64)$$

$$\begin{array}{l} \text{Inverted} \\ \text{Y-scheme} \end{array} \quad \alpha_Y^{(D)} = \frac{2 M_c + 2 M_b + 2 M_b \frac{h}{e} + 2 M_d \frac{h}{e}}{Fh} \quad (2.65)$$

The design criterion needed to avoid B-type mechanism requires the fulfilment of the following inequality generally expressed as:

$$\alpha^{(A)} \leq \alpha^{(B)} \quad (2.66)$$

which become:

- for EBFs with D-scheme:

$$\alpha_D^{(A)} \leq \alpha_D^{(B)} \rightarrow 2 M^{(A)} \frac{L}{e} \leq \frac{M_b \phi_p^{(B)}}{\theta} + \frac{M_d \phi_p^{(B)}}{\theta} + \frac{M^{(B)} \phi_p^{(B)}}{\theta} + \frac{V^{(B)} v_p^{(B)}}{\theta} \quad (2.67)$$

- for EBFs with inverted V-scheme:

$$\alpha_V^{(A)} \leq \alpha_V^{(B)} \rightarrow 4 M^{(A)} \frac{L}{e} \leq 2 \frac{M_b \phi_p^{(B)}}{\theta} + 2 \frac{M_d \phi_p^{(B)}}{\theta} + 2 \frac{M^{(B)} \phi_p^{(B)}}{\theta} + 2 \frac{V^{(B)} v_p^{(B)}}{\theta} \quad (2.68)$$

- for EBFs with inverted Y-scheme:

$$\alpha_Y^{(A)} \leq \alpha_Y^{(B)} \rightarrow 2 M^{(A)} \frac{h}{e} \leq \frac{2 M_b \phi_p^{(B)}}{\theta} + \frac{M^{(B)} \phi_p^{(B)}}{\theta} + \frac{V^{(B)} v_p^{(B)}}{\theta} \quad (2.69)$$

Rearranging these equations by using Eq. (2.15) for A-type mechanism and Eqs. (2.37) to (2.39) for B-type mechanism the following inequalities are provided:

$$\text{D-scheme} \quad V^{(A)} L \theta \leq V^{(B)} e \phi_p^{(B)} + v_p^{(B)} V^{(B)} \quad (2.70)$$

$$\text{V-scheme} \quad 2V^{(A)} L \theta \leq 2V^{(B)} e \phi_p^{(B)} + 2v_p^{(B)} V^{(B)} \quad (2.71)$$

$$\text{Inverted Y-scheme} \quad V^{(A)} h \theta \leq V^{(B)} e \phi_p^{(B)} + v_p^{(B)} V^{(B)} \quad (2.72)$$

and, by means of kinematic compatibility equations, they become:

$$\text{D-scheme and Y-scheme} \quad V^{(A)} \leq V^{(B)} \quad (2.73)$$

$$\text{Inverted V-scheme} \quad 2V^{(A)} \leq V^{(B)} \quad (2.74)$$

By substituting Eq. (2.37) and Eq. (2.41) into the design condition (2.73) the following relationship is obtained:

$$\frac{W}{e} \leq \frac{1}{e} \left( \frac{M_f \left( 1 - \frac{X}{M_f} \frac{M_w^2}{V_p^2 e^2} \right) + M_w \sqrt{1 - \frac{(M_f + X)^2}{V_p^2 e^2} + \frac{M_w^2}{V_p^2 e^2}}}{1 + \frac{M_w^2}{V_p^2 e^2}} + X \right) \quad (2.75)$$

where the terms  $X$  and  $W$  are equal to:

$$\text{D-scheme} \quad X = M_b + M_d \quad W = 2M^{(A)} \quad (2.76)$$

$$\text{V scheme} \quad X = M_b + M_d \quad W = 4M^{(A)} \quad (2.77)$$

$$\text{Inverted Y-scheme} \quad X = 2M_b \quad W = 2M^{(A)} \quad (2.78)$$

which, by introducing the non-dimensional parameters:

$$\bar{W} = \frac{W}{V_p e} \quad \bar{M}_f = \frac{M_f}{V_p e} \quad \bar{M}_w = \frac{M_w}{V_p e} \quad \bar{X} = \frac{X}{V_p e} \quad (2.79)$$

provides:

$$\bar{W}(1 + \bar{M}_w^2) - (\bar{M}_f + \bar{X}) \leq \bar{M}_w \sqrt{1 - (\bar{M}_f + \bar{X}) + \bar{M}_w^2} \quad (2.80)$$

The solution of the irrational inequality (2.80) leads to the following design conditions:

$$\left\{ \begin{array}{l} \bar{X} \leq \bar{M}_{X.lim.1} = \sqrt{1 + \bar{M}_w^2} - \bar{M}_f \\ \bar{X} \leq \bar{M}_{X.lim.2} = \bar{W}(1 + \bar{M}_w^2) - \bar{M}_f \\ \bar{M}_{X.lim.3} \leq \bar{X} \leq \bar{M}_{X.lim.4} \end{array} \right. \cup \left\{ \begin{array}{l} \bar{M}_X \leq \bar{M}_{X.lim.1} \\ \bar{M}_X > \bar{M}_{X.lim.2} \end{array} \right. \quad (2.81)$$

where  $\cup$  is the union symbol and:

$$\bar{M}_{X.lim.3} = (\bar{W} - \bar{M}_f) - \sqrt{1 + \bar{W}^2} \quad \bar{M}_{X.lim.4} = (\bar{W} - \bar{M}_f) + \sqrt{1 + \bar{W}^2} \quad (2.82)$$

Taking into account Eq. (2.9) and Eq. (2.15), it is easy to show that:

$$\bar{M}_{X.lim.3} = \bar{M}_A \quad \bar{M}_{X.lim.4} = 3\bar{M}_A - 2\bar{M}_f \quad (2.83)$$

In the same way, the design criterion to be applied to avoid C-type mechanism, which occurs only for inverted Y-scheme can be obtained by means of Eq. (2.59) and Eq. (2.61) by imposing the following requirement:

$$\alpha^{(A)} \leq \alpha^{(C)} \quad \rightarrow \quad V^{(A)} \leq V^{(C)} \quad (2.84)$$

which provides the limit value of the plastic moment of the diagonal braces by means of relationships formally coincident with equations (2.81), (2.82) and (2.83) where the parameter  $\bar{X}$  has to be substituted by the non-dimensional plastic moment of the diagonal brace:

$$\bar{X} = \frac{X}{V_p e} = \frac{2M_d}{V_p e} \quad (2.85)$$

Finally, the design criterion needed to avoid D-type mechanism requires the fulfilment of the following inequality generally expressed as:

$$\alpha^{(A)} \leq \alpha^{(D)} \quad (2.86)$$

that become both for EBFs with K-scheme and inverted Y-scheme:

$$\alpha_K^{(A)} \leq \alpha_K^{(D)} \text{ and } \alpha_Y^{(A)} \leq \alpha_Y^{(D)} \rightarrow M^{(A)} \leq M_b + M_d \quad (2.87)$$

## 2.5.2 Hierarchy Criteria for Long links

In case of long links, the plastic shear deformation  $v_p$  is equal to zero, so that the internal work corresponding to the possible kinematic mechanisms can be immediately derived.

In case of A-type mechanism (Figure 2.3), considering the compatibility equations (2.49) and (2.50), the internal work of the link can be expressed as:

$$W_{link}^{(A)} = W\gamma \quad (2.88)$$

being the bending  $W$  provided by Eqs. (2.76), (2.77) and (2.78) where the term  $M^{(A)}$  takes the meaning of plastic moment of the link, because there is no interaction with moment and shear for long links. Such consideration obviously is also valid for the other mechanism typologies depicted in Figure 2.3.

In order to avoid the undesired mechanisms, the kinematically admissible multiplier of the seismic horizontal force for A-Type mechanism has to be less than those corresponding to B-type, C-type and D-type mechanisms.

The internal virtual work for the kinematic mechanisms illustrated in Figure 2.3 is expressed by means of the following relationships for A-type mechanism:

$$W_{K.li}^{(A)} = W_{D.li}^{(A)} = 2M_p \theta \frac{L}{e} + 2M_c \theta \quad (2.89)$$

$$W_{V.li}^{(A)} = 4M_p \theta \frac{L}{e} + 2M_c \theta \quad (2.90)$$

$$W_{Y.li}^{(A)} = 2M_p \theta \frac{h}{e} + 2M_b \theta + 2M_c \theta \quad (2.91)$$

B-type mechanism:

$$W_{D.li}^{(B)} = 2M_c \theta + M_b \theta \frac{L}{e} + M_d \theta \frac{L}{e} + M_p \theta \frac{L}{e} \quad (2.92)$$

$$W_{V.li}^{(B)} = 2M_c \theta + 2M_b \theta \frac{L}{e} + 2M_d \theta \frac{L}{e} + 2M_p \theta \frac{L}{e} \quad (2.93)$$

$$W_{Y.li}^{(B)} = 2M_c \theta + 2M_b \theta + 2M_b \theta \frac{h}{e} + M_p \theta \frac{h}{e} \quad (2.94)$$

C-type mechanism:

$$W_{Y.li}^{(C)} = 2M_c \theta + 2M_b \theta + 2M_d \theta \frac{h}{e} + M_p \theta \frac{h}{e} \quad (2.95)$$

D-type mechanism:

$$W_{K.li}^{(A)} = 2M_b \theta \frac{L}{e} + 2M_d \theta \frac{L}{e} + 2M_c \theta \quad (2.96)$$

$$W_{Y.li}^{(A)} = 2M_c \theta + 2M_b \theta + 2M_b \theta \frac{h}{e} + 2M_b \theta \frac{h}{e} \quad (2.97)$$

Being the external virtual work still expressed by Eqs. (2.54) and (2.55), the kinematically admissible horizontal force multipliers corresponding to the different mechanisms are obtained by equating the internal work to the external work as follows:

▪ A-type mechanism:

$$\text{K-scheme} \quad \alpha_K^{(A)} = \frac{2M_p \frac{L}{e} + 2M_c}{Fh} \quad (2.98)$$

$$\text{D-scheme} \quad \alpha_D^{(A)} = \frac{2M_p \frac{L}{e} + 2M_c - q \frac{L(L-e)}{2}}{Fh} \quad (2.99)$$

$$\text{V-scheme} \quad \alpha_V^{(A)} = \frac{4M_p \frac{L}{e} + 2M_c}{Fh} \quad (2.100)$$

$$\text{Inverted Y-scheme} \quad \alpha_Y^{(A)} = \frac{2M_p \frac{h}{e} + 2M_b + 2M_c}{Fh} \quad (2.101)$$

▪ B-type mechanism:

$$\text{D-scheme} \quad \alpha_D^{(B)} = \frac{2M_c + M_b \frac{L}{e} + M_d \frac{L}{e} + M_p \frac{L}{e} - q \frac{L(L-e)}{2}}{Fh} \quad (2.102)$$

$$\text{V-scheme} \quad \alpha_V^{(B)} = \frac{2M_c + 2M_b \frac{L}{e} + 2M_d \frac{L}{e} + 2M_p \frac{L}{e}}{Fh} \quad (2.103)$$

$$\text{Inverted Y-scheme} \quad \alpha_Y^{(B)} = \frac{2M_c + 2M_b + 2M_b \frac{h}{e} + M_p \frac{h}{e}}{Fh} \quad (2.104)$$

- C-type mechanism:

$$\text{Inverted Y-scheme} \quad \alpha_Y^{(C)} = \frac{2M_c + 2M_b + 2M_d \frac{h}{e} + M_p \frac{h}{e}}{Fh} \quad (2.105)$$

- D-type mechanism:

$$\text{K-scheme} \quad \alpha_K^{(D)} = \frac{2M_b \frac{L}{e} + 2M_d \frac{L}{e} + 2M_c}{Fh} \quad (2.106)$$

$$\text{Inverted Y-scheme} \quad \alpha_Y^{(D)} = \frac{2M_c + 2M_b + 2M_b \frac{h}{e} + 2M_b \frac{h}{e}}{Fh} \quad (2.107)$$

The design criterion needed to avoid B-type mechanism requires the fulfilment of the following inequality generally expressed as:

$$\alpha^{(A)} \leq \alpha^{(B)} \quad (2.108)$$

which become:

- for EBFs with D-scheme:

$$\begin{aligned} \alpha_D^{(A)} \leq \alpha_D^{(B)} &\rightarrow 2M_p \frac{L}{e} + 2M_c - q \frac{L(L-e)}{2} \\ &\leq 2M_c + M_b \frac{L}{e} + M_d \frac{L}{e} + M_p \frac{L}{e} - q \frac{L(L-e)}{2} \end{aligned} \quad (2.109)$$

- for EBFs with inverted V-scheme:

$$\alpha_V^{(A)} \leq \alpha_V^{(B)} \rightarrow 4M_p \frac{L}{e} + 2M_c \leq 2M_c + 2M_b \frac{L}{e} + 2M_d \frac{L}{e} + 2M_p \frac{L}{e} \quad (2.110)$$

- for EBFs with inverted Y-scheme:

$$\alpha_Y^{(A)} \leq \alpha_Y^{(B)} \rightarrow 2M_p \frac{h}{e} + 2M_b + 2M_c \leq 2M_c + 2M_b + 2M_b \frac{h}{e} + M_p \frac{h}{e} \quad (2.111)$$

Rearranging these equations, the following design conditions are provided:

$$\text{D-scheme} \quad M_p \leq M_b + M_d \quad (2.112)$$

$$\text{V-scheme} \quad M_p \leq M_b + M_d \quad (2.113)$$

$$\text{Inverted Y-scheme} \quad M_p \leq 2M_b \quad (2.114)$$

In the same way, the design criterion to be applied to avoid C-type mechanism, which occurs only for inverted Y-scheme can be obtained by means of Eq. (2.101) and Eq. (2.105) by imposing the following requirement:

$$\alpha_Y^{(A)} \leq \alpha_Y^{(B)} \rightarrow 2M_p \frac{h}{e} + 2M_b + 2M_c \leq 2M_c + 2M_b + 2M_d \frac{h}{e} + M_p \frac{h}{e} \quad (2.115)$$

Eq. (2.115), being rearranged become:

$$\text{Inverted Y-scheme} \quad M_p \leq 2M_d \quad (2.116)$$

Finally, the design criterion needed to avoid D-type mechanism requires the fulfilment of the following inequality generally expressed as:

$$\alpha^{(A)} \leq \alpha^{(D)} \quad (2.117)$$

which become both for EBFs with K-scheme and inverted Y-scheme:

$$\alpha_K^{(A)} \leq \alpha_K^{(D)} \text{ and } \alpha_Y^{(A)} \leq \alpha_Y^{(D)} \rightarrow M_p \leq M_b + M_d \quad (2.118)$$

### 2.5.3 Hierarchy Criteria for Short Links

In case of short links, the interaction between shear and bending moment is negligible as depicted in Figure 2.3, so that they are subjected to plastic shear deformation  $v_p$  only, being  $\phi_p$  equal to zero according to the normal plastic flow rule. As a consequence, the internal work of short links in case of A-type mechanism is given by (Figure 2.3):

$$W_{s.link}^{(A)} = V_p \gamma e = V_p \theta h \quad (2.119)$$

In case of short links, B-type mechanism and C-type mechanism cannot develop, because the link ends are not subjected to plastic rotations, so that, due to compatibility requirements, both the beam ends at the link-to-beam connection and the top ends of diagonals are not subjected to plastic rotations. In other words, with reference to Figure 2.3, the plastic rotation  $\phi_p$  required for B-type and C-type mechanisms is equal to zero. Therefore, in case of short links, only A-type and D-Type mechanisms can be developed. In D-type mechanism  $v_p$  is equal to zero, so that the internal work of the link is equal to zero and the compatibility requirement is given by Eqs. (2.49) and (2.50). The conditions to avoid D-type mechanism for short link has to be applied for EBFs with K-scheme and Y-scheme only. The internal virtual work is, for A-type mechanism, given by:



$$W_{K.s.i}^{(A)} = 2M_c\theta + V_p\theta L \quad (2.120)$$

$$W_{Y.li}^{(A)} = 2M_c\theta + 2M_b\theta + V_p\theta h \quad (2.121)$$

while for D-type mechanism is given by:

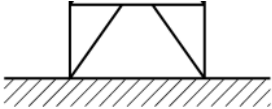
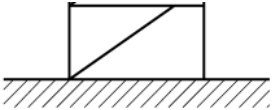
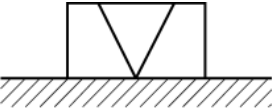
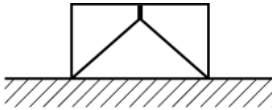
$$W_{K.s.i}^{(D)} = 2M_c\theta + 2M_b\theta \frac{L}{e} + 2M_d\theta \frac{L}{e} \quad (2.122)$$

$$W_{Y.li}^{(D)} = 2M_c\theta + 2M_b\theta + 2M_b\theta \frac{h}{e} + 2M_d\theta \frac{h}{e} \quad (2.123)$$

Considering the external work provided by Eq. (2.55), the application of the kinematic theorem of plastic collapse (Eq. (2.117)) leads to the following design criterion to be satisfied to avoid the undesired D-type mechanism:

$$\alpha_K^{(A)} \leq \alpha_K^{(D)} \text{ and } \alpha_Y^{(A)} \leq \alpha_Y^{(D)} \rightarrow \frac{V_p e}{2} \leq M_b + M_d \quad (2.124)$$

**Table 2.1** – Design conditions to avoid undesired mechanisms

EBFs configuration	Short link $e \leq 1.6 \frac{M_p}{V_p}$	Intermediate link $1.6 \frac{M_p}{V_p} \leq e \leq 3 \frac{M_p}{V_p}$	Long link $e \geq 3 \frac{M_p}{V_p}$
	$\frac{V_p e}{2} \leq M_b + M_d$	$M^{(A)} \leq M_b + M_d$	$M_p \leq M_b + M_d$
	No condition	$V^{(A)} \leq V^{(B)}$	$M_p \leq M_b + M_d$
	No condition	$2V^{(A)} \leq V^{(B)}$	$M_p \leq M_b + M_d$
	$\frac{V_p e}{2} \leq M_b + M_d$	$V^{(A)} \leq V^{(B)}$ $V^{(A)} \leq V^{(C)}$ $M^{(A)} \leq M_b + M_d$	$M_p \leq 2M_b$ $M_p \leq 2M_d$ $M_p \leq M_b + M_d$

Finally a summary of all the design conditions needed to avoid partial mechanism such as B-type, C-type and D-type are reported in Table 2.1 where  $M^{(A)}$  and  $V^{(A)}$  are provided by Eqs. (2.16) and (2.17), respectively while  $M_p$  and  $V_p$  are the link plastic moment and the link plastic shear.

Therefore, the hierarchy criteria derived in Table 2.1 have to be applied by making reference to the ultimate domain rather than to the plastic domain of the link. To this scope, a non-homothetic expansion of the plastic domain considering an ultimate value of the bending moment is obtained by means of an overstrength factor equal to 1.20 while the ultimate shear is obtained by means of an overstrength factor equal to 1.50. As soon as such expansion of the plastic domain is carried out to obtain the ultimate domain, all the relationships reported in Table 2.1 remain valid provided that reference is made to the ultimate values of  $M$  and  $V$ .

## 2.6 Validation and numerical examples

Aiming at the validation of the derived hierarchy criteria, with particular attention paid to the case of intermediate links where moment-shear interaction is of primary importance, the obtained design criteria have been applied to a one-storey EB-Frame with inverted Y-scheme. The inelastic behaviour of the designed structure has been successively examined by means of a push-over analysis, aimed to check the fulfilment of the design goal, i.e. the achievement of A-type mechanism.

The vertical link is constituted by an HEB200 profile made of S235 steel grade ( $f_{yk} = 235 \text{ MPa}$ ). Regarding the link classification, reference is made to Eurocode 8 [11] where links are classified as short links when the following condition occurs:

$$e \leq 1.6 \frac{M_{p.link}}{V_{p.link}} \quad (2.125)$$

where  $M_{p.link} = M_f = b_f t_f f_y (d - t_f)$  and  $V_{p.link} = V_p = (d - 2t_f)t_w f_y / \sqrt{3}$ .

It is useful to note that due to strain-hardening the flexural overstrength is about 20% while the shear overstrength is about 50%, so that due to link equilibrium requirement, the condition corresponding to the balance point of the ultimate domain provides [56]:

$$e = 2.0 \frac{M_u}{V_u} = 2.0 \frac{1.20 M_{p.link}}{1.50 V_{p.link}} = 1.6 \frac{M_{p.link}}{V_{p.link}} \quad (2.126)$$

Therefore, the ultimate moment-shear domain to be consistent with link classification needs to be obtained by a non-homothetic expansion starting from Neal plastic domain [49]. Such non-homothetic expansion is depicted in Figure 2.6 with reference to an HEB200 profile made of S235 steel grade, i.e. the link section. BPP is the balance point of the plastic domain while BPU is the balance point of the ultimate domain.

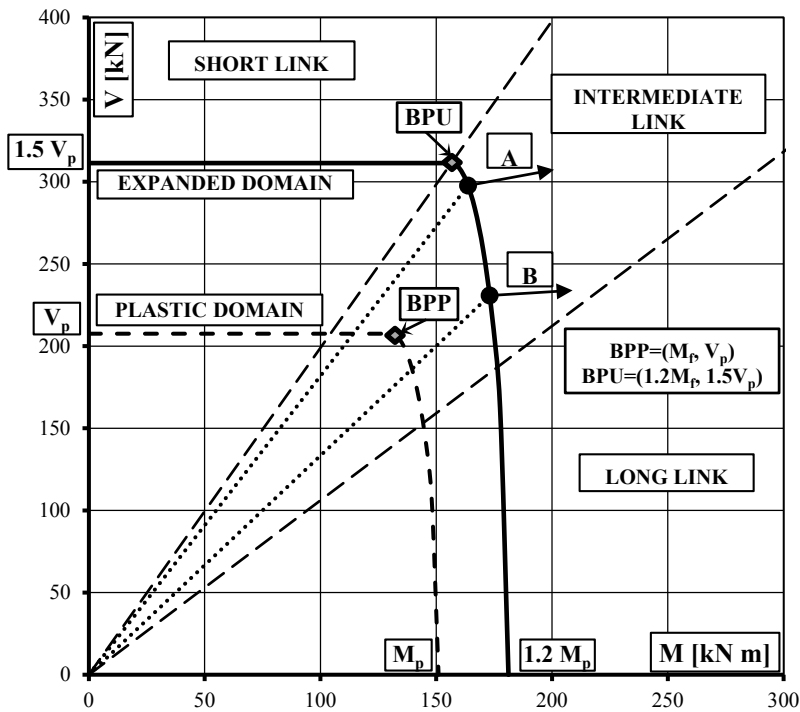


Figure 2.6 – Modelling of link moment-shear interaction for rigid-plastic analysis

The limit value provided by Eq. (2.87) for the above link section is equal to 1.005 m. Therefore, in order to validate the derived hierarchy criteria with particular reference to the case of intermediate links, i.e. the case where code provisions are not consistent with rigorous plastic design theory, two cases are

analysed, namely “Case A” and “Case B”. In “Case A” reference is made to an intermediate link whose length is equal to 1.10 m, i.e. very close to the short link range; conversely, in “Case B” reference is made to an intermediate link whose length is equal to 1.50 m. In both cases, reference is made to the structural scheme depicted in Figure 2.7. The bay span is  $L = 6.0\text{ m}$ , the interstorey height is  $h = 3.5\text{ m}$ .

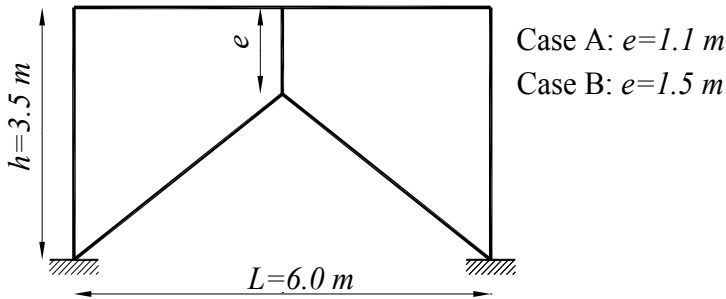


Figure 2.7 – Analysed scheme

As already underlined, overstrength plays a paramount role in the application of capacity design principles, because non-dissipative zones have to be designed considering the maximum internal actions that yielded and strain-hardened dissipative zones are able to transmit. Therefore, the hierarchy criteria derived have to be applied by making reference to the ultimate domain rather than to the plastic domain of the link.

With reference to the analysed cases, the application of the relationships given in Table 2.1 for intermediate links provides the values given in Table 2.2. The points A and B corresponding to the attainment of the ultimate conditions, for “Case A” and “Case B” respectively, are also given on the ultimate domain shown in Figure 2.6, where also the plastic deformation vectors according to the normal flow rule are depicted.

The  $M_b$  value required to avoid undesired mechanisms is derived according to Eq. (2.81) with reference to the notation reported in Eq. (2.78). With reference to “Case A” the limit values of  $\bar{M}_b$  are given in Table 1, so that the solution of the system of inequalities corresponding to the left hand side of Eq. (2.80) is  $0.239 \leq \bar{M}_b \leq 0.252$  while the solution for the right hand side is  $0.252 \leq \bar{M}_b \leq 0.273$ . Therefore, the union of the two solutions provides  $0.239 \leq \bar{M}_b \leq 0.273$ . As a

consequence, the minimum flexural resistance required to the beam to satisfy hierarchy criteria is  $M_b = \bar{M}_b V_p e = 0.239 \times 342.52 = 81.87 \text{ kNm}$ , given the needed substitutions.

Similarly, in "Case B", the minimum flexural resistance required to satisfy hierarchy criteria is obtained, being equal to  $86.54 \text{ kNm}$  (Table 2.2).

The limit value of the plastic moment of diagonal braces required to avoid C-type mechanism is coincident with the limit value of  $M_b$  given in Table 2.2, but from the design point of view it has to be remembered that it is a plastic moment reduced due to the contemporary action of the axial force. This axial force can easily be evaluated starting from the knowledge of the shear action  $V^{(A)}$  transmitted by the link which is equilibrated by the axial forces of the diagonal braces in tension and compression.

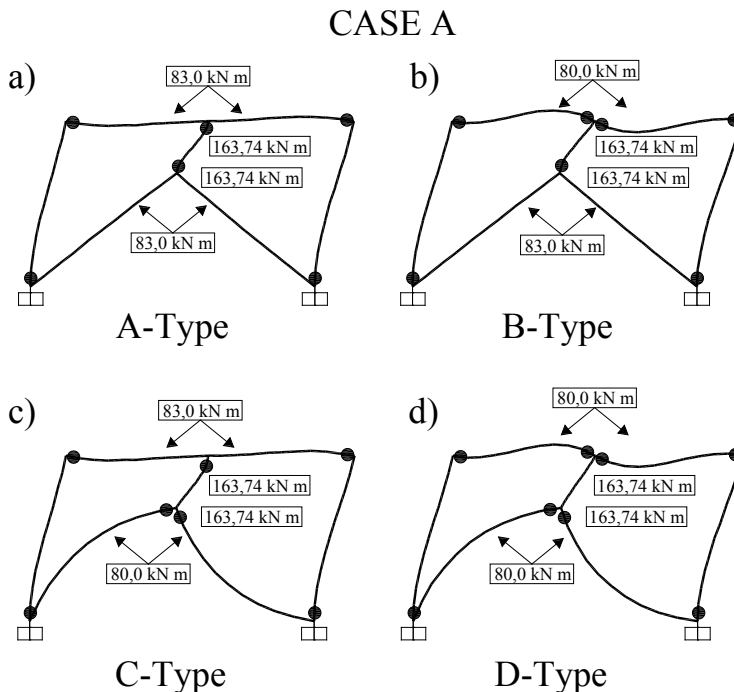


**Figure 2.8** - Analysed structures for "Case A"

Finally, regarding the column sections, they are dimensioned by assuring the fulfilment of the following requirement:

$$M_c \geq M_b \quad (2.127)$$

where  $M_c$  is the plastic moment of columns. Column sections HEB200 have been adopted for the structure depicted in Figure 2.7.

In order to assess the accuracy of the hierarchy criteria previously explained, a variety of structural solutions for the scheme depicted in Figure 2.7 has been examined by means of static pushover analyses with SAP2000 computer program [57]. Each examined structural solution has been selected in order to obtain a predetermined pattern of yielding. With reference to the beam and the diagonal braces, structural sections having predefined values of the plastic moment rather than standard shapes have been used to provide a more robust check of the expected results, i.e. in order to avoid possible beneficial effects coming from overstrength due to standard shape selection.

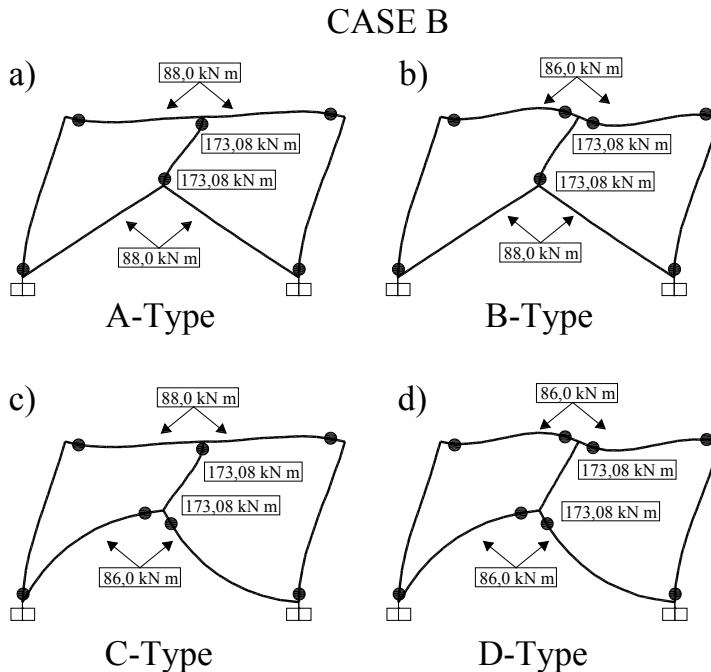
The first examined structure (a) (Figure 2.8a for “Case A” and Figure 2.9a for “Case B”) is characterized by beams and diagonal braces whose plastic moment just exceeds the limit value delivered in Table 2.2. Therefore, structure (a) fails according to A-type mechanism.

The second structure (b) is characterized by diagonal sections whose plastic moment just exceeds the limit value given in Table 2.2 (Figure 2.8b for “Case A” and Figure 2.9b for “Case B”) while beam sections are characterized by a plastic moment just below the limit provided in Table 2.2. Therefore, structure (b) fails according to B-type mechanism.

The third structure (c) is characterized by diagonal sections whose plastic moment is just below the limit value given in Table 2.2 (Figure 2.8c for “Case A” and Figure 2.9c for “Case B”) while beam sections are characterized by a plastic moment just exceeding the limit provided in Table 2.2. Therefore, structure (c) fails according to C-type mechanism.

Finally, in case of diagonal and beam sections whose plastic moment is just below the limit value given in Table 2.2 (Figure 2.8d for “Case A” and Figure 2.9d for “Case B”) D-type mechanism, i.e. (d) structures, occurs. Therefore, all the collapse mechanisms resulting from push-over analyses confirm the prediction coming from the formulations preliminarily discussed.

In all the examined cases, as SAP2000 [57] does not allow to define a moment-shear interaction domain, the link has been modelled by means of a beam-column element with plastic hinges at its ends whose plastic moment is equal to the equivalent plastic moment previously defined. In other words, the plastic hinge properties are characterised by a plastic moment equal to  $M^{(A)}$  so that the corresponding internal work can be simply expressed as  $W_{link} = 2M^{(A)}\gamma = 2M_{p,eq}\gamma$ , where  $M^{(A)}$  accounts for moment-shear interaction. As a further assessment of the accuracy of the suggested hierarchy criteria, it has been checked that the value of the corresponding shear is less than  $V^{(A)}$  when no hinges are developed. The value of  $V^{(A)}$  is also delivered in Table 2.2.



The obtained results are pointed out in the same Figure 2.8 and Figure 2.9 where the deformed configurations for a top sway displacement assuring the complete development of a kinematic mechanism are depicted for all the analysed cases. The moments at the member ends used to design the different

schemes are also shown. The obtained patterns of yielding confirm the accuracy of the proposed design procedure. In fact, by respecting design relationships in Table 2.1 A-type mechanism is assured; conversely, if one or more of such design conditions are not satisfied, undesired collapse mechanisms develop (B-type, C-type or D-type).

**Table 2.2** - Results of moment-shear interaction and hierarchy criteria

	Case A (e=1.10 m)	Case B (e=1.50 m)		Case A (e=1.10 m)	Case B (e=1.50 m)
$M^{(A)}$ (kNm)	163.74	173.08	$\bar{M}_{X.lim.1}$	0.273	0.333
$V^{(A)}$ (kN)	297.72	230.78	$\bar{M}_{X.lim.2}$	0.252	0.204
$\theta$ (rad)	0.04	0.04	$\bar{M}_{X.lim.3}$	0.239	0.185
$\phi_p^{(A)}$ (rad)	0.0866	0.0836	$\bar{M}_{X.lim.4}$	0.260	0.221
$v_p^{(A)}$ (m)	0.0224	0.0073	$\bar{M}_b$	0.239	0.185
$V_u e$ (kNm)	342.52	467.07	$M_b$ (kNm)	81.87	86.54

It has also been checked that the developed pattern of yielding is compatible with the local ductility supply. Obviously, as soon as the kinematic mechanism is completely developed, the ultimate lateral displacement is dependent on the plastic rotation supply of members.

## 2.7 Summary notes

In this chapter, a rigorous treatment of moment-shear interaction occurring in intermediate links of EB-Frames has been reported. The whole analysis has been carried out within the framework of rigid-plastic design by exploiting the plastic domain, the normal flow rule, the kinematic compatibility requirements and the kinematic theorem of plastic collapse. Therefore, the derived hierarchy criteria are characterised by the robustness of their theoretical background.

In particular, analytical formulations for evaluating the internal actions and the plastic deformations of intermediate links have been derived and appropriate hierarchy criteria to avoid undesired collapse mechanisms have been established.

From the design point of view, the influence of the strain-hardening leading to link overstrength can be properly accounted for by means of an appropriate



expansion of the plastic domain. The derived theoretical formulations remain valid both in case of homothetic and in case of non-homothetic expansions of the plastic domain, needed to define an appropriate ultimate domain.

The obtained results are needed for a theoretically consistent application of capacity design principles for seismic design of EB-Frames. In addition, the obtained results are propaedeutic to the development of a design procedure for failure mode control of multi-storey MRF-EBF dual systems reported in Chapter 4. It means that the final purpose of the presented work is the setting up of a rigorous design procedure assuring the attainment of a collapse mechanism of global type, i.e. characterized by the yielding of the links and of the beam ends at all the storeys, while all the diagonal braces and the columns remain in elastic range, with the only exception of base sections of first storey columns.

Finally, within the above framework, from the design point of view, it is useful to underline that if the interaction between bending moment and shear is neglected in the application of local hierarchy criteria devoted to the design of beams and diagonal braces, a safe side solution can be obtained considering, in every case, an ultimate shear force equal to  $1.5 V_p$  and an ultimate bending moment equal to  $1.2 M_p$ , but both beams and diagonal braces are oversized. As a consequence, more severe design conditions are obtained, in case of multi-storey structures, regarding the column sections required to prevent partial collapse mechanisms. This general oversizing can lead to uneconomical solutions for EB-Frames with intermediate links.



# CHAPTER 3

## THEORY OF PLASTIC MECHANISM CONTROL (TPMC): STATE OF THE ART AND NEW ADVANCES

### 3.1 Introduction

In this Chapter the state of the art and the important improvement leading to a closed form solution for the Theory of Plastic Mechanism Control (TPMC) are reported. In particular, reference is made to MR-Frames which constitute the most simple structural typology and also the first one TPMC has been applied. The reasonings reported in this chapter are of paramount importance for the comprehension of the following chapters, where TPMC is presented for MRF-EBF dual systems.

As it is known, a fundamental principle of capacity design of MR-Frames is that plastic hinge formation in columns during an earthquake should be avoided, in order to make sure that the seismic energy is dissipated by the beams only. Therefore, the optimisation of the energy dissipation capacity of structures is achieved when a collapse mechanism of global type develops [1-3].

In order to decrease the probability of plastic hinge formation in columns, MR-Frames must be designed to have strong columns and weak beams. To this scope, different simplified design criteria have been proposed [4-10] and the so-called beam-column hierarchy criterion has been introduced in Eurocode 8 [11].

However, Eurocode 8 is able to avoid only soft storey mechanism but it does not assure the development of a collapse mechanism of global type. There are a

number of reasons why the beam-column hierarchy criterion cannot achieve the above mentioned design goal and these have been widely discussed in Chapter 1 but, probably the most important and difficult to be accounted for in a simplified design approach, is the shifting of the contraflexure point in columns during the seismic excitation. This considerable shifting leads to a bending moment distribution substantially different from that resulting from code-prescribed design rules [11]. The shift of the contraflexure point is caused by the formation of hinges in beams adjacent to the column and even in part of the columns. All these factors alter the stiffness of beam-column subassemblage, hence the moment distribution.

The main reason why the above issue cannot be accounted for by means of a simplified design rule, such as the beam-column hierarchy criterion, is that the second principle of capacity design cannot be easily applied in case of multiple resisting mechanisms not located in series. In fact, according to the second principle of capacity design, non-dissipative zones (i.e. the columns in case of MR-Frames) need to be designed considering the maximum internal actions which the dissipative zones (i.e. the beam ends in case of MR-Frames) are able to transmit at their ultimate conditions.

For this reason, a rigorous design procedure, based on the kinematic theorem of plastic collapse, has been presented in 1997 [17], aiming to guarantee a collapse mechanism of global type where plastic hinges develop at the beam ends only, while all the columns remain in elastic range. Obviously, exception is made for base section of first storey columns, leading to a kinematic mechanism. Starting from this first work, TPCM has been outlined as a useful tool for the seismic design of steel structures. It consists on the extension of the kinematic theorem of plastic collapse to the concept of mechanism equilibrium curve. In fact, for any given structural typology, the design conditions to be applied in order to prevent undesired collapse mechanisms can be derived by imposing that the mechanism equilibrium curve corresponding to the global mechanism has to be located below those corresponding to all the other undesired mechanisms up to a top sway displacement level compatible with the local ductility supply of dissipative zones.

The problem of failure mode control aiming to assure a strong column-weak beam seismic behaviour has been also faced by Lee and Goel [31] with reference to moment-resisting frames. The proposed design procedure is aimed not only

to assure a pre-selected yield mechanism, but also to assure a given target drift within the framework of performance based design. To this scope the authors preliminarily provide the design base shear as a function of the target plastic drift by exploiting the energy balance equation following an approach originally developed by Leelataviwat et al. [58], but introducing an energy modification factor accounting for the relationship between the ductility factor and the force reduction factor [59]. Moreover, the design procedure suggested by Goel and his co-authors is also characterised by a new distribution of lateral design forces that is based on relative distribution of maximum storey shears consistent with inelastic dynamic results [60], [61]. Therefore, the main components of such design methodology are the determination of design base shear, lateral force distribution and plastic design. The method [31] has been successively extended to the design of eccentrically braced frames [40] and to the case of special truss moment frames [62].

Starting from the above background, in this chapter new advances in the application of the Theory of Plastic Mechanism Control are reported. In particular, by means of new considerations regarding collapse mechanism typologies, a closed form solution has been found. The design conditions to be satisfied to prevent undesired collapse mechanisms can now be solved without any iterative procedure, so that the unknown of the design problem, i.e. column sections at each storey, can now be directly derived. The extreme simplicity of the resulting design procedure will be emphasised by means of a worked example aiming to show its practical application which can now be carried out even by means of hand calculations. In addition, static inelastic analysis (push-over analysis) and incremental dynamic analyses are successively carried out to compare the actual inelastic behaviour of the designed frame with the design goal. Despite the detailed comparison between TPMC and the design methodology suggested by Goel et al. [31] is out of the scope of this work.

### 3.2 Theory of Plastic Mechanism Control

The theory of plastic mechanism control, originally proposed by Mazzolani and Piluso [17], is based on the upper bound theorem of plastic collapse extended to the concept of mechanism equilibrium curve. Before then, rigid-plastic analysis was used only for the computation of the collapse load multiplier of structures completely defined from the mechanical point of view, i.e. already

designed structures whose load carrying capacity was under investigation. Conversely, thanks to TPMC rigid-plastic analysis was for the first time recognised as a useful tool for seismic design of structures.

In particular, TPMC allows the theoretical solution of the problem of designing a structure failing in global mode, i.e. assuring that plastic hinges develop only at beam ends while all the columns remain in elastic range with the only exception of base sections at first storey columns. The beam sections are assumed to be known quantities, because they are preliminarily designed to withstand vertical loads according to the non-seismic load combination, or to withstand the design value of the seismic horizontal forces while the unknowns of the design problem are the column sections needed to assure the desired collapse mechanism, i.e. the global mechanism.

To this scope, TPMC is based on the kinematic or upper bound theorem of plastic collapse within the framework of limit analysis. According to the theory of limit analysis, the assumption of a rigid-plastic behaviour of the structure until the complete development of a collapse mechanism is made. It means that the attention is focused on the condition the structure exhibits in the collapse state by neglecting each intermediate condition. Given the above, it is possible to recognise three main collapse mechanism typologies the structure is able to exhibit. These mechanisms, depicted in Figure 3.1, have to be considered undesired, because they do not involve all the dissipative zones. The global mechanism, representing the design goal, is a particular case of type-2 mechanism involving all the storeys.

However, the simple application of the kinematic theorem of plastic collapse is not sufficient to assure the desired collapse mechanism, because high horizontal displacements occur before the complete development of the kinematic mechanism. These displacements give rise to significant second order effects which cannot be neglected in the seismic design of structures, particularly in case of moment-resisting steel frames. Therefore, the basic principle of TPMC is essentially constituted by the extension of the kinematic theorem of plastic collapse to the concept of mechanism equilibrium curve.

Within the framework of a kinematic approach, for any given collapse mechanism, the mechanism equilibrium curve can be easily derived by equating the external work to the internal work due to the plastic hinges involved in the

collapse mechanism, provided that the external second-order work due to vertical loads is also evaluated [17].

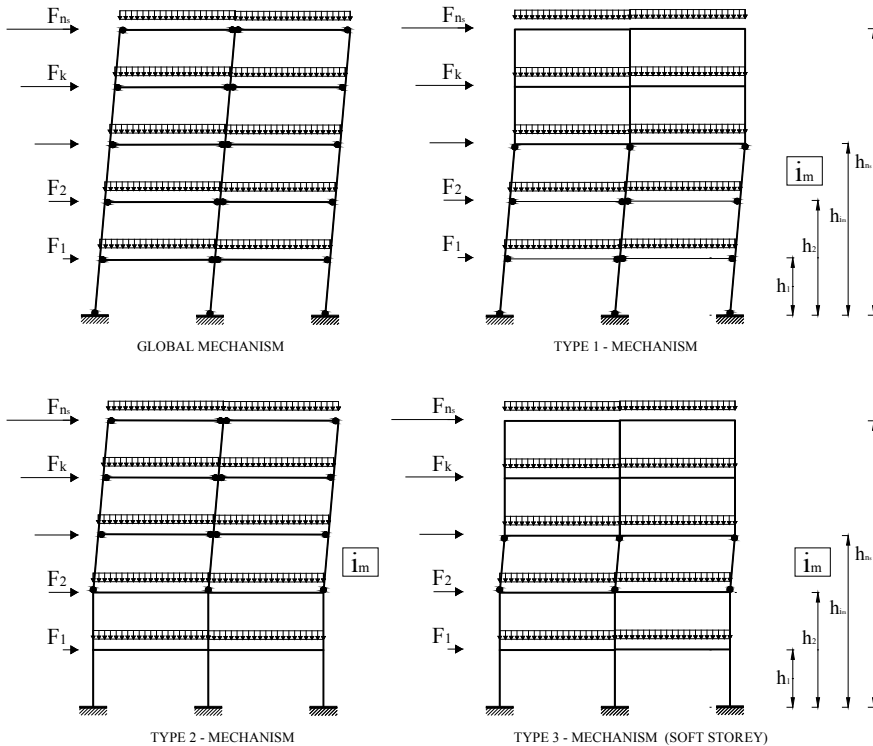


Figure 3.1 – Collapse mechanism of MR-Frames

In the following, for sake of simplicity, reference is made to the case of uniform vertical loads acting on the beams satisfying the limitation [17]:

$$q_{jk} \leq \frac{4 M_{b,jk}}{l_j^2} \quad (3.1)$$

where  $q_{jk}$  is the uniform vertical load applied to the beam of  $j$ -th bay and  $k$ -th storey,  $M_{b,jk}$  is the corresponding beam plastic moment and  $l_j$  is the  $j$ -th bay span. Such limitation assures that beam plastic hinges develop at the beam ends. It can be demonstrated [17] that in case of vertical loads exceeding the above limit the

second plastic hinge in the beam develops in an intermediate section, so that the external work due to the uniform vertical loads has also to be considered.

As an example, in case of global mechanism the external work due to a virtual rotation  $d\theta$  of columns plastic hinges is given by:

$$W_e = \alpha \sum_{k=1}^{n_s} F_k h_k d\theta + \frac{\delta}{h_{n_s}} \sum_{k=1}^{n_s} V_k h_k d\theta \quad (3.2)$$

where  $\alpha$  is the multiplier of horizontal forces,  $F_k$  and  $h_k$  are, respectively, the seismic force applied at k-th storey and the k-th storey height with respect to the foundation level,  $h_{n_s}$  is the value of  $h_k$  at the top storey,  $\delta$  is the top sway displacement and  $V_k$  is the total vertical load acting at k-th storey.

The first term of Eq. (3.2) represents the external work due to seismic horizontal forces, while the second term is the second order work due to vertical loads. In order to compute the slope of the mechanism equilibrium curve, it is necessary to evaluate the second-order work due to vertical loads. With reference to Figure 3.2, it can be observed that the horizontal displacement of the k-th storey involved in the generic mechanism is given by  $u_k = r_k \sin\theta$ , where  $r_k$  is the distance of the k-th storey from the centre of rotation C and  $\theta$  the angle of rotation. The top sway displacement is given by  $\delta = h_{n_s} \sin\theta$ .

The relationship between vertical and horizontal virtual displacements is given by  $dv_k \tan\theta \approx du_k \sin\theta$ . It shows that, as the ratio  $dv_k / du_k$  is independent of the storey, vertical and horizontal virtual displacement vectors have the same shape. In fact, the virtual horizontal displacements are given by  $du_k = r_k \cos\theta d\theta \approx r_k d\theta$ , where  $r_k$  defines the shape of the virtual horizontal displacement vector, while the virtual vertical displacements are given by  $dv_k = \frac{\delta}{h_{n_s}} r_k d\theta$  and, therefore, they have the same shape  $r_k$  of the horizontal ones. It can be concluded that:

$$dv_k = \frac{\delta}{h_{n_s}} h_k d\theta \quad (3.3)$$

where  $dv_k$  is the vertical virtual displacement occurring at k-th storey.

The internal work due to a virtual rotation  $d\theta$  of column plastic hinges is:

$$W_i = \left( \sum_{k=1}^{n_c} M_{c,i1} + 2 \sum_{k=1}^{n_s} \sum_{j=1}^{n_b} M_{b,jk} \right) d\theta \quad (3.4)$$



where  $M_{c,ik}$  is the plastic moment of  $i$ -th column of  $k$ -th storey reduced due to the contemporary action of the axial force;  $n_c$ ,  $n_b$  and  $n_s$  are the number of columns, bays and storeys, respectively.

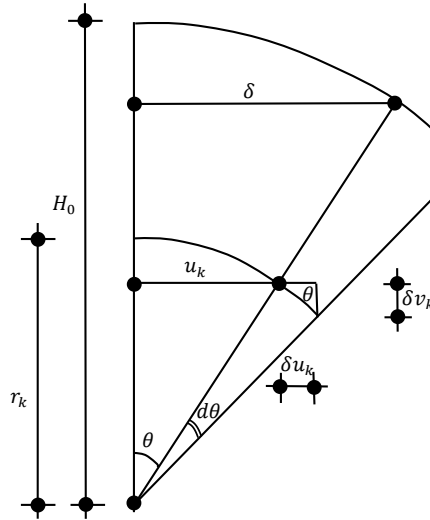


Figure 3.2 – Second order vertical displacements

By equating the internal work to the external one, the following relationship is obtained:

$$\alpha = \frac{\sum_{k=1}^{n_c} M_{c,i1} + 2 \sum_{k=1}^{n_s} \sum_{j=1}^{n_b} M_{b,jk}}{\sum_{k=1}^{n_s} F_k h_k} - \frac{1}{h_{n_s}} \frac{\sum_{k=1}^{n_s} V_k h_k}{\sum_{k=1}^{n_s} F_k h_k} \delta \quad (3.5)$$

From this equation, it is immediately recognized that the mechanism equilibrium curve is a straight line which can be generally expressed in the form:

$$\alpha = \alpha_0 - \gamma \delta \quad (3.6)$$

where  $\alpha_0$  is the kinematically admissible multiplier of horizontal forces according to first order rigid-plastic analysis and  $\gamma$  is the slope of the mechanism equilibrium curve [17].

In the case of global type mechanism, as shown in Figure 3.1, kinematically admissible multiplier of horizontal forces is:

$$\alpha_0^{(g)} = \frac{\sum_{i=1}^{n_c} M_{c.i1} + 2 \sum_{k=1}^{n_s} \sum_{j=1}^{n_b} M_{b.jk}}{\sum_{k=1}^{n_s} F_k h_k} \quad (3.7)$$

Regarding the slope  $\gamma^{(g)}$  of the mechanism equilibrium curve, it is given by:

$$\gamma^{(g)} = \frac{1 \sum_{k=1}^{n_s} V_k h_k}{h_{n_s} \sum_{k=1}^{n_s} F_k h_k} \quad (3.8)$$

The parameters of the mechanism equilibrium curves for type-1, type-2 and type-3 mechanism typologies are derived in a similar way.

With reference to  $i_m$ th mechanism of type-1, the kinematically admissible multiplier of seismic horizontal forces, for  $i_m = 1$ , is given by:

$$\alpha_{0.1}^{(1)} = \frac{2 \sum_{i=1}^{n_c} M_{c.i1}}{h_1 \sum_{k=1}^{n_s} F_k} \quad (3.9)$$

and, for  $i_m > 1$ , is given by:

$$\alpha_{i_m}^{(1)} = \frac{\sum_{i=1}^{n_c} M_{c.i1} + 2 \sum_{k=1}^{i_m-1} \sum_{j=1}^{n_b} M_{b.jk} + \sum_{i=1}^{n_c} M_{c.ii_m}}{\sum_{k=1}^{i_m} F_k h_k + h_{i_m} \sum_{k=i_m+1}^{n_s} F_k} \quad (3.10)$$

while the slope of the mechanism equilibrium curve is [17]:

$$\gamma_{i_m}^{(1)} = \frac{1 \sum_{k=1}^{i_m} V_k h_k + h_{i_m} \sum_{k=i_m+1}^{n_s} V_k}{h_{i_m} \sum_{k=1}^{i_m} F_k h_k + h_{i_m} \sum_{k=i_m+1}^{n_s} F_k} \quad (3.11)$$

With reference to  $i_m$ th mechanism of type-2, the kinematically admissible multiplier of seismic horizontal forces is given by:

$$\alpha_{0.i_m}^{(2)} = \frac{\sum_{i=1}^{n_c} M_{c.i.i_m} + 2 \sum_{k=i_m}^{n_s} \sum_{j=1}^{n_b} M_{b.jk}}{\sum_{k=i_m}^{n_s} F_k (h_k - h_{i_m-1})} \quad (3.12)$$

while the slope of the mechanism equilibrium curve is [17]:

$$\gamma_{i_m}^{(2)} = \frac{1 \sum_{k=i_m}^{n_s} V_k (h_k - h_{i_m-1})}{h_{n_s} - h_{i_m-1} \sum_{k=i_m}^{n_s} F_k (h_k - h_{i_m-1})} \quad (3.13)$$

It is useful to note that, for  $i_m=1$  Eq. (3.12) and Eq. (3.13) are coincident with Eq. (3.7) and (3.8), respectively, because in such case the mechanism is coincident with the global one.

Finally, with reference to  $i_m$ th mechanism of type-3, the kinematically admissible multiplier of horizontal forces, for  $i_m = 1$ , is given by:

$$\alpha_{0.1}^{(3)} = \frac{2 \sum_{i=1}^{n_c} M_{c.i1}}{h_1 \sum_{k=1}^{n_s} F_k} \quad (3.14)$$

and, for  $i_m > 1$ , is given by:

$$\alpha_{0.i_m}^{(3)} = \frac{2 \sum_{i=1}^{n_c} M_{c.ii_m}}{(h_{i_m} - h_{i_m-1}) \sum_{k=i_m}^{n_s} F_k} \quad (3.15)$$

In addition, the corresponding slope of the mechanism equilibrium curve is given by [17]:

$$\gamma_{i_m}^{(3)} = \frac{1}{h_{i_m} - h_{i_m-1}} \frac{\sum_{k=i_m}^{n_s} V_k}{\sum_{k=i_m}^{n_s} F_k} \quad (3.16)$$

It is important to underline that, for any given geometry of the structural system, the slope of mechanism equilibrium curve attains its minimum value when the global type mechanism is developed [2]. This issue assumes a paramount importance in TPMC exploiting the extension of the kinematic theorem of plastic collapse to the concept of mechanism equilibrium curve.

In fact, according to the kinematic theorem of plastic collapse, extended to the concept of mechanism equilibrium curve, the design conditions to be fulfilled in order to avoid all the undesired collapse mechanisms require that the mechanism equilibrium curve corresponding to the global mechanism has to be located below those corresponding to all the undesired mechanisms within a top sway displacement range,  $\delta_u$ , compatible with the ductility supply of structural members ([17]):

$$\alpha_0^{(g)} - \gamma^{(g)} \delta_u \leq \alpha_{i_m}^{(t)} - \gamma_{i_m}^{(t)} \delta_u \quad \text{for } i_m = 1, 2, 3, \dots, n_s \quad t = 1, 2, 3 \quad (3.17)$$

Eq. (3.17) constitutes the statement of the theory of plastic mechanism control and it is valid independently of the structural typology. This is the reason why TPMC has been applied with success to MR-Frames, EB-Frames, knee braced frames, MRF-CBF dual systems and dissipative truss-moment frames. Therefore, TPMC really constitutes a general approach to the seismic design of structures aiming to the control of the collapse mechanism. The robustness of the theory is founded on the kinematic theorem of plastic collapse and on second-order rigid-plastic analysis.

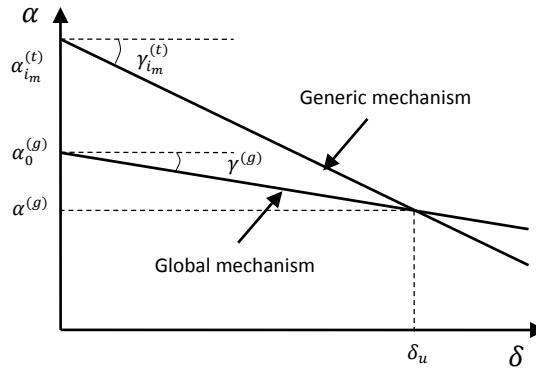


**Figure 3.3** - Design conditions

Conversely, hierarchy criteria commonly suggested in modern seismic codes often do not exhibit any sound theoretical basis. As an example, the beam-column hierarchy criterion, suggested for the column design of MR-Frames, is merely based on the joint equilibrium occurring when the beam ends are yielded and strain-hardened up to their ultimate limit state, but no information can be theoretically derived about the distribution of bending moments between the columns converging in the joint. As a consequence, beam-column hierarchy criterion can only be an approximate application of the second principle of capacity design.

### 3.3 Closed Form Solution

As already stated, TPMC was originally developed in nineties, so that the design conditions given by Eq. (3.17) do not constitute any new. However, aiming to the solution of the set of inequalities, the original procedure was iterative, so that the application of TPMC required the development of specific computer programs. The advances presented in this work are based on new observations leading to a closed form solution of Eq. (3.17). The resulting design procedure is now easier and well suited even for hand calculations.

In particular, the solution is obtained according to the following steps:

- a) Selection of a design top sway displacement  $\delta_u$  compatible with the ductility supply of structural members. To this scope, in the following,

the plastic rotation capacity of beams is assumed equal to 0.04 rad so that  $\delta_u = 0.04 h_{ns}$  where  $h_{ns}$  is the height of the structure.

- b) Computation of the slopes of mechanism equilibrium curves  $\gamma_{i_m}^{(t)}$  by means of Eqs. (3.11), (3.13) and (3.16). The slope of the global mechanism equilibrium curve,  $\gamma^{(g)}$ , is provided by Eq. (3.8) and it is the minimum among the  $\gamma_{i_m}^{(t)}$  values computed before.
- c) Computation of the axial load acting in the columns at collapse state, i.e. when a collapse mechanism of global type is completely developed.
- d) This step, probably the most important, consists in the design of beam sections and of first storey columns. To this scope two cases can be identified. The first case occurs when the moment resisting frame is orthogonal to the secondary beams of the building decks, so that the beams are subjected to significant vertical loads. In such a case, the preliminary design of beams can be simply carried out by properly estimating the maximum bending moment occurring in the non-seismic load combination. In such a case (high gravity loads), the required sum of plastic moment of columns, reduced due to the contemporary action of the axial force,  $\sum_{i=1}^{n_c} M_{c,i1}$ , for  $i_m = 1$ , i.e. at the first storey, is computed by means of the following relation:

$$\sum_{i=1}^{n_c} M_{c,i1} \geq \frac{2 \sum_{k=1}^{n_s} \sum_{j=1}^{n_b} M_{b,jk} + (\gamma_1^{(3)} - \gamma^{(g)}) \delta_u \sum_{k=1}^{n_s} F_k h_k}{2 \frac{\sum_{k=1}^{n_s} F_k h_k}{h_1 \sum_{k=1}^{n_s} F_k} - 1} \quad (3.18)$$

Equation (3.18) is derived from design conditions (3.17) for  $i_m = 1$  and  $t = 1$  or  $t = 3$ , because for  $i_m = 1$  type-1 mechanism and type-3 mechanism are coincident as depicted in Figure 3.4. Furthermore, it is important to underline that, for  $i_m = 1$ , type 2 mechanism is coincident with the global mechanism so that Eq. (3.17), for  $i_m = 1$  and  $t = 2$  becomes an identity. The above observations are of paramount importance from the practical point of view, because they allow to design first storey columns directly by means of Eq. (3.18) and to avoid any iterative procedure leading to a closed form solution easy to be applied by hand calculations.

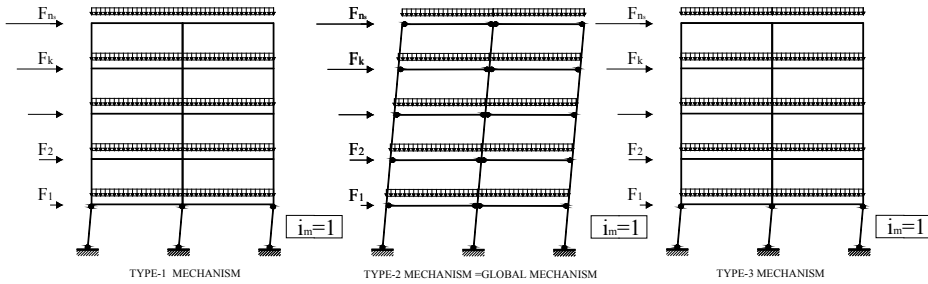


**Figure 3.4** - Collapse mechanism of MR-Frames for  $i_m = 1$

The second case occurs when the moment resisting frame is parallel to the secondary beams of the decks. In such a case, being the tributary area for the gravity loads small, the simple design of beams for vertical loads only would lead to beam sections too small which could be not sufficient to withstand the seismic load combination in elastic range and/or to allow for drift limitation as required for serviceability limit states. In this second case, according to [31] it is desirable to have the distribution of the beam flexural strength along the building height that follows the distribution of the design storey shears, i.e.  $M_{b,jk} = \beta_k M_{b,jn_s}$  where  $\beta_k$  is the ratio between the design seismic shear at k-th storey and the design seismic shear at the top storey. By means of this design choice, the equilibrium equation under the design horizontal forces can be expressed in the following form:

$$\sum_{k=1}^{n_s} F_k h_k + \sum_{k=1}^{n_s} V_k h_k \frac{\delta_y}{h_{n_s}} = \sum_{i=1}^{n_c} M_{c.i.1} + 2 \sum_{k=1}^{n_s} \beta_k M_{b.jn_s} \quad (3.19)$$

where  $\delta_y$  is the top sway displacement corresponding to the estimated first yielding drift (a value  $\theta_y = \delta_y/h_{n_s} = 0.01$  rad can be generally assumed). Similarly, Eq. (3.18) can be rearranged in the following form:

$$\sum_{i=1}^{n_c} M_{c.i.1} \geq \frac{2 \sum_{k=1}^{n_s} \beta_k M_{b.jn_s} + (\gamma_1^{(3)} - \gamma^{(g)}) \delta_u \sum_{k=1}^{n_s} F_k h_k}{\frac{2 \sum_{k=1}^{n_s} F_k h_k}{h_1 \sum_{k=1}^{n_s} F_k} - 1} \quad (3.20)$$

Therefore, combining Eq. (3.19) and Eq. (3.20) both the sum of the reduced plastic moments of first storey columns (i.e.  $\sum_{i=1}^{n_c} M_{c.i.1}$ ) and the

sum of the plastic moment of top storey beams (i.e.  $\sum_{i=1}^{n_c} M_{b,jn_s}$ ) can be designed. As a consequence, the beam plastic moment of the other storey are derived as:  $M_{b,jk} = \beta_k M_{b,jn_s}$ .

It is useful to underline that, despite this procedure is similar to the one suggested by Goel et al. [31] two important differences can be identified. First of all, Eq. (3.19) accounts for second order effects occurring at the estimated yield drift level. In addition, second order effects occurring when the ultimate design displacement is reached are explicitly and rigorously accounted for by a kinematic approach leading to Eq. (3.20).

- e) The sum of the required plastic moments of columns at first storey is distributed among the columns proportionally to the axial load acting at the collapse state, so that, the design internal actions ( $M_{c,i1}, N_{c,i1}$  for  $i = 1, 2, \dots, n_c$ ) are derived and the column sections at first storey can be designed. As column sections are selected from standard shapes, the value obtained of  $\sum_{i=1}^{n_c} M_{c,i1}$ , namely  $\sum_{i=1}^{n_c} M_{c,i1}^*$  is generally greater than the required minimum value provided by Eq. (3.18). Therefore, the mechanism equilibrium curve  $\alpha = \alpha_0^{(g)} - \gamma^{(g)} \delta$  has to be evaluated accordingly, i.e. by means of Eq. (3.20) by replacing the term  $\sum_{i=1}^{n_c} M_{c,i1}$ , with the value  $\sum_{i=1}^{n_c} M_{c,i1}^*$  resulting from standard shapes. In addition, the multiplier of seismic horizontal forces corresponding to the ultimate design displacement can be computed as  $\alpha^{(g)} = \alpha_0^{(g)} - \gamma^{(g)} \delta_u$  (Figure 3.3).
- f) Computation of the required sum of plastic moment of columns, reduced due to the contemporary action of the axial force,  $\sum_{i=1}^{n_c} M_{c,ii_m}^{(t)}$  for  $i_m > 1$  and  $t = 1, 2, 3$  by means of the following relations:

$$\sum_{i=1}^{n_c} M_{c,ii_m}^{(1)} \geq (\alpha^{(g)} + \gamma_{i_m}^{(1)} \delta_u) \left( \sum_{k=1}^{i_m} F_k h_k + h_{i_m} \sum_{k=i_m+1}^{n_s} F_k \right) - \sum_{i=1}^{n_c} M_{c,i1}^* - 2 \sum_{k=1}^{i_m-1} \sum_{j=1}^{n_b} M_{b,jk} \quad (3.21)$$

needed to avoid type-1 mechanisms;

$$\sum_{i=1}^{n_c} M_{c.ii_m}^{(2)} \geq (\alpha^{(g)} + \gamma_{i_m}^{(2)} \delta_u) \sum_{k=i_m}^{n_s} F_k (h_k - h_{i_m-1}) - 2 \sum_{k=i_m}^{n_s} \sum_{j=1}^{n_b} M_{b.jk} \quad (3.22)$$

needed to avoid type-2 mechanisms;

$$\sum_{i=1}^{n_c} M_{c.ii_m}^{(3)} \geq (\alpha^{(g)} + \gamma_{i_m}^{(3)} \delta_u) \frac{(h_{i_m} - h_{i_m-1})}{2} \sum_{k=i_m}^{n_s} F_k \quad (3.23)$$

needed to avoid type-3 mechanisms.

Eq. (3.21), (3.22) and (3.23) have been directly derived from Eq. (3.17) for  $i_m > 1$  and  $t = 1$ ,  $t = 2$  and  $t = 3$ , respectively.

- g) Computation of the required sum of the reduced plastic moments of columns for each storey as the maximum value among those coming from the above design conditions:

$$\sum_{i=1}^{n_c} M_{c.ii_m} = \max \left\{ \sum_{i=1}^{n_c} M_{c.ii_m}^{(1)}, \sum_{i=1}^{n_c} M_{c.ii_m}^{(2)}, \sum_{i=1}^{n_c} M_{c.ii_m}^{(3)} \right\} \quad (3.24)$$

- h) The sum of the required plastic moment of columns at each storey, reduced for the contemporary action of the axial force, is distributed among all the storey columns, proportionally to the axial force acting at collapse state. The knowledge of these plastic moments  $M_{c.ii_m}$ , coupled with the axial force  $N_{c.ii_m}$  at the collapse state, allows the design of column sections from standard shapes.
- i) If necessary, a technological condition is imposed by requiring, starting from the base, that the column sections cannot increase along the building height. If this condition requires the change of column sections at first storey then the procedure needs to be repeated from point e). In fact, in this case, a new value of  $\sum_{i=1}^{n_c} M_{c.i1}^*$  is obtained and, as a consequence, the value of the sum of the required plastic moments of columns at each storey (Eq. (3.24)) changes. It is important to underline that the possibility of a revision of column sections is due to their selection from standard shapes while the theory provides a closed form solution. In order to avoid any revision of the column sections and to minimise the column sections at upper storeys, the use of dog-bones at the base of first storey columns can be suggested. This choice has two



advantages, because, on one hand, it allows to fix the value of  $\sum_{i=1}^{n_c} M_{c,i1}$  satisfying Eq. (3.20) by equality and, on the other hand, can promote the safeguard of column base connections making easier their design.

It is important to underline that TPMC is aimed at the control of the collapse mechanism, being devoted to the seismic design of structures against the ultimate limit state requirements. However, as far as the member of storeys increase, the lateral stiffness requirements needed to fulfil serviceability limit state requirements could impose the use of bigger sections.

In order to design structures failing in a global mode, but also satisfying such damage limitation, an iterative design procedure can be applied [66]. It consists in repeating the proposed design methodology for failure mode control by assuming increased sections of beams (strategy 1). In such case (strategy 1), because of the increase in beam resistance (i.e. the increase in the internal work due to the beams), in order to guarantee the development of a global mechanism, column sections are required, so that also the lateral stiffness increases. Obviously, by increasing beam and column sections, a considerable increase in construction steel weight is also obtained.

As an alternative (strategy 2) the design value of the ultimate top sway displacement can be increased. In such a case, because of increased second order effects, the fulfilment of the design requirements expressed by Eq. (3.17) leads to a further increase of column sections and, as a consequence, to the increase of the lateral stiffness as needed to satisfy serviceability limit states.

### 3.4 Worked example

In order to present in detail the practical application of TPMC, the seismic design of a six-bay five-storey moment resisting frame is shown. The inelastic behaviour of the designed structure is successively examined by means of both static and dynamic non-linear analyses, confirming the fulfilment of the design goal, i.e. the achievement of a collapse mechanism of global type and pointing out the excellent seismic performance obtained.

The structural scheme of the frame to be designed is shown in Fig. 4. The bay span is equal to 6.5 m; the interstorey height is equal to 3.20 m. For sake of simplicity, a structural scheme where the beam sections are governed by gravity loads is examined. The characteristic values of the vertical loads acting on the beams are equal to 15 and 10 kN/m for permanent ( $G_k$ ) and live ( $Q_k$ ) actions, respectively. The structural material adopted for the structure is steel grade S275.

According to Eurocode 8 [11], the value of the period of vibration to be used for preliminary design is:

$$T = 0.085 H^{3/4} = 0.085 \times 16^{3/4} \approx 0.68 \text{ s} \quad (3.25)$$

where  $H$  is the total height of the frame.

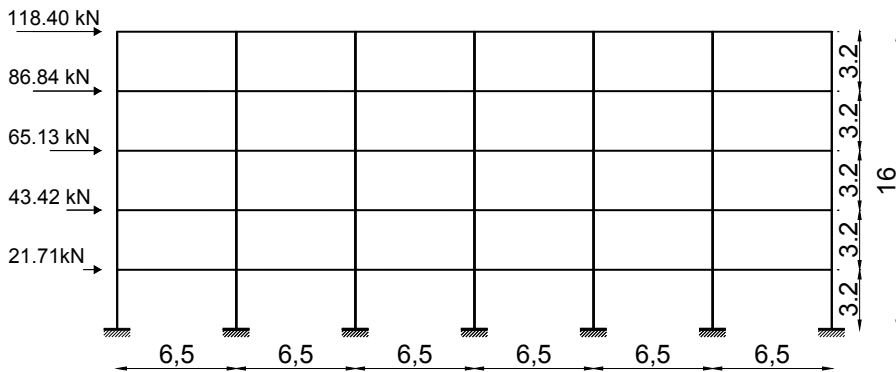


**Figure 3.5** - Structural scheme of the example frame (dimension in m)

With reference to the design spectrum for stiff soil conditions (soil class A of Eurocode 8) and by assuming a behaviour factor  $q$  equal to 6 the horizontal seismic forces are those depicted in Figure 3.5 corresponding to a design base shear equal to 335.5 kN. Despite the worked example herein presented is developed with reference to the seismic force distribution provided by Eurocode 8, it is useful to underline that TPMC can be applied to any seismic force distribution. In the following, the numerical development of the design steps for the structural scheme described above is provided.

**a) Selection of the design top sway displacement**

The selection of the maximum top sway displacement up to which the global mechanism has to be assured is a very important design issue, because the value of this displacement governs the magnitude of second order effects accounted for in the design procedure. In addition, the complete development of the collapse mechanism could be prevented by the occurrence of a plastic rotation demand exceeding the local ductility supply. Therefore, a good criterion to choose the design ultimate displacement  $\delta_u$  is to relate it to the plastic rotation supply of beams or beam-to-column connections by assuming  $\delta_u = \theta_u h_{n_s}$  (where  $\theta_u$  is the plastic rotation supply, considered in this case equal to 0.04 rad). As a consequence, the design value of the top sway displacement has been assumed equal to:

$$\delta_u = 0.04 h_{n_s} = 0.04 \cdot 16 = 0.64 \text{ m} \quad (3.26)$$

**b) Computation of the slopes of mechanism equilibrium curve  $\gamma_{i_m}^{(t)}$**

By means of Eqs. (3.11), (3.13) and (3.16) the slopes of mechanism equilibrium curves are computed. These values are reported in Table 3.1. The slope value corresponding to the global mechanism,  $\gamma^{(g)}$  is the minimum among all the  $\gamma_{i_m}^{(t)}$  values:

$$\gamma^{(g)} = 0.005293 \text{ cm}^{-1} \quad (3.27)$$

**Table 3.1-** Slopes of mechanism equilibrium curves ( $\text{cm}^{-1}$ )

STOREY $i_m$	$\gamma_{i_m}^{(1)}$	$\gamma_{i_m}^{(2)}$	$\gamma_{i_m}^{(3)}$
1	0.0327	0.0053	0.0327
2	0.0152	0.0060	0.0280
3	0.0095	0.0074	0.0243
4	0.0068	0.0102	0.0214
5	0.0053	0.0185	0.0185

*c) Computation of the axial load acting at collapse state in the columns*

In agreement with the global mechanism, axial forces in the columns at collapse state depend both on distributed loads acting on the beams and on the shear action coming from the development of plastic hinges at the beam ends, as depicted in Figure 3.6. So that, the total load transmitted by the beams to the columns is the sum of two contributions. The first one,  $N_q$ , is related to the vertical loads acting in the seismic load combination (i.e. the sum of  $ql/2$  type contributions). The second one,  $N_f$ , is related to the shear actions due to the plastic hinges developed at the beams ends (i.e. the sum of  $2M_{b,jk}/l$  type contributions).

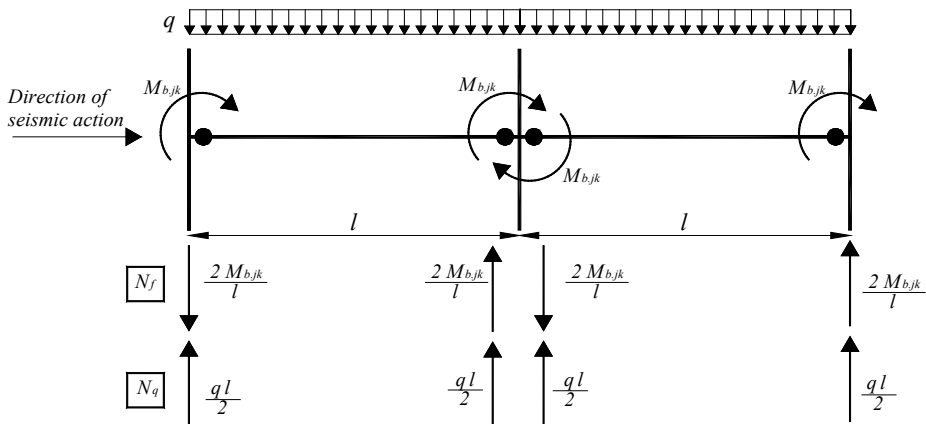


**Figure 3.6** - Loads transmitted by the beams to the columns at collapse state

However, seismic actions can be acting either in the positive direction or in the negative direction, so that the maximum axial forces has to be considered.

In Table 3.2 the two contributions,  $N_q$  and  $N_f$  and the total value,  $N_{totr}$ , of the axial force are reported for each storey both for internal columns and for external columns.

**Table 3.2** - Axial forces acting at collapse state in the columns

STOREY	External columns			Internal columns			
	$i_m$	$N_q$ (kN)	$N_f$ (kN)	$N_{tot}$ (kN)	$N_q$ (kN)	$N_f$ (kN)	$N_{tot}$ (kN)
1		292.500	369.310	661.810	585.000	0	585.000
2		234.000	295.440	529.440	468.000	0	468.000
3		175.500	221.580	397.080	351.000	0	351.000
4		117.000	147.720	264.720	234.000	0	234.000
5		58.500	73.860	132.360	117.000	0	117.000

**d) Design of beam sections and overall flexural resistance of first storey columns**

The combination of actions corresponding to the frame subjected to vertical loads only is:

$$q_v = 1.3 G_k + 1.5 Q_k = 34.5 \text{ kN/m} \quad (3.28)$$

Therefore, in order to withstand such uniform vertical load an IPE300 section is adopted for the beams.

With reference to the seismic design situation, corresponding to the combination of actions,  $G_k + \psi_2 Q_k + E_d$ , the uniform vertical load acting on the beams is ( $\psi_2 = 0.3$  for residential buildings):

$$q = 15 + 0.3 \times 10 = 18 \text{ kN/m} \quad (3.29)$$

The average plastic resistance of beams is:

$$M_{b,m} = W_{pl} f_{ym} = (628.4 \times 10^{-6})(310.66 \times 10^3) = 195.2 \text{ kNm} \quad (3.30)$$

where  $W_{pl}$  is the plastic modulus and  $f_{ym}$  is the average yield stress whose value is assumed equal to 310.66 MPa for S275 steel grade. Therefore, the limit value of the uniform vertical load is:

$$q_{lim} = \frac{4M_{b,m}}{L^2} = \frac{4 \times 195.2}{(6.50)^2} \approx 18.48 \text{ kN/m} \quad (3.31)$$

With reference to the seismic design situation, this limit value is not exceeded; therefore, plastic hinges develop at the beam ends.

Moreover, it is important to underline that according to the second principle of capacity design non-dissipative members, i.e. the column sections, have to be designed considering the maximum internal action which the dissipative zones, i.e. the beam sections, are able to transmit in their fully yielded and strain-hardened state. Therefore, the amount of strain-hardening which the beams are able to develop up to the complete development of local buckling has been computed according to the formulation given in [11] accounting for flange and web slenderness. As a result, in case of an IPE300 beam, made of S275 steel grade, the overstrength factor due to strain-hardening is equal to 1.23. As a consequence the ultimate average resistance of beams,  $M_b$ , to be applied in the application of TPMC, is equal to  $1.23 \times 195.2 = 240 \text{ kNm}$ .

Regarding the design of first storey columns, i.e. the sum of the reduced plastic moments  $\sum_{i=1}^{n_c} M_{c.i1}$ , as the beam sections are governed by gravity loads, so that they are immediately dimensioned (Eqs. (3.28-3.31)), Eq. (3.18) can be directly applied. In the examined case, Eq. (3.18) provides a value of  $\sum_{i=1}^{n_c} M_{c.i1}$  equal to 3334.5 kNm and has to be distributed among the columns proportionally to the total axial force acting at collapse state.

#### e) *Design of first storey columns*

As already stated, the overall flexural resistance,  $\sum_{i=1}^{n_c} M_{c.i1}$ , of first storey columns obtained at the end of step c) has to be distributed among the different columns proportionally to the axial forces obtained in step d). Therefore, the bending moment required for each column,  $M_{req.c.i1}$ , the plastic modulus required,  $W_{pl.req}$ , the plastic modulus obtained,  $W_{pl.obt}$ , the profile selected and the bending resistance obtained for internal and external column,  $M_{obt.c.i1}$ , are reported in Table 3.

As reported in Table 3.3 the selected profile of first storey columns are HE300B for internal columns and HE320B for external columns so that, the sum of column plastic moments obtained at first storey,  $\sum_{i=1}^{n_c} M_{c.i1}^*$ , is:

$$\sum_{i=1}^{n_c} M_{c.i1}^* = 3637.93 \text{ kNm} \quad (3.32)$$

which is greater than the required one because of the column selection from the standard shapes. In addition, the value of  $\alpha^{(g)}$  is provided, by replacing  $\sum_{i=1}^{n_c} M_{c.i1}^*$  with  $\sum_{i=1}^{n_c} M_{c.i1}$ , by Eq. (3.5) with  $\delta = \delta_u$ :

$$\alpha^{(g)} = \alpha_0^{(g)} - \gamma^{(g)} \delta_u = \frac{\sum_{i=1}^{n_c} M_{c.i1}^* + 2 \sum_{k=1}^{n_s} \sum_{j=1}^{n_b} M_{b.jk}}{\sum_{k=1}^{n_s} F_k h_k} - \gamma^{(g)} \delta_u \quad (3.33)$$

$$= 4.1917$$

so that, the multiplier of seismic horizontal forces corresponding to the ultimate displacement is now a known quantity.

**Table 3.3** - Design of the column sections at first storey

	$N_{tot}$ (kN)	$M_{req.c.i1}$ (kN m)	$W_{pl.req}$ (cm <sup>3</sup> )	$W_{pl.obt}$ (cm <sup>3</sup> )	PROFILE	$M_{obt.c.i1}$ (kN m)
External columns	661.810	519.4	1887.5	2149.0	HE 320 B	570.6
Internal columns	585.000	459.1	1683.2	1869.0	HE 300 B	499.3

- f) *Computation of the sum of plastic moment of columns, reduced due to the contemporary action of the axial load,  $\sum_{i=1}^{n_c} M_{c.i1}^{(t)}$ , required at any storey to avoid undesired mechanisms.*

**Table 3.4** - Sum of reduced plastic moment of columns required at each storey to avoid undesired mechanisms

STOREY $i_m$	$\sum_{i=1}^{n_c} M_{c.i1}^{(1)}$ (kN m)	$\sum_{i=1}^{n_c} M_{c.i1}^{(2)}$ (kN m)	$\sum_{i=1}^{n_c} M_{c.i1}^{(3)}$ (kN m)
1	<u>3621.93</u>	[-]	3621.93
2	<u>4225.43</u>	1778.31	3001.87
3	<u>4746.65</u>	225.73	2486.19
4	<u>4394.74</u>	-744.77	1824.99
5	<u>2878.68</u>	-842.15	1018.27

The sum of plastic moments of columns, reduced due to the contemporary action of axial loads, required at each storey to prevent undesired collapse mechanisms is computed by means of Eqs. (21-23). The values obtained are delivered in Table 3.4.

*g) Computation of the maximum value of  $\sum_{i=1}^{n_c} M_{c.ii_m}$ .*

The sum of the plastic moment of columns governing the column design at each storey is given in Table 3.4 by the underlined values. It can be recognized that, in the examined case, the need to avoid type-1 mechanisms always governs the design of columns.

*h) Design of column sections at each storey*

The required sum of column plastic moments reduced due to the contemporary action of the axial load  $M_{req.c.ii_m}$ , the plastic modulus required,  $W_{pl.req}$  and obtained  $W_{pl.obt}$ , the standard shapes selected and the plastic moment obtained  $M_{obt.c.ii_m}$  are given in Table 3.5.

**Table 3.5 - Design of column sections at each storey**

STOREY $i_m$	$N_{tot}$ (kN)	$M_{req.c.ii_m}$ (kN m)	$W_{pl.req}$ (cm <sup>3</sup> )	$W_{pl.obt}$ (cm <sup>3</sup> )	PROFILE	$M_{obt.c.ii_m}$ (kN m)	
2°	External columns	529.440	658.0266	2392.82	3232	HE 400 B	888.8000
	Internal columns	468.000	581.8745	2115.91	2408	HE 340 B	662.2000
3°	External columns	397.080	739.1963	2687.99	3232	HE 400 B	888.8000
	Internal columns	351.000	653.6506	2376.91	2408	HE 340 B	662.2000
4°	External columns	264.720	684.3944	2488.71	2683	HE 400 B	737.8250
	Internal columns	234.000	605.1908	2200.69	2408	HE 340 B	662.2000
5°	External columns	132.360	448.2971	1630.17	1869	HE 300 B	513.9750
	Internal columns	117.000	396.4166	1441.51	1534	HE 280 B	421.8500



*i) Checking of technological condition*

As the column sections obtained at the first storey are smaller than those required at some storeys above, the technological condition occurs, so that the column sections at first storey are revised by using HE340B standard shapes. As a consequence, the value of  $\sum_{i=1}^{n_c} M_{c,i1}^*$  needs to be updated, being now equal to 5081.45 kNm and the procedure needs to be repeated from step e). The new results are reported in Table 3.6 and Table 3.7. The resulting mechanism equilibrium curve is now  $\alpha = 4.8973 - 0.005293\delta$ .

**Table 3.6** - *Sum of reduced plastic moment of column required at each storey to avoid undesired mechanisms*

STOREY $i_m$	$\sum_{i=1}^{n_c} M_{c,i i_m}^{(1)}$ (kN m)	$\sum_{i=1}^{n_c} M_{c,i i_m}^{(2)}$ (kN m)	$\sum_{i=1}^{n_c} M_{c,i i_m}^{(3)}$ (kN m)
1	<u>5044.64</u>	0.00	5044.64
2	<u>3545.70</u>	2817.11	3181.40
3	<u>4376.30</u>	905.46	2640.88
4	<u>4259.26</u>	-374.43	1942.42
5	<u>2878.68</u>	-706.66	1086.01

It is important to note that column sections at 4<sup>th</sup> storey are now different from those initially reported in Table 3.5. In particular, for internal columns, HE320B in place of HE340B sections, while, for external columns, HE360B in place of HE340B has been selected (Table 3.7). This apparently weird situation occurs because, by increasing the sum of column plastic moments at first storey, the sum of required column plastic moments for  $i_m > 1$  is affected by the increase of the first right hand side term of Eq. (3.21) and the increase of the subtracting second term at right hand side of Eq. (3.21).

Finally, it is useful to underline that, in the examined case, the elastic structural analysis carried out to check serviceability requirements has pointed out that the designed structure fulfil also the corresponding drift limitation required by Eurocode 8. Therefore, there is no any need for iterating the design procedure by increasing the beam sections or the design ultimate displacement.

**Table 3.7 - Design of column sections at each storey**

STOREY $i_m$	$N_{tot}$ (kN)	$M_{req.c.i.i_m}$ (kN m)	$W_{pl.req}$ (cm <sup>3</sup> )	$W_{pl.obt}$ (cm <sup>3</sup> )	PROFILE	$M_{obt.c.i.i_m}$ (kN m)	
1°	External columns	661.810	519.0571	1887	3232	HE 400 B	589.5
	Internal columns	585.000	458.9877	1669	2408	HE 340 B	592.2
2°	External columns	529.440	552.1726	2478	2683	HE 360 B	602.0
	Internal columns	468.000	488.2708	2191	2408	HE 340 B	602.0
3°	External columns	397.080	681.5228	2478	2683	HE 360 B	602.0
	Internal columns	351.000	602.6515	2191	2408	HE 340 B	602.0
4°	External columns	264.720	663.2952	2411	2683	HE 360 B	602.0
	Internal columns	234.000	586.5334	2132	2149	HE 320 B	537.2
5°	External columns	132.360	448.2971	1630	1869	HE 300 B	383.5
	Internal columns	117.000	396.4165	1441	1534	HE 280 B	383.5

### 3.5 Validation of the design procedure for MR-Frames

In order to validate the design procedure, both static non linear analysis (push-over) and incremental dynamic non-linear analyses have been carried out, by means of SAP 2000 computer program [57], to investigate the actual seismic response of the designed frame. These analyses have the primary aim to confirm the development of the desired collapse mechanism typology and to evaluate the obtained energy dissipation capacity, testing the accuracy of the proposed design methodology.

Regarding the structural modelling, all the members are modelled by means of beam-column elements, whose mechanical non-linearities have been concentrated at their ends by means of plastic hinge elements. In particular, beam plastic hinges are based on the cyclic envelope depicted in Table 3.7 according to FEMA 356 [52] with strength degradation modelled following the suggestions

given in [67] and the amount of strain hardening evaluated as a function of flange and web slenderness according to the formulation given in [11]. Conversely, column plastic hinges account also for the interaction between axial force and bending moment.

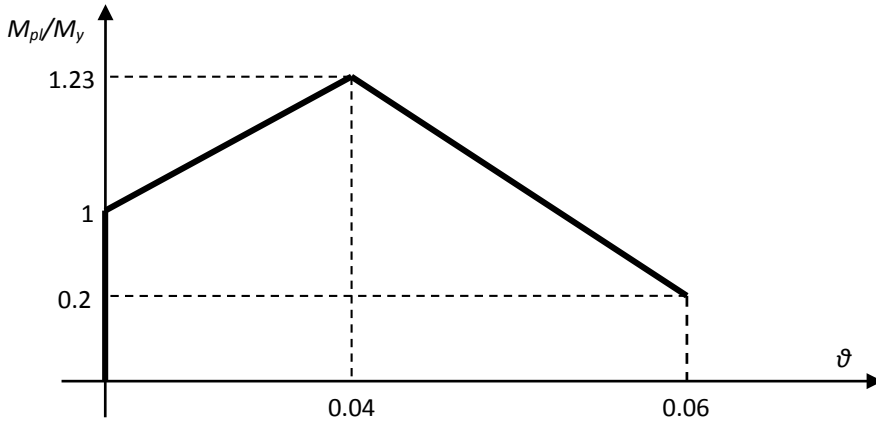


**Figure 3.7** - Cyclic envelope of rigid plastic hinge elements adopted in structural modelling

The push-over analysis has been led under displacement control taking into account both geometrical and mechanical non-linearities. The results of the push-over analysis are mainly constituted by the frame capacity curve. In Figure 3.8 the push-over curve is provided with reference to two different structural models, the first one is based on the use of simple rigid-perfectly plastic hinges while the second one refers to the hinge modelling according to Figure 3.7. The purpose of the push-over curve based on rigid-perfectly plastic hinges is to provide a better comparison with the mechanism equilibrium curve derived by means of rigid-plastic analysis. Therefore, in the same figure, also two straight lines are given: the first one corresponding to the linear elastic analysis and the second one corresponding to the linearised mechanism equilibrium curve whose expression, for the designed frame, is:

$$\alpha = 4.8973 - 0.005293 \delta \quad (3.34)$$

Obviously, the base shear depicted in Figure 3.8 is, in this case, obtained by multiplying the value of  $\alpha$ , by the design base shear corresponding to  $\alpha = 1$ . Such design base shear, as already stated, is equal to 335.5 kN. Figure 3.8 points out that the first yield base shear is equal to about 800 kN so that it is confirmed that in the examined case the size of the beam sections is governed by gravity loads rather than the design seismic forces. Despite it is out of the scope of the work herein presented, it is useful to underline that, in such a case, i.e. beam size governed by gravity loads, the use of RBS connections can be particularly convenient to promote the development of a global mechanism with reduced column sections compared to those needed when the full plastic moment of the beam gross cross-section is developed.

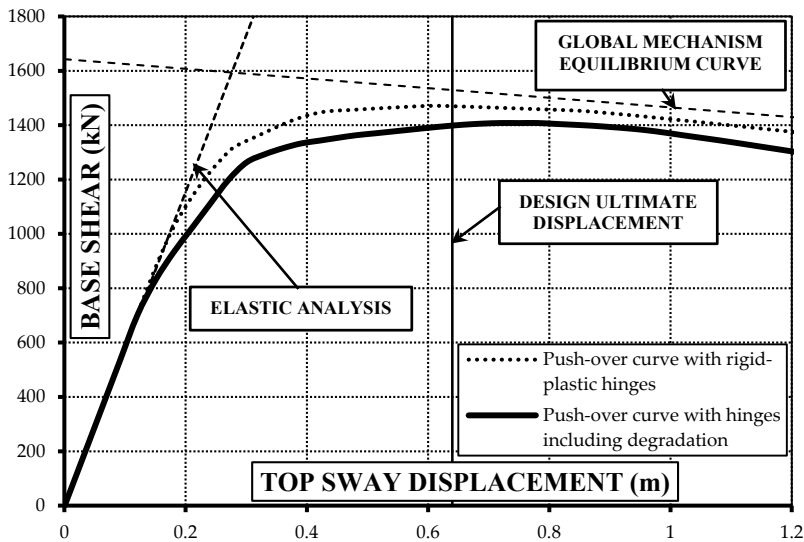


**Figure 3.8** - Behavioural curves of the designed frame and comparison with the corresponding bilinear approximation

The comparison between the capacity curve and the above straight lines provides a first confirmation of the accuracy of the proposed design procedure. Under this point of view, it is useful to underline that for  $E \rightarrow \infty$ , being  $E$  the elastic modulus, the capacity curve tends to the bilinear curve given by the vertical axis and the mechanism equilibrium curve.

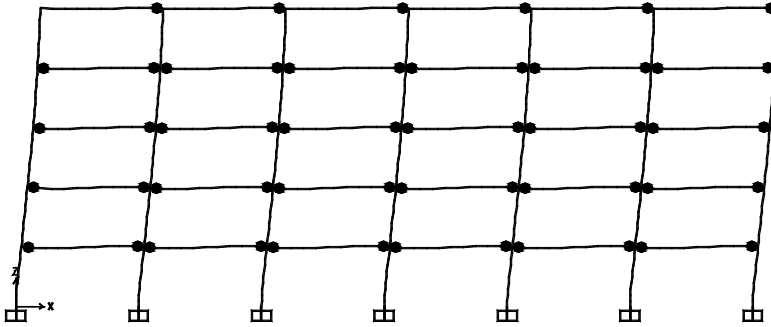


Figure 3.9 - Pattern of yielding of the designed frame at  $\delta = \delta_u$

A further confirmation, even the most important, of the fulfilment of the design objective is represented by the pattern of yielding developed at the occurrence of the design ultimate top sway displacement. In fact, developed plastic hinges are shown in Figure 3.9 and their pattern is in perfect agreement with the global mechanism. However, the complete development of the collapse mechanism does not occur, because plastic hinges at the first end of top storey beams are not still formed and column base sections are still in elastic range, and the structure remains stable even when the design ultimate displacement has been attained. For a displacement greater than the ultimate one, the global mechanism is completely developed according to the design goal.

In order to provide a more robust validation of the design methodology, non-linear incremental dynamic analyses have been carried out with reference to the same structural model used for push-over analyses, with plastic hinges having a cyclic envelope curve according to Figure 3.7, and described above. In addition, 5% damping according to Rayleigh modelling has been assumed.

Record-to-record variability has been accounted for considering 7 recorded accelerograms selected from PEER [68] data base. In Table 8, the main features of the records (name, date, magnitude, ratio between PGA and gravity acceleration, length and step recording) are given. These earthquake records have been selected to approximately match the linear elastic design response spectrum of Eurocode 8, for type A soil. Moreover, in order to perform IDA analyses, each ground motion has been scaled to obtain the same value of the spectral acceleration  $S_a(T_1)$  corresponding to the fundamental period of vibration  $T_1$  of the

structure ( $T_1=1.0$  s). This is the seismic intensity measure (IM) adopted for IDA analyses where  $S_a(T_1)$  values have been progressively increased until the occurrence of structural collapse, corresponding to anyone of the following ultimate limit states: column buckling, complete development of a collapse mechanism, attainment of the limit value of plastic rotation of beams or columns.

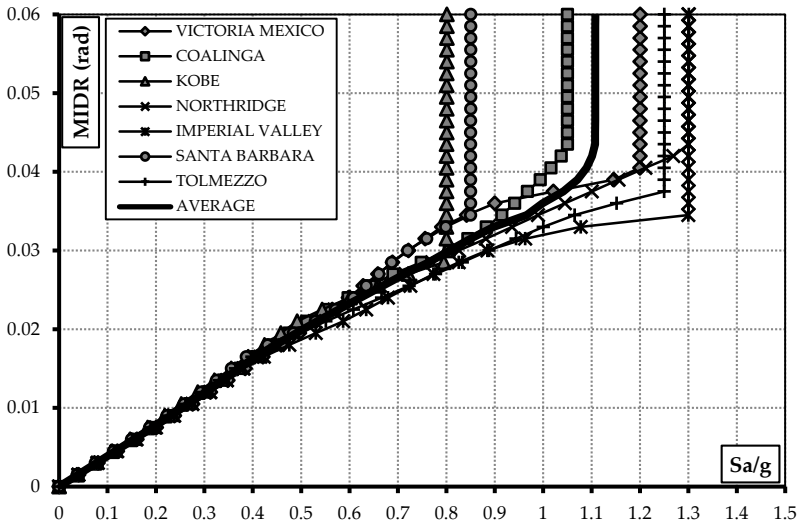


**Figure 3.10** - Maximum interstorey drift ratio versus  $S_a(T_1)$

In Figure 3.10, the maximum interstorey drift ratio (MIDR) versus spectral acceleration curve is reported. MIDR curves appear quite regular and increasing without exhibiting dynamic instability. In addition, for each record the obtained pattern of yielding has been monitored for increasing values of  $S_a(T_1)$  by checking that plastic hinge development is always in perfect agreement with the global mechanism. This result testifies the accuracy of the proposed design procedure even under actual seismic actions.

As an example, Figure 3.11 provides the distribution of plastic hinges for increasing value of  $S_a(T_1)$  with reference to Kobe earthquake record. As a consequence of the obtained design goal, the spectral acceleration values leading to collapse, given in Table 9, are very high and compatible with the adoption of the designed structure even in the case of destructive earthquakes. In particular,

the average value of  $S_a(T_1)$  leading to collapse is very close to 1.1 g while the average PGA is about 1.335 g. These very high values of spectral acceleration and PGA the structure is able to withstand testify the effectiveness of the design procedure to provide structures with excellent performances against life safety and collapse prevention limit states.

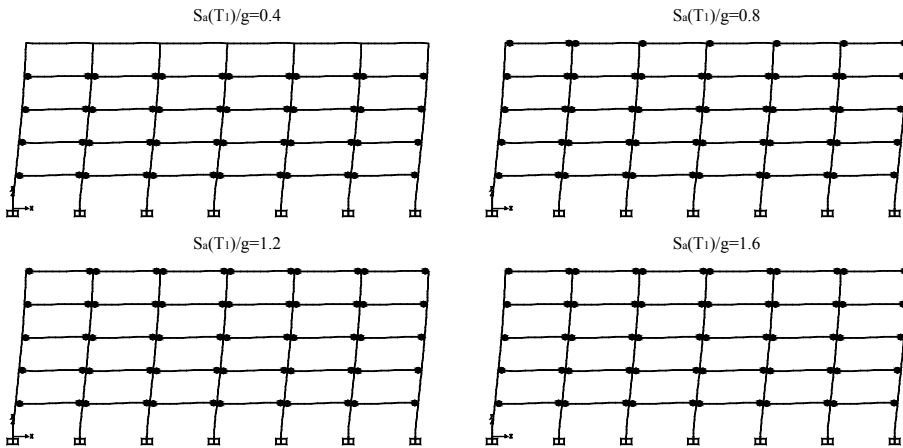


**Figure 3.11** - Pattern of yielding of the designed frame for increasing value of  $S_a(T_1)$  with reference to Kobe earthquake record

### 3.6 The influence of geometry, loads and steel grade for the development of a specific collapse type

As observed in §3.4 the columns of the structure reported in the worked example have been designed by selecting the maximum sum of reduced plastic moment of column required at each storey to avoid undesired mechanisms (Eq. (3.24)). The maximum value belongs, for the analysed structure, to the condition to avoid type-1 mechanism. It means that type-1 mechanism governs the design of the structure so that type-2 and type-3 mechanism, in this case, appear not decisive. Now it is important to point out what are the parameters deciding the influence of type-1 mechanism and if it is possible to preliminarily decide, on the basis of geometrical characteristics, loads and steel grade which one of the three undesired mechanism governs the design of the structure.

In order to answer these questions a parametric analysis has been led by varying geometry, loads and steel grade on MR-Frames with the scope to observe whether there a type mechanism which mostly governs the collapse of structure.

As regards the parameters involved, the geometry has been varied in term of number of storeys, number of bays, storey height and bay length. In particular the number of storey adopted goes from 3 to 8 while the number of bays goes from 2 to 6. Storey height have been assumed equal to 3 m, 4 m and 5 m while bay length has been considered equal to 3 m, 3.5 m, 4 m, 4.5 m, 5 m, 5.5 m, 6 m, 6.5 m and 7 m. Permanent loads,  $G_k$ , has been adopted equal to 4 kN/m<sup>2</sup> while live loads  $Q_k$  has been assumed as equal to 2 and 3 kN/m<sup>2</sup>. Loads have been combined following this relation:  $G_k+0.3Q_k$ . In addition, the influence light of the loads acting on the beams goes from 1 m to 6 m. Beams have been designed on the basis of the acting loads with a minimum and maximum bending moment of  $q_d l^2/16$  and their shapes have been selected from the IPE standard profiles. The adopted steel grades are S275, S355, S450. Seismic forces distribution has been assumed as increasing with the storey height by neglecting their magnitude because, as underlined in the previous paragraphs, it is irrelevant for the design result of the procedure.

The whole of the analysed number of cases is equal to 176960 but 12690 of these ones have beams incompatible with the assigned loads, so that the real number of analysed cases is equal to 162270.

After the application of TPMC to the analysed cases the following results have been observed: the number of cases governed by a mechanism typology different by the type-1 without the occurrence of the technological condition, i.e. at the step g) of the procedure reported in §3.3, are 197 while the number of cases that are governed by a mechanism typology different by the type-1 after the occurrence of the technological condition, i.e. at the step i) of the procedure, are 22260. It means that, as preliminarily stated, at the occurrence of the technological condition the sum of required column plastic moments for  $i_m > 1$  is affected by the increase of the first right hand side term of Eq. (3.21) and the increase of the subtracting second term at right hand side of Eq. (3.21) and for this reason type-2 and type-3 mechanism become determinant for the design of the structure.

However, by stopping the attention on the procedure without the occurrence of technological condition is important to observe that only the 0.12% of the analysed cases is governed by a collapse typology different from type-1



and for this reason, it is possible to confirm that type-1 mechanism governs, in the most of the cases, the design of MR-Frames.

Many advantages belong to this observation: first of all the chance to use a simplified version of TPMC to design MR-Frames. This simplified version starts from the preliminary assumption that column sections are pin-jointed at their bases. As a consequence, Eq.(3.20) becomes:

$$\sum_{i=1}^{n_c} M_{c,i1} \geq \frac{2 \sum_{k=1}^{n_s} \sum_{j=1}^{n_b} M_{b,jk} + (\gamma_1^{(3)} - \gamma^{(g)}) \delta_u \sum_{k=1}^{n_s} F_k h_k}{\frac{\sum_{k=1}^{n_s} F_k h_k}{h_1 \sum_{k=1}^{n_s} F_k} - 1} \quad (3.35)$$

and Eqs. (3.21), (3.22) and (3.23), become:

$$\sum_{i=1}^{n_c} M_{c,ii_m}^{(1)} \geq (\alpha^{(g)} + \gamma_{i_m}^{(1)} \delta_u) \left( \sum_{k=1}^{i_m} F_k h_k + h_{i_m} \sum_{k=i_m+1}^{n_s} F_k \right) - 2 \sum_{k=1}^{i_m-1} \sum_{j=1}^{n_b} M_{b,jk} \quad (3.36)$$

needed to avoid type-1 mechanisms;

$$\sum_{i=1}^{n_c} M_{c,ii_m}^{(2)} \geq (\alpha^{(g)} + \gamma_{i_m}^{(2)} \delta_u) \sum_{k=i_m}^{n_s} F_k (h_k - h_{i_m-1}) - 2 \sum_{k=i_m}^{n_s} \sum_{j=1}^{n_b} M_{b,jk} \quad (3.37)$$

needed to avoid type-2 mechanisms;

$$\sum_{i=1}^{n_c} M_{c,ii_m}^{(3)} \geq (\alpha^{(g)} + \gamma_{i_m}^{(3)} \delta_u) \frac{(h_{i_m} - h_{i_m-1})}{2} \sum_{k=i_m}^{n_s} F_k \quad (3.38)$$

needed to avoid type-3 mechanisms; where  $\alpha^{(g)}$  does not depend on the sum of the reduced plastic moments of columns at the first storey  $\sum_{i=1}^{n_c} M_{c,i1}$  and it is provided by the following relation:

$$\alpha^{(g)} = \frac{\sum_{k=1}^{n_s} \sum_{j=1}^{n_b} 2B_{jk} R_{b,jk}}{\sum_{k=1}^{n_s} F_k h_k} \quad (3.39)$$

being Eqs. (3.21), (3.22) and (3.23) independent of the sum of the reduced plastic moments of columns at the first storey,  $\sum_{i=1}^{n_c} M_{c,i1}$ , the column sections at first storey are provided starting by Eq. (3.35) while the column sections at each storey required to avoid undesired mechanism are directly provided starting by Eq. (3.36), (3.37) and (3.38) without the preliminary design of column sections at first storey. In this way, each storey is independent of the other storey and in particular, of the first one, so that, even if the technological condition occurs the column sections at each storey do not need to be revised. In addition, the solution provided in the framework of the hypothesis of pin-jointed column bases (simplified TPMC) constitutes a safe side solution with reference to the original

TPMC proposed in §3.3, only in the case of type-1 mechanism governing the design procedure.

### **3.7 Summary notes**

In this chapter the state of the art and the important improvement leading to a closed form solution for the Theory of Plastic Mechanism Control (TPMC) have been presented with reference to MR-Frames.

This closed form solution constitutes a significant improvement compared to the original algorithm developed by Mazzolani and Piluso [17] in nineties that required an iterative solution. On the bases of the extension of the kinematic theorem of plastic collapse to the concept of mechanism equilibrium curve, the Theory of Plastic Mechanism Control allows to evaluate the sum of the plastic moments of columns required at each storey to obtain a collapse mechanism of global type. This information has to be coupled with the computation of the axial forces occurring in the columns when the global mechanism is completely developed. The knowledge of bending moment  $M$  and axial force  $N$  allows the design of the column sections required to prevent any partial or storey mechanism.

The closed form solution of the design conditions makes now the design procedure very easy to be applied even by means of hand calculations and, therefore, it could be suggested for code purposes by definitely solving the problem of collapse mechanism control whose importance in seismic design is universally recognised. Beam-column hierarchy criterion, commonly suggested by seismic codes, appears only as a very rough approximation when compared to TPMC and its theoretical background.

It has also to be underlined that TPMC can be applied with reference to any desired distribution of design seismic forces and to any criterion of design seismic forces and to any criterion to derive the design base shear, so that it can be properly introduced within the framework of procedures devoted to performance based plastic design of steel structures. Given this background in Chapter 4, the TPMC has been extended to MRF-EBF dual systems with both horizontal link and vertical link making the needed difference for the computation of the virtual internal work.

# CHAPTER 4

## TPMC FOR MRF ECCENTRICALLY BRACED FRAMES:

### MRF-EBF DUAL SYSTEMS

#### 4.1 Introduction

In this chapter, the closed form solution of Theory of Plastic Mechanism Control (TPMC), presented in the Chapter 3 for the case of MR-Frames, is extended to the case of Moment Resisting Frames-Eccentrically braced frames (MRF-EBF) dual systems.

Eccentrically braced frames constitute a suitable compromise between seismic resistant MR-frames and concentrically braced frames. In fact, they exhibit both adequate lateral stiffness, due to the high contribution coming from the diagonal braces, and ductile behaviour, due to the ability of the links, constituting the dissipative zones of this structural typology, in developing wide and stable hysteresis loops. Therefore, the coupling of MRF and EBF constitute a much safe and dissipative compromise because the resulting dual system is characterised by a first fail-safe system constituted by the eccentrically braced frames, and a secondary fail-safe system, constituted by moment resisting frame. This secondary one can be considered as an additional dissipative system where plastic hinges are concentrated at the beam ends. Conversely, the main dissipative system is constituted by the link members located in the braced frames of MRF-EBF dual system which can horizontal (K-braced, D-braced and V-braced) or vertical (inverted Y-braced) (Figure 2.1). In addition, diagonals constituting the bracing system are considered in this work as pinned at their

bases. It means that they are assumed unable to transmit the bending moments and, therefore, are modelled with actual hinges in the structural scheme.

However, in the project concerned, capacity design principles needs to be applied to assure that yielding occurs in the link elements only while beams, columns and diagonal braces remain in elastic range.

In fact, it is universally recognized that one of the primary aims of seismic resistant design is to avoid partial collapse mechanisms and soft storey mechanisms that significantly undermine the energy dissipation capacity of the structure. The optimization of the seismic structural response is, conversely, obtained when a collapse mechanism of global type is developed, because, in such case, all the dissipative zones are involved in the corresponding pattern of yielding, leaving all the other structural parts in elastic range.

TPMC allows the theoretical solution of the problem of designing a structure failing in global mode, i.e. assuring that the yielding involves only dissipative zones while all the columns, which are the unknown of the design problem, remain in elastic range with the only exception of base sections at first storey columns. Conversely, link, beam and diagonal sections are assumed as known quantities.

## **4.2 Plastic mechanism typologies**

The number of possible collapse mechanisms of eccentrically braced frames is very high, because at each storey yielding can develop in links, beams, columns and diagonal braces depending on the relative flexural strength of members. For this reason, the attention need to be preliminarily focused on one-storey structure to derive the design conditions to be satisfied in order to assure that yielding occurs according to the desired collapse mechanism, namely A-type, in Figure 2.3, Figure 2.4 and Figure 2.5. These design conditions have been derived and reported in Chapter 2, in which also the interaction between shear and moment in link members has been addressed. In fact, even with reference to a simple one-storey scheme, it is needed to consider that EB-Frames can develop alternative undesired collapse mechanism (Figure 2.3, Figure 2.4 and Figure 2.5), namely B-type, C-type and D-type. All these collapse mechanisms are able to develop only in the case of EB-Frame with vertical link (inverted Y scheme) while in the case

of horizontal link only one undesired mechanism typology can affect the behaviour of the one storey structure.

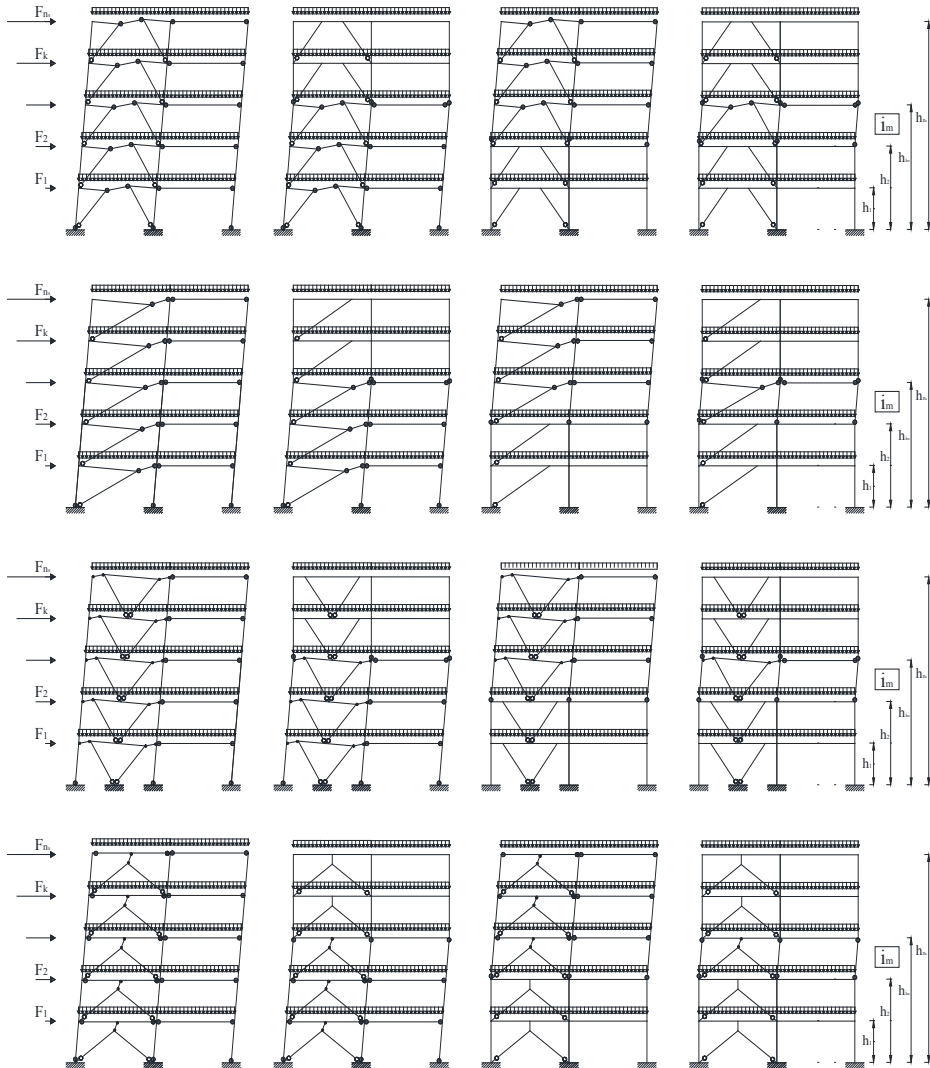


**Figure 4.1** – Collapse mechanism typologies for MRF-EBF dual systems when A-type is assured

In case of multi-storey MRF-EBF dual systems, dealing with the overall behaviour of the structure, and being assured the A-type mechanism at storey level, collapse mechanisms can be considered as belonging to three main typologies as depicted in Figure 4.1. These mechanisms, have to be considered undesired, because they do not involve all the dissipative zones. The global mechanism, representing the design goal, is generally considered, a particular case of type-2 mechanism involving all the storeys. However, in the case of MRF-EBF dual systems with horizontal link also type-1 mechanism involving all the storeys is coincident with the global mechanism. This peculiarity only valid for this structural typology is of paramount importance for the development of TPMC in closed form solution. Conversely, MRF-EBF dual systems with vertical links conform the undesired mechanism of MRFs.

Other differences between the undesired mechanisms of horizontal and vertical link structures are, for type-1 mechanism, that column plastic hinges of undesired mechanism do not develop at the top end of the  $i_m$ -th storey as the same as the vertical link EBFs but at the column bases of the  $i_m$ -th +1 storey. The same happens in the case of type-3 mechanism where the plastic hinges of columns of the storey affected by the soft storey mechanism develop at the bottom end of the  $i_m$ -th storey and at the bottom end of the  $i_m$ -th+1 storey. Finally, it is important to observe that, diagonal members, being pinned at their bases do not constitute dissipative zone and are assured to remain in elastic range when the A-type mechanism at storey level is respected.

Given the above, in order to face the problem of plastic mechanism control from the overall point of view, the Theory of Plastic Mechanism Control (TPMC) need to be applied to assure the development of a global type mechanism. The design problem is constituted by the definition of the column sections required at each storey to assure the desired collapse mechanism, whereas beam, diagonal and link sections are assumed as known properties. The algorithm of TPMC for the case of EB-Frames with both horizontal and vertical link will be reported in the following paragraphs.

### 4.3 Design of links

The so-called seismic links constitute the dissipative zones of eccentrically braced frames. Seismic links can be disposed horizontally; this is the case of EBFs

with K-scheme, V-scheme and D-scheme or vertically as the EBFs with Inverted Y-scheme Figure 2.1.

According to the first principle of capacity design, links are preliminarily designed to withstand the internal actions due to the design seismic shear acting at the storey level. Regarding the rate of seismic action the braced part has to bear, ASCE 7-10 [69] requires for a dual system that the moment frames shall be capable of resisting at least 25 percent of the design seismic forces while the remaining part is entrusted to the EBF. However, the percentage proposed by ASCE 7-10 can be seen only as a suggestion, therefore, in this work the whole seismic action has been entrusted to the EBF.

Regarding the link design, there are some differences in the computation of the internal shear action for horizontal and vertical link configuration. In fact, while in the case of EBFs with vertical link the dissipative zones have to be designed to withstand the whole seismic action that the designer intends to entrust to the braced bay, in the case of EBFs with horizontal link the maximum internal action has to be computed by means of the approximate equilibrium equation around point A of Figure 4.2 applied at each storey.

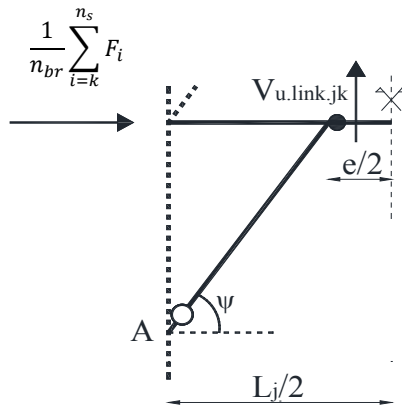


**Figure 4.2** – Estimation of link design shear

This equilibrium is carried out on the basis of the following assumptions: the link member is subject to a bi-triangular diagram of bending moment with

zero value at the midspan; the bending moment at the column bottom end is negligible. In this conditions the following design formula for both horizontal and vertical link in the hypothesis of more than one bay is braced are provided:

$$V_{link.H.Sd} = \frac{1}{n_{br}} \frac{\sum_{i=k}^{n_s} F_i}{L} h_k \leq V_{link.Rd} \quad (4.1)$$

$$V_{link.V.Sd} = \frac{1}{n_{br}} \sum_{i=k}^{n_s} F_i \leq V_{link.Rd} \quad (4.2)$$

where  $F_i$  is the storey seismic horizontal force,  $L_j$  is the length of the  $j$ -th bay,  $V_{link.Rd}$  is the link shear resistance at  $k$ -th storey, and  $n_{br}$  is the number of braced bays. It follows that all the braced bays are assumed as sharing the same amount of the storey shear.

#### 4.4 Design of beams and diagonals

According to the second principle of capacity design, non-dissipative zones need to be designed considering the maximum internal actions which the dissipative zones are able to transmit in their fully yielded and strain-hardened state.

For this reason, in order to account for the significant strain-hardening occurring in link elements [19], [20] reference is made to an overstrength equal to 50% in case of shear links and to an overstrength equal to 20% in case of long links, according to the following equations:

$$V_u = 1.5f_y t_w (h - t_f) / \sqrt{3} \quad (4.3)$$

$$M_u = 1.2f_y W_{pl} \quad (4.4)$$

$$M_{fu} = 1.2f_y b_f t_f (h - t_f) \quad (4.5)$$

$$M_{wu} = M_u - M_{fu} \quad (4.6)$$

where  $W_{pl}$  is the plastic modulus of the link section,  $h$  is the height,  $b_f$  and  $t_f$  are the flange width and thickness, respectively,  $t_w$  is the web thickness and  $f_y$  is the yield strength of steel.

In order to account for the influence of the link length on their plastic behaviour, the concept of equivalent plastic bending moment is used. It allows



the development of rigid-plastic analyses accounting for moment-shear interaction, so that short, intermediate and long links can be properly modelled.

The equivalent moment [24], [25] accounts for the mechanical behaviour of the link as short, intermediate or long, according to the classification reported in Eurocode 8 [11]. It allows modelling the link as an element with plastic hinge in simple bending, with the scope to write the internal work simply as the product between the equivalent plastic moment and the equivalent plastic rotation, even in the case of moment-shear interaction. Virtual internal work can be written for EBFs with horizontal link as:

$$W_i^{link} = 2M_{eq} \frac{\theta L_j}{e} \quad (4.7)$$

and for vertical link as:

$$W_i^{link} = 2M_{eq} \frac{\theta H_i}{e} \quad (4.8)$$

where  $H$  and  $\theta$  are the interstorey height and plastic rotation at beam ends, respectively and  $M_{eq}$  is the equivalent plastic moment of the link for the desired mechanism, accounting for the influence of the link length, given by [19]:

$$M_{eq}^{(short)} = \frac{V_u e}{2} \quad (4.9)$$

$$M_{eq}^{(intermediate)} = \frac{M_{fu} + M_{wu} \sqrt{1 - 4 \frac{M_{fu}^2 - M_{wu}^2}{V_u^2 e^2}}}{1 + 4 \frac{M_{wu}^2}{V_u^2 e^2}} \quad (4.10)$$

$$M_{eq}^{(long)} = M_u \quad (4.11)$$

where  $V_u$  and  $M_u$  denote the ultimate shear resistance and the ultimate moment resistance, respectively. In addition,  $M_{fu}$  and  $M_{wu}$  represent the contribution of the flanges and web, respectively, to the ultimate moment of the section and  $e$  denotes the link length.

The beam and the brace sections are preliminarily designed to assure that, at each storey, yielding occurs in the link only, i.e. by imposing the design requirements given in Chapter 2. In this way only A-type mechanism can develop. It means that beam and diagonal sections have to be selected to satisfy the relationship reported in Table 2.1.

In addition, it is required that beam sections have to resist also vertical loads according to the load combinations provided by seismic code. Finally, beam-to-column connections in the structural modelling are assumed as rigid full-strength.

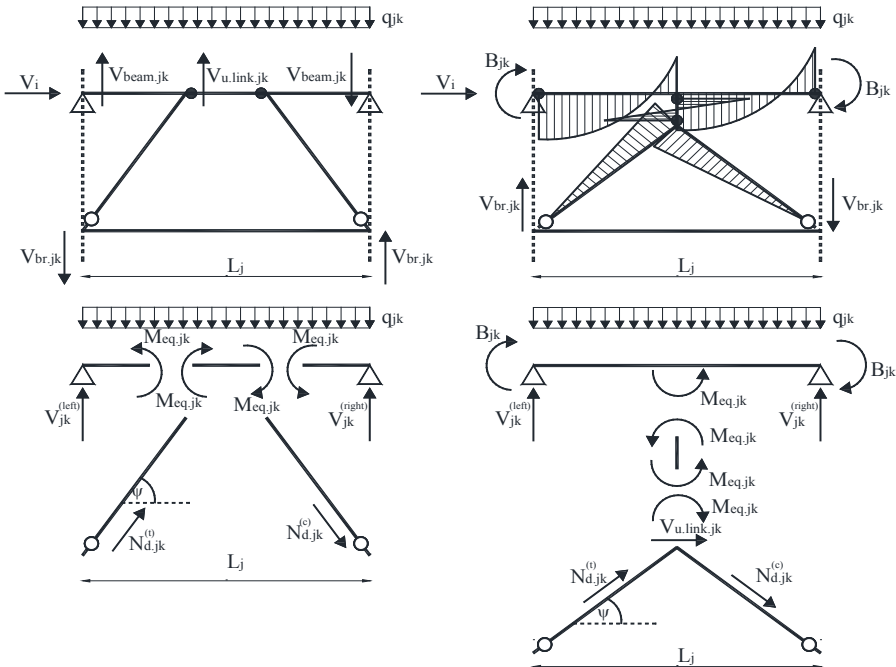


**Figure 4.3 – Bending moment diagram in beam, link and diagonal braces in ultimate conditions and corresponding free body internal actions**

The axial forces in the diagonal braces in the ultimate conditions, according to the second principle of capacity design, can be derived from the knowledge of the maximum shear force,  $V_{u,link,jk}$ , which the vertical link is able to transmit (Figure 4.3).

As regards the EBFs with horizontal link, the axial load acting in the diagonals when the global mechanism is completely developed can be obtained by means of simplified equilibrium equations around point B, as suggested by

Kasai and Han [34], [35]. Therefore, with reference to the  $j$ -th bay and the  $k$ -th storey, the axial force in the tensile  $N_{d,jk}^{(t)}$  and compressed  $N_{d,jk}^{(c)}$  diagonal are given by:

$$N_{d,jk}^{(t)} = N_{d,jk}^{(c)} = \frac{V_{u.link,jk} L_j}{2(h_k - h_{k1}) \cos \psi} \quad (4.12)$$

while, as regards EBFs with vertical link the axial force in the tensile  $N_{d,jk}^{(t)}$  and compressed  $N_{d,jk}^{(c)}$  diagonal are given by:

$$N_{d,jk}^{(t)} = N_{d,jk}^{(c)} = \frac{V_{u.link,jk}}{2 \cos \psi} \quad (4.13)$$

As a consequence, the section of diagonal braces has to be selected in order to comply with in-plane stability check under the action of a bending moment  $M_{d,jk}$  needed to avoid local undesired mechanisms at the one-storey level and an axial load given by Eq. (4.12) and Eq. (4.13) for EBFs with horizontal and vertical link, respectively. Moreover, out-plane buckling under the axial force given by Eq. (4.12) and Eq. (4.13) needs also to be checked.

## 4.5 Column Axial Forces at Collapse

The design of the column sections requires the knowledge of the flexural resistance needed to avoid the undesired collapse mechanisms. This flexural resistance is obtained by means of the TPMC. Such flexural resistance is the required plastic moment reduced due to the contemporary action of the axial load. Therefore, in order to the design column sections also the axial loads acting in the columns at collapse, i.e. when the global mechanism is completely developed, are required. In the following, the relation for the computation of axial loads acting at the collapse state are reported for both the EBFs with horizontal link and vertical link.

### 4.5.1 EBFs with horizontal link

The value of the axial load acting in the columns when the global mechanism is completely developed can be obtained by means of simplified equilibrium equations, as suggested by Kasai and Han [34], [35]. In Figure 4.3 the corresponding simplified schemes are reported. According to capacity design the internal actions are calculated on the basis of the maximum shear force (i.e. the ultimate shear  $V_{u.link,jk}$ ) that the link in the fully yielded and strain-hardened

condition, is able to transmit. In particular, with reference to Figure 4.3, by assuming that the bending moment at the beam ends and at the bottom end of braces is negligible, the vertical equilibrium equation provides:

$$V_{beam.jk} = N_{d.jk} \sin\psi - V_{u.link.jk} \quad (4.14)$$

In addition, the shear action due to the distributed load acting on beams need to be taken in account and it has the following expression:

$$V_{q.jk} = \frac{q_{jk} L_j}{2} \quad (4.15)$$

So that, the vertical equilibrium equation provides the following relationship:

$$N_{c.ik} = N_{c.ik+1} + \frac{q_{jk} L_j}{2} + N_{d.jk+1} \sin\psi - V_{beam.jk} \quad (4.16)$$

Eq. (4.16) provides the axial load at the collapse state,  $N_{c.ik}$ , for each diagonal and each column. In particular, Eq. (4.16) has to be applied starting from the top storey (so that  $N_{c.ik}$  and  $N_{d.jk}$  are equal to 0) and continuing up to the first storey.

#### 4.5.2 EBFs with vertical link

The value of the axial load acting in the columns when the global mechanism is completely developed can be obtained as the sum of the shear forces transmitted by the adjacent beams at and above the considered storey and of the vertical components of the axial forces in the diagonal braces above the considered storey.

With reference to the  $j$ -th beam of the  $k$ -th storey, the shear force transmitted by the beam to the columns at collapse can be easily derived as (Figure 4.4):

$$V_{jk} = V_{q.jk} \pm V_{M.jk} = \frac{q_{jk} l_j}{2} \pm \frac{2B_{i,k} + M_{eq.jk}}{l_j} \quad (4.17)$$

where the sign plus is valid for  $V_{jk}^{(right)}$  and the sign minus is valid for  $V_{jk}^{(left)}$ ;  $B_{j,k}$  is the beam plastic moment;  $M_{eq.jk}$  is the link equivalent plastic moment considering accounting for moment-shear interaction when needed and  $l_j$  is the bay span.

The vertical component of the axial force in the diagonal braces is given by:

$$V_{br.jk} = \frac{V_{u.link.jk}}{2} \operatorname{tg}\psi \quad (4.18)$$

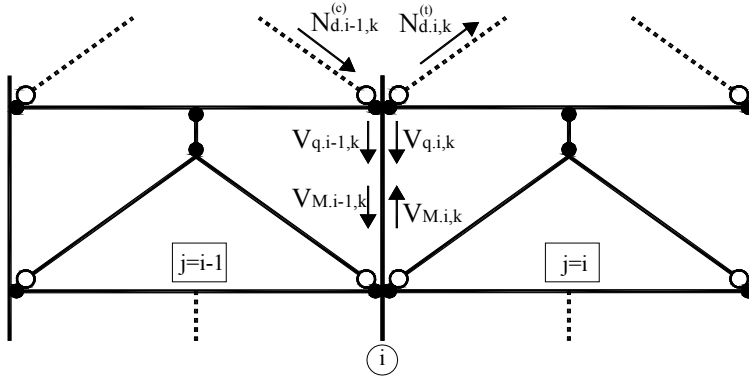


**Figure 4.4** - Evaluation of column axial forces at collapse

Therefore, the axial load acting at collapse state in the  $i$ -th column of the  $k$ -th storey, being  $j = i - 1$  and  $j = i$  the adjacent bays, can be computed as:

$$\begin{aligned}
 N_{c,ik} = & \sum_{m=k}^{n_s} (V_{q,i-1,m} + V_{q,i,m}) + \sum_{m=k}^{n_s} (V_{M,i-1,m} - V_{M,i,m}) \\
 & + \sum_{m=k}^{n_s} (V_{br,i-1,m} - V_{br,i,m})
 \end{aligned} \tag{4.19}$$

being the first sum representative of the contribution due to the uniform loads acting on the beams, namely  $N_{q,ik}$ , the second sum the contribution due to the bending moment transmitted by the link to the beam and to the bending moments at the beam ends, namely  $N_{M,ik}$  and the third sum the contribution due to the actions transmitted by the diagonal braces, namely  $N_{br,ik}$ . Obviously, the design of the column sections has to be carried out considering, for each column, the most severe axial load deriving from both positive and negative direction of seismic horizontal forces.

## 4.6 Equilibrium Curves of the Analysed Plastic Mechanisms

The Theory of Plastic Mechanism Control (TPMC) which has the primary aim to assure the development of a collapse mechanism of global type is based

on the kinematic theorem of plastic collapse and on second order rigid-plastic analysis. The design problem is constituted by the definition of the column sections required at each storey to assure the desired collapse mechanism, whereas beam, brace and link sections are assumed as known properties designed by means of the relationships reported in the previous paragraphs.

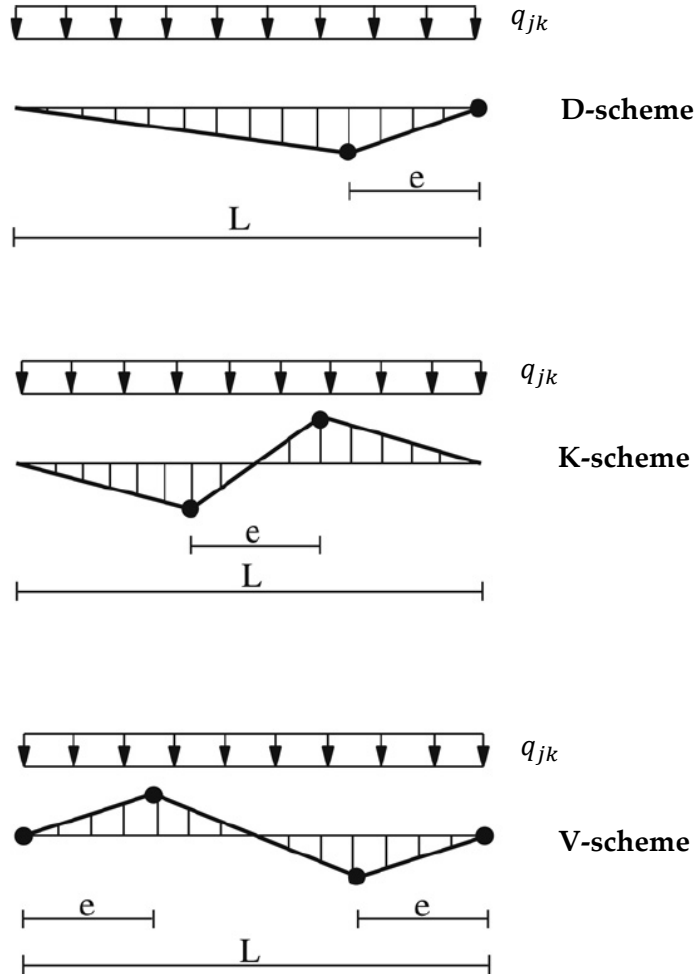


Figure 4.5 – Vertical displacement diagram

The TPMC is based on the extension of the kinematic theorem of plastic collapse to the concept of mechanism equilibrium curve. Therefore, it accounts also for the influence of second order effects in plastic range that cannot be neglected in the seismic design of steel structures. In particular, the plastic section modulus of each column has to be defined by imposing that the mechanism equilibrium curve corresponding to the global mechanism, i.e. the desired mechanism, has to lie below those corresponding to all the undesired mechanism within a displacement range compatible with the local ductility supply of members. It means that, according to the upper bound theorem, the true collapse mechanism is the global mechanism.

As reported in Chapter 3 for the case of MRFs the mechanism equilibrium curve can be easily derived by equating the external work to the internal work, due to the dissipative zones involved in the collapse mechanism, provided that the external second-order work due to vertical loads is also evaluated [17].

Regarding the beams, it is preliminarily useful to remember that when the following limitation reported in Eq. (3.1) is fulfilled beam plastic hinges develop only at the beam ends. Conversely, it can be demonstrated [17] that, in case of vertical loads exceeding the above limit, the first plastic hinge in the beam develops at the end where the bending moments due to gravity loads and to seismic forces have the same sign (hogging moments) while the second plastic hinge in the beam develops in an intermediate section whose abscissa is given by  $x_{jk} = L_j - 2(M_{b,jk}/q_{jk})^{0.5}$ , so that the external work due to the uniform vertical loads has also to be considered as equal to:

$$W_{q,jk} = q_{jk} \frac{L_j x_{jk}}{2} \quad (4.20)$$

This is the case of the MRF part of the MRF-EBF dual systems, where plastic hinges of the beams can develop in intermediate sections. As regard the EBF part, it can be difficult that plastic hinges develop in section of the beams different from the end sections. However, the virtual external work due to the vertical loads cannot be negligible in the particular case of EBFs with horizontal link and D-scheme. In such case (Figure 4.5) virtual external work due to the distributed load,  $q_{jk}$  is always present in correspondence of the braced bay and assumes the following form:

$$W_{q,jk} = q_{jk} \frac{L_j(L_j - e_{jk})}{2} \quad (4.21)$$

As an example, in the case of global mechanism, for the most general case, the external work due to a virtual rotation  $d\theta$  of columns plastic hinges is given by:

$$W_e = \alpha \sum_{k=1}^{n_s} F_k h_k d\theta + \frac{\delta}{h_{n_s}} \sum_{k=1}^{n_s} V_k h_k d\theta + \sum_{k=1}^{n_s} \sum_{j=1}^{n_b} W_{q,jk} d\theta \quad (4.22)$$

where  $\alpha$  is the multiplier of horizontal forces,  $F_k$  and  $h_k$  are, respectively, the seismic force applied at  $k$ -th storey and the  $k$ -th storey height with respect to the foundation level,  $h_{n_s}$  is the value of  $h_k$  at the top storey,  $\delta$  is the top sway displacement and  $V_k$  is the total vertical load acting at  $k$ -th storey.

The first term of Eq. (4.22) represents the external work due to seismic horizontal forces, the second term is the second order work due to vertical loads as reported in Chapter 3 (Eq. (3.3)) while the third term is the virtual external work due to the vertical loads in the case of plastic hinge formation at an intermediate section of the beam (case of MRF part of EBF-Dual or EBF part of D scheme).

In the case of a global mechanism, the internal work due to a virtual rotation  $d\theta$  of column plastic hinges can be written as:

$$W_i = \left( \sum_{k=1}^{n_c} M_{c,i1} + \sum_{k=1}^{n_s} \sum_{j=1}^{n_b} W_{d,jk} \right) d\theta \quad (4.23)$$

where  $M_{c,ik}$  is the plastic moment of  $i$ -th column of  $k$ -th storey ( $k=1$  in this case) reduced due to the contemporary action of the axial force;  $W_{d,jk}$  is the internal work due to the dissipative zones located in the  $j$ -th bay of  $k$ -th storey, to be evaluated depending on the structural typology as it will be discussed in the following;  $n_c$ ,  $n_b$  and  $n_s$  are the number of columns, bays and storeys, respectively.

By equating the internal work to the external one, the following relationship is obtained:

$$\alpha = \frac{\sum_{k=1}^{n_c} M_{c,i1} + \sum_{k=1}^{n_s} \sum_{j=1}^{n_b} (W_{d,jk} - W_{q,jk})}{\sum_{k=1}^{n_s} F_k h_k} - \frac{1}{h_{n_s}} \frac{\sum_{k=1}^{n_s} V_k h_k}{\sum_{k=1}^{n_s} F_k h_k} \delta \quad (4.24)$$

From this equation, it is immediately recognized the mechanism equilibrium curve mathematical structure:



$$\alpha = \alpha_0 - \gamma\delta \quad (4.25)$$

where  $\alpha_0$  is the kinematically admissible multiplier of horizontal forces according to first order rigid-plastic analysis and  $\gamma$  is the slope of the mechanism equilibrium curve.

In the case of global mechanism, as shown in Figure 4.1, the kinematically admissible multiplier of horizontal forces is given by:

$$\alpha_0^{(g)} = \frac{\sum_{i=1}^{n_c} M_{c.i1} + \sum_{k=1}^{n_s} \sum_{j=1}^{n_b} (W_{d.jk} - W_{q.jk})}{\sum_{k=1}^{n_s} F_k h_k} \quad (4.26)$$

while the slope of the mechanism equilibrium curve  $\gamma^{(g)}$  is the same given by Eq. (2.8).

As the undesired collapse mechanism are different for MRF-EBF dual system with horizontal link and vertical link as described in §4.2 also the term  $\alpha_{0,i_m}^{(t)}$  are different while the slope of mechanism equilibrium curves are the same because the slope of the mechanism equilibrium curve is independent of structural typology as it is related only to the magnitude of vertical loads, the collapse mechanism typology and index. However, for any given geometry of the structural system, the slope of mechanism equilibrium curve attains its minimum value when the global type mechanism is developed. This second issue assumes a paramount importance in TPMC allowing to exploit the extension of the kinematic theorem of plastic collapse to the concept of mechanism equilibrium curve.

In the following the collapse mechanism multiplier of the undesired mechanism for MRF-EBF dual system either with horizontal link or vertical link are reported. The collapse mechanism multiplier  $\alpha_0^{(g)}$  of the global mechanism is the same in both the cases. The parameters of the mechanism equilibrium curves for type-1, type-2 and type-3 mechanism typologies are derived at the same way reported for the global mechanism.

### 4.6.1 Mechanism equilibrium curve for MRF-EBF dual system with horizontal link

With reference to  $i_m$ -th mechanism of type-1, the kinematically admissible multiplier of seismic horizontal forces, for  $1 \leq i_m < n_s$  is given by:

$$\alpha_{0.i_m}^{(1)} = \frac{\sum_{i=1}^{n_c} M_{c.i1} + \sum_{i=1}^{n_c} M_{c.ii_{m+1}} + \sum_{k=1}^{i_m} \sum_{j=1}^{n_b} W_{d.jk} - \sum_{k=1}^{i_m} \sum_{j=1}^{n_b} W_{q.jk}}{\sum_{k=1}^{i_m} F_k h_k + h_{i_m} \sum_{k=i_m+1}^{n_s} F_k} \quad (4.27)$$

and for  $i_m = n_s$  is given by:

$$\alpha_{0.n_s}^{(1)} = \frac{\sum_{i=1}^{n_c} M_{c.i1} + \sum_{k=1}^{i_m} \sum_{j=1}^{n_b} W_{d.jk} - \sum_{k=1}^{i_m} \sum_{j=1}^{n_b} W_{q.jk}}{\sum_{k=1}^{n_s} F_k h_k} \quad (4.28)$$

where  $\sum_{j=1}^{n_b} W_{d.jk}$  is the term due to the internal work of the dissipative zones and the slope of the mechanism equilibrium curve is the same given by Eq. (3.11).

With reference to  $i_m$ th mechanism of type-2, the kinematically admissible multiplier of seismic horizontal forces is given by:

$$\alpha_{0.i_m}^{(2)} = \frac{\sum_{i=1}^{n_c} M_{c.ii_m} + \sum_{k=i_m}^{n_s} \sum_{j=1}^{n_b} (W_{d.jk} - W_{q.jk})}{\sum_{k=i_m}^{n_s} F_k (h_k - h_{i_m-1})} \quad (4.29)$$

while the slope of the mechanism equilibrium curve is the same given by Eq. (3.13). It is useful to note that, Eq. (4.29) for  $i_m=1$ , Eq. (4.26) and Eq. (4.26) are coincident, because the type-1 mechanism for  $i_m = n_s$  and type-2 mechanism for  $i_m=1$  are coincident with the global one.

Finally, with reference to  $i_m$ th mechanism of type-3, the kinematically admissible multiplier of horizontal forces, for  $i_m = 1$ , is given by:

$$\alpha_{0.1}^{(3)} = \frac{\sum_{i=1}^{n_c} M_{c.i1} + \sum_{i=1}^{n_c} M_{c.i2} + \sum_{j=1}^{n_b} W_{d.j1} - \sum_{j=1}^{n_b} W_{q.j1}}{h_1 \sum_{k=1}^{n_s} F_k} \quad (4.30)$$

for  $1 < i_m < n_s$ , is given by:

$$\alpha_{0.i_m}^{(3)} = \frac{\sum_{i=1}^{n_c} M_{c.ii_m} + \sum_{i=1}^{n_c} M_{c.ii_{m+1}} + \sum_{j=1}^{n_b} W_{d.ji_m} - \sum_{j=1}^{n_b} W_{q.ji_m}}{(h_{i_m} - h_{i_m-1}) \sum_{k=i_m}^{n_s} F_k} \quad (4.31)$$

and for  $i_m = n_s$  is given by:

$$\alpha_{0.n_s}^{(3)} = \frac{\sum_{i=1}^{n_c} M_{c.in_s} + \sum_{j=1}^{n_b} W_{d.jn_s} - \sum_{j=1}^{n_b} W_{q.jn_s}}{F_{n_s} (h_{n_s} - h_{n_s-1})} \quad (4.32)$$

where  $\sum_{j=1}^{n_b} W_{d,jk}$  is the term due to the internal work of the dissipative zones. In addition, the corresponding slope of the mechanism equilibrium curve is given by Eq. (3.16). It is of paramount importance to note, for the development of the design algorithm that Eq. (4.29) for  $i_m = n_s$  and Eq. (4.32) are coincident.

#### 4.6.2 Mechanism equilibrium curve for MRF-EBF dual system with vertical link (Inverted Y-scheme)

By observing Figure 4.1, it is possible to take over that undesired mechanism involving MRF-EBF dual systems with vertical link are very similar to those involving MRFs (Figure 3.1) with the only difference due to the link yielding at the  $i_m$ th storey. In addition, beam ends of the  $i_m$ th storey are not involved in the mechanism as the same as MRFs. For this reason collapse mechanism multipliers of undesired mechanism have the same form of the MRFs one with the only addition of the term related to the virtual internal work of the links.

Therefore, with reference to  $i_m$ th mechanism of type-1, the kinematically admissible multiplier of seismic horizontal forces, for  $i_m = 1$  is given by:

$$\alpha_{0.1}^{(1)} = \frac{2 \sum_{i=1}^{n_c} M_{c.i1} + \sum_{j=1}^{n_b} W_{d.j1}}{h_1 \sum_{k=1}^{n_s} F_k} \quad (4.33)$$

where  $\sum_{j=1}^{n_b} W_{d.j1}$  is the term due to the internal work of links only because in this case beams are not involved in the undesired mechanism.

Similarly, for  $i_m > 1$ , the kinematically admissible multiplier of seismic horizontal forces is given by:

$$\alpha_{0.i_m}^{(1)} = \frac{\sum_{i=1}^{n_c} M_{c.i1} + \sum_{i=1}^{n_c} M_{c.ii_m} + \sum_{k=1}^{i_m} \sum_{j=1}^{n_b} W_{d.jk} - \sum_{k=1}^{i_m-1} \sum_{j=1}^{n_b} W_{q.j}}{\sum_{k=1}^{i_m} F_k h_k + h_{i_m} \sum_{k=i_m+1}^{n_s} F_k} \quad (4.34)$$

where  $\sum_{j=1}^{n_b} W_{d.jk}$  is the term due to the internal work of the dissipative zones, i.e. link sections and beam ends for the MRF part while the slope of the mechanism equilibrium curve is the same given by Eq. (3.11).

With reference to  $i_m$ th mechanism of type-2, the kinematically admissible multiplier of seismic horizontal forces is given by:

$$\alpha_{0.i_m}^{(2)} = \frac{\sum_{i=1}^{n_c} M_{c.ii_m} + \sum_{k=i_m}^{n_s} \sum_{j=1}^{n_b} (W_{d.jk} - W_{q.jk})}{\sum_{k=i_m}^{n_s} F_k (h_k - h_{i_m-1})} \quad (4.35)$$

while the slope of the mechanism equilibrium curve is the same given by Eq. (3.13). It is useful to note that, for  $i_m=1$  Eq. (4.35) and Eq. (4.26) are coincident as Eq. (3.13) and (3.8), because in such case the type-2 mechanism is coincident with the global one.

Finally, with reference to  $i_m$ th mechanism of type-3, the kinematically admissible multiplier of horizontal forces, for  $i_m = 1$ , is given by:

$$\alpha_{0.1}^{(3)} = \frac{2 \sum_{i=1}^{n_c} M_{c.i1} + \sum_{j=1}^{n_b} W_{d.j1}}{h_1 \sum_{k=1}^{n_s} F_k} \quad (4.36)$$

where  $\sum_{j=1}^{n_b} W_{d.j1}$  is the term due to the internal work of links and, for  $i_m > 1$ , is given by:

$$\alpha_{0.i_m}^{(3)} = \frac{2 \sum_{i=1}^{n_c} M_{c.ii_m} + \sum_{j=1}^{n_b} W_{d.ji_m} - \sum_{j=1}^{n_b} W_{q.ji_m}}{(h_{i_m} - h_{i_m-1}) \sum_{k=i_m}^{n_s} F_k} \quad (4.37)$$

where  $\sum_{j=1}^{n_b} W_{d.ji_m}$  is the term due to the internal work of links at  $i_m$ th storey.

In addition, the corresponding slope of the mechanism equilibrium curve is given by Eq. (3.16). Regarding the internal work  $W_{d.jk}$  due to the dissipative zones of  $j$ -th bay of  $k$ -th storey, it has to be computed accounting for the specific structural typology, as briefly summarised in Table 4.1.

In such table,  $M_{eq.l.jk}$  is the equivalent plastic moment of the link of  $j$ -th braced bay and  $k$ -th storey accounting for moment-shear interaction when needed and  $e_{jk}$  is the corresponding link length,  $R_{b.jk}$  is a coefficient which is equal to 0 if the bay is braced and 1 if it is unbraced and  $R_{l.jk}$  is a coefficient equal to 0 if the bay is unbraced and 1 if it is braced.

**Table 4.1** - Computation of the internal work due to the dissipative zones of  $j$ -th bay of  $k$ -th storey

Structural typology	$W_{d.jk}$	$W_{q.jk}$
<b>K-scheme</b>	$2R_{b.jk}M_{b.jk} \frac{L_j}{L_j - x_{jk}} + 2R_{l.jk}M_{eq.l.jk} \frac{L_j}{e_{jk}}$	$q_{jk} \frac{L_j x_{jk}}{2}$
<b>D-scheme</b>	$2R_{b.jk}M_{b.jk} \frac{L_j}{L_j - x_{jk}} + 2R_{l.jk}M_{eq.l.jk} \frac{L_j}{e_{jk}}$	$q_{jk} L_j \left[ \frac{x_{jk}}{2} + \frac{(L_j - e_{jk})}{2} \right]$
<b>V-scheme</b>	$2R_{b.jk}M_{b.jk} \frac{L_j}{L_j - x_{jk}} + 4R_{l.jk}M_{eq.l.jk} \frac{L_j}{2e_{jk}}$	$q_{jk} \frac{L_j x_{jk}}{2}$
<b>Inverted Y-scheme</b>	$2M_{b.jk} \frac{L_j}{L_j - x_{jk}} + 2R_{l.jk}M_{eq.l.jk} \frac{h_k - h_{k-1}}{e_{jk}}$	$q_{jk} \frac{L_j x_{jk}}{2}$

In addition, Eqs. (4.27) to (4.37) become suitable also for the case of simple EBFs by neglecting the contribution given by plastic moment of beam ends.

#### 4.7 Column design requirements to prevent undesired collapse mechanisms

The design conditions that column sections have to satisfy in order to prevent the undesired failure modes can be derived by the direct application of TPMC, i.e. by explicating the design conditions given by Eq. (3.17) as functions of the unknown column plastic moments.

In fact, as reported in Chapter 3, according to the kinematic theorem of plastic collapse, extended to the concept of mechanism equilibrium curve, the design conditions to be fulfilled in order to avoid all the undesired collapse mechanisms require that the mechanism equilibrium curve corresponding to the global mechanism has to be located below those corresponding to all the undesired mechanisms within a top sway displacement range,  $\delta_u$ , compatible with the ductility supply of dissipative zones, i.e. the plastic rotation of members which govern the design procedure.

In particular, the dissipative zones in MRF-EBF dual systems are both the beam and link members, so that the ultimate design displacement is the minimum among those corresponding to the beams and links rotational capacity. The ultimate plastic rotation of links,  $\gamma_u$ , is assumed equal to 0.08 rad for short link, 0.02 rad for long link and the interpolation between this two values for intermediate link while plastic rotation of beams is assumed equal to 0.04 rad. However in the whole of case is the link capacity that governs the structural capacity, so that, the ultimate design displacement is provided by means of the following relations:

$$\delta_u = \gamma_u (e/L_j) h_{n_s} \text{ for K-Scheme, D-scheme and V-scheme} \quad (4.38)$$

$$\delta_u = \gamma_u (e/h_i) h_{n_s} \text{ for Inverted Y-Scheme} \quad (4.39)$$

Eq. (2.17) constitutes the statement of the theory of plastic mechanism control and it is valid independently of the structural typology. The representation of the design statement is reported in Figure 3.3.

## 4.8 Closed form solution

As already stated, the original application of TPMC was based on an iterative procedure, so that the application of TPMC required the development of specific computer programs. The advances presented in this work are based on new observations leading to a closed form solution of Eq. (3.17). The resulting design procedure is now more simple and well suited even for hand calculations.

In the following paragraphs closed form solution is given both for MRF-EBF dual systems with horizontal link and vertical links.

### 4.8.1 Closed form solution for MRF-EBF dual system with horizontal link

Closed form solution algorithm of MRF-EBF dual systems with horizontal link presents some differences with reference to the design algorithm proposed for MRFs. As widely defined in Chapter 3 the observation that leads to the closed form solution regards the coincidence between type-1 and type-3 mechanisms for  $i_m = 1$  (at first storey) as depicted in Figure 3.4. As a consequence by substituting  $\alpha_0^{(g)}, \gamma^{(g)}, \alpha_{0,1}^{(1)}, \gamma_1^{(1)}$  and  $\alpha_{0,1}^{(3)}, \gamma_1^{(3)}$ , in Eq. (3.17), respectively the same design condition is provided. In addition type-2 mechanism for  $i_m = 1$  is coincident with the global one. In the case of MRF-EBF dual system with horizontal link type-1 and type-3 mechanisms for  $i_m = 1$  are coincident but by substituting the expression of their  $\alpha_0^{(g)}, \gamma^{(g)}, \alpha_{0,1}^{(1)}, \gamma_1^{(1)}$  and  $\alpha_{0,1}^{(3)}, \gamma_1^{(3)}$  respectively in Eq. (3.17) it is not possible to univocally determine the sum of reduced plastic moment at first storey because Eq. (4.27) for  $i_m = 1$  and Eq. (4.30) contain two unknown quantities, i.e. the sum of the plastic moment reduced due to the contemporary action of axial load at the first,  $\sum_{i=1}^{n_c} M_{c.i1}$ , and the second storey  $\sum_{i=1}^{n_c} M_{c.i2}$ . Therefore, a couple of other two undesired mechanism coincident are needed.

Our aid arrives the observation that type-2 and type-3 mechanism for  $i_m = n_s$  are coincident as same as their collapse mechanism multipliers  $\alpha_{0,n_s}^{(2)}$  and  $\alpha_{0,n_s}^{(3)}$  provided by Eq. (4.29) for  $i_m = n_s$  and Eq. (4.32), respectively. In addition type-1 mechanism for  $i_m = n_s$  is coincident with the global one and for this reason does not provide any design condition.

Starting from these observations the closed form solution is obtained according to the following steps:

- a) Selection of a design top sway displacement  $\delta_u$  compatible with the ductility supply of structural members (Eq. (4.38)).
- b) Computation of the slopes of mechanism equilibrium curves  $\gamma_{i_m}^{(t)}$  by means of Eqs. (3.11), (3.13) and (3.16). The slope of the global mechanism equilibrium curve,  $\gamma^{(g)}$ , is provided by Eq. (3.8) and it is the minimum among the  $\gamma_{i_m}^{(t)}$  values computed before.
- c) Design of dissipative zones, i.e. link and beam ends.
- d) Computation of the axial load acting in the columns at collapse state, i.e. when a collapse mechanism of global type is completely developed (4.16).
- e) Computation of the required sum of plastic moment of columns, reduced due to the contemporary action of the axial force,  $\sum_{i=1}^{n_c} M_{c.i.1'}$  for  $i_m = 1$ , i.e. at the first storey, by means of the following relation:

$$\sum_{i=1}^{n_c} M_{c.i.1} \geq \frac{\sum_{k=1}^{n_s} \sum_{j=1}^{n_b} W_{d.j.1} + (\gamma_1^{(3)} - \gamma^{(g)}) \delta_u \sum_{k=1}^{n_s} F_k h_k}{2 \frac{\sum_{k=1}^{n_s} F_k h_k}{h_1 \sum_{k=1}^{n_s} F_k} - 1} \quad (4.40)$$

Equation (4.40) is derived from design conditions (3.17) for  $i_m = 1$  and  $t = 1$  or  $t = 3$ , because for  $i_m = 1$  type-1 mechanism and type-3 mechanism are coincident as depicted in Figure 3.4 by assuming, as a first attempt,  $\sum_{i=1}^{n_c} M_{c.i.1}$  equal to  $\sum_{i=1}^{n_c} M_{c.i.2}$ . This assumption is, in any case, permissible because second storey columns can be at least equal or lighter than first storey one.

- f) The sum of the required plastic moments of columns at first storey is distributed among the columns proportionally to the axial load acting at the collapse state, so that, the design internal actions ( $M_{c.i.1}, N_{c.i.1}$  for  $i = 1, 2, \dots, n_c$ ) are derived and the column sections at first storey can be designed. As column sections are selected from standard shapes, the value obtained of  $\sum_{i=1}^{n_c} M_{c.i.1}$ , namely  $\sum_{i=1}^{n_c} M_{c.i.1}^*$  is generally greater than the required minimum value provided by Eq. (4.40). Therefore, the mechanism equilibrium curve  $\alpha = \alpha_0^{(g)} - \gamma^{(g)} \delta$  has to be evaluated

- accordingly, i.e. by means of Eq. (4.40) by replacing the term  $\sum_{i=1}^{n_c} M_{c.i.1}$ , with the value  $\sum_{i=1}^{n_c} M_{c.i.1}^*$  resulting from standard shapes. In addition, the multiplier of seismic horizontal forces corresponding to the ultimate design displacement can be computed as  $\alpha^{(g)} = \alpha_0^{(g)} - \gamma^{(g)} \delta_u$ .
- g) Computation of the required sum of plastic moment of columns, reduced due to the contemporary action of the axial force,  $\sum_{i=1}^{n_c} M_{c.in_s}^{(t)}$  for  $i_m = n_s$  by means of the following relation:

$$\sum_{i=1}^{n_c} M_{c.in_s}^{(3)} \geq (\alpha^{(g)} + \gamma_{n_s}^{(3)} \delta_u) F_{n_s} (h_{n_s} - h_{n_s-1}) - \sum_{j=1}^{n_b} W_{d.jn_s} + \sum_{j=1}^{n_b} W_{q.jn_s} \quad (4.41)$$

Eq. (4.41) is derived from design conditions (3.17) for  $i_m = n_s$  and  $t = 2$  or  $t = 3$ , because for  $i_m = n_s$  type-2 mechanism and type-3 mechanism are coincident as depicted in Figure 4.6.

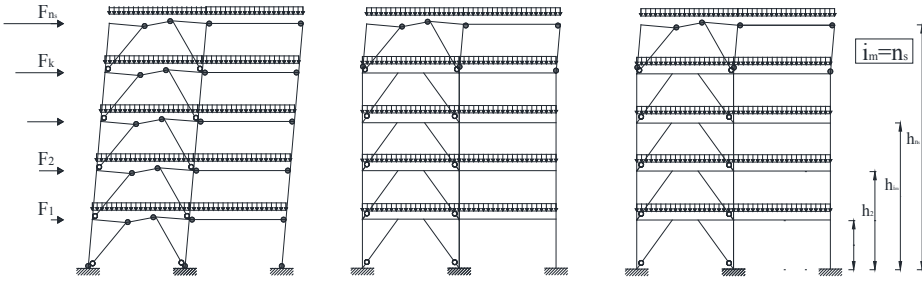


Figure 4.6 - Collapse mechanism of MRF-EBF dual systems for  $i_m = n_s$

- h) Starting from the top storey, computation of the required sum of plastic moment of columns, reduced due to the contemporary action of the axial force,  $\sum_{i=1}^{n_c} M_{c.ii_m}^{(t)}$  for  $1 \leq i_m < n_s$  and  $t = 1, 2, 3$  by means of the following relations:

$$\sum_{i=1}^{n_c} M_{c.ii_m}^{(1)} \geq (\alpha^{(g)} + \gamma_{i_m}^{(1)} \delta_u) \left( \sum_{k=1}^{i_m} F_k h_k + h_{i_m} \sum_{k=i_m+1}^{n_s} F_k \right) - \sum_{i=1}^{n_c} M_{c.i1}^* - \sum_{k=1}^{i_m} \sum_{j=1}^{n_b} W_{d.jk} + \sum_{k=1}^{i_m} \sum_{j=1}^{n_b} W_{q.jk} \quad (4.42)$$



needed to avoid type-1 mechanisms;

$$\sum_{i=1}^{n_c} M_{c.ii_m}^{(2)} \geq (\alpha^{(g)} + \gamma_{i_m}^{(2)} \delta_u) \sum_{k=i_m}^{n_s} F_k (h_k - h_{i_m-1}) - \sum_{k=i_m}^{n_s} \sum_{j=1}^{n_b} W_{d.jk} + \sum_{k=i_m}^{n_s} \sum_{j=1}^{n_b} W_{q.jk} \quad (4.43)$$

needed to avoid type-2 mechanisms;

$$\sum_{i=1}^{n_c} M_{c.ii_m}^{(3)} \geq (\alpha^{(g)} + \gamma_{i_m}^{(3)} \delta_u) (h_{i_m} - h_{i_m-1}) \sum_{k=i_m}^{n_s} F_k - \sum_{i=1}^{n_c} M_{c.ii_{m+1}}^{(3)} - \sum_{j=1}^{n_b} W_{d.ji_m} + \sum_{j=1}^{n_b} W_{q.ji_m} \quad (4.44)$$

needed to avoid type-3 mechanisms.

Eq. (4.42), (4.43) and (4.44) have been directly derived from Eq. (3.17) for  $i_m > 1$  and  $t = 1$ ,  $t = 2$  and  $t = 3$ , respectively. The term  $W_{d.jk}$  which accounts for the virtual internal work of dissipative zones, is provided in

Table 4.1.

- i) Computation of the required sum of the reduced plastic moments of columns for each storey as the maximum value among those coming from the above design conditions:

$$\sum_{i=1}^{n_c} M_{c.ii_m} = \max \left\{ \sum_{i=1}^{n_c} M_{c.ii_m}^{(1)}, \sum_{i=1}^{n_c} M_{c.ii_m}^{(2)}, \sum_{i=1}^{n_c} M_{c.ii_m}^{(3)} \right\} \quad (4.45)$$

- j) The sum of the required plastic moment of columns at each storey, reduced for the contemporary action of the axial force, is distributed among all the storey columns, proportionally to the axial force acting at collapse state. The knowledge of these plastic moments  $M_{c.ii_m}$ , coupled with the axial force  $N_{c.ii_m}$  at the collapse state, allows the design of column sections from standard shapes.

- k) If the new value of  $\sum_{i=1}^{n_c} M_{c,i1}^*$  provided by Eq. (4.45) is greater than the original value provided by Eq. (4.40) the procedure has to be restarted from point g).

#### 4.8.2 Closed form solution for MRF-EBF dual system with vertical link (Inverted Y-scheme)

Closed form solution algorithm for MRF-EBF dual systems with vertical link is the same proposed in Chapter 3 for MRFs with the only exception given by the internal virtual work related to the dissipative zones that, in this particular case, take in account also the link member which are known quantities as well as the beam sections. For this reason, Eq. (3.18) becomes as:

$$\sum_{i=1}^{n_c} M_{c,i1} \geq \frac{\sum_{k=1}^{n_s} \sum_{j=1}^{n_b} W_{d,jk} + (\gamma_1^{(3)} - \gamma^{(g)}) \delta_u \sum_{k=1}^{n_s} F_k h_k}{2 \frac{\sum_{k=1}^{n_s} F_k h_k}{h_1 \sum_{k=1}^{n_s} F_k} - 1} \quad (4.46)$$

while Eqs. (3.21), (3.22) and (3.23) become:

$$\begin{aligned} \sum_{i=1}^{n_c} M_{c,ii_m}^{(1)} \geq & (\alpha^{(g)} + \gamma_{i_m}^{(1)} \delta_u) \left( \sum_{k=1}^{i_m} F_k h_k + h_{i_m} \sum_{k=i_m+1}^{n_s} F_k \right) - \sum_{i=1}^{n_c} M_{c,i.1}^* \\ & - \sum_{k=1}^{i_m-1} \sum_{j=1}^{n_b} W_{d,jk} \end{aligned} \quad (4.47)$$

needed to avoid type-1 mechanisms;

$$\sum_{i=1}^{n_c} M_{c,ii_m}^{(2)} \geq (\alpha^{(g)} + \gamma_{i_m}^{(2)} \delta_u) \sum_{k=i_m}^{n_s} F_k (h_k - h_{i_m-1}) - \sum_{k=i_m}^{n_s} \sum_{j=1}^{n_b} W_{d,jk} \quad (4.48)$$

needed to avoid type-2 mechanisms;

$$\sum_{i=1}^{n_c} M_{c,ii_m}^{(3)} \geq (\alpha^{(g)} + \gamma_{i_m}^{(3)} \delta_u) \frac{(h_{i_m} - h_{i_m-1})}{2} \sum_{k=i_m}^{n_s} F_k - \sum_{j=1}^{n_b} W_{d,ji_m} \quad (4.49)$$

needed to avoid type-3 mechanisms, respectively.

In addition the term  $W_{d,jk}$  which accounts for the virtual internal work of dissipative zones, is provided in Table 4.1.

## 4.9 Eurocode 8 design provisions for MRF-EBF dual systems

Eurocode 8 does not provide specific hierarchy criteria for MRF-EBF dual systems, so that the design procedure for EBFs is based on simplified hierarchy criteria following the same principle also applied in case of MRFs. In particular, the application rules to design the columns is based on the use of an amplifying factor whose aim is the prevention of yielding or buckling of non-dissipative elements when the most stressed dissipative zone is yielded and strain-hardened up to its ultimate condition. Dissipative zones are constituted by link elements whose stress level is related to the following ratios [11]:

$$\Omega_i = 1.5 \frac{V_{p.link.i}}{V_{Ed.i}} \quad (4.50)$$

in case of short links, and:

$$\Omega_i = 1.5 \frac{M_{p.link.i}}{M_{Ed.i}} \quad (4.51)$$

in case of intermediate and long links, where  $V_{p.link.i}$  and  $M_{p.link.i}$  are the plastic design resistance under pure shear and bending respectively, 1.5 is an overstrength factor and  $V_{Ed.i}$  and  $M_{Ed.i}$  are the internal actions, shear and bending moment respectively, occurring in the  $i$ -th link element under the seismic load combination.

The minimum value among all the  $\Omega_i$  ratios, computed for each link element, obviously identifies the most stressed link. In order to assure as more as possible a uniform participation of all the links to the dissipation of the earthquake input energy, Eurocode 8 suggests that the difference between the maximum and the minimum value of  $\Omega_i$  should not be greater than 25% of the minimum value. Regarding non-dissipative elements, i.e. columns, beams and diagonal braces the most unfavourable combination of the axial force and bending moments has to be considered to check the following requirement [11]:

$$N_{pl.Rd}(M_{Ed}, V_{Ed}) \geq N_{Ed,G} + 1.1\gamma_{ov}\Omega N_{Ed,E} \quad (4.52)$$

where:

- $N_{pl,Rd}(M_{Ed}, V_{Ed})$  is the axial design resistance evaluated considering the interaction with the bending moment,  $M_{Ed}$ , and the shear,  $V_{Ed}$ , occurring in the seismic load combination;

$N_{Ed,G}$  is the axial force due to non-seismic loads included in the seismic load combination;

- $N_{Ed,E}$  is the axial force due to seismic loads only;
- $\gamma_{ov}$  is an overstreight coefficient taking in account random material variability;
- $\Omega$  is the minimum value of  $\Omega_i$  computed among all the links.

It is easy to recognize that the above design criterion is able to prevent yielding or buckling of non-dissipative elements before yielding of the most stressed link element, but cannot assure a pattern of yielding involving all the links. In fact, seismic resistant structural schemes, as the one herein examined, are complex systems where resistant mechanisms are partly located in series and partly in parallel or like a combination of resistant mechanisms in series and resistant mechanisms in parallel. Eq. (4.52) does not possess any theoretical background under the point of view of failure mode control.

The analyses of the case studies presented and discussed in Chapter 5 demonstrate that, even in the case of a dual system where EBFs are integrated by MRFs, acting as a secondary fail safe system, the use of Eq. (4.52) is not able to prevent the development of partial mechanisms and for some earthquake records even the occurrence of soft-storey mechanisms.

# CHAPTER 5

## NUMERICAL APPLICATIONS AND VALIDATION OF TPMC

### 5.1 Introduction

In this chapter, numerical applications and a first validation of the Theory of Plastic Mechanism Control (TPMC) are reported. It is important to underline that the validation of the design procedure is usually carried out in two phases. After designing a significant number of structural schemes, the first phase requires that the structures have analysed by means of push-over analysis while in a second phase also incremental dynamic non-linear analyses (IDA) are developed in order to investigate the pattern of yielding under severe seismic motions and the possible influence of higher mode effects. These analyses, constituting the complete validation of the proposed design procedure, will be presented in Chapter 6. Conversely, in this chapter the validation of the TPMC design procedure has been led with reference only to push-over analyses.

In Chapter 4 two different approaches for the design of MRF-EBF dual system have been proposed. The first one is based on TPMC in its closed form solution for MRF-EBF dual systems, the second one is the design methodology proposed by Eurocode 8. Both this methods have the main aim to assure an adequate post-elastic behaviour of the structure in term of ductility against of seismic events. This goal can be reached by concentrating the yielding only in the dissipative zones, i.e. link and beam ends, and trying to assure that non dissipative zones, such as the column remain in elastic range. However, only

TPMC assures the development of a global type, that is the considered the optimum mechanism typology, while EC8 provisions are able only to prevent soft storey mechanisms.

Aiming at the evaluation of its accuracy, the TPMC has been implemented and applied to dimension an adequate number of MRF-EBF dual system (in this work only a sample of 8 structures designed by TPMC are reported). The validation of the procedure has been carried out both comparing the theoretical curve, i.e. the collapse mechanism equilibrium curve with the push-over one than comparing the pattern hinge distribution obtained by the push-over analysis with that corresponding to the global mechanism (Appendix A).

It is also important to observe that only short link have been considered for the design of structures because they present more advantages respect to the long and intermediate links. In fact, the main parameter governing the seismic response of such structural typology, both in elastic and post-elastic range, is the length  $e$  of the links, constituting the dissipative zones. In fact, this parameter influences the lateral stiffness of the structure, the ability to dissipate the seismic input energy and the link plastic rotation demands. In particular, the lateral stiffness of the bracing system increases as far as the link length decreases [50]. It is possible to recognise that eccentrically braced frames are very sensitive to the variation of the ratio between the link length and the bay span  $e/L$ , since, at least for  $e/L < 0.4$ , a little decrease of this parameter is responsible of a significant increase in lateral stiffness. This effect is more and more important as far as  $e/L$  decreases, and it is more evident in K scheme (where two diagonal braces are connected at the ends of the link located at beam mid-span) rather than in D ones (where there is only one brace element and the link is connected directly to the column). The limit case  $e/L = 0$  can be ideally associated to the case of concentrically braced frames providing the highest lateral stiffness, while, conversely, the case of  $e/L = 1$  is representative of moment resisting frames, providing the minimum lateral stiffness.

In addition, depending on the length  $e$ , the mechanical behaviour of links varies from pure shear to pure bending and it governs the cyclic response, i.e. the dissipative capacity of the structure. It is well known that, under this point of view, links are classified into three categories, namely short, intermediate and long links, depending on the ratio  $M_p/V_p$  as reported in Chapter 2. The shear action is dominant for  $e \leq 1.6M_p/V_p$  (i.e. in case of short links), while the bending

moment becomes more and more relevant as far as the link length  $e$  increases, until it becomes dominant for  $e \geq 3M_p/V_p$  (i.e. in case of long links).

Due to their performance in terms of both stiffness and ductility, short links are in several cases the most suitable choice for seismic-resistant EBFs. In fact, the cyclic behaviour of short links is characterised by wide and stable cycles allowing the development of high energy dissipation capacity, provided that adequate web stiffeners are adopted along the element length to prevent web local buckling. In such a case, high rotation capacity has been experimentally exhibited by short links when compared to intermediate and long ones [46], [63-64]. Several tests have clearly shown that a properly stiffened short link can sustain plastic rotations up to  $\pm 0.08$  [11] rad under cyclic loading conditions or up to 0.20 rad under monotonic loading conditions. Despite of web stiffeners, shear buckling has been typically observed as the controlling failure mode, but the mechanism is delayed allowing the complete distribution of the inelastic shear strains over the whole length of the link.

Conversely, long links are characterised by a completely different failure mechanism where large flexural deformations lead to the fracture of tensile flanges or to the lateral torsional buckling of compressed ones. As a result, maximum plastic rotations up to  $\pm 0.02$  rad have been experimentally measured [7]. Finally, intermediate links are characterised by a combination of the previously discussed effects, depending on the combination of shear force and bending moment.

From the design point of view, on one hand, it has to be considered that short links provide the highest plastic rotation supply, but also, on the other hand, the highest plastic rotation demand for a given lateral displacement; the opposite case occurs when long links are adopted, while intermediate links provide an intermediate behaviour. For this reason, care has to be taken in the selection of the link length, which governs the overall ultimate behaviour, the local ductility (both demand and supply) and the stiffness of the structure. Consequently, the main goal of the design process of an eccentrically braced frame is the identification of the best compromise between the need, on one hand, to develop high lateral stiffness and plastic rotation supply which increase as far as the link length decreases and, on the other hand, the need to reduce the plastic rotation demands which, conversely, decrease as far as the link length increases.

For this series of resonances, only short links are used to design the structures reported in this work.

## 5.2 Study cases

The study cases herein investigated are referred to a building whose plan configuration is depicted in Figure 5.1. The seismic resistant structural system is a perimeter system constituted by MRF-EBF dual systems while the inner bays are pinned and designed only for gravity loads. The building constituting the study cases are of both 6-storeys and 8-storeys and have been designed, both according to TPMC and EC8. As regards the resistant scheme it is a MRF-EBF dual system whose EBF part is configured with K-scheme, D-scheme, V-scheme and inverted Y-scheme. Therefore, a total of 16 study cases have been analysed. The seismic response of the buildings is herein analyzed with reference to the longitudinal direction only. The corresponding seismic resistant schemes are depicted in Figure 5.2, Figure 5.3, Figure 5.4 and Figure 5.5, for the K-scheme, D-scheme, V-scheme and inverted Y-scheme, respectively. In addition in such figures also the leaning column adopted in structural modelling to account for second order effects due to the internal gravity load resisting system is reported. The scope of the leaning column is to take into account the gravity loads acting in the leaning part of the structure which cannot be negligible both in term of structural seismic masses than in term of second order effects. Being the structural schemes adopted both with horizontal and vertical link the selection of the link length become of relevant importance because governs the ultimate design displacement. They have been selected equal to 1.20 m for the K-scheme, D-scheme and V-scheme buildings and 0.70 m for the inverted Y-scheme, at each storey. The characteristic values of the vertical loads are equal to 4.0 kN/m<sup>2</sup> and 2.0 kN/m<sup>2</sup> for permanent ( $G_k$ ) and live ( $Q_k$ ) loads, respectively. As a consequence, with reference to the seismic load combination provided by EC8 [11],  $G_k + \psi_2 Q_k + E_d$  (where  $\psi_2$  is the coefficient for the quasi-permanent value of the variable actions, equal to 0.3 for residential buildings), the vertical loads acting on the floor are equal to 4.6 kN/m<sup>2</sup>. The structural material adopted for all the members is S355 steel grade ( $f_{yk} = 355 \text{ MPa}$ ). The beams of the MRF part have been designed to withstand vertical loads accounting also for serviceability requirements. They are delivered in Figure 5.2, Figure 5.3, Figure 5.4 and Figure 5.5, for the K-scheme, D-scheme, V-scheme and inverted Y-scheme, respectively,



and are the same both for the buildings designed according to TPMC and for the buildings designed according to Eurocode 8. The design horizontal forces have been determined according to EC8, assuming a peak ground acceleration equal to 0.35g, a seismic response factor equal to 2.5, a behaviour factor equal to 6 [11]. On the basis of such force distribution, the design shear action of link members has been obtained by assuming that the storey shear is completely entrusted to the link. The sections of the links which are considered as short links, are the same both for TPMC and EC8 designed structures. Link length has been defined in order to assure that the ultimate design displacement,  $\delta_u$ , of TPMC based designed is the same both for the K-scheme and inverted Y-scheme, according to the following relations for K-scheme, D-scheme, V-scheme:

$$\delta_u = \gamma_u (e/L_j) h_{n_s} = 0.08(1.2/6) h_{n_s} = 0.016 h_{n_s} \quad (5.1)$$

and inverted Y-scheme:

$$\delta_u = \gamma_u (e/h_i) h_{n_s} = 0.08(0.7/3.5) h_{n_s} = 0.016 h_{n_s} \quad (5.2)$$

where  $\gamma_u$  is the target link plastic rotation,  $e$  is the link length,  $L_j$  is the braced bay length,  $h_i$  is the interstorey height and  $h_{n_s}$  is the building height. In Table 5.1, Table 5.2, Table 5.3 and Table 5.4 the link and diagonal sections for the designed structures are reported. In addition, in the same tables, the values of the overstrength factor,  $\Omega_i$ , of link elements computed according to EC8 are reported. It can be observed that the ratio between the maximum  $\Omega_i$  value and the minimum one is not ever less than the limit value suggested by EC8 (equal to 1.25) to promote the yielding of all the link elements. Notwithstanding, the results of push-over analyses, presented in the following, have pointed out that all the links are yielded. Conversely, the design methodology significantly affects the column sections (Table 5.5, Table 5.6, Table 5.7 and Table 5.8). In particular, the application of the TPMC leads to bigger columns at all the storeys. In addition, in Table 5.9 the collapse mechanism multipliers,  $\alpha_0$ , and the slopes of mechanism equilibrium curves,  $\gamma$ , for the structure designed by means of TPMC are reported. In these tables it is also useful to observe that for the same structural height the slope of the mechanism equilibrium curve are the same because they are only related to the second order effects.

Regarding the application of Eurocode 8, the requirements reported in §4.9 have been used. In addition, it has also to be considered that, in the analysed design examples, also the beam-to-column hierarchy criterion, usually suggested

for MRFs, has been applied in column design. As it will be observed in the following section, the main benefit coming from the use of dual systems is due to the ability of the moment-resisting part to work as a survival secondary structural system which is engaged in plastic range after the spreading of yielding in the primary structural system constituted by the braced part.

Finally, serviceability requirements for all the designed structures have been checked.

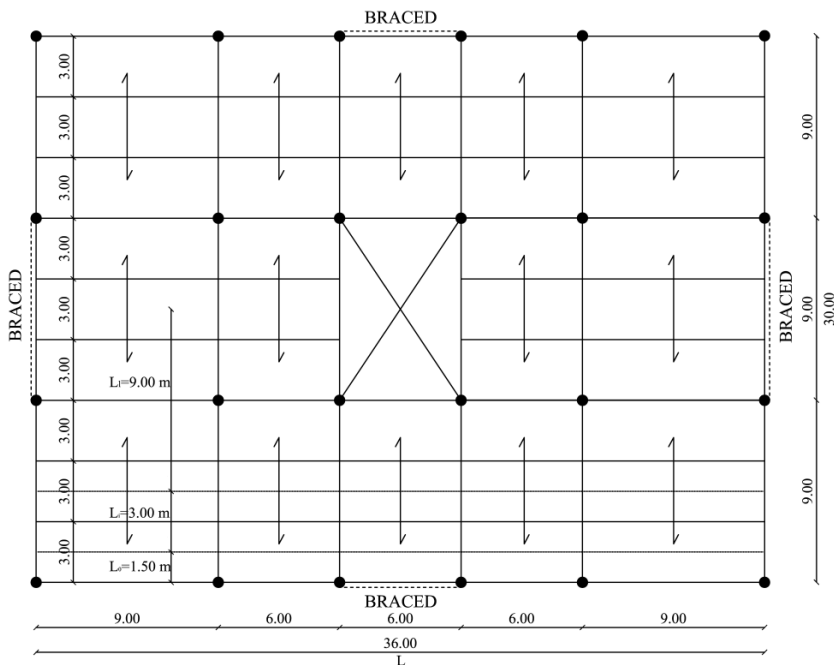


**Figure 5.1** - Plan configuration of the analyzed buildings

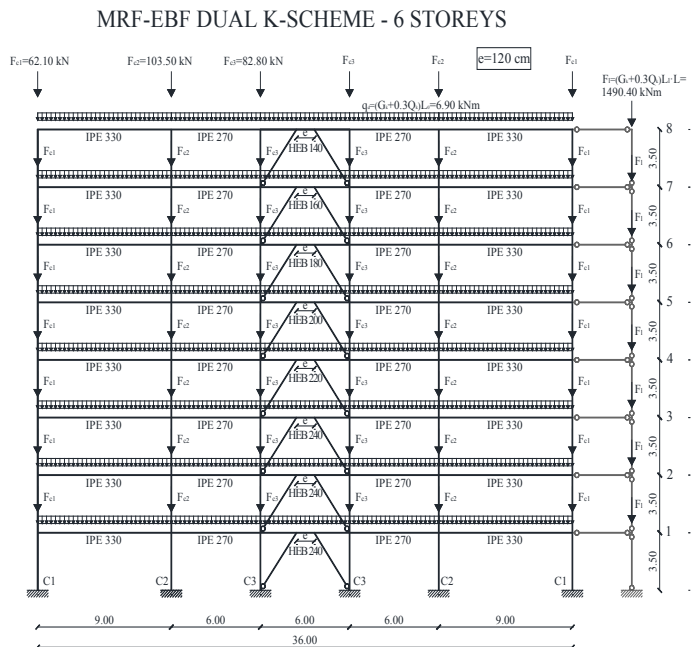
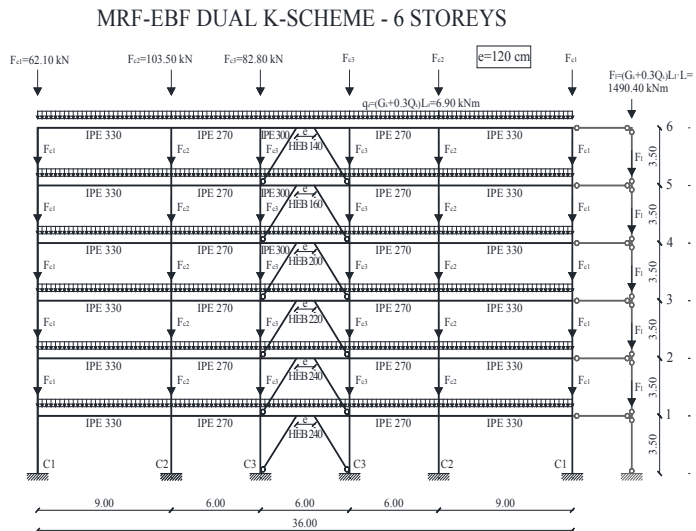


**Figure 5.2 - Structural schemes of the longitudinal seismic resistant system for 6-storey and 8-storey building (K-scheme)**

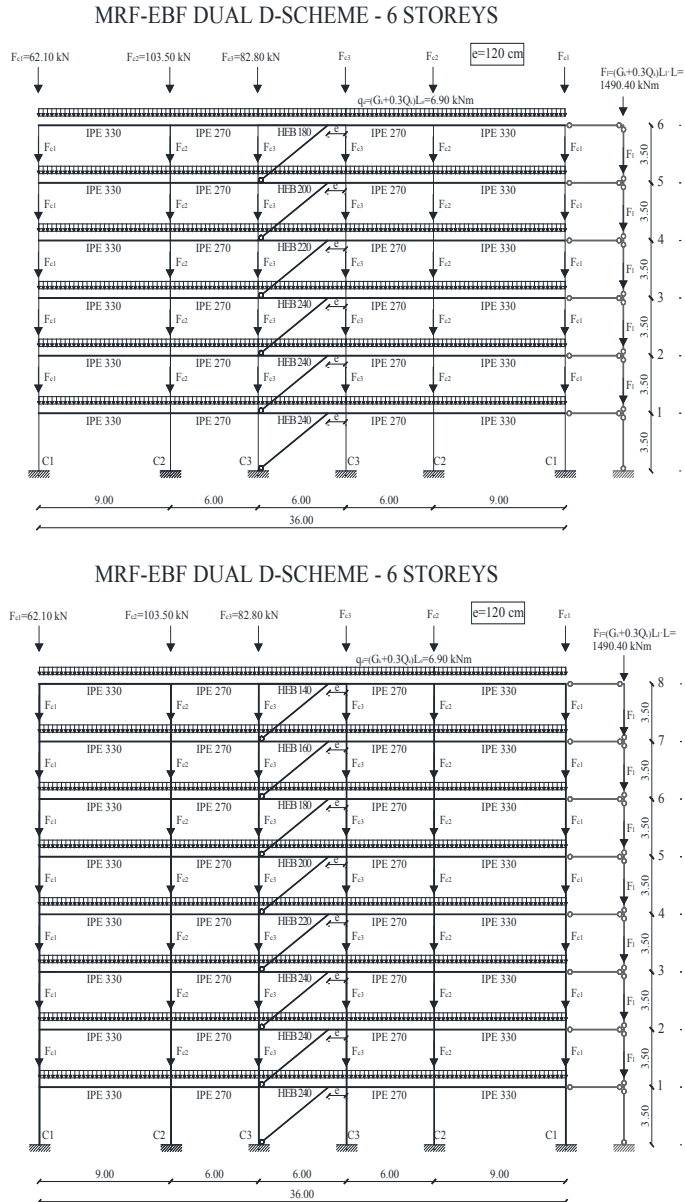
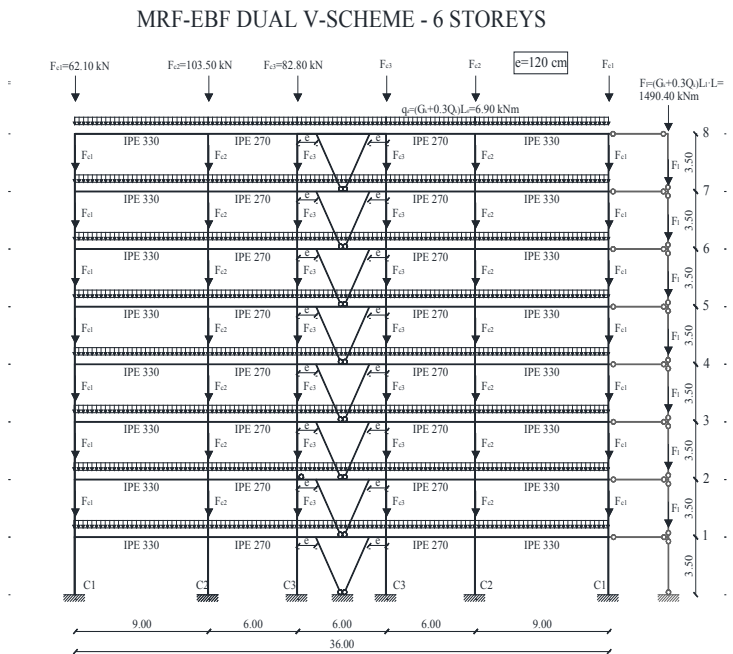
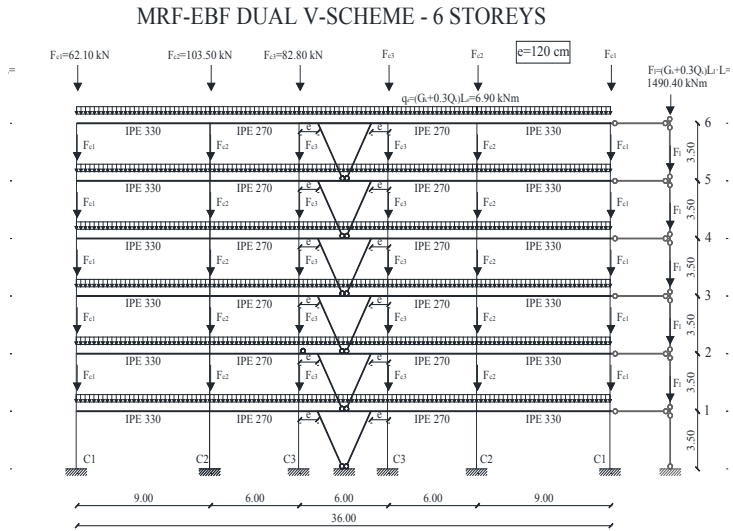


Figure 5.3 - Structural schemes of the longitudinal seismic resistant system for 6-storey and 8-storey building (D-scheme)



**Figure 5.4 - Structural schemes of the longitudinal seismic resistant system for 6-storey and 8-storey building (V-scheme)**

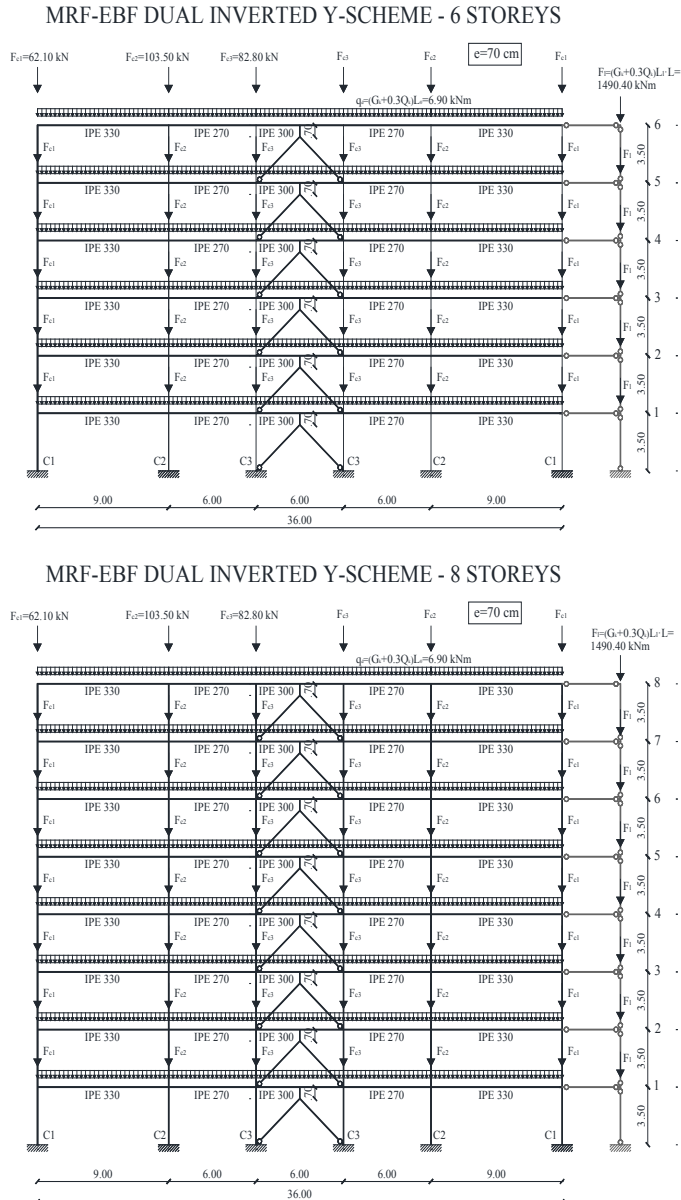


Figure 5.5 - Structural schemes of the longitudinal seismic resistant system for 6-storey and 8-storey building (inverted Y-scheme)

**Table 5.1** - Design seismic forces, link and diagonal sections for K-scheme buildings

	STOREY $i_m$	F [kN]	LINKS (K-scheme)	$\Omega_i$ (K-scheme)	DIAGONAL SECTIONS
	6-STORY BUILDING	1	50.643	HE 240 B	1.53
2		101.285	HE 240 B	1.24	CHS 355.6x16
3		151.928	HE 220 B	1.24	CHS 355.6x16
4		202.571	HE 200 B	1.29	CHS 355.6x16
5		253.214	HE 160 B	1.38	CHS 355.6x16
6		303.856	HE 140 B	2.01	CHS 355.6x16
	STOREY $i_m$	F [kN]	LINKS (K-scheme)	$\Omega_i$ (K-scheme)	DIAGONAL SECTIONS
	8-STORY BUILDING	1	31.745	HE 240 B	1.74
2		63.489	HE 240 B	1.21	CHS 406.4x32
3		95.234	HE 240 B	1.22	CHS 406.4x32
4		126.978	HE 220 B	1.20	CHS 406.4x32
5		158.723	HE 200 B	1.23	CHS 406.4x32
6		190.467	HE 180 B	1.34	CHS 406.4x32
7		222.212	HE 160 B	1.64	CHS 406.4x32
8		253.956	HE 140 B	2.63	CHS 406.4x32

**Table 5.2** - Design seismic forces, link and diagonal sections for D-scheme buildings

	STOREY $i_m$	F [kN]	LINKS (D-scheme)	$\Omega_i$ (D-scheme)	DIAGONAL SECTIONS
	6-STORY BUILDING	1	50.643	HEB 200	1.34
2		101.285	HEB 200	1.28	CHS 355.6x16
3		151.928	HEB 200	1.29	CHS 355.6x16
4		202.571	HEB 180	1.39	CHS 355.6x16
5		253.214	HEB 160	1.46	CHS 355.6x16
6		303.856	HEB 160	2.68	CHS 355.6x16
	STOREY $i_m$	F [kN]	LINKS (D-scheme)	$\Omega_i$ (D-scheme)	DIAGONAL SECTIONS
	8-STORY BUILDING	1	31.745	HEB 340	1.36
2		63.489	HEB 340	1.15	CHS 406.4x32
3		95.234	HEB 320	1.24	CHS 406.4x32
4		126.978	HEB 300	1.22	CHS 406.4x32
5		158.723	HEB 280	1.24	CHS 406.4x32
6		190.467	HEB 240	1.37	CHS 406.4x32
7		222.212	HEB 200	1.79	CHS 406.4x32
8		253.956	HEB 140	3.73	CHS 406.4x32

**Table 5.3** - Design seismic forces, link and diagonal sections for V-scheme buildings

	STOREY $i_m$	F [kN]	LINKS	$\Omega_i$	DIAGONAL
			(V-scheme)	(V-scheme)	SECTIONS
6-STORY BUILDING	1	50.643	HE 240 B	1.59	CHS 355.6x16
	2	101.285	HE 240 B	1.29	CHS 355.6x16
	3	151.928	HE 220 B	1.33	CHS 355.6x16
	4	202.571	HE 200 B	1.41	CHS 355.6x16
	5	253.214	HE 160 B	1.74	CHS 355.6x16
	6	303.856	HE 140 B	2.43	CHS 355.6x16
8-STORY BUILDING	1	31.745	HE 240 B	1.73	CHS 406.4x32
	2	63.489	HE 240 B	1.22	CHS 406.4x32
	3	95.234	HE 240 B	1.28	CHS 406.4x32
	4	126.978	HE 220 B	1.39	CHS 406.4x32
	5	158.723	HE 200 B	1.36	CHS 406.4x32
	6	190.467	HE 180 B	1.56	CHS 406.4x32
	7	222.212	HE 160 B	2.15	CHS 406.4x32
	8	253.956	HE 140 B	5.50	CHS 406.4x32

**Table 5.4** - Design seismic forces, link and diagonal sections for inverted Y-scheme buildings

	STOREY $i_m$	F [kN]	LINKS	$\Omega_i$	DIAGONAL
			(Inv. Y-scheme)	(Inv. Y-scheme)	SECTIONS
6-STORY BUILDING	1	50.643	HEB 200	1.20	CHS 244.5x20
	2	101.285	HEB 200	1.16	CHS 244.5x20
	3	151.928	HEB 200	1.19	CHS 244.5x20
	4	202.571	HEB 180	1.16	CHS 244.5x20
	5	253.214	HEB 160	1.29	CHS 244.5x20
	6	303.856	HEB 160	1.44	CHS 244.5x20
8-STORY BUILDING	1	31.745	HEB 340	1.26	CHS 406.4x32
	2	63.489	HEB 340	1.22	CHS 406.4x32
	3	95.234	HEB 320	1.17	CHS 406.4x32
	4	126.978	HEB 300	1.19	CHS 406.4x32
	5	158.723	HEB 280	1.28	CHS 406.4x32
	6	190.467	HEB 240	1.28	CHS 406.4x32
	7	222.212	HEB 200	1.37	CHS 406.4x32
	8	253.956	HEB 140	1.91	CHS 406.4x32



**Table 5.5** – Column sections for the K-scheme buildings

	STOREY	TPMC			EUROCODE 8			
		$t_m$	C1	C2	C3	C1	C2	C3
K-scheme	6-STORY BUILDING	1	HEB 300	HEB 300	HEB 500	HEB 200	HEB 240	HEB 400
		2	HEB 300	HEB 300	HEB 450	HEB 200	HEB 240	HEB 340
		3	HEB 300	HEB 300	HEB 450	HEB 200	HEB 240	HEB 280
		4	HEB 300	HEB 300	HEB 450	HEB 200	HEB 240	HEB 260
		5	HEB 300	HEB 300	HEB 360	HEB 200	HEB 240	HEB 220
		6	HEB 240	HEB 260	HEB 260	HEB 200	HEB 240	HEB 220
	8-STORY BUILDING	1	HEB 320	HEB 340	HEB 650	HEB 220	HEB 240	HEB 500
		2	HEB 320	HEB 340	HEB 600	HEB 220	HEB 240	HEB 400
		3	HEB 320	HEB 340	HEB 600	HEB 220	HEB 240	HEB 360
		4	HEB 320	HEB 340	HEB 550	HEB 220	HEB 240	HEB 360
		5	HEB 320	HEB 340	HEB 500	HEB 220	HEB 240	HEB 340
		6	HEB 320	HEB 320	HEB 450	HEB 220	HEB 240	HEB 320
		7	HEB 300	HEB 300	HEB 360	HEB 220	HEB 240	HEB 300
		8	HEB260	HEB260	HEB260	HEB 220	HEB 240	HEB 260

**Table 5.6** – Column sections for the V-scheme buildings

	STOREY	TPMC			EUROCODE 8			
		$t_m$	C1	C2	C3	C1	C2	C3
V-scheme	6-STORY BUILDING	1	HEB 280	HEB 280	HEB 550	HEB 200	HEB 240	HEB 500
		2	HEB 280	HEB 280	HEB 500	HEB 200	HEB 240	HEB 500
		3	HEB 280	HEB 280	HEB 450	HEB 200	HEB 240	HEB 500
		4	HEB 280	HEB 280	HEB 450	HEB 200	HEB 240	HEB 500
		5	HEB 280	HEB 280	HEB 400	HEB 200	HEB 240	HEB 500
		6	HEB 260	HEB 260	HEB 360	HEB 200	HEB 240	HEB 400
	8-STORY BUILDING	1	HEB 300	HEB 320	HEB 700	HEB 220	HEB 240	HEB 650
		2	HEB 300	HEB 320	HEB 650	HEB 220	HEB 240	HEB 450
		3	HEB 300	HEB 320	HEB 600	HEB 220	HEB 240	HEB 360
		4	HEB 300	HEB 320	HEB 600	HEB 220	HEB 240	HEB 300
		5	HEB 300	HEB 320	HEB 550	HEB 220	HEB 240	HEB 260
		6	HEB 300	HEB 320	HEB 550	HEB 220	HEB 240	HEB 220
		7	HEB 300	HEB 300	HEB 500	HEB 220	HEB 240	HEB 220
		8	HEB 280	HEB 280	HEB 400	HEB 220	HEB 240	HEB 220

Table 5.7 – Column sections for the D-scheme buildings

	STOREY	TPMC			EUROCODE 8			
		$i_m$	C1	C2	C3	C1	C2	C3
D-scheme	6-STOREY BUILDING	1	HEB 280	HEB 280	R=HEB 550 L=HEB 500	HEB 200	HEB 240	HEB 360
		2	HEB 280	HEB 280	R=HEB 500 L=HEB 450	HEB 200	HEB 240	R=HEB 340 L=HEB 300
		3	HEB 280	HEB 280	R=HEB 450 L=HEB 400	HEB 200	HEB 240	R=HEB 300 L=HEB 240
		4	HEB 280	HEB 280	R=HEB 450 L=HEB 400	HEB 200	HEB 240	R=HEB 280 L=HEB 240
		5	HEB 280	HEB 280	R=HEB 450 L=HEB 340	HEB 200	HEB 240	R=HEB 280 L=HEB 240
		6	HEB 280	HEB 280	R=HEB 400 L=HEB 260	HEB 200	HEB 240	R=HEB 240 L=HEB 220
	8-STOREY BUILDING	1	HEB 300	HEB 320	HEB 700	HEB 220	HEB 240	R=HEB 700 L=HEB 600
		2	HEB 300	HEB 320	HEB 650	HEB 220	HEB 240	HEB 500
		3	HEB 300	HEB 320	HEB 600	HEB 220	HEB 240	R=HEB 400 L=HEB 340
		4	HEB 300	HEB 320	R=HEB 600 L=HEB 550	HEB 220	HEB 240	R=HEB 320 L=HEB 300
		5	HEB 300	HEB 320	HEB 550	HEB 220	HEB 240	R=HEB 280 L=HEB 260
		6	HEB 300	HEB 320	R=HEB 550 L=HEB 500	HEB 220	HEB 240	R=HEB 260 L=HEB 240
		7	HEB 300	HEB 320	R=HEB 500 L=HEB 400	HEB 220	HEB 240	R=HEB 240 L=HEB 220
		8	HEB 300	HEB 300	R=HEB 400 L=HEB 280	HEB 220	HEB 240	R=HEB 200 L=HEB 180

**Table 5.8** – Column sections for the inverted Y-scheme buildings

	STOREY	TPMC			EUROCODE 8			
		$i_m$	C1	C2	C3	C1	C2	C3
Inverted Y-scheme	6-STORY BUILDING	1	HEB 300	HEB 300	HEB 500	HEB 200	HEB 240	HEB 400
		2	HEB 300	HEB 300	HEB 450	HEB 200	HEB 240	HEB 340
		3	HEB 300	HEB 300	HEB 450	HEB 200	HEB 240	HEB 280
		4	HEB 300	HEB 300	HEB 450	HEB 200	HEB 240	HEB 260
		5	HEB 300	HEB 300	HEB 360	HEB 200	HEB 240	HEB 220
		6	HEB 240	HEB 260	HEB 260	HEB 200	HEB 240	HEB 220
	8-STORY BUILDING	1	HEB 320	HEB 340	HEB 650	HEB 220	HEB 240	HEB 500
		2	HEB 320	HEB 340	HEB 600	HEB 220	HEB 240	HEB 400
		3	HEB 320	HEB 340	HEB 600	HEB 220	HEB 240	HEB 360
		4	HEB 320	HEB 340	HEB 550	HEB 220	HEB 240	HEB 360
		5	HEB 320	HEB 340	HEB 500	HEB 220	HEB 240	HEB 340
		6	HEB 320	HEB 320	HEB 450	HEB 220	HEB 240	HEB 320
		7	HEB 300	HEB 300	HEB 360	HEB 220	HEB 240	HEB 300
		8	HEB260	HEB260	HEB260	HEB 220	HEB 240	HEB 260

**Table 5.9** – Collapse mechanism multiplier and slope of mechanism equilibrium curve of TPMC designed structures

	K-scheme		D-scheme		V-scheme		Inv. Y-scheme	
	$\alpha_0$	$\gamma$	$\alpha_0$	$\gamma$	$\alpha_0$	$\gamma$	$\alpha_0$	$\gamma$
<b>6-storey</b>	2.1428	0.004851	2.1009	0.004851	2.1394	0.004851	2.1994	0.004851
<b>8-storey</b>	2.0803	0.004439	2.0415	0.004439	2.0567	0.004439	2.1279	0.004439

### 5.3 Validation by means of push-over analyses

With reference to the longitudinal seismic resistant system of the designed buildings, push-over analyses have been carried out by means of SAP2000 computer program [57] both for the structures designed by means of TPMC and EC8. The aim of these analyses is to check the collapse mechanism actually developed to provide a first quick comparison between the performances in plastic range of the structures designed.

Member yielding has been taken in account by modelling the dissipative zones by means of hinge elements, i.e. with a lumped plasticity model. Column, beam, diagonal and link members have been modelled with an elastic beam-column frame element with two rigid-plastic hinge elements located at the member ends. With reference to beams, plastic hinge properties are defined in

pure bending (M3 hinge) while in case of columns and diagonals plastic hinge properties are defined to account for the interaction between bending and axial force (P-M3 hinges). Despite of diagonal members are also subjected to compression, so that their buckling in compression could be modelled as suggested in D'Aniello et al. [70], their modelling has been carried out by neglecting the possibility of occurrence of buckling, because they are designed to assure a buckling resistance greater than the axial force transmitted by the link elements in their fully yielded and strain-hardened state corresponding to the ultimate conditions. Both of them have a rigid plastic constitutive model for the moment rotation behaviour. Regarding link members, as short links yielding in shear are of concern, their behaviour is governed by shear. However, as preliminarily reported in previous chapters it is more useful to exploit the concept of equivalent moment (Eq. (4.9)). For this reason, plastic hinges in pure bending moment (M3) have been considered, with a tri-linear bending moment versus plastic rotation rigid-hardening-perfectly plastic as depicted in Figure 5.6. In particular, in this case, an overstrength of 1.5 has been confirmed for a link plastic rotation of 0.08 rad [71-72]. However, for very short links, with compact cross sections and perfect axial restraints, and for built up links with very compact shape and short length, larger values of shear overstrength are expected.

The use of a rigid-hardening behaviour for the plastic shear hinges of link elements is justified because of the significant overstrength that link elements are able to exhibit [3], [33], [38], [42]. Even though many doubts have been raised concerning the amount of overstrength arising in short links due to strain-hardening ([44-46], [48], [54-55]) the overstrength factor has been assumed equal to 1.50 as suggested in code provisions for short link. This choice is further justified considering the results of a recent research activity aimed at the investigation of the shear overstrength of links by means of FE model analyses [71]. In particular, the authors pointed out that three basic parameters have a combined effect on link shear overstrength: (i) axial forces, (ii) the ratio of flange over web area and (iii) the ratio of link length and cross section depth. By means of an analytical model for predicting the overstrength of shear links with or without restraint, they underlined that the larger is the area of flanges and the shorter is the link, the larger is the link shear force developed at a given link rotation, for given boundary conditions.

The push-over analyses have been led under displacement control taking into account both geometrical and mechanical non-linearities. In addition, out-

of-plane stability checks of compressed members have been performed at each step of the non-linear analysis for both the examined structures.

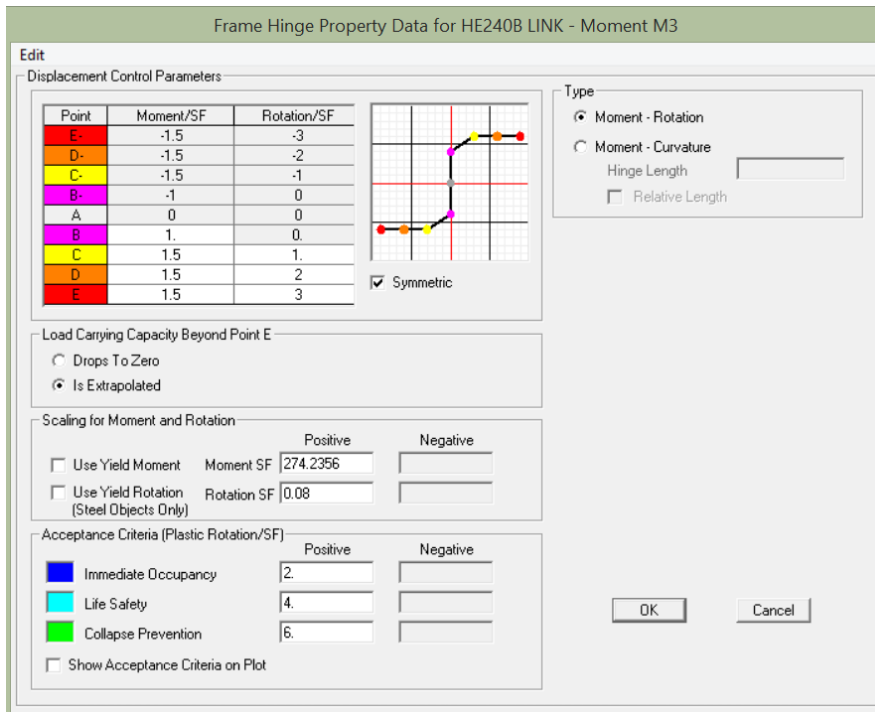


**Figure 5.6** – Plastic hinge modeling of the link using the concept of equivalent moment

The results provided by the pushover analyses are reported in Figure 5.7, Figure 5.8 where both the push-over curves and the mechanism equilibrium curves corresponding to the global mechanism are depicted. In particular, the results provided by the analyses show that the softening branch of the push-over curve corresponding to the structure designed by means of the proposed procedure, i.e. TPMC, tends towards the mechanism equilibrium curve obtained by means of second order rigid-plastic analysis. It is also useful to underline that, in the examined cases, push-over curves exhibit a softening behavior, because the occurrence of strain-hardening in shear links does not counterbalance the softening due to second order effects.

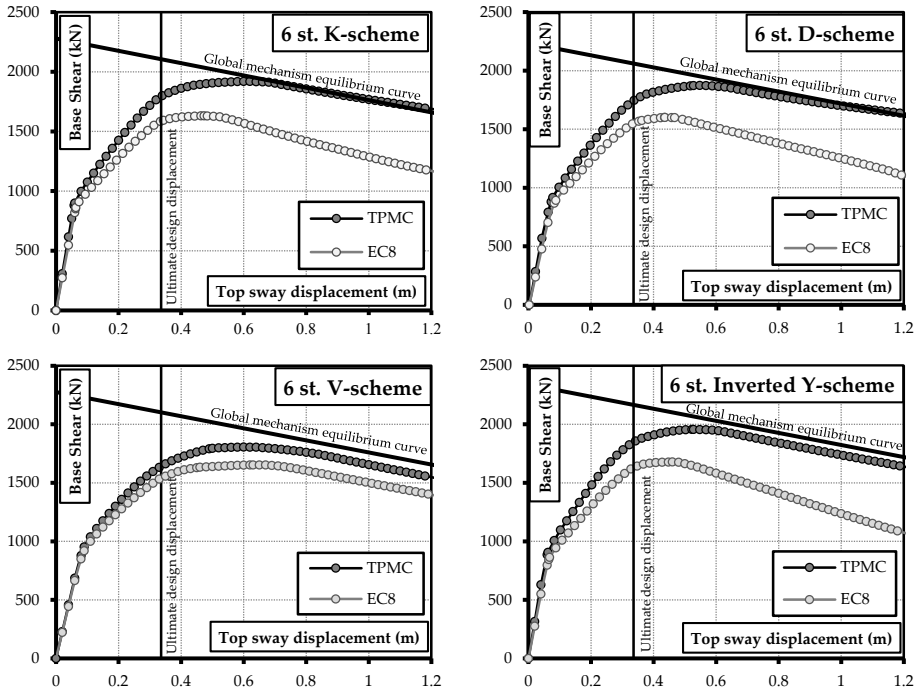
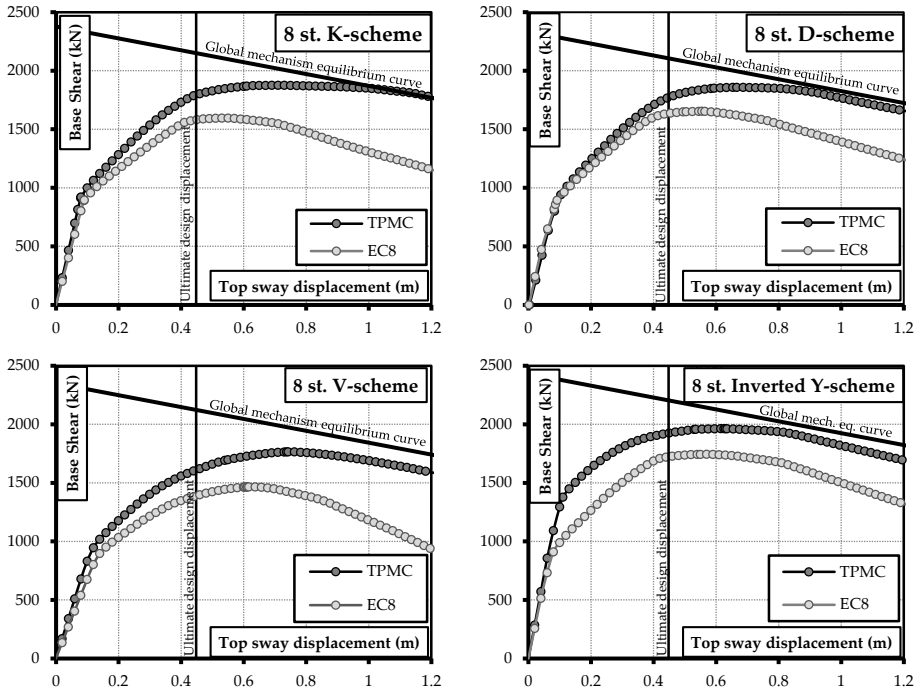


Figure 5.7 – Push-over curves for 6-storey structures designed with TPMC and EC8

Regarding the push-over curves of structures designed by means of Eurocode 8, it can be observed that they exhibit a less stiffness and strength compared to the proposed design procedure. However, the most important difference between the two structural solutions is the collapse mechanism typology pointed out by the push-over analyses plastic hinge patterns reported in the Appendix A. In particular, with reference to the proposed design procedure, these figures show the distribution of plastic hinges developed when for a level of the top sway displacement equal to the ultimate design displacement,  $\delta_u$ . The results confirm the accuracy of the proposed design procedure, being the pattern of yielding in perfect agreement with the global mechanism.

Conversely, the structures designed according to Eurocode 8 always exhibit a partial storey mechanisms which goes from a minimum of two storeys involved (6-storey building with inverted Y-scheme) to a maximum of three storey

(Appendix A). However, because of its high lateral stiffness, the braced part of the structural scheme is able to promote the spreading of yielding at all the storey, so that all the links are yielded.



**Figure 5.8** – Push-over curves for 8-storey structures designed with TPMC and EC8





# CHAPTER 6

## EC8 VS TPMC: PERFORMANCE EVALUATION

### 6.1 Introduction

In this chapter the investigation of the seismic response of MRF-EBF dual systems is reported. In particular, a further validation of the proposed design methodology called Theory of Plastic Mechanism Control (TPMC) has been gained by means of Incremental Dynamic Analyses (IDA) [73] which are aimed, on one hand, to confirm the pattern of yielding actually developed and, on the other hand, to compare the structural solutions in terms of local ductility demands, under seismic actions and energy dissipation capacity. In particular, in this chapter only the K-scheme and inverted Y-scheme 6-storey and 8-storey frame are analysed. K-scheme has been selected because it is the most common EBF scheme with horizontal link configuration.

Both the structures designed according to Eurocode 8 and those designed according to TPMC have been subjected to IDA analyses carried out using the Sap2000 computer program [57] by means of the same structural model already adopted for push-over analyses reported in Chapter 5. Rayleigh formulation for a 5% damping has been assumed with the proportional factors computed with reference to the first and third mode of vibration. They are reported in Table 6.2 for the examined structures. Record-to-record variability has been accounted for by considering 10 recorded accelerograms selected from PEER data base [68]. In Table 6.1 the analysed records (name, date, magnitude, ratio between PGA and

gravity acceleration, length and step recording) have been reported. These recorded accelerograms have been selected to approximately match the linear elastic design response spectrum of Eurocode 8, for soil type A and PGA of 0.35 g.

**Table 6.1 - Analyzed ground motion records**

Earthquake (record)	Component [-]	Date [-]	PGA/g [-]	Length (s)	Step recording (s)
Victoria, Mexico (Chihuahua)	CHI102	1980/06/09	0.150	26.91	0.01
Coalinga (Slack Canyon)	H-SCN045	1985/05/02	0.166	29.99	0.01
Kobe (Kakogawa)	KAK000	1995/01/16	0.251	40.95	0.01
Spitak, Armenia (Gukasian)	GUK000	1988/12/17	0.199	19.89	0.01
Northridge (Stone Canyon)	SCR000	1994/01/17	0.252	39.99	0.01
Imperial Valley (Agrarias)	H-AGR003	1979/10/15	0.370	28.35	0.01
Palm Springs (San Jacinto)	PALMSPR/H08000	1986/07/08	0.250	26.00	0.005
Santa Barbara (Courthouse)	SBA132	1978/08/13	0.102	12.57	0.01
Friuli, Italy (Buia)	B-BUI000	1976/09/15	0.110	26.38	0.005
Irpinia, Italy (Calitri)	A-CTR000	1980/11/23	0.132	35.79	0.0024

In Figure 6.1 and Figure 6.2 the spectra of recorded ground motions (Table 6.1) scaled to the same  $S_a$  value for the period of vibration of the 6-storey K-scheme structure designed by means of the TPMC ( $T_1=1.38$  s) and 8-storey K-scheme designed by EC8 ( $T_1=1.92$  s) are reported, respectively. The periods of such structures are the minimum and the maximum among all the 8 designed

structures. Therefore, if the mean spectrum curve approximately matches the Eurocode 8 spectrum curve for this two extreme values of the period of vibration it is permissible to admit that the same happens also for the other values of the period  $T_1$  that are included in this range. In addition, each ground motion has been scaled to obtain the same value of the spectral acceleration,  $S_a(T_1)$ , corresponding to the fundamental period of vibration  $T_1$  of the structure under examination; successively  $S_a(T_1)$  values have been progressively increased.

**Table 6.2 - First and third vibration mode period of buildings designed**

BUILDINGS	TPMC		EUROCODE 8	
	$T_1$ (s)	$T_3$ (s)	$T_1$ (s)	$T_3$ (s)
6-STOREY K-scheme	1.38	0.56	1.46	0.60
8-STOREY K-scheme	1.80	0.67	1.92	0.73
6-STOREY Inverted Y-scheme	1.39	0.54	1.47	0.58
8-STOREY Inverted Y-scheme	1.62	0.60	1.70	0.63

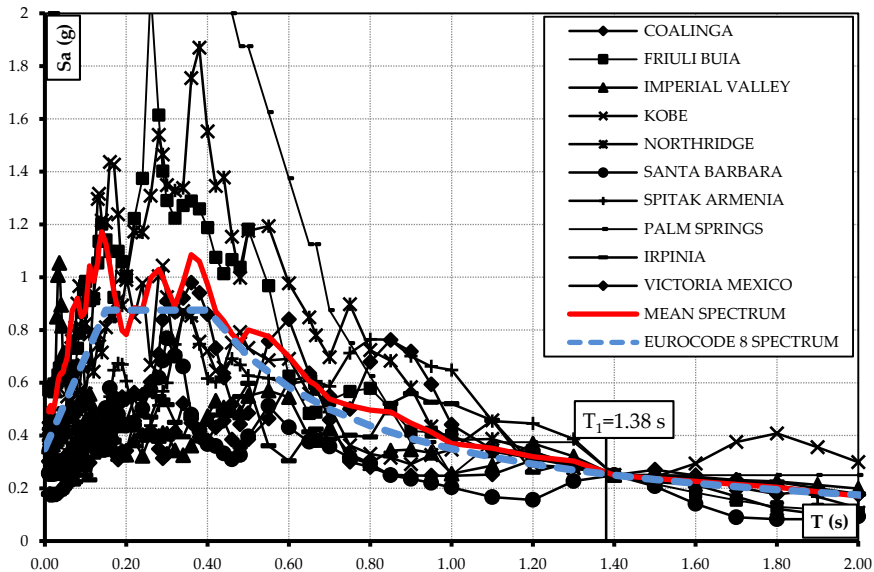


**Figure 6.1 - Response spectra (soil type A,  $\zeta=5\%$ ) scaled at the same value of  $S_a$  for  $T_1=1.38$**

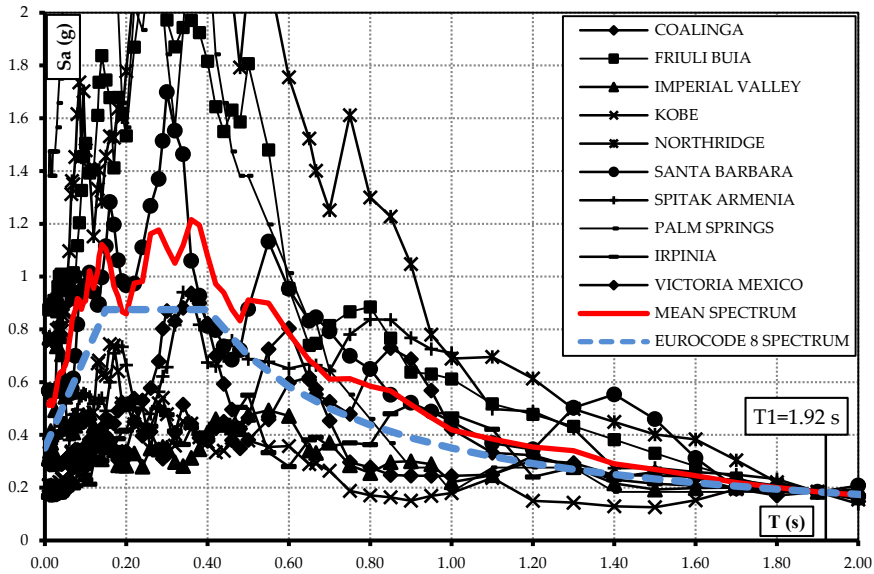


Figure 6.2 - Response spectra (soil type A,  $\zeta=5\%$ ) scaled at the same value of  $S_a$  for  $T_1=1.92$

The Incremental Dynamic Analyses have been carried out by increasing the  $S_a(T_1)/g$  value until the occurrence of structural collapse, corresponding to:

- column or diagonal buckling;
- the attainment of the limit value of the chord rotation of beam, diagonal and column members, which has been assumed equal to 0.04 rad
- the attainment of the limit value of the chord rotation of link members which has been assumed equal to 0.08 rad as a target design value, 0.11 rad at Life Safety Limit State and 0.14 rad at Collapse Prevention Limit State as suggested by FEMA 356 [52].

## 6.2 Incremental Dynamic Analyses Results

Incremental Dynamic Analyses results have been reported with reference to the Link Plastic Rotation (Figure 6.3 and Figure 6.4) and to the Maximum Interstorey Drift (MIDR) (Figure 6.5 and Figure 6.6).

Plastic rotation demands are depicted in Figure 6.3 with reference to the 6-storey and in Figure 6.4 with reference to 8-storey structures designed by TPMC and EC8 where the  $S_a(T_1)/g$  value corresponding to the achievement of a plastic rotation equal to 0.08 rad (assumed as target rotation) can be easily identified. In addition, it is useful to consider that FEMA 356 [52] provisions suggest limit values of the link plastic rotation demands equal to 0.11 rad and 0.14 rad with reference to the Life Safety (LS) and to the Collapse Prevention (CP) limit states, respectively. In particular, by comparing the average value of  $S_a(T_1)/g$  corresponding to such limit state it is possible to observe that, given the design approach, limit state is achieved, first by the K-braced structures and successively by the inverted Y-schemes. It means that, in the examined cases, the inverted Y-scheme is able to provide better seismic performances compared to the K-scheme. In addition, given the scheme, EC8 designed structures achieve the considered limit states before the TPMC designed structures. This points out the higher performances of TPMC designed structures, which assuring a collapse mechanism of global type are able to fully exploit the ductility supply of the structure. Both push-over and dynamic non-linear analyses have pointed out the different seismic performances which can be obtained by means of the investigated design procedures.

Starting from this preliminar consideration, if the TPMC designed structures achieve the collapse when the plastic link rotation assumes the maximum value corresponding to CP Limit State 0.14 rad EC8 structures are subjected to the occurrence of a different collapse which regards in most cases the column out of plane buckling or the achievement of a partial mechanism involving few storeys. The  $S_a(T_1)$  collapse values are reported in Table 6.3 and Table 6.4 with reference to 6-storey structures and 8-storey structures respectively. In addition, in such tables also the average collapse values are reported. By comparing the average  $S_a(T_1)$  collapse values it is possible to observe that the difference in term of performance between the structure TPMC designed and EC8 designed are even greater than what was evident in the first comparison given in terms of link plastic rotation.

In addition, it is useful to observe that K-scheme structures show worse performances compared to the inverted Y-scheme structures, given the design approach. It means that the structural typology deeply influences the structural performances.

**Table 6.3** –  $S_a(T_1)$  values corresponding to the attainment of the collapse condition for the 6-storey structures

	6-storey K TPMC	6-storey K EC8	6-storey Inv. Y TPMC	6-storey Inv. Y EC8
	$S_a(T_1)$	$S_a(T_1)$	$S_a(T_1)$	$S_a(T_1)$
Coalinga	1.15g	0.30 g	1.30g	1.30g
Friuli, Italy	0.95g	0.30 g	0.95g	0.80g
Imperial Valley	0.80g	0.30 g	0.85g	0.60g
Irpinia, Italy	1.00g	0.40 g	1.20g	1.00g
Kobe	1.05g	0.40 g	1.20g	0.70g
Northridge	0.83g	0.20 g	1.20g	0.80g
Palm Springs	0.50g	0.10 g	1.30g	0.40g
Santa Barbara	1.55g	0.30 g	1.70g	0.90g
Spitak Armenia	0.80g	0.30 g	0.90g	0.80g
Victoria Mexico	1.10g	0.40 g	1.20g	0.80g
<b>Mean value</b>	<b>0.97g</b>	<b>0.30g</b>	<b>1.06g</b>	<b>0.81g</b>

**Table 6.4** –  $S_a(T_1)$  values corresponding to the attainment of the collapse condition for the 8-storey structures

	8-storey K TPMC	8-storey K EC8	8-storey Inv. Y TPMC	8-storey Inv. Y EC8
	$S_a(T_1)$	$S_a(T_1)$	$S_a(T_1)$	$S_a(T_1)$
Coalinga	1.10g	0.50g	1.10g	0.70g
Friuli, Italy	1.25g	0.80g	1.30g	0.90g
Imperial Valley	0.75g	0.60g	0.80g	0.90g
Irpinia, Italy	0.88g	0.62g	1.00g	0.90g
Kobe	1.85g	1.15g	1.00g	0.95g
Northridge	0.75g	0.40g	0.90g	0.60g
Palm Springs	0.40g	0.30g	0.50g	0.30g
Santa Barbara	0.65g	0.40g	0.95g	0.40g
Spitak Armenia	0.68g	0.40g	0.70g	0.60g
Victoria Mexico	1.05g	0.70g	0.90g	0.60g
<b>Mean value</b>	<b>0.75g</b>	<b>0.50g</b>	<b>0.92g</b>	<b>0.60g</b>

It is also helpful to underline that link, beam and diagonal sections are the same for the two design methodologies, so that the different seismic performances are due to the increase of column sections required by TPMC to assure a collapse mechanism of global type.

In addition, being the analysed structural system a MRF-EBF dual system it is useful to point out the influence of the MRF part. It can be obtained by

observing the Maximum Interstorey Drift (MIDR) curves that can be significant to highlight the achievement of maximum plastic rotation in the beam ends.

It is possible to observe that, by comparing the average results reported in Table 6.3 and Table 6.4 for the 6-storey structures and 8-storey structures, respectively, the average MIDR curves achieve the target value of 0.04 rad for  $S_a(T_1)$  values greater or almost equal to the collapse average values in term of  $S_a(T_1)$  reported in Table 6.3 and Table 6.4. It confirms that the MRF part of MRF-EBF dual system really constitutes a supplementary fail safe system as foretold in Chapter 1 whose contribution to the seismic performances of the structures is more and more important as the seismic intensity measure increases. However, the development of plastic hinges at beam ends can be anticipated by sharing different rates of the base shear between the link and column members. As an example, ASCE 7-10 [69] requires for a dual system that the moment frames shall be capable of resisting at least 25 percent of the design seismic forces. Between the range going from the 0% to 25% of the base shear entrusted to the MRF part of the dual systems many solutions are possible but only one is able to give the optimum in term of weight performances ratio.

In addition, it should be interesting to observe the pattern of yielding actually developed by the structures under earthquake ground motions. They are reported in Appendix B both for the TPMC that for EC8 designed structures for a  $S_a(T_1)$  value equal to the attainment of the structural collapse. It is important also to underline that the pattern of yielding of the structures designed according to TPMC results to be in perfect agreement with the one already pointed out by means of push-over analysis (Appendix A) and, in turn, corresponding to the global mechanism. Conversely, the structures designed according to Eurocode 8 are not always able to prevent dangerous soft storey mechanisms or partial mechanisms. However, some spurious hinges develop at the beam and diagonal ends converging in the link members. These hinges are called spurious because they do not participate to the collapse mechanism being their plastic rotation not increasing during the collapse mechanism evolution.

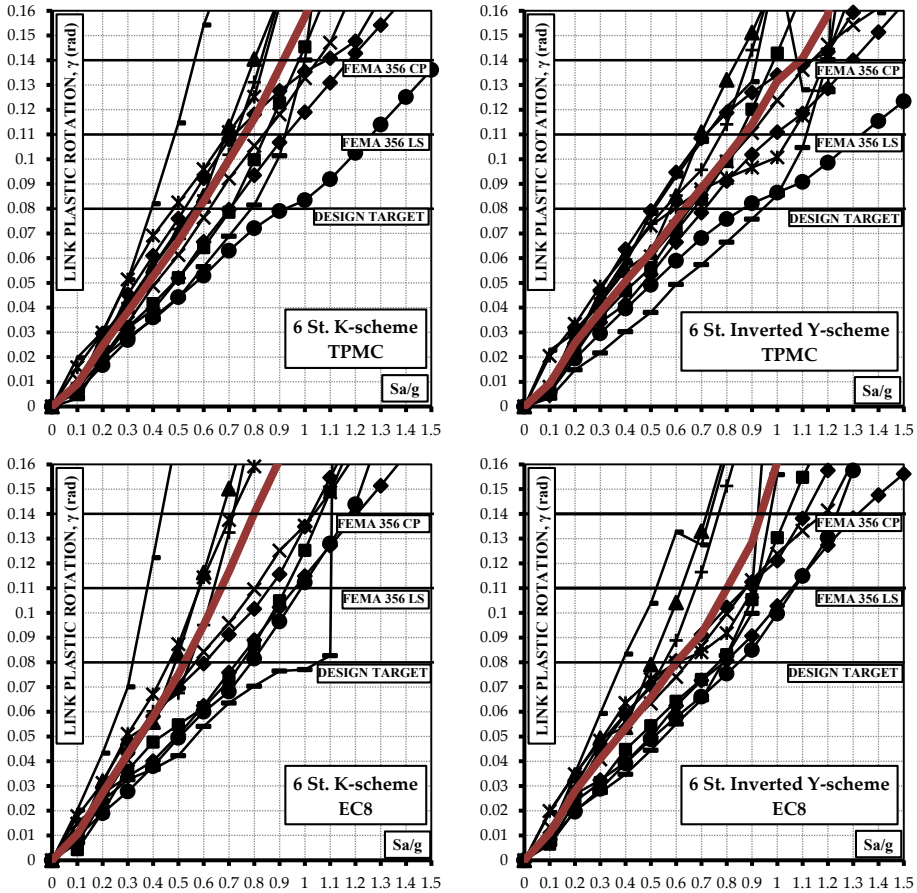


Figure 6.3 - Maximum plastic rotation of link versus spectral acceleration for the 6-storey structures designed according to TPMC and according to Eurocode 8



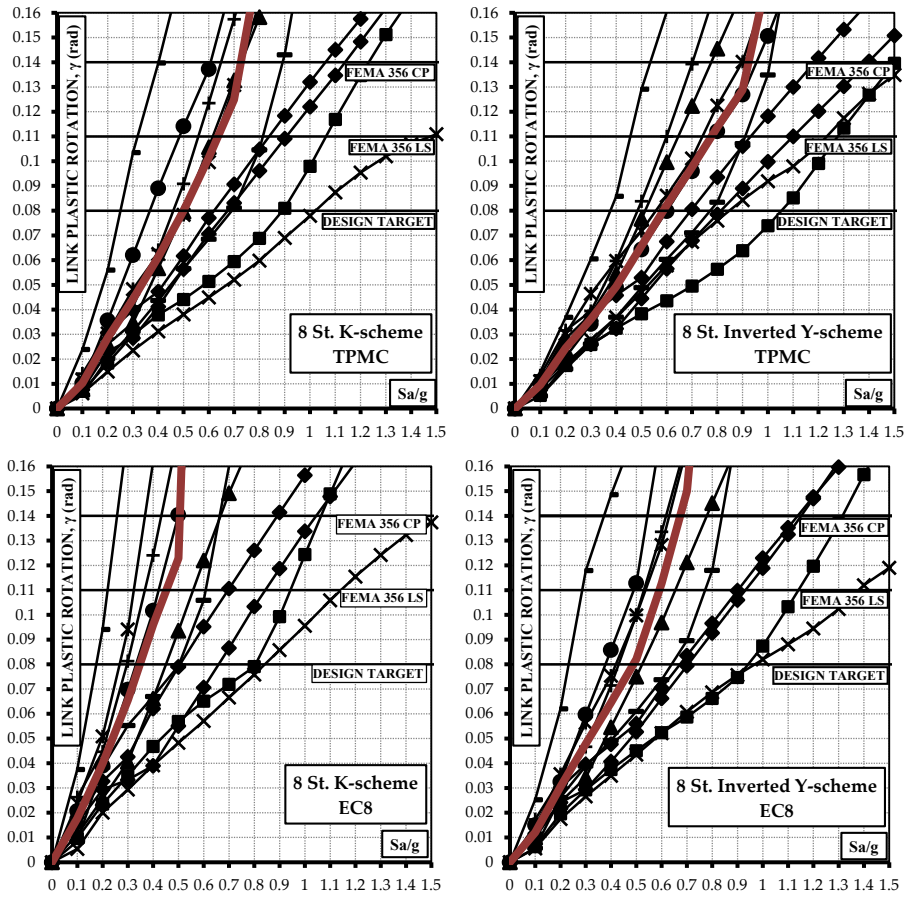
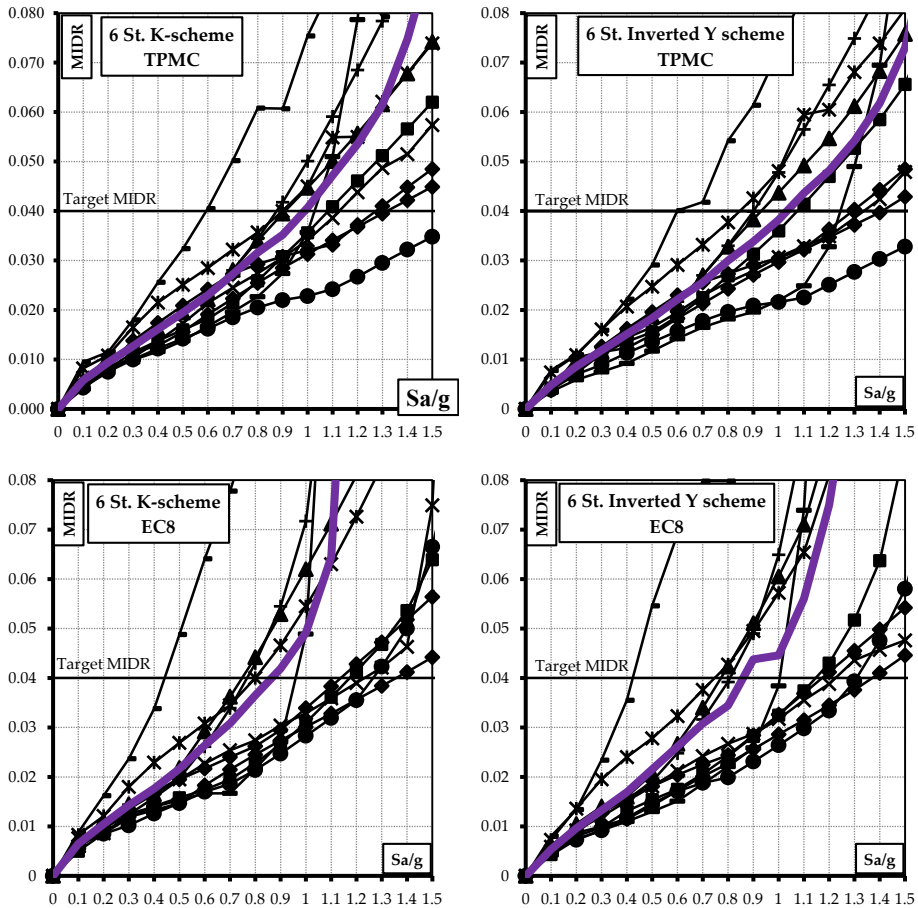
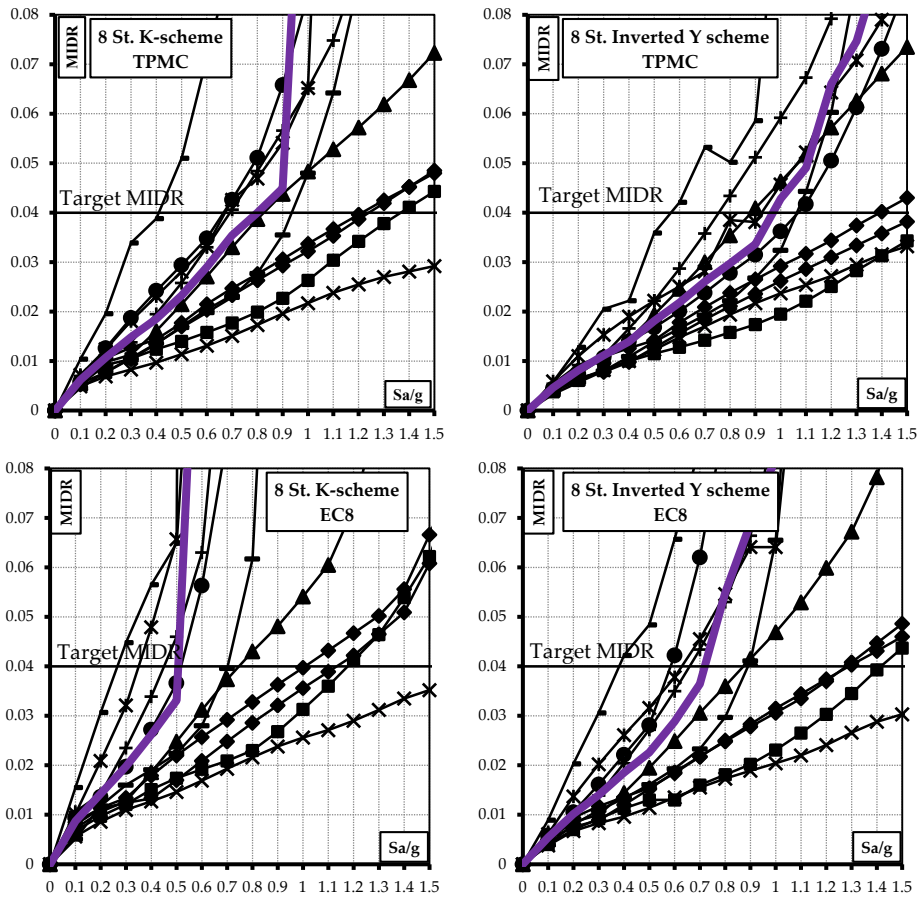


Figure 6.4 - Maximum plastic rotation of link versus spectral acceleration for the 8-storey structures designed according to TPMC and according to Eurocode 8



**Figure 6.5** - Maximum Interstorey Drift Ratio (MIDR) versus spectral acceleration for the 6-storey structures designed according to TPMC and according to Eurocode 8



**Figure 6.6** - Maximum Interstorey Drift Ratio (MIDR) versus spectral acceleration for the 8-storey structures designed according to TPMC and according to Eurocode 8

### 6.3 Considerations on economic issues

Aiming to provide a more exhaustive comparison between the two considered design procedures, i.e. TPMC and EC8, and between the analysed structural typologies (6-storey and 8-storey MRF-EBF dual systems) it is useful to face the topic also from the economic point of view. First of all, it can be assumed that the cost of the Whole Structure is proportional to its weight:

$$C_{WS,EC8} = \beta W_{WS,EC8} \quad (6.1)$$

$$C_{WS.TPMC} = \beta W_{WS.TPMC} \quad (6.2)$$

where the second index denote either the structure designed according to EC8 or that designed according to TPMC. It follows that the cost of the whole structure designed according to TPMC can be expressed as:

$$C_{WS.TPMC} = C_{WS.EC8} \frac{W_{WS.TPMC}}{W_{WS.EC8}} \quad (6.3)$$

The weight of the whole structure has to be considered as the sum of the weight of the Seismic Resistant (SR) part and the weight of the Gravity Load part (GL):

$$W_{WS.TPMC} = W_{SR.TPMC} + W_{GL} \quad (6.4)$$

The weight of the gravity load part is equal for both the structure designed by means of TPMC and EC8, and it is equal to 80000 kg and 140000 kg, for the 6-storey and 8-storey structures, respectively. The whole structural weights of the exhamined structures are reported in Table 6.5 for TPMC and EC8, respectively while the ratio between the weighth of the structures TPMC designed and EC8 designed, given the structural scheme, are reported in Figure 6.7. It means that TPMC design procedure causes a maximum increase of 11% of structural weight, corresponding to the 8-storey K-scheme structure. Similar consideration, can be made making a comparison between the structural weights, at equal design. The ratios between the K-scheme structures and Inverted Y-scheme structure are reported in Figure 6.8. It is possible to observe that in the case of 6-storey structures the K-scheme structures result heavier than the inverted Y-scheme structures, the opposite occurs in the case of 8-storey structures.

**Table 6.5 – Weight of the designed structures**

BUILDINGS	TPMC	EUROCODE 8
	Weight (kg)	Weight (kg)
6-STOREY K-scheme	152590	138021
8-STOREY K-scheme	240190	219560
6-STOREY Inverted Y-scheme	147170	135993
8-STOREY Inverted Y-scheme	259524	244839

However, according to the common design experience, it is important to observe that the cost of the whole structure represents a typical percentage of the whole building cost depending on its destination of use, so that, the difference

deriving from the different design procedure become less relevant if the cost of whole building is considered.

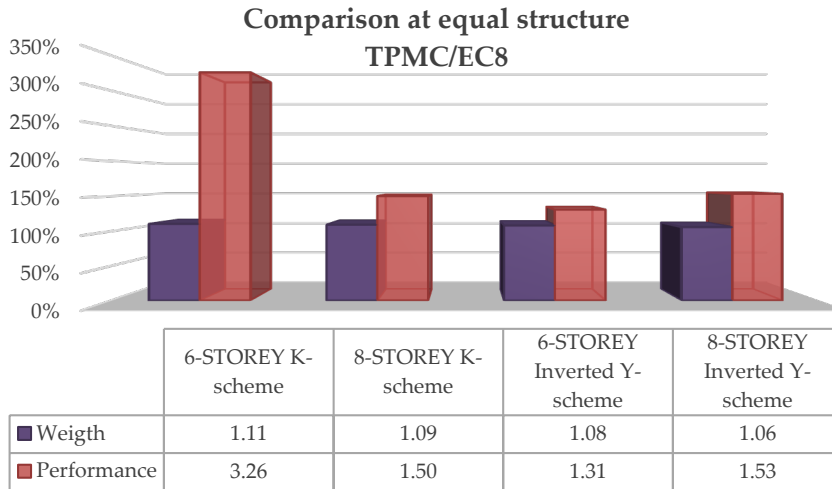


**Figure 6.7** – Comparison between the weight and performances in terms of  $S_a(T_1)$  of the TPMC and EC8 designed structures, given the structural scheme

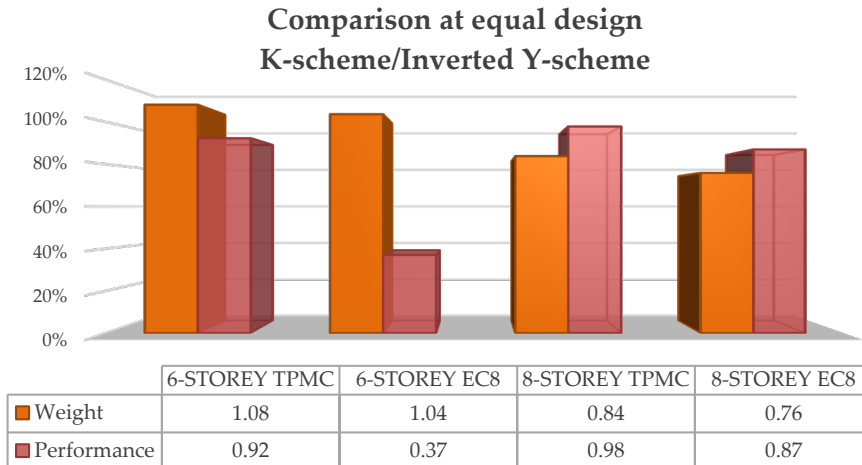


**Figure 6.8** – Comparison between the weight and performances in terms of  $S_a(T_1)$  of the TPMC and EC8 designed structures, given the design approach

## 6.4 Summary notes

In this chapter, the same structural systems, 6-storey MRF-EBF dual systems and 8-storey MRF-EBF dual systems with K-scheme and inverted Y-scheme, have been designed according to two different procedures. The first one is Theory of Plastic Mechanism Control (TPMC) whose robustness is based on the kinematic theorem of plastic collapse and its extension to the concept of mechanism equilibrium curve. The second one corresponds to the combined application of Eurocode 8 (EC8) provisions devoted to moment-resisting frames and to eccentrically braced frames.

Both push-over analyses reported in Chapter 5 and dynamic non-linear analyses have pointed out the different seismic performances which can be obtained by means of the investigated design procedures. In particular, the results of both push-over and IDA analyses have pointed out the accuracy of TPMC. As testified by the obtained pattern of yielding (Appendix B), it allows the control of the failure mode assuring a collapse mechanism of global type. The application of TPMC has led to the fulfilment of the design goal, i.e. the involvement of all the dissipative zones (links and beam ends) reaching high values of the spectral acceleration leading to collapse. This performance is due to the control of the failure mode which assures a dual system behaviour where the contribution of the moment-resisting part in the sharing of the seismic base shear increases as far as the seismic intensity measure increases. Conversely, despite the application of hierarchy criteria, structures designed according to Eurocode 8 do not satisfy the code promises, because they do not exhibit a pattern of yielding consistent with the required energy dissipation capacity which the  $q$ -factor is based on. In fact, as pointed out by both push-over and IDA analyses, the structures exhibit partial mechanisms which undermines the seismic response as testified by the quite low values of the spectral acceleration leading to the collapse. In the examined study cases, on average, K-scheme structures exhibit worse performances compared to the inverted Y-scheme structure, given the approach. Conversely, given the structural scheme, the buildings designed by means of TPMC exhibit better performance compared to the EC8 structures. In addition, despite an increase in term of weight for the TPMC designed structures, they exhibit an higher behaviour in term of seismic performances.

Even though the preliminary performance assessment of the designed building is based on IDA analyses limited to only ten records, the obtained

results are very encouraging about the performance improvements which can be attained by applying TPMC. However, it has be recognized that seismic response of structures is highly affected by the frequency content of the ground motion, so that, record-to-record variability has to be more accurately considered.





## CONCLUSIONS

The present work is devoted to the design of Moment Resisting Frame-Eccentrically Braced Frames dual systems (MRF-EBFs dual systems) in the framework of a complete procedure able to assure the design of structure exhibiting at collapse a collapse mechanism of global type.

Eccentrically Braced Frames constitute a suitable compromise between seismic resistant MR-Frames and concentrically braced frames because they exhibit both adequate lateral stiffness, due to the high contribution coming from the diagonal braces, and ductile behaviour, due to the ability of the links, constituting the dissipative zones of this structural typology, in developing wide and stable hysteresis loops. Therefore, the coupling of MRF and EBF constitute an excellent dual system where the primary structural system is constituted by the EBF part, and a secondary fail-safe system is constituted by the MRF part. This secondary one can be considered as an additional dissipative system where plastic hinges are concentrated at the beam ends. However, the main dissipative system is constituted by the link members located in the braced bay of MRF-EBF dual system that can be horizontal (K-scheme, D-scheme and V-scheme) or vertical (inverted Y-scheme). In addition, links can be short, long or intermediate themselves depending on their length and, consequently, on the stress they are governed by. In fact, link length deeply influences the seismic behaviour. Short links, whereas they are governed by shear, are able to show higher plastic rotations while long links, bending moment depending, are those less dissipative. Intermediate links show an intermediate behaviour respect to short

and long link and the interaction between shear force and bending moment is not negligible in the prediction of their ultimate behaviour.

For this reason one of the primary aim of the present work has regarded the development a rigorous treatment of moment-shear interaction occurring in intermediate links in order to provide local hierarchy criteria at “storey level” able to assure that the yielding is concentrated only in the link members, while the other members, such as beams and diagonals remain in elastic range. The whole analysis has been carried out within the framework of rigid-plastic design by exploiting the plastic domain, the normal flow rule, the kinematic compatibility requirements and the kinematic theorem of plastic collapse. Therefore, the derived hierarchy criteria, characterised by the robustness of their theoretical background constitutes the first step for the development of the design procedure able to design structures developing a collapse mechanism of global type. In fact, in such case, all the dissipative zones are involved in the corresponding pattern of yielding, leaving all the other structural parts in elastic range.

Theory of Plastic Mechanism Control (TPMC) is able to assure this ambitious design goal. Such theory was proposed for the first time by Mazzolani and Piluso in nineties with reference to MRFs with rigid full-strength beam-to-column connections. This theory ranks in the framework of plastic analysis since then only used to check the structural safety and not as a powerful tool to design structures exhibiting a predetermined collapse mechanism. It consists on the extension of the kinematic theorem of plastic collapse to the concept of mechanism equilibrium curve. In fact, for any given structural typology, the design conditions to be applied in order to prevent undesired collapse mechanisms can be derived by imposing that the mechanism equilibrium curve corresponding to the global mechanism has to be located below those corresponding to all the other undesired mechanisms up to a top sway displacement level compatible with the local ductility supply of dissipative zones.

Starting from the original procedure, in this work recent important improvement to the TPMC have been achieved. In particular, by means of new considerations regarding the collapse mechanism typologies, a closed form solution has been found. The design conditions to be satisfied to prevent undesired collapse mechanisms can now be solved without any iterative

procedure, so that the unknown of the design problem, i.e. column sections at each storey, can now be directly derived also by means of end calculations. This new advances in Theory of Plastic Mechanism Control have been implemented not only for MRFs but also for Moment Resisting Frame-Eccentrically Braced Frames dual systems (MRF-EBFs dual systems) which constitute the main topic of this work.

Aiming at the evaluation of TPMC accuracy, an adequate number of MRF-EBF dual systems, have been designed according to two different procedures. The first one is properly TPMC while the second one corresponds to the combined application of Eurocode 8 (EC8) provisions devoted to moment-resisting frames and to eccentrically braced frames.

Both push-over analyses and dynamic non-linear analyses have pointed out the different seismic performances which can be obtained by means of the investigated design procedures. In particular, the results have pointed out the accuracy of TPMC, whose robustness is based on the kinematic theorem of plastic collapse and its extension to the concept of mechanism equilibrium curve. As testified by the obtained hinge pattern of yielding, it allows the control of the failure mode assuring a collapse mechanism of global type. The application of TPMC has led to the fulfilment of the design goal, i.e. the involvement of all the dissipative zones reaching high values of the spectral acceleration leading to collapse. This performance is due to the control of the failure mode which assures a dual system behaviour where the contribution of the moment-resisting part in the sharing of the seismic base shear increases as far as the seismic intensity measure increases. Conversely, despite the application of hierarchy criteria, the structures designed according to Eurocode 8 does not satisfy the code promises, because do not exhibit a pattern of yielding consistent with the required energy dissipation capacity. In fact, as pointed out both by push-over and IDA analyses, the structures exhibit a partial mechanism which undermines the seismic response as testified by the quite low values of the spectral acceleration leading to the collapse.

In the examined study cases, on average, K-scheme structures exhibit worse performances compared to the inverted Y-scheme structure, given the approach. Conversely, given the structural scheme, the buildings designed by means of TPMC exhibit better performance compared to the EC8 structures.

In addition, also the economic issue has been faced. It has been observed that despite an increase in term of weight of the whole structure for the TPMC designed structures, they exhibit an higher behaviour in term of seismic performances. The differencet between seismic performances and weight become more and more relevant considering the weigth of the whole building, i.e. also the non structural elements.

Even though the preliminary performance assessment of the designed building is based on IDA analyses limited to only ten records, the obtained results are very encouraging about the performance improvements which can be attained by applying Theory of Plastic Mechanism Control which in spite of the procedured reported in the codes confirms able to assure the full control of the collapse mechanism with the achievement of a collapse mechanism of global type.

Therefore, the future development of such research line will require the application of TPMC to design MRF-EBF dual systems whose beam section are governed by seismic actions, i.e. whose configuration is parallel to the direction of the warping of deck slab; the evaluation of the differences in terms of behaviour factor occurring for the different EBF schemes, i.e. with horizontal or vertical link; the application of a probabilistic approach aiming to evaluate the seismic reliability of TPMC in terms of mean annual frequency of exceeding specified limit states and in terms of seismic loss hazard.

## REFERENCES

- [1] **Park R.:** "Ductile Design Approach for Reinforced Concrete Frames", Earthquake Spectra, EERI, 2(3), pp. 565-619, 1986.
- [2] **Mazzolani F.M., Piluso V.:** "Theory and Design of Seismic Resistant Steel Frames", E&FN Spon, an imprint of Chapman & Hall, 1996.
- [3] **Bruneau M., Uang C.M., Sabelli R.S.E.:** "Ductile Design of Steel Structures", McGraw-Hill, 2011.
- [4] **Akiyama H.:** "Earthquake Resistant Limit State Design for Building" University of Tokyo Press, Tokyo, 1985.
- [5] **Rosenblueth E. (ed.):** "Design of Earthquake Resistant Structures", Pentech Press, London, 1980.
- [6] **Dowrich D.J.:** "Earthquake Resistant Design", A Manual for Engineers and Architects, Wiley, New York, 1977.
- [7] **Paulay T., Priestley M.J.N.:** "Seismic Design of Reinforced Concrete and Masonry Buildings", Wiley, New York, 1995.
- [8] **Wakabayashi M.:** "Design of Earthquake Resistant Buildings", McGraw-Hill, New York, 1986, p. 229.
- [9] **Bertero V. V., Popov E. P.:** "Seismic behaviour of ductile moment-resisting reinforced concrete frames", in Reinforced Concrete Structures in Seismic Zones, ACI Publication SP-53, American Concrete Institute, Detroit, 1977, pp. 247-291.
- [10] **Lee H.S.:** "Revised rule for concept of strong-column weak-girder design", J. struct. eng. ASCE, 122, 359D364 (1996).
- [11] **EN 1998-1:** "Eurocode 8: Design of Structures for Earthquake Resistance – Part 1: general Rules, Seismic Actions and Rules for Buildings", CEN, 2004
- [12] **Paulay T.:** "Deterministic Design Procedure for Ductile Frames in Seismic Areas", ACI Publication SP-63, American Concrete Institute, Detroit, 1980, pp. 357-381.

- [13] **Paulay T.:** "Seismic design of ductile moment resisting reinforced concrete frames, columns: evaluation of actions", Bull. New Zealand Natl. Soc. Earthquake Eng., 10, 85-94,1977.
- [14] **Paulay T.:** "Capacity design of earthquake resisting ductile multistorey reinforced concrete frames", Proc. 3rd Canad. conf. on earthquake eng., Montreal, Vol. 2, pp. 917-948, 1979.
- [15] **New Zealand Standard Code of Practice for the Design of Concrete Structures:** NZS 3101:Part 1; Commentary NZS 3101: Part 2; Standard Association of New Zealand, Wellington, New Zealand, 1982.
- [16] **Panelis G.G., Kappos A.J.:** "Earthquake-Resistant Concrete Structures", E&FN Spon, an imprint of Chapman & Hall, 1997.
- [17] **Mazzolani F.M., Piluso V.:** "Plastic Design of Seismic Resistant Steel Frames", Earthquake Engineering and Structural Dynamics, Vol. 26, pp. 167-191, 1997.
- [18] **Park R., Paulay T.:** Reinforced Concrete Structures, Wiley, New York, 1975, pp. 566-568, 602-604.
- [19] **Kappos, A.J.:** "Evaluation of the Inelastic Seismic Behaviour of Multistorey Reinforced Concrete Buildings", PhD Thesis (in Greek), Scientific Annual of the Faculty of Engineering, Aristotle University of Thessaloniki, 1986.
- [20] **Engelhardt M.D., Popov E.P.:** "Behaviour of long links in eccentrically braced frames", Report N. UCB/EERC-89/01, EarthquakeEngineering Research Center, University of California, Berkeley, 1989.
- [21] **Montuori R., Piluso V.:** "Design of Semi-Rigid Steel Frames for Failure Mode Control", Moment Resistant Connections of Steel Frames: Design and Reliability, London: E&FN Spon, Taylor & Francis Group, pp. 461-483, 2000.
- [22] **Montuori R., Piluso V.:** "L'Uso dei "Dog Bones" nella Progettazione a Collasso Controllato dei Telai Sismo-Resistenti", XVII Congresso C.T.A. Italian Conference on Steel Construction, Napoli, 3-5 Ottobre, vol. 1, pp. 301-310, 1999.

- [23] **Mastrandrea L., Montuori R., Piluso V.:** "Failure mode control of seismic resistant EB-frames", Stessa, 4<sup>th</sup> International Conference on Behavior of Steel Structures in Seismic Areas, 2003.
- [24] **Mastrandrea L., Montuori R., Piluso V.:** "Shear-moment interaction in plastic design: eccentrically braced frames", STESSA 2003, 4<sup>th</sup> International Conference on Behavior of Steel Structures in Seismic Areas, Naples, Italy, 9-12 June. Rotterdam: Balkema, 2003.
- [25] **Montuori R., Nastri E., Piluso V.:** "Rigid-plastic analysis and Moment-shear interaction for Hierarchy Criteria of Inverted Y EB-Frames", accepted for publication on Journal of Constructional Steel Research, 2014.
- [26] **Montuori R., Nastri E., Piluso V.:** "Theory of Plastic Mechanism Control for Eccentrically Braced Frames with inverted Y-scheme", Journal of Constructional Steel Research, Volume 93, pp. 122-135, 2014.
- [27] **Conti M.A., Mastandrea L., Piluso V.:** "Plastic Design and Seismic Response of Knee Braced Frames", Advanced Steel Costructions, Vol. 5, n.3 September, pp. 343-363, 2009.
- [28] **Longo A., Montuori R., Piluso V.:** "Theory of Plastic Mechanism Control of Dissipative Truss Moment Frames", Engineering Structures, Vol. 37, pp. 63-75, 2012.
- [29] **Longo A., Montuori R., Piluso V.:** "Failure Mode Control and Seismic Response of Dissipative Truss Moment Frames", Journal of Structural Engineering, Vol. 138, pp.1388-1397, 2012.
- [30] **Longo A., Montuori R., Piluso V.:** "Theory of plastic mechanism control for MRF-CBF dual systems and its validation." Bulletin of Earthquake Engineering (2014): 1-31.
- [31] **Lee S-S., Goel S.C.:** "Performance-Based Design of Steel Moment Frames using Target Drift and Yield Mechanism", Research Report UMCEE 01-17, University of Michigan, December 2011.
- [32] **Piluso V., Nastri E., Montuori R.:** "Advances in Theory of Plastic Mechanism Control: Closed Form Solution for Mr-Frames", Earthquake Engineering and Structural Dynamics, 2015.

- [33] **Kasai K., Popov E.P.:** "General behavior of WF steel shear link beams", ASCE Journal of Structural Engineering, Vol. 112, Issue 2, pp. 362-382, 1986.
- [34] **Kasai K., Han X.:** "New EBF design method and applications: Redesign and analysis of US-Japan EBF. Proceedings of Stessa 97 – 2<sup>nd</sup> international conference on behaviour of steel structures in seismic areas, 1997.
- [35] **Kasai K., Han X.:** "Refined Design and Analysis of Eccentrically Braced Frames", Journal of Structural Engineering, ASCE, 1997.
- [36] **Hera Publication P4001:2013,** "Seismic Design of Eccentrically Braced Frames", Earthquake Engineering, 2013.
- [37] **Roeder C.W., Popov E.P.:** "Eccentrically braced steel frames for earthquakes", ASCE, Journal of Structural Division, Vol. 104, Issue 3, pp. 391-412, 1978.
- [38] **Hjelmstad K.D., Popov E.P.:** "Cyclic behavior and design of link beams", ASCE Journal of Structural Engineering, Vol. 109, Issue 10, pp. 2387-2403, 1983.
- [39] **Mastrandrea L., Piluso V.:** "Failure mode control of seismic resistant EB-frames", Plastic Design of Eccentrically Braced Frames, II: Failure Mode Control", Journal of Constructional Steel Research, pp. 1015-1028, 2009.
- [40] **Chao S.H., Goel S.C.:** "Performance-Based Seismic Design of Eccentrically Braced Frames using target drift and yield mechanism as Performance Criteria ", Engineering Journal, Third Quarter, 2006.
- [41] **Montuori R., Nastri E., Piluso V.:** Theory of plastic mechanism control for the seismic design of braced frames equipped with friction dampers - Mechanics Research Communications – Vol. 58. pp. 112-123, 2014.
- [42] **Balendra T., Sam M.T., Liaw C.Y., Lee S.L.:** "Preliminary studies into the behavior of knee braced frames subjected to seismic loading", Engineering Structures, Vol. 13, Issue 1, pp. 67-74, 1991.
- [43] **Rai D.C., Wallace B.J.:** "Aluminium shear-links for enhanced seismic resistance", Earthquake Engineering and Structural Dynamics, Vol. 27, Issue 4, pp. 315-342, 1998.



- [44] **Dusicka P.**: "Hysteretic shear links utilising innovative steels for earthquake protection of long span bridges", Ph.D. Dissertation, Reno, NV: University of Nevada, 2004.
- [45] **Dusicka P., Itani A.M., Buckle I.G.**: "Evaluation of conventional and specialty steels in shear link hysteretic energy dissipators", In: Proceedings of 13th WCEE, Paper No. 522, 2004.
- [46] **Okazaki T., Arce G., Ryu H.C., Engelhardt M.D.**: "Recent Research on Link Performance in Steel Eccentrically Braced Frames", 13th World Conference on Earthquake Engineering, 13th WCEE, Vancouver, Canada, August 1-6, Paper No. 302, 2004.
- [47] **AISC**: "Seismic provisions for structural steel buildings", Standard ANSI/AISC 341-10, Chicago (IL): American Institute of Steel Construction, 2010.
- [48] **Okazaki T., Engelhardt M.D., Drolias A., Schell E., Hong J.K., Uang C.M.**: "Experimental investigation of link-to-column connections in eccentrically braced frames", Journal of Constructional Steel Research, Vol. 65, pp. 1401-1412, 2009.
- [49] **Neal B.G.**: "Effect of shear force on the fully plastic moment of an I-beam". Journal of Mechanics and Engineering Science, Vol. 3, Issue 3, pp. 258-268, 1961.
- [50] **Hjelmstad K.D., Popov E.P.**: "Seismic behavior of active beam link in eccentrically braced frames", EERC Report No. 83-15, Berkeley: Earthquake Engineering Research Center, University of California, 1983.
- [51] **Malley J.O., Popov E.P.**: "Design consideration for shear links in eccentrically braced frames", EERC Report No. 83-24, Berkeley: Earthquake Engineering Research Center, University of California, 1983.
- [52] **FEMA 356**. "Prestandard and Commentary for the Seismic Rehabilitation of Buildings", November 2000.
- [53] **EN 1993-1-1:2005**. "Eurocode 3: Design of steel structures. Part 1: General rules and rules for buildings", Comité Européen de Normalisation, CEN/TC 250, 2005.

- [54] **Itani A., Douglas B.M., El-Fass S.:** "Cyclic behavior of shear links in retrofitted Richmond-San Rafael bridge towers", In: Proceedings of the First World Congress on Structural Engineering, San Francisco: Elsevier Science; 1998. Paper No.T155-3, 1998.
- [55] **Mc Daniel C.C., Uang C.M., Seible F.:** "Cyclic testing of built-up steel shear links for the new bay bridge", ASCE Journal of Structural Engineering, Vol. 129, Issue 6, pp. 801-809, 2003.
- [56] **Barecchia E., Della Corte G., Mazzolani F.M.:** "Plastic over-strength of short and intermediate links", In: Proceedings of STESSA 2006 Conference on Behaviour of Steel Structures in Seismic Areas, pp. 177-183, 2006.
- [57] **CSI 2007.** SAP 2000: Integrated Finite Element Analysis and Design of Structures. Analysis Reference. Computer and Structure Inc. University of California, Berkeley.
- [58] **Leelataviwat S., Goel S.C., Stojadinovic B.:** "Toward Performance Based Design of Structures", Earthquake Spectra, EERI, 15, 435-461, 1999.
- [59] **Goel S.C., Liao W-C., Bayat M.R., Chao S-H.:** "Performance Based Plastic Design (PBDP) Method for Earthquake-Resistant Structures: An Overview", The Structural Design of Tall and Special Buildings, 19, 115-137, 2010.
- [60] **Chao S-H., Goel S.C., Lee S-S.:** "A Seismic Design Lateral Force Distribution Based on Inelastic State of Structures", Earthquake Spectra, EERI, 23:3, 547-569, 2007.
- [61] **Goel S.C., Chao S-H.:** "Performance-Based Plastic Design: Earthquake Resistant steel Structures", International Code Council: Washington, DC, 2008.
- [62] **Chao S-H., Goel S.C.:** "Performance-Based Plastic Design of Seismic Resistant Special Truss Moment Frames", AISC Engineering Journal, Second Quarter, 127-150, 2008.
- [63] **Ohsaki M., Nakajima T.:** "Optimization of Link Member of Eccentrically Braced Frames for Maximum Energy Dissipation", Journal of Constructional Steel Research, Vol. 75, 2012, pp. 38-44, 2012.

- [64] **Gulec C.K., Gibbons B., Chen A., Whittaker A.S.:** "Damage States and Fragility Functions for Link Beams", *Journal of Constructional Steel Research*, Vol. 67, 2011, pp. 1299-1309, 2011.
- [65] **Mastandrea L., Nastro E., Piluso V.:** "Validation of a Design Procedure for Failure Mode Control of EB-Frames: Push-over and IDA analyses", *The Open Construction and Building Technology Journal*, 7, 193-207, 2013.
- [66] **Giugliano M.T., Longo A., Montuori R., Piluso V.:** "Failure Mode and Drift Control of MR-CBF Dual Systems", *The Open Journal of Construction and Building Technology*, Vol. 4, pp.121-133, 2010.
- [67] **Deierlein, G.G., Reinhorn, A. M., Willford M. R.:** "Nonlinear Structural Analysis For Seismic Design", *NERPH Seismic Design Technical Brief No.4, NIST GCR 10-917-5*
- [68] **Pacific Earthquake Engineering Research Center,** PEER Strong Motion Database, <http://peer.berkeley.edu.smcat>.
- [69] **ASCE:** "ASCE Standard 7-10: Minimum Design Loads for Buildings and Other Structures", *American Society of Civil Engineers*, 2010.
- [70] **D'Aniello M., La Manna Ambrosino G., Portioli F., Landolfo R.:** "Modelling aspects of the seismic response of steel concentric braced frames". *Steel and Composite Structures, An International Journal*, Vol. 15, No. 5, November 2013, 539-566, 2013.
- [71] **Della Corte G., D'Aniello M., Mazzolani F.M.:** "Inelastic response of shear links with axial restraints: numerical vs. analytical results" *5th International Conference on Advances in Steel Structures*, Singapore, 5 – 7 December, 2007.
- [72] **Della Corte G., D'Aniello M., Landolfo R.:** "Analytical and numerical study of plastic overstrength of shear links", *Journal of Constructional Steel Research*, 82, 19–32, 2013.
- [73] **Vamvatsikos D., Cornell C.A.:** "Incremental dynamic analysis", *Earthquake Engineering and Structural Dynamics*, 2002.



# APPENDIX A

## PUSH-OVER HINGE PATTERNS

In this section the plastic hinge distribution for the study cases described in Chapter 5 are reported. A total number of 16 structures, 8 designed exploiting the Theory of Plastic Mechanism Control and 8 the Eurocode 8 have been considered. These structures have been analysed by means of push-over analyses carried out by SAP2000 computer program.

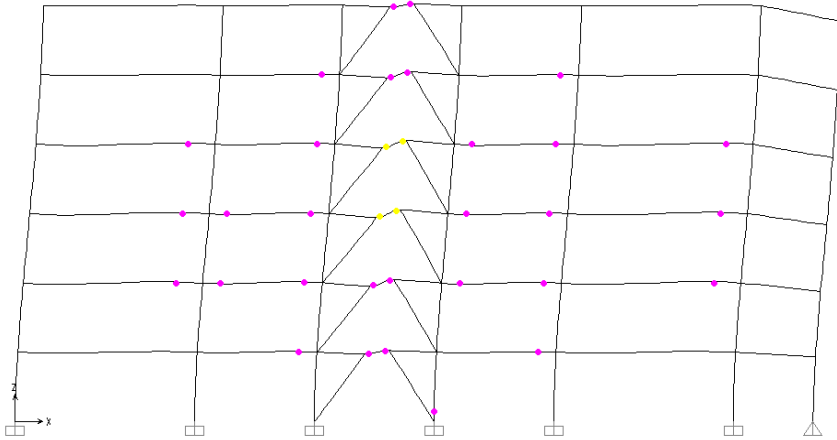
For each structure the figures representing the push-over hinge pattern for the ultimate design displacement ( $\delta_u$ ) and for a displacement equal to two times the ultimate design displacement ( $2\delta_u$ ) are reported. These figures originate from the SAP2000 Computer Program screenshot.

In order to identificate the exhamined structures the following notation has been used:

- **MRF-EBF K-scheme** for the MRF-EBF dual systems whose braced bay is an EBF with K-scheme;
- **MRF-EBF D-scheme** for the MRF-EBF dual systems whose braced bay is an EBF with D-scheme;
- **MRF-EBF V-scheme** for the MRF-EBF dual systems whose braced bay is an EBF with V-scheme;
- **MRF-EBF inv. Y-scheme** for the MRF-EBF dual systems whose braced bay is an EBF with inverted Y-scheme.

**MRF-EBF K-SCHEME 6-STOREY TPMC**

(a)



(b)

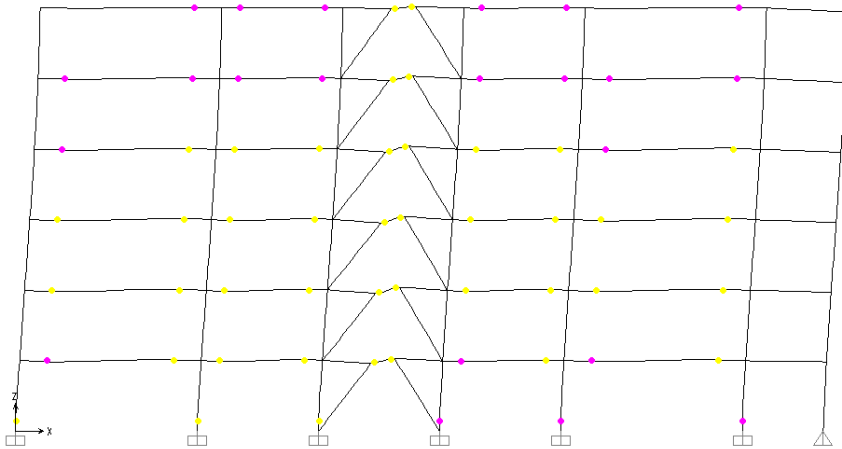
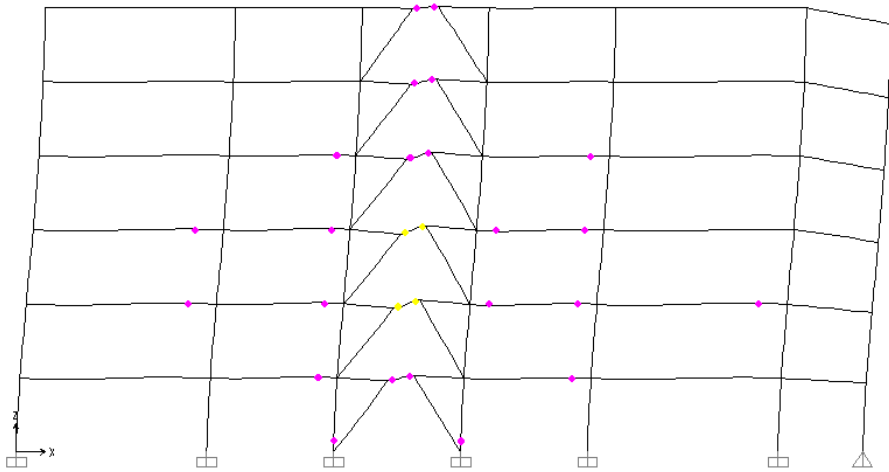


**Figure A.1** - Push-over hinge pattern 6-storey K-scheme TPMC for the ultimate design displacement (a) and for a displacement equal to two times the ultimate design displacement (b)

MRF-EBF K-SCHEME 6-STOREY EC8

(a)



(b)

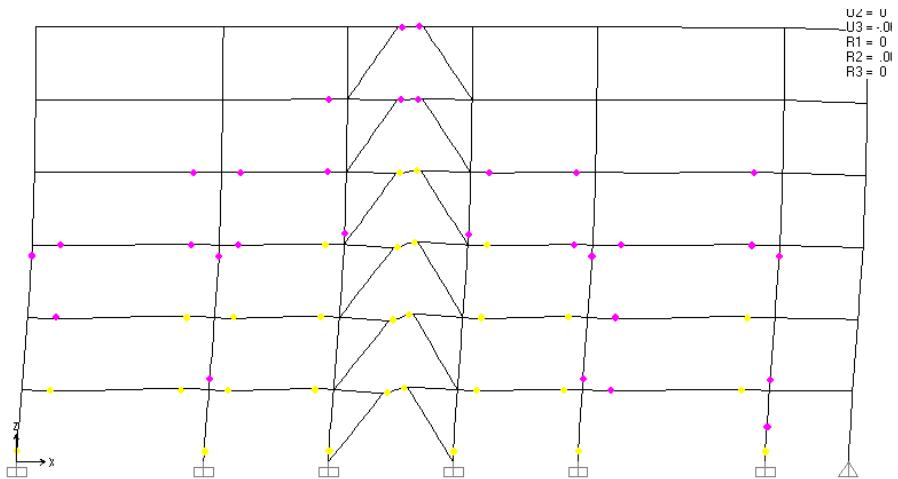


**Figure A.2** - Push-over hinge pattern 6 storey K-scheme EC8 for the ultimate design displacement (a) and for a displacement equal to two times the ultimate design displacement (b)

## MRF-EBF K-SCHEME 8-STOREY TPMC

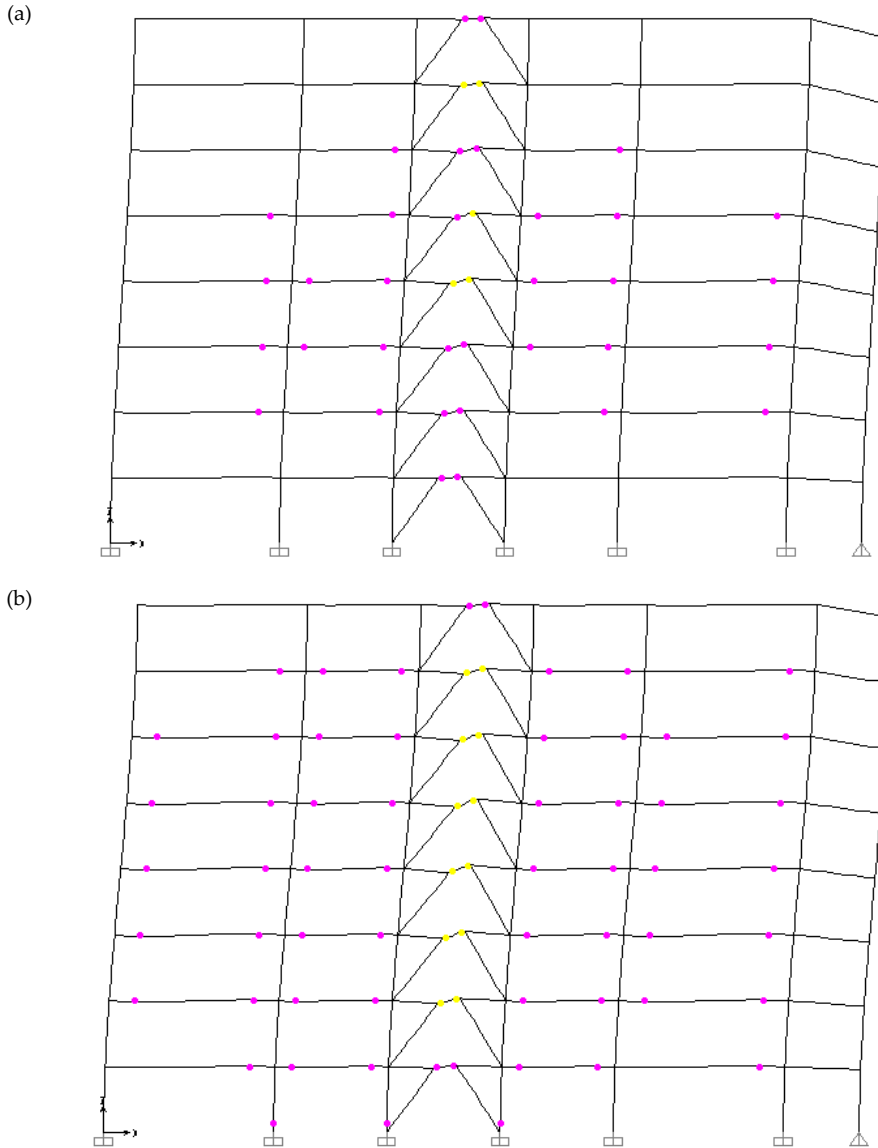


**Figure A.3** – Push-over hinge pattern 8 storey K-scheme TPMC for the ultimate design displacement (a) and for a displacement equal to two times the ultimate design displacement (b)



## MRF-EBF K-SCHEME 8-STOREY EC8

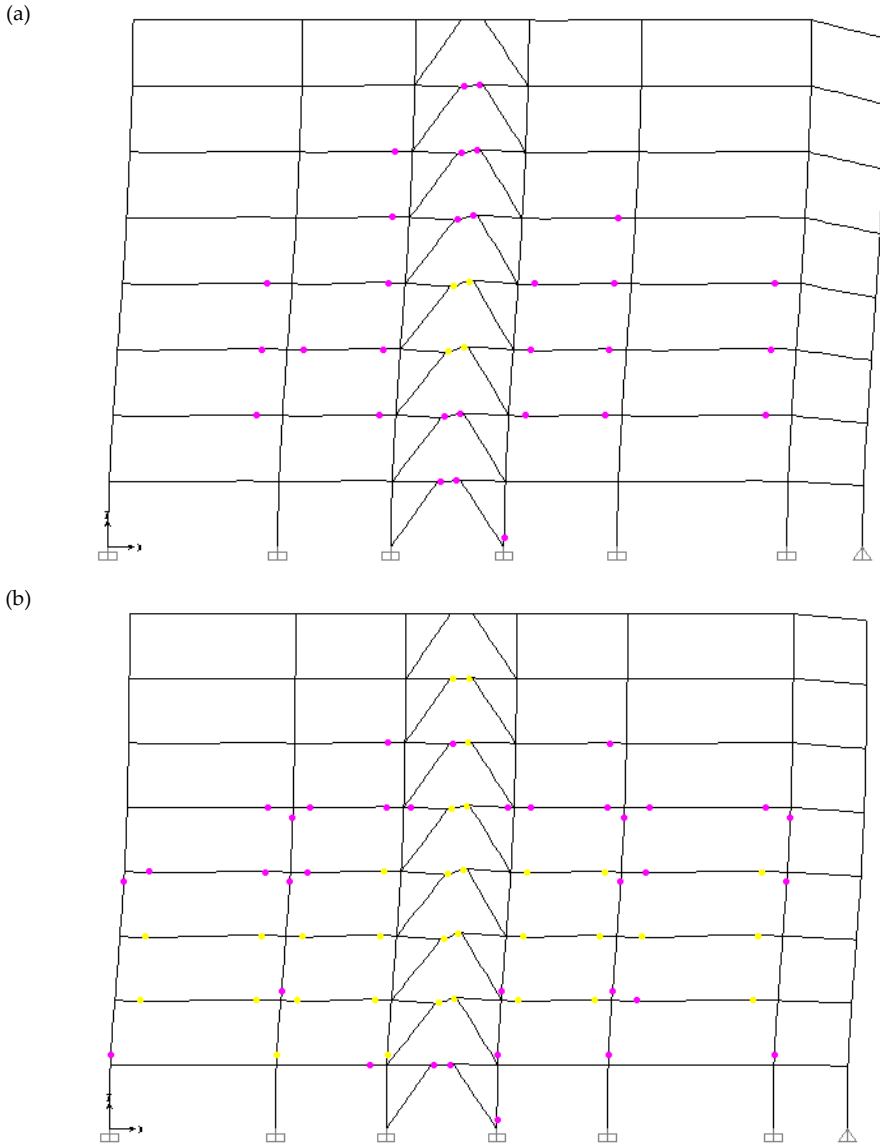
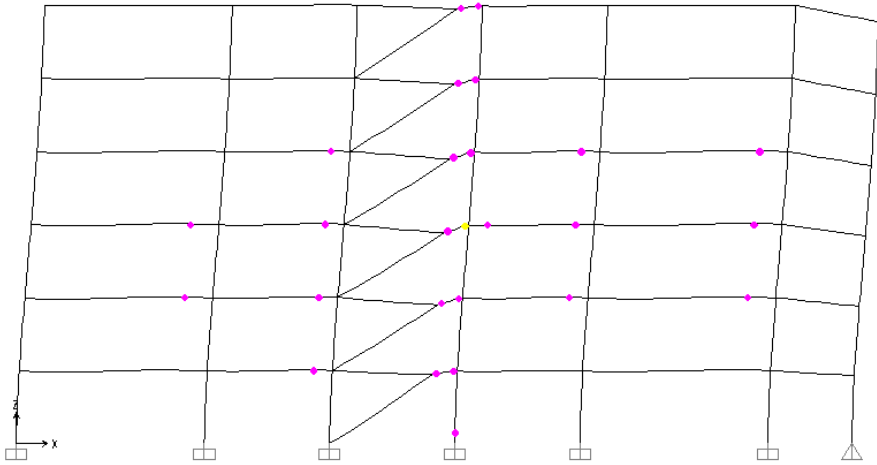


**Figure A.4** – Push-over hinge pattern 6 storey D-scheme EC8 for the ultimate design displacement (a) and for a displacement equal to two times the ultimate design displacement (b)

## MRF-EBF D-SCHEME 6-STOREY TPMC

(a)



(b)

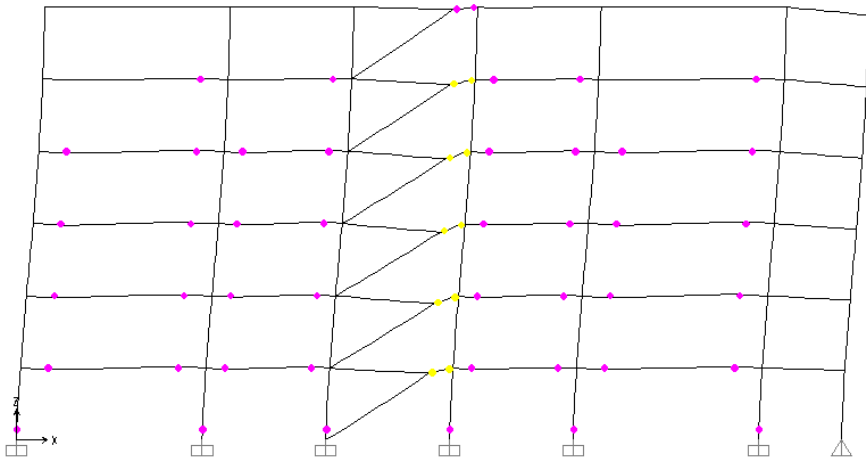
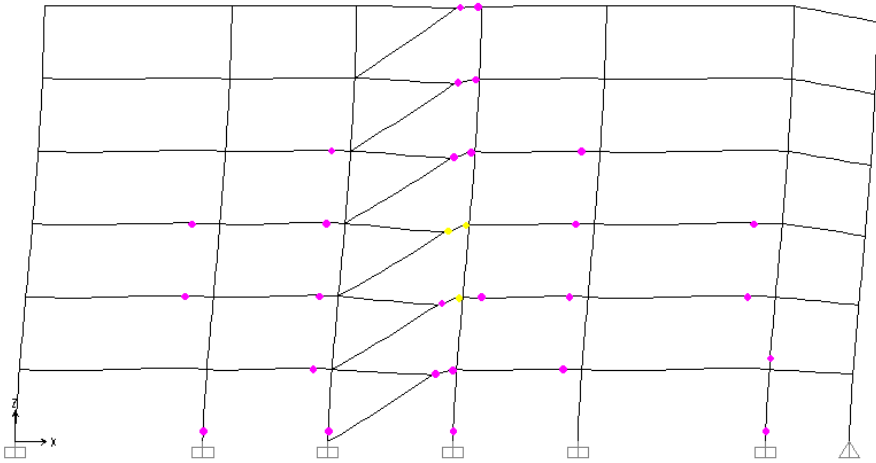


**Figure A.5** – Push-over hinge pattern 8 storey D-scheme TPMC for the ultimate design displacement (a) and for a displacement equal to two times the ultimate design displacement (b)

## MRF-EBF D-SCHEME 6-STOREY EC8

(a)



(b)

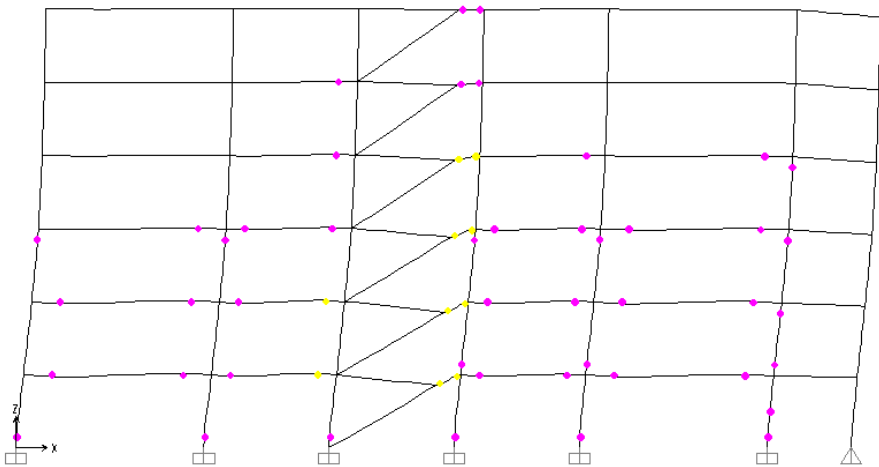
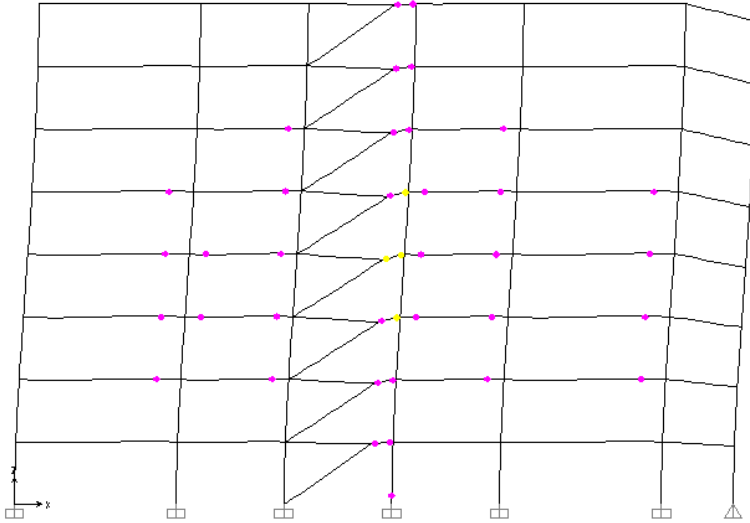


**Figure A.6** – Push-over hinge pattern 6 storey D-scheme EC8 for the ultimate design displacement (a) and for a displacement equal to two times the ultimate design displacement (b)

**MRF-EBF D-SCHEME 8-STOREY TPMC**

(a)



(b)

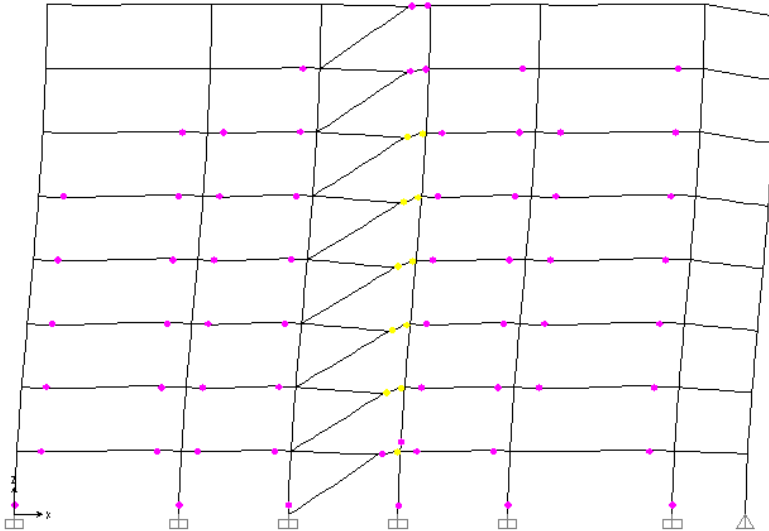
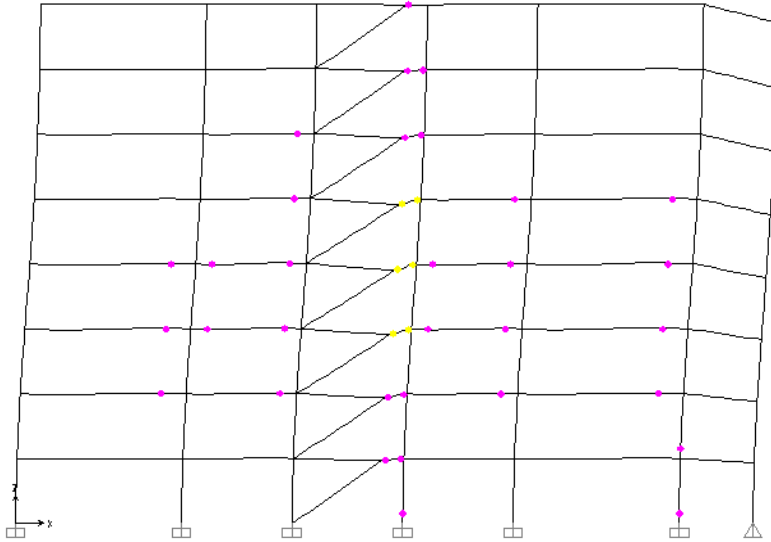


**Figure A.7** – Push-over hinge pattern 8 storey D-scheme TPMC for the ultimate design displacement (a) and for a displacement equal to two times the ultimate design displacement (b)

## MRF-EBF D-SCHEME 8-STOREY EC8

(a)



(b)

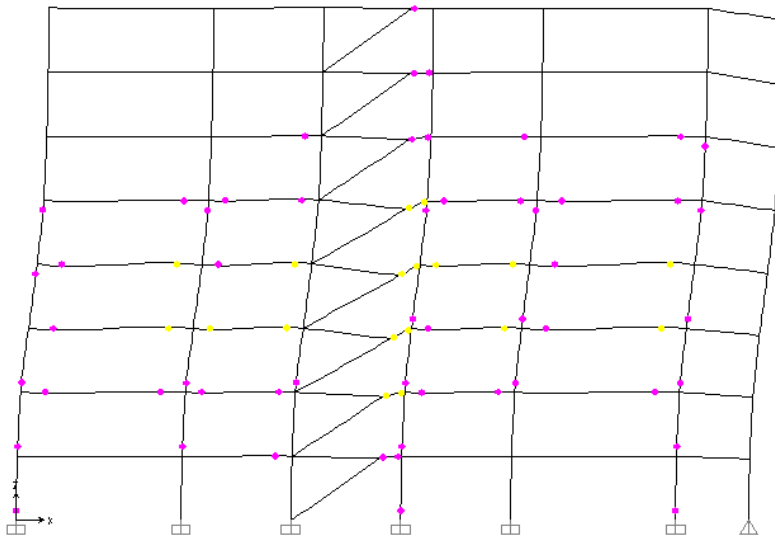
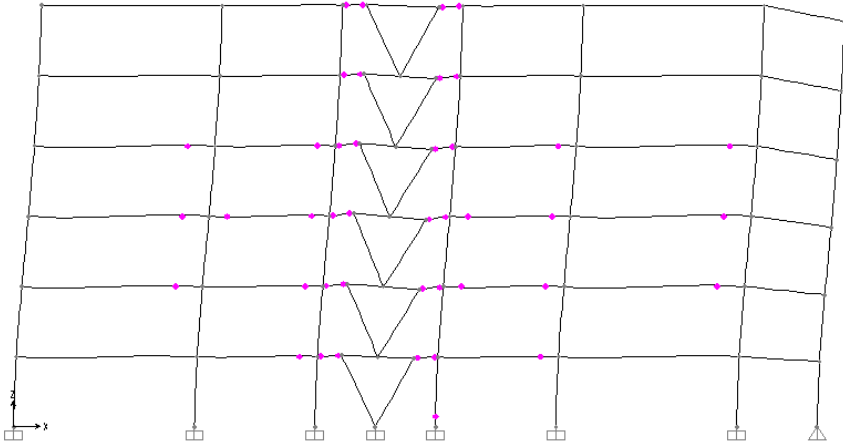


**Figure A.8** – Push-over hinge pattern 8 storey D-scheme EC8 for the ultimate design displacement (a) and for a displacement equal to two times the ultimate design displacement (b)

## MRF-EBF V-SCHEME 6-STOREY TPMC

(a)



(b)

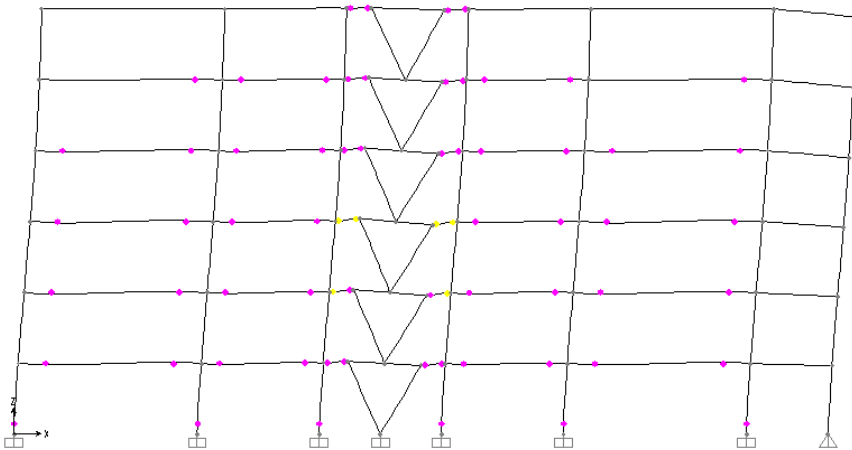
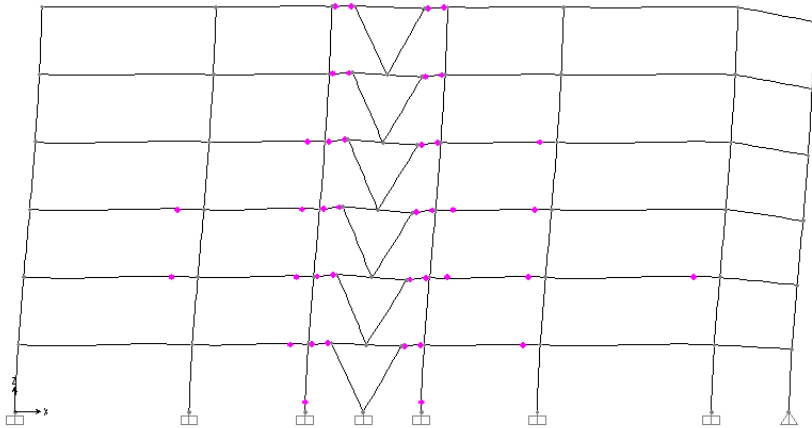


**Figure A.9** – Push-over hinge pattern 6 storey V-scheme TPMC for the ultimate design displacement (a) and for a displacement equal to two times the ultimate design displacement (b)

**MRF-EBF V-SCHEME 6-STOREY EC8**

(a)



(b)

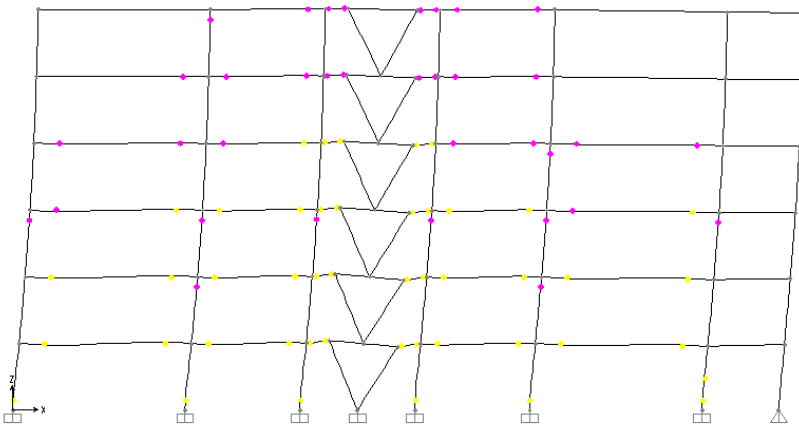


**Figure A.10** – Push-over hinge pattern 6 storey V-scheme EC8 for the ultimate design displacement (a) and for a displacement equal to two times the ultimate design displacement (b)

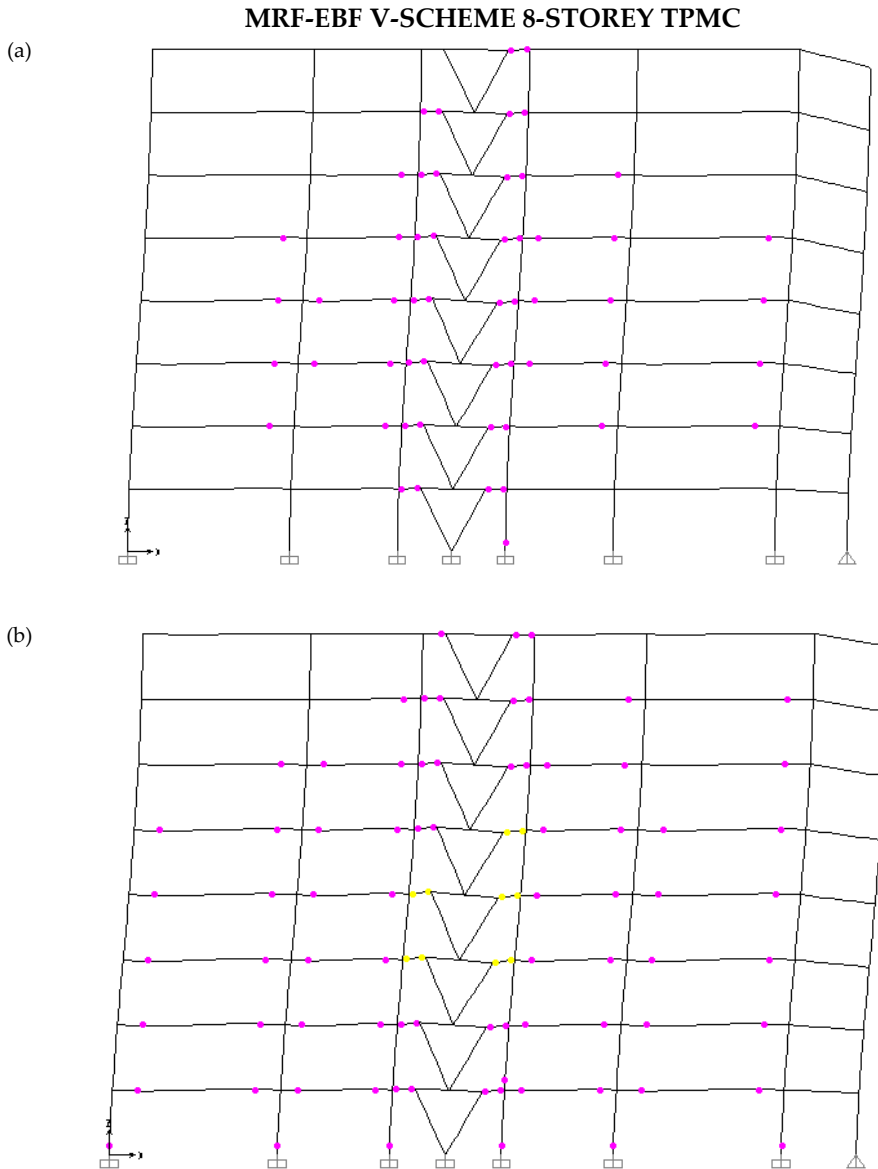
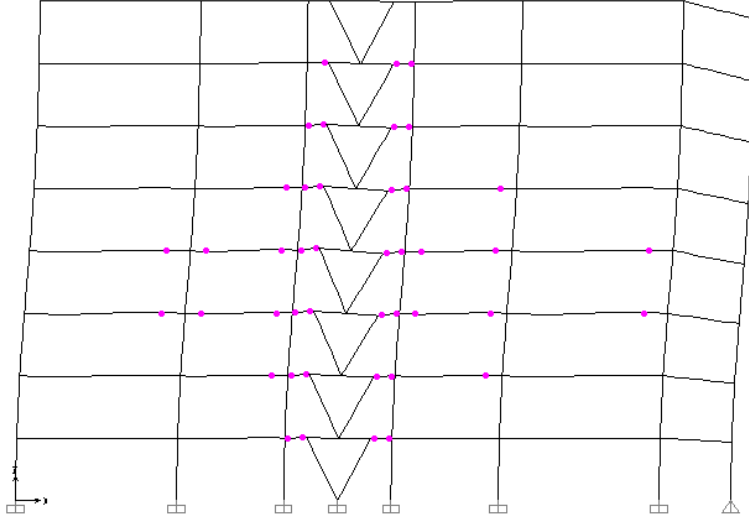


**Figure A.11** - Push-over hinge pattern 8 storey V-scheme TPMC for the ultimate design displacement (a) and for a displacement equal to two times the ultimate design displacement (b)



## MRF-EBF V-SCHEME 8-STOREY EC8

(a)



(b)

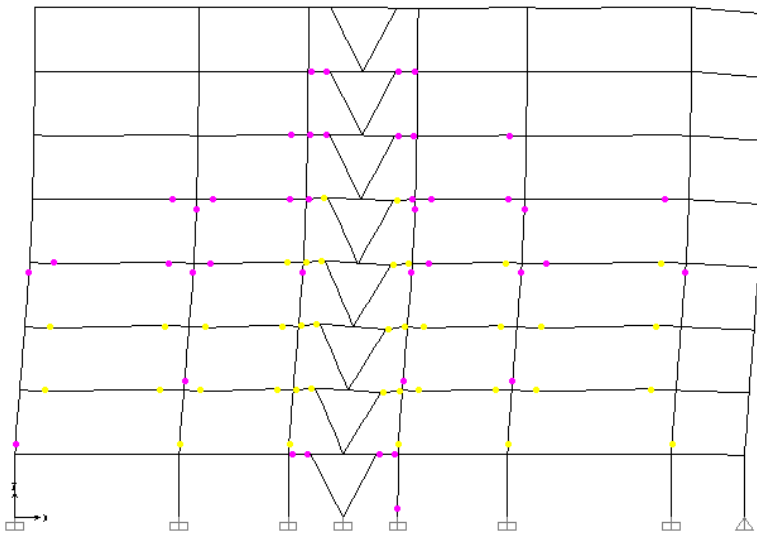
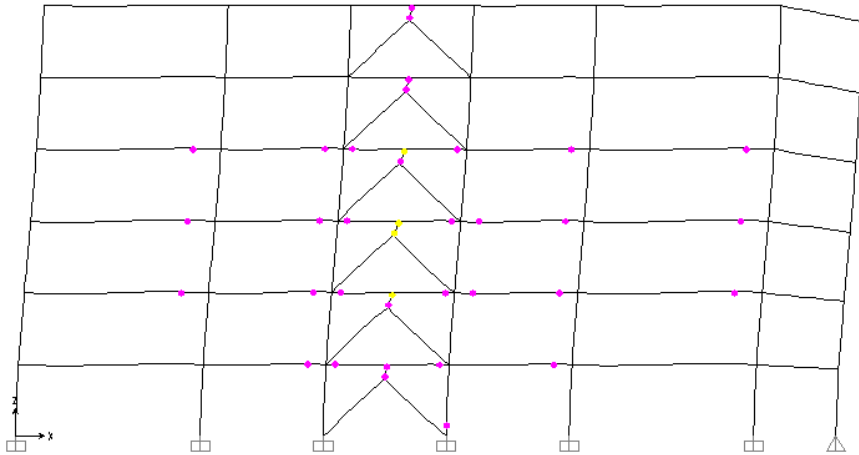


**Figure A.12** - Push-over hinge pattern 8 storey V-scheme TPMC for the ultimate design displacement (a) and for a displacement equal to two times the ultimate design displacement (b)

## MRF-EBF INV. Y-SCHEME 6-STOREY TPMC

(a)



(b)

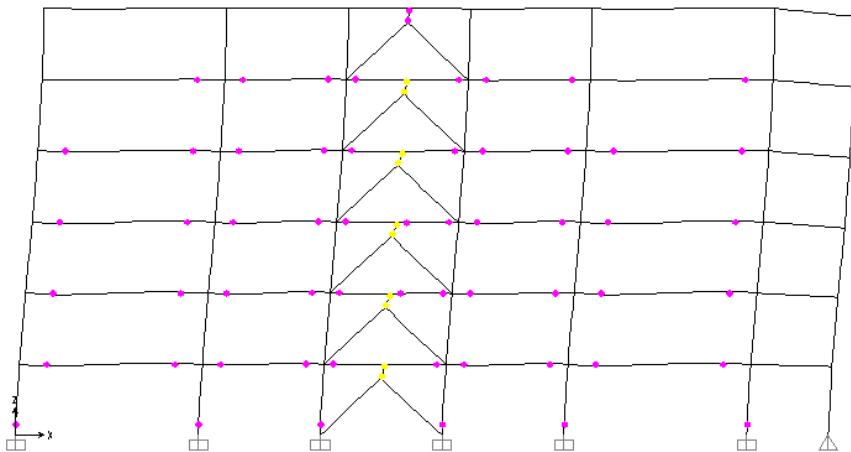
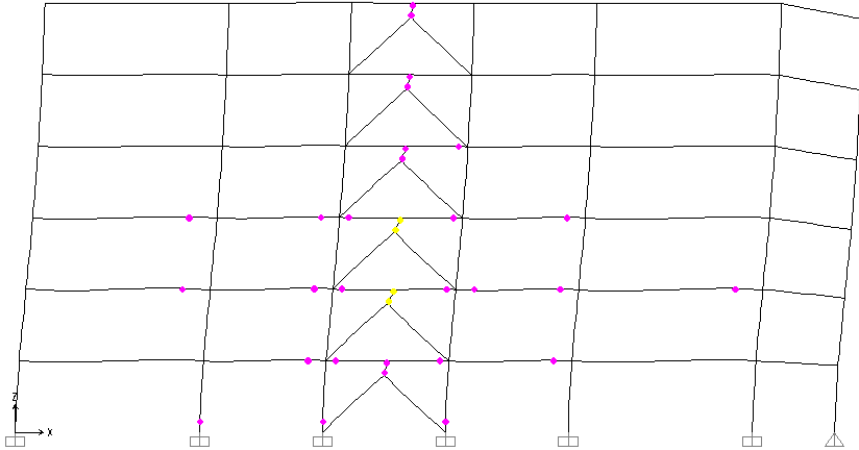


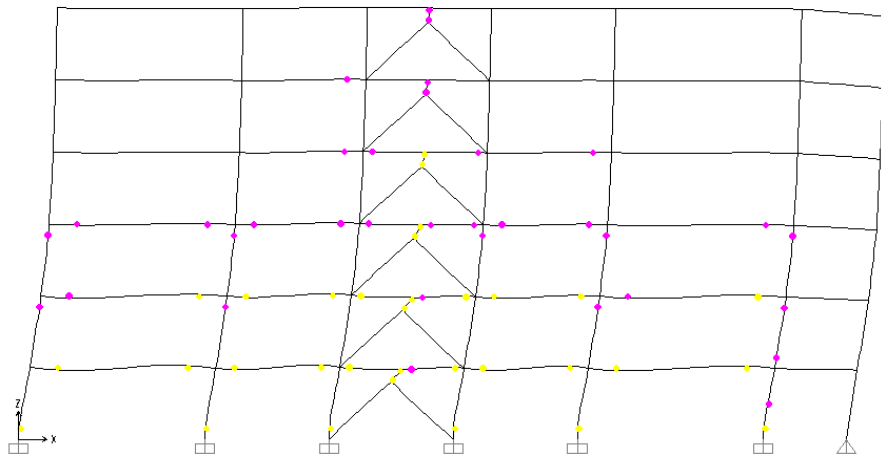
**Figure A.13** - Push-over hinge pattern 6 storey inverted Y-scheme TPMC for the ultimate design displacement (a) and for a displacement equal to two times the ultimate design displacement (b)

## MRF-EBF INV. Y-SCHEME 6-STOREY EC8

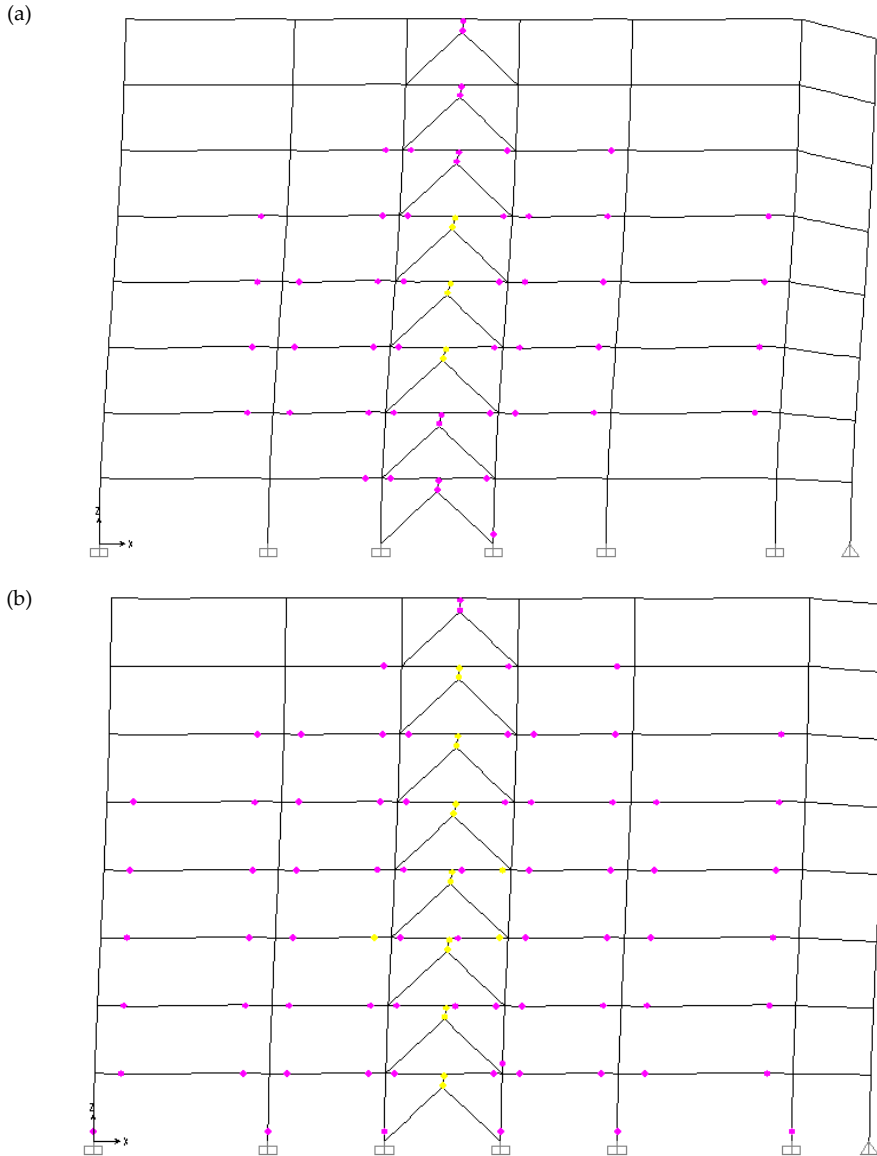
(a)



(b)



**Figure A.14** - Push-over hinge pattern 6 storey inverted Y-scheme EC8 for the ultimate design displacement (a) and for a displacement equal to two times the ultimate design displacement (b)

**MRF-EBF INV. Y-SCHEME 8-STOREY TPMC**

**Figure A.15** - Push-over hinge pattern 8 storey inverted Y-scheme TPMC for the ultimate design displacement (a) and for a displacement equal to two times the ultimate design displacement (b)

## MRF-EBF INV. Y-SCHEME 8-STOREY EC8

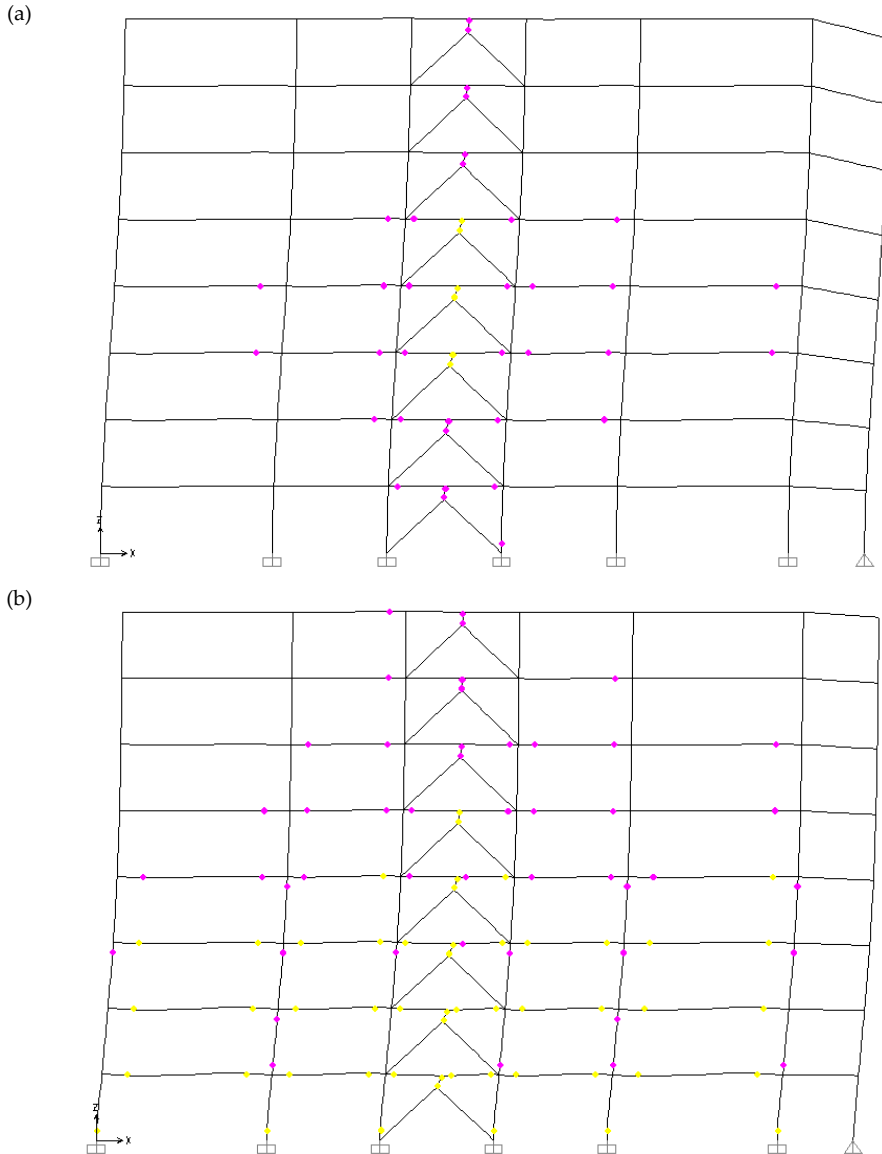


**Figure A.16** - Push-over hinge pattern 8 storey inverted Y-scheme EC8 for the ultimate design displacement (a) and for a displacement equal to two times the ultimate design displacement (b)



# APPENDIX B

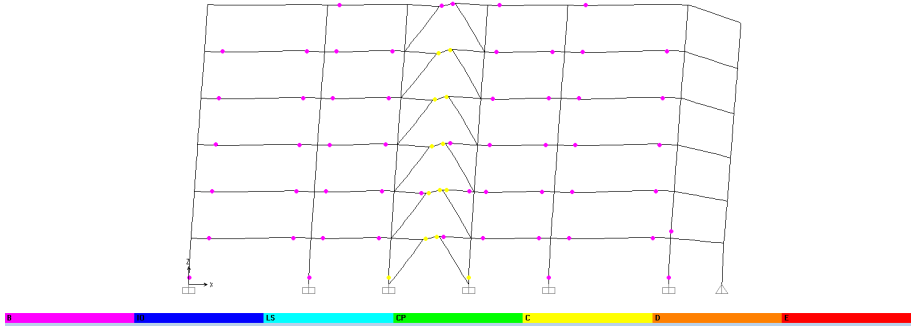
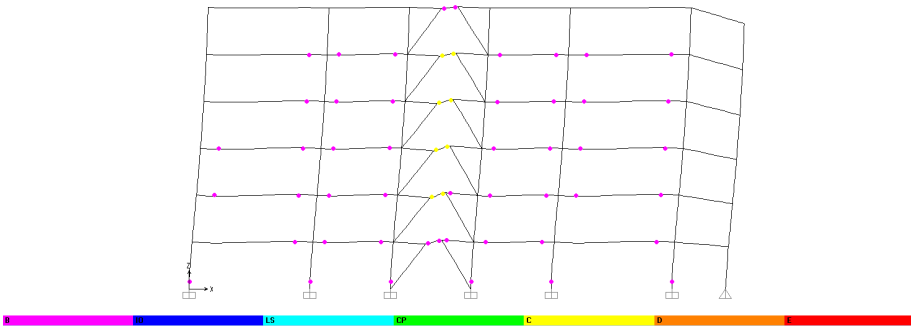
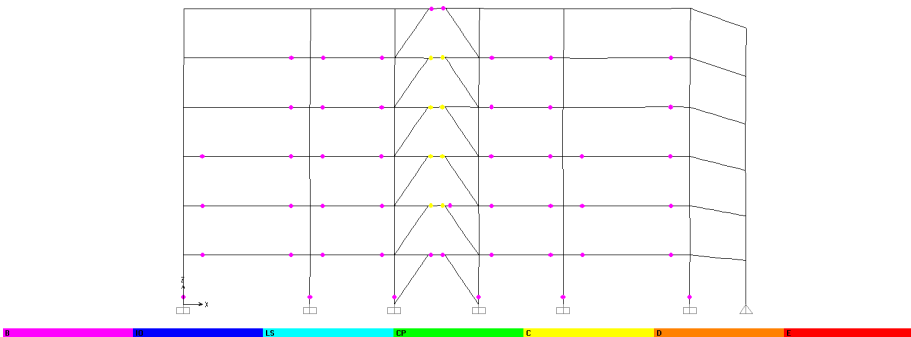
## INCREMENTAL DYNAMIC ANALYSES HINGE PATTERNS

In this section the plastic hinge distribution for the study cases described in Chapter 5 are reported. A total number of 8 structures, 4 designed exploiting Theory of Plastic Mechanism Control and 4 Eurocode 8 have been considered. These structures have been analysed by means of Incremental Dynamic Analyses (IDA) carried out by SAP2000 computer program.

The figures representing hinge patterns for each ground motion and for the  $S_a/g(T_i)$  corresponding to the achievement of the collapse condition are reported with reference to each analysed structure. These figures originate from the SAP2000 Computer Program screenshot.

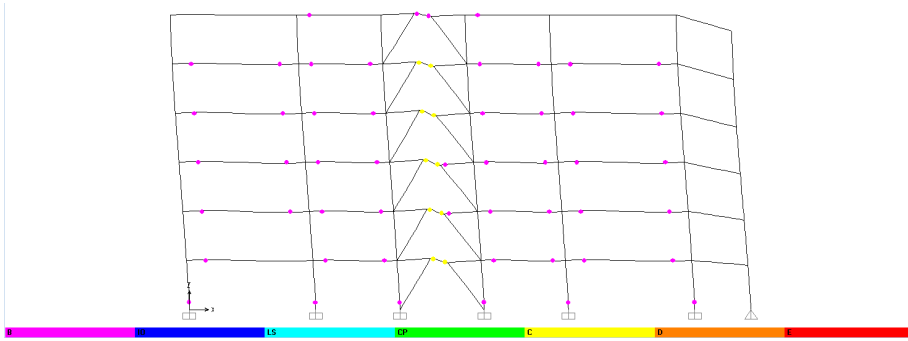
In order to identificate the exhamined structures the following notation has been used:

- **MRF-EBF K-scheme** for the MRF-EBF dual systems whose braced bay is an EBF with K-scheme;
- **MRF-EBF D-scheme** for the MRF-EBF dual systems whose braced bay is an EBF with D-scheme;
- **MRF-EBF V-scheme** for the MRF-EBF dual systems whose braced bay is an EBF with V-scheme;
- **MRF-EBF inv. Y-scheme** for the MRF-EBF dual systems whose braced bay is an EBF with inverted Y-scheme.

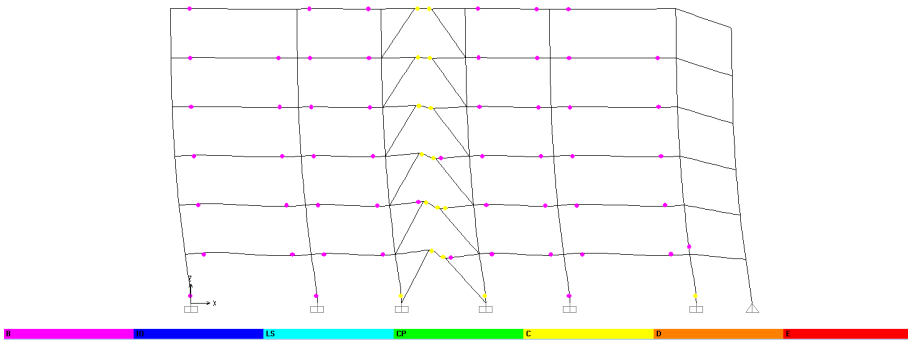
**6 STOREY K-SCHEME TPMC - COALINGA  $S_a(T_1)=1.15g$** **6 STOREY K-SCHEME TPMC – FRIULI BUIA  $S_a(T_1)=0.95g$** **6 STOREY K-SCHEME TPMC – IMPERIAL VALLEY  $S_a(T_1)=0.80g$** 



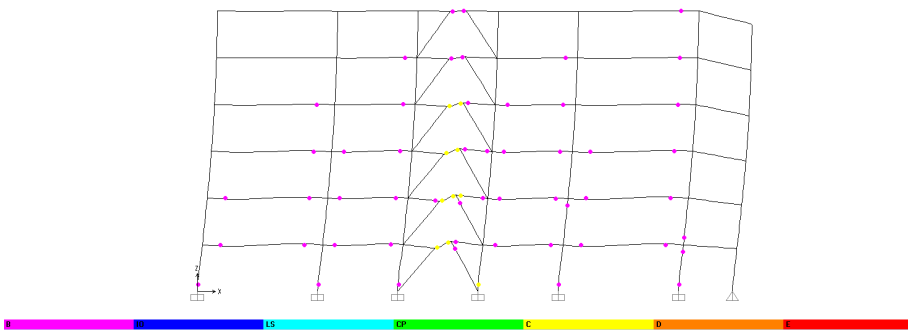
**6 STOREY K-SCHEME TPMC – IRPINIA  $S_a(T_1)=1.00g$**

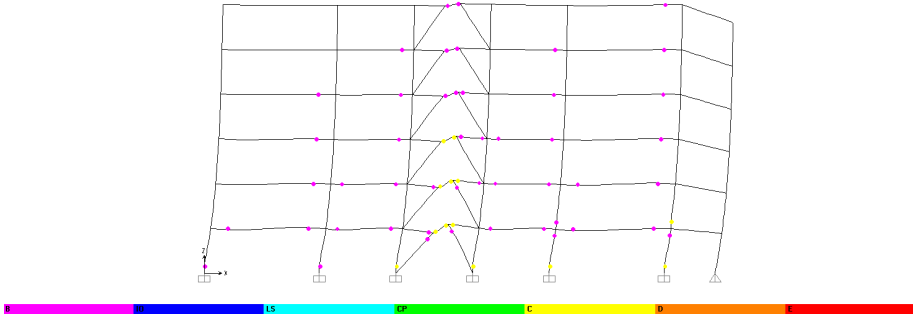
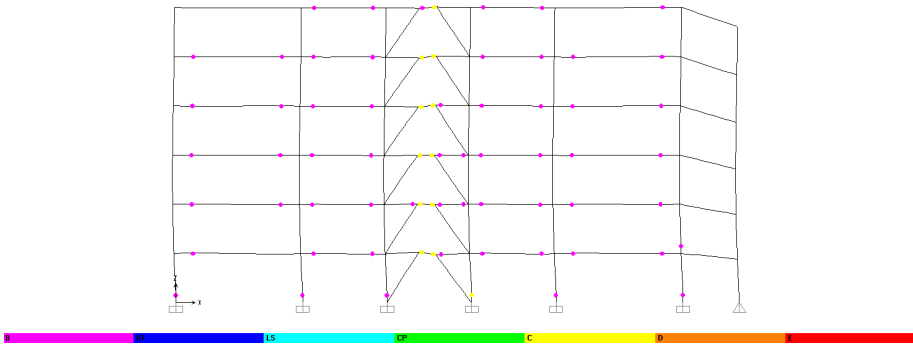
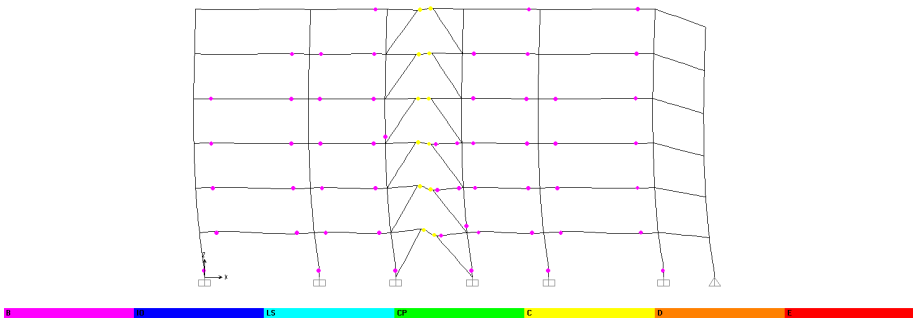


**6 STOREY K-SCHEME TPMC - KOBE  $S_a(T_1)=1.05g$**

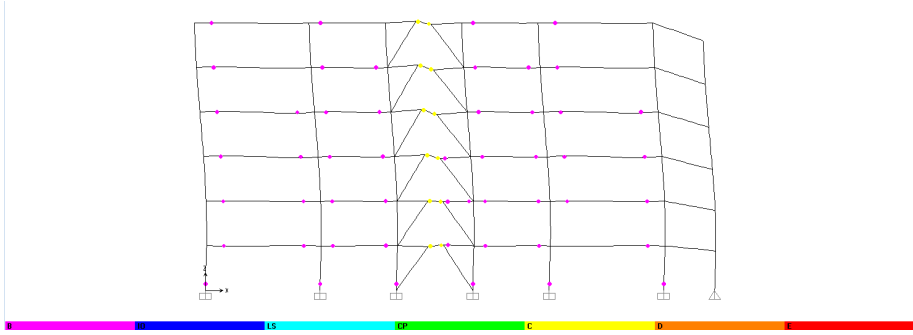


**6 STOREY K-SCHEME TPMC – NORTHRIDGE  $S_a(T_1)=0.83g$**

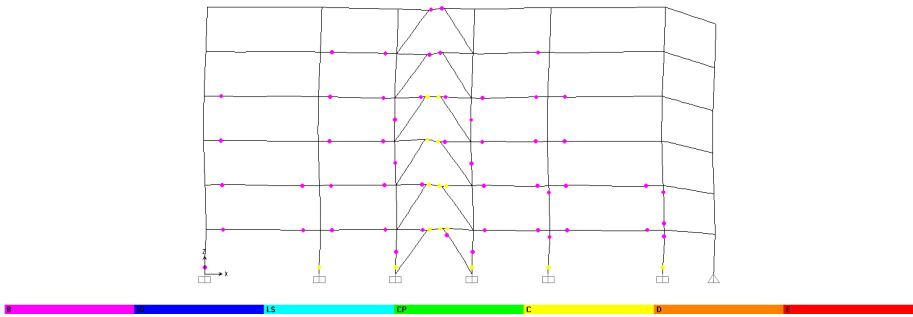


**6 STOREY K-SCHEME TPMC – PALM SPRINGS  $S_a(T_1)=0.50g$** **6 STOREY K-SCHEME TPMC – SANTA BARBARA  $S_a(T_1)=1.55g$** **6 STOREY K-SCHEME TPMC – SPITAK ARMENIA  $S_a(T_1)=0.80g$** 

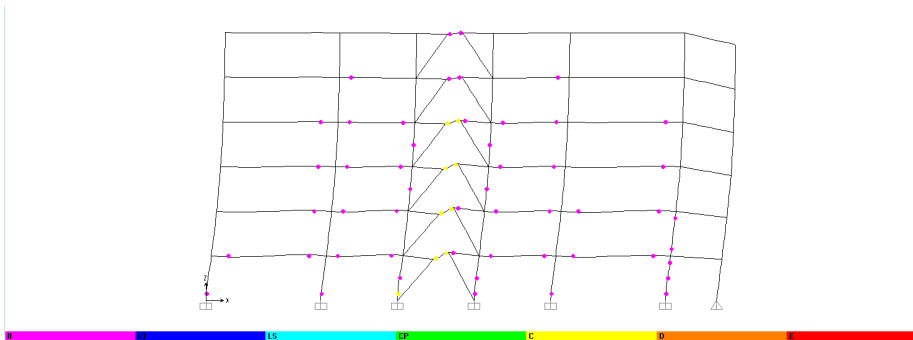
**6 STOREY K-SCHEME TPMC – VICTORIA MEXICO  $S_a(T_1)=1.10g$**

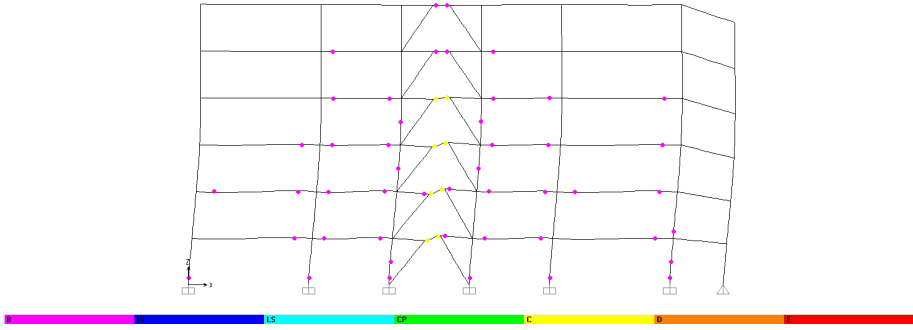
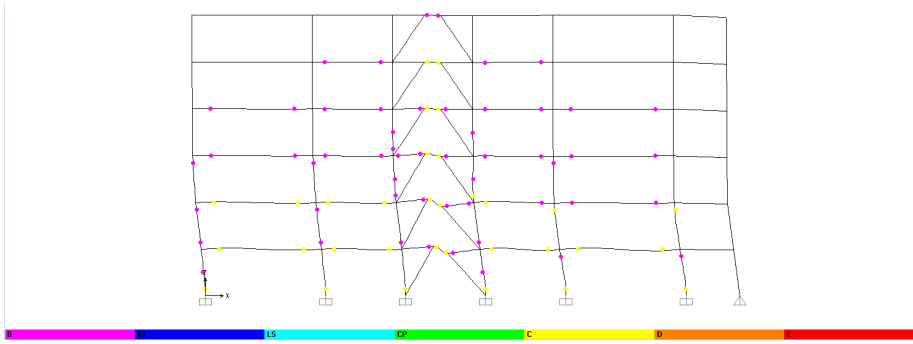
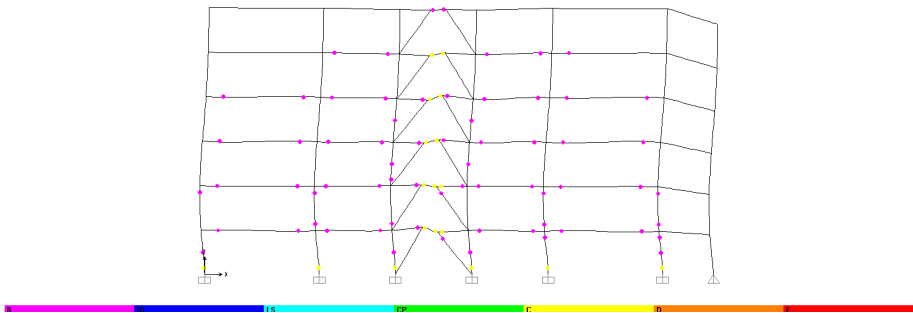


**6 STOREY K-SCHEME EC8 - COALINGA  $S_a(T_1)=0.30g$**

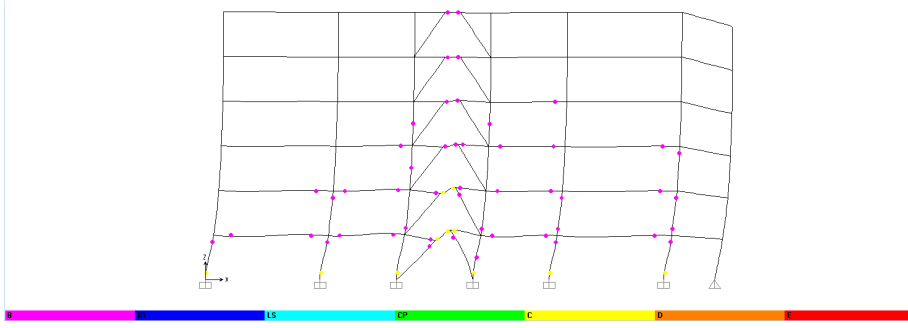


**6 STOREY K-SCHEME EC8 - FRIULI BUIA  $S_a(T_1)=0.30g$**

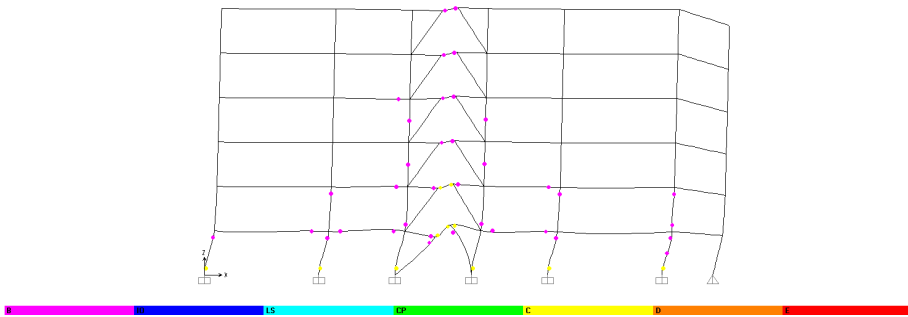


**6 STOREY K-SCHEME EC8 – IMPERIAL VALLEY  $S_a(T_1)=0.30g$** **6 STOREY K-SCHEME EC8 – IRPINIA  $S_a(T_1)=0.40g$** **6 STOREY K-SCHEME EC8 – KOBE  $S_a(T_1)=0.40g$** 

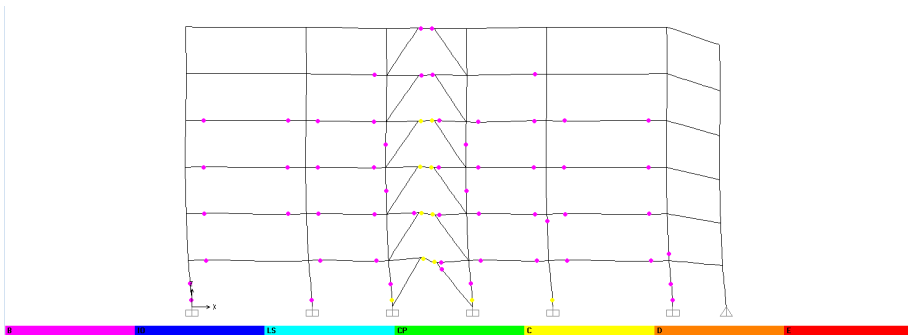
**6 STOREY K-SCHEME EC8 – NORTHRIDGE  $S_a(T_1)=0.20g$**

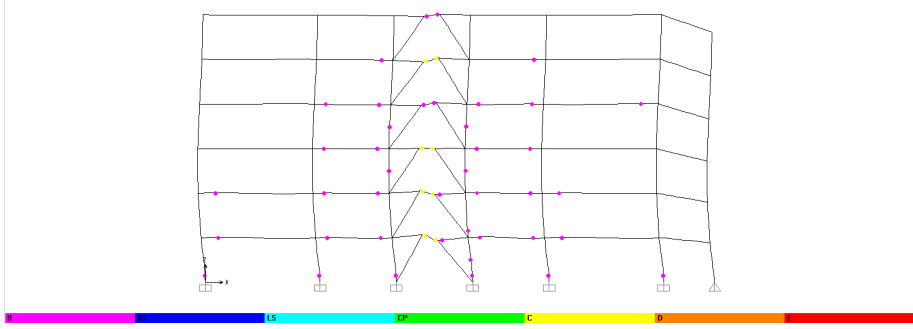
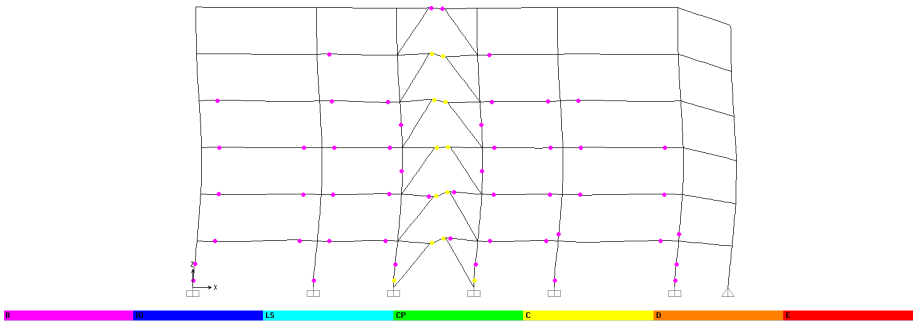
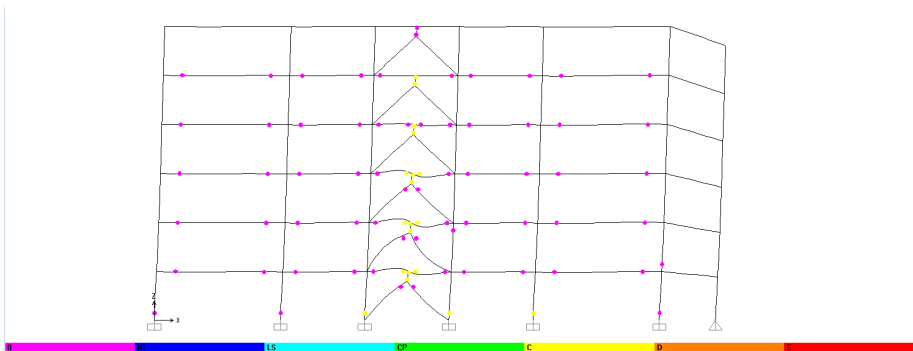


**5 STOREY K-SCHEME EC8 – PALM SPRINGS  $S_a(T_1)=0.10g$**

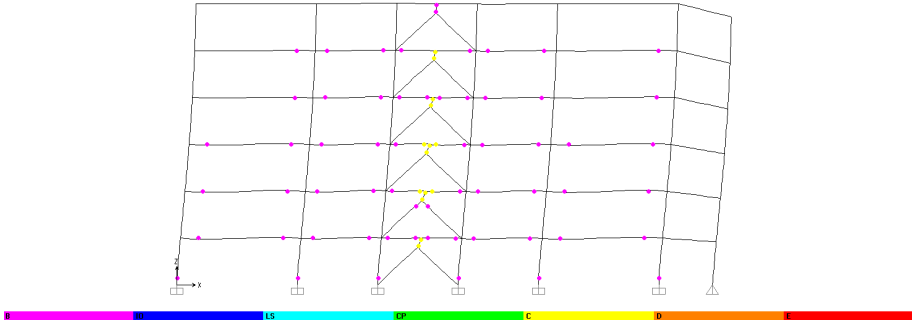


**6 STOREY K-SCHEME EC8 – SANTA BARBARA  $S_a(T_1)=0.30g$**

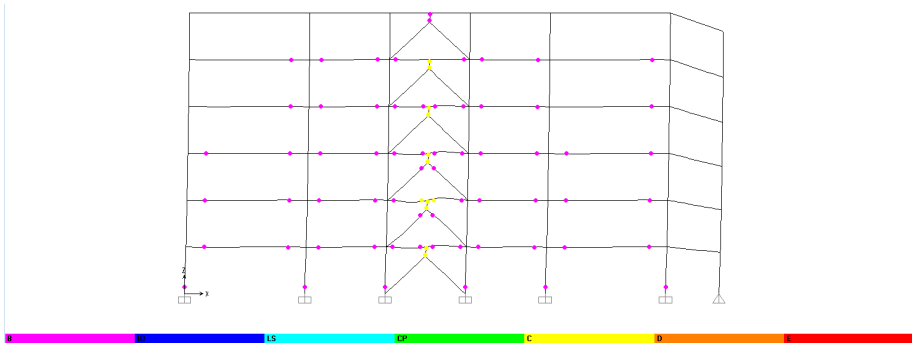


**6 STOREY K-SCHEME EC8 – SPITAK ARMENIA  $S_a(T_1)=0.30g$** **6 STOREY K-SCHEME EC8 – VICTORIA MEXICO  $S_a(T_1)=0.40g$** **6 STOREY INV. Y-SCHEME TPMC - COALINGA  $S_a(T_1)=1.30g$** 

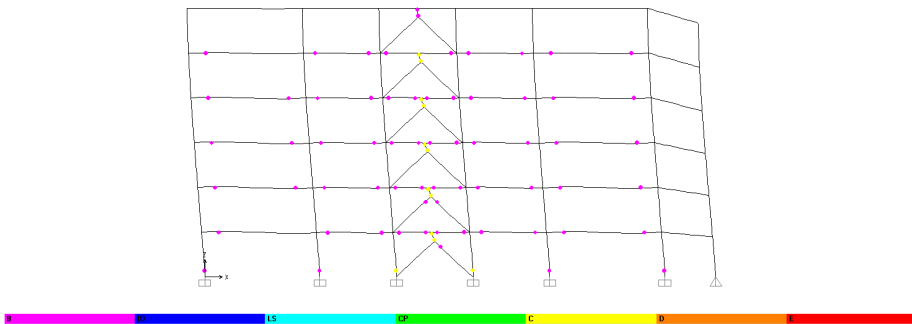
**6 STOREY INV. Y-SCHEME TPMC – FRIULI BUIA  $S_a(T_1)=0.95g$**

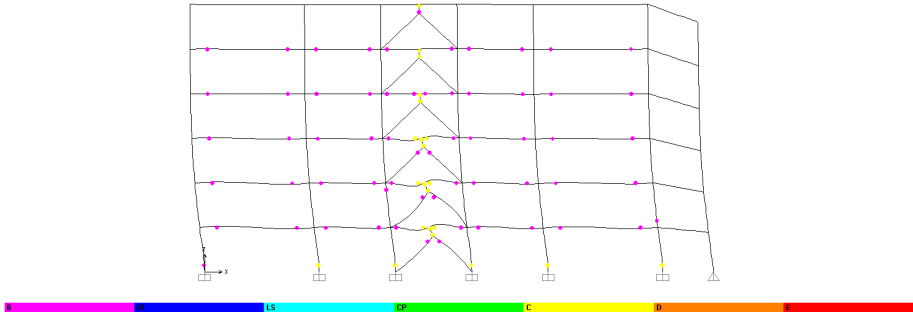
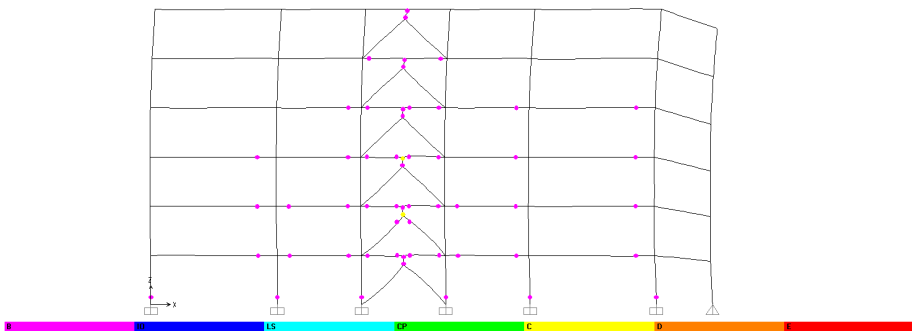
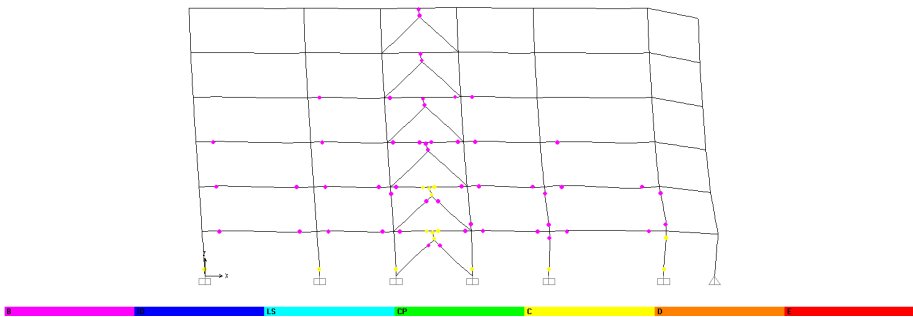


**6 STOREY INV. Y-SCHEME TPMC – IMPERIAL VALLEY  $S_a(T_1)=0.85g$**



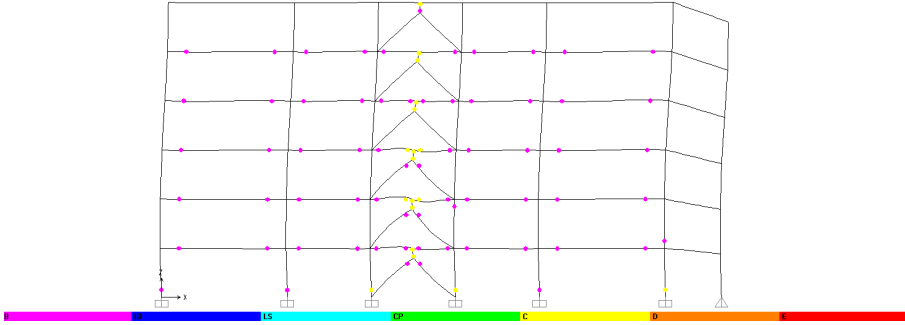
**6 STOREY INV. Y-SCHEME TPMC – IRPINIA  $S_a(T_1)=1.20g$**



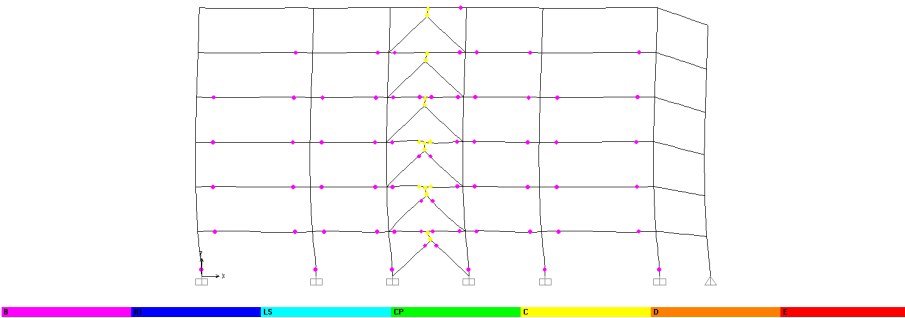
**6 STOREY INV. Y-SCHEME TPMC - KOBE  $S_a(T_1)=1.20g$** **6 STOREY INV. Y-SCHEME TPMC - NORTHRIDGE  $S_a(T_1)=1.20g$** **6 STOREY INV. Y-SCHEME TPMC - PALM SPRINGS  $S_a(T_1)=1.30g$** 



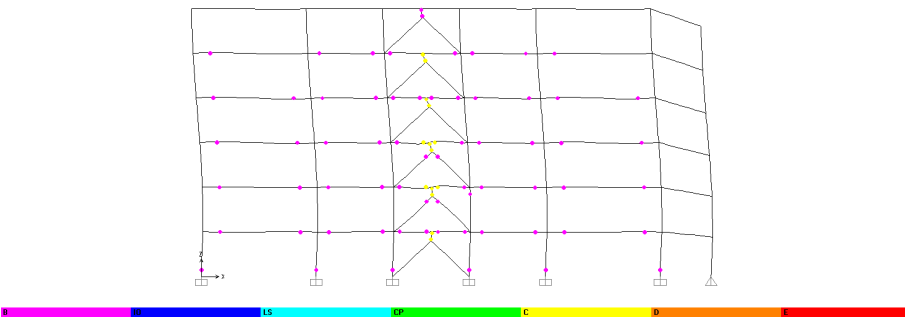
**6 STOREY INV. Y-SCHEME TPMC – SANTA BARBARA  $S_a(T_1)=1.70g$**

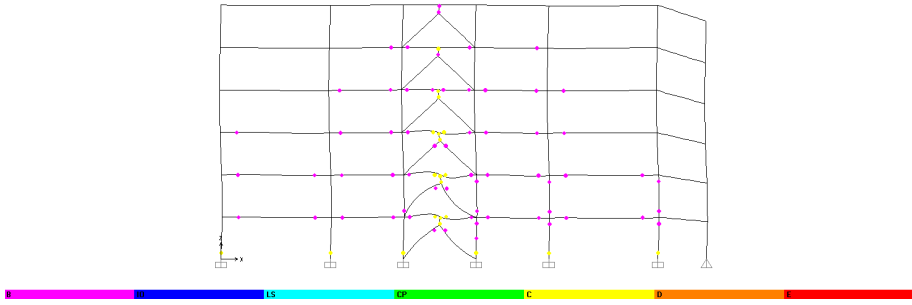
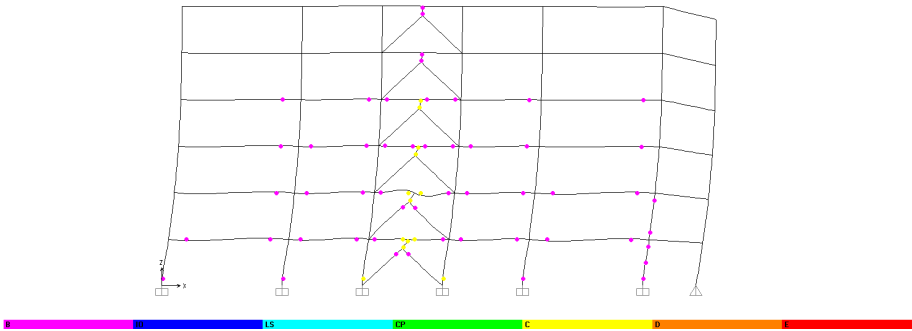
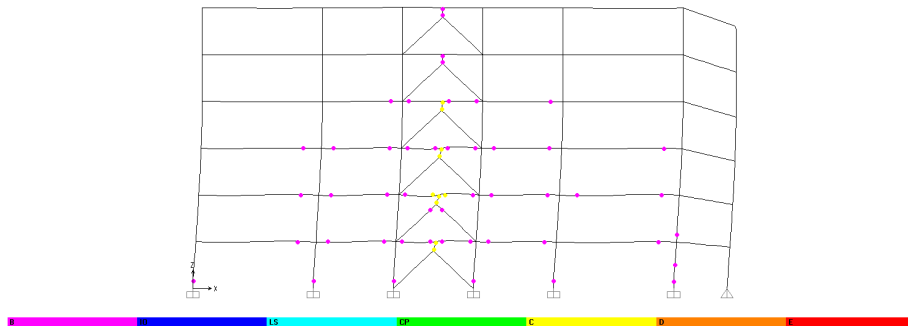


**6 STOREY INV. Y-SCHEME TPMC – SPITAK ARMENIA  $S_a(T_1)=0.90g$**

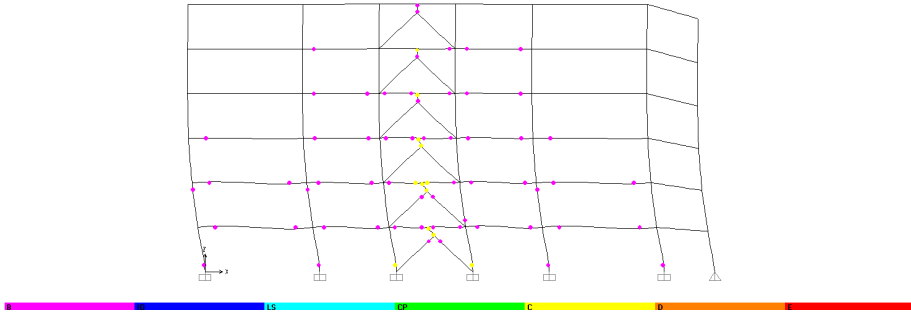


**6 STOREY INV. Y-SCHEME TPMC – VICTORIA MEXICO  $S_a(T_1)=1.20g$**

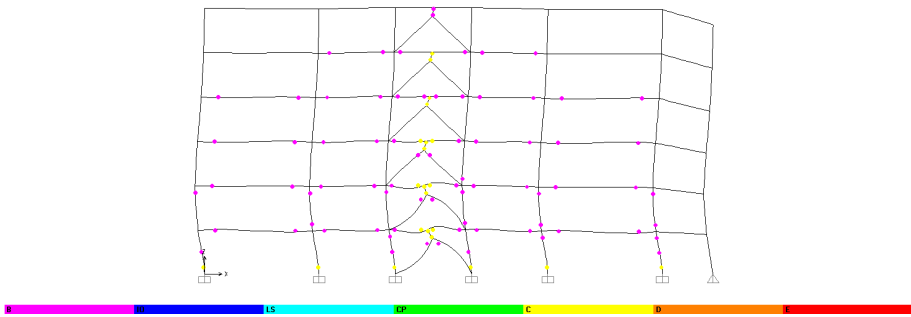


**6 STOREY INV. Y-SCHEME EC8 – COALINGA  $S_a(T_1)=1.30g$** **6 STOREY INV. Y-SCHEME EC8 – FRIULI BUIA  $S_a(T_1)=0.80g$** **6 STOREY INV. Y-SCHEME EC8 – IMPERIAL VALLEY  $S_a(T_1)=0.60g$** 

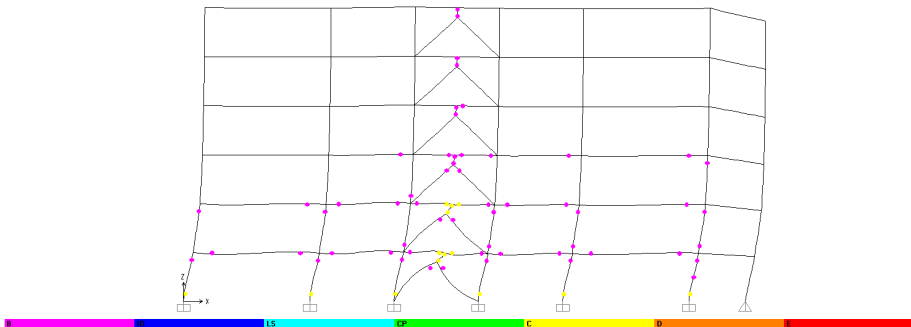
**6 STOREY INV. Y-SCHEME EC8 – IRPINIA  $S_a(T_1)=1.00g$**

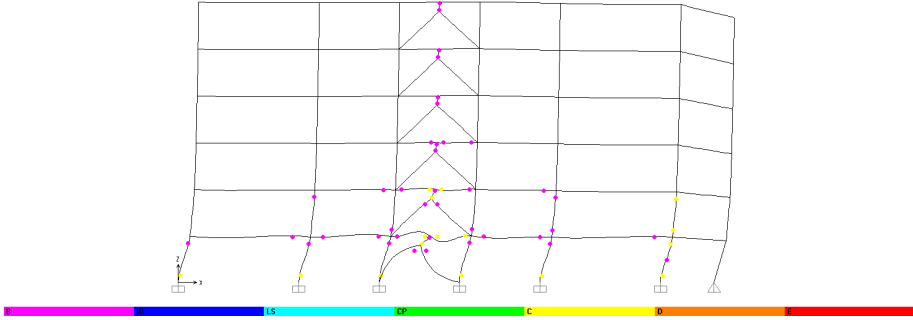
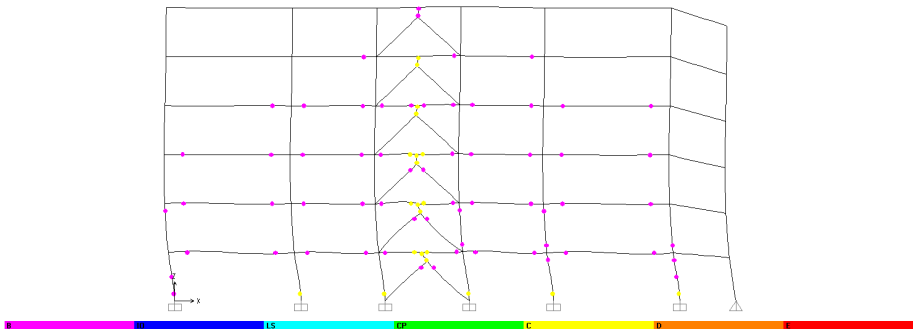
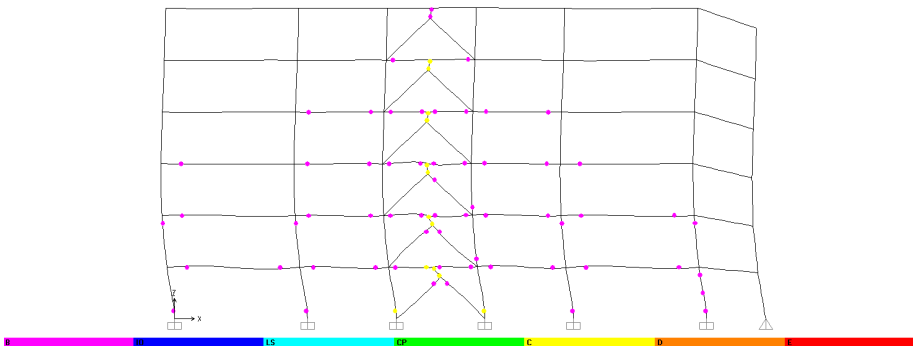


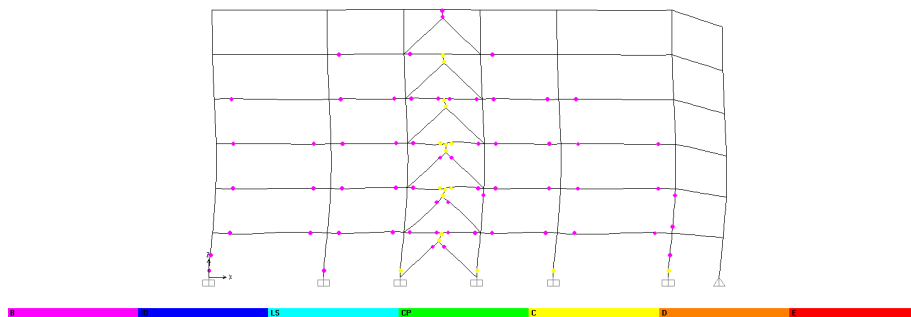
**6 STOREY INV. Y-SCHEME EC8 – KOBE  $S_a(T_1)=0.70g$**



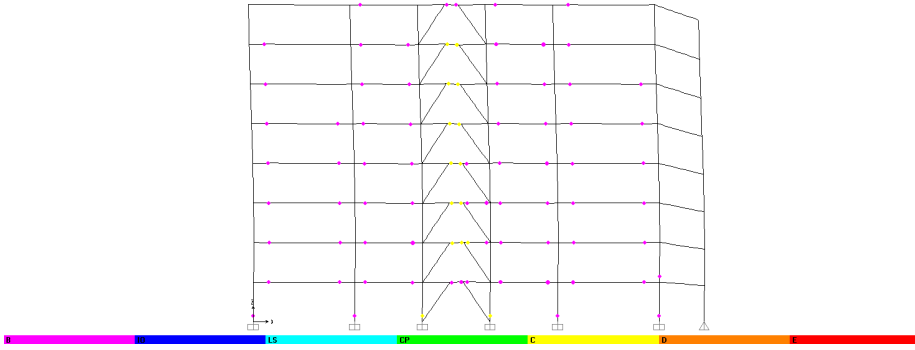
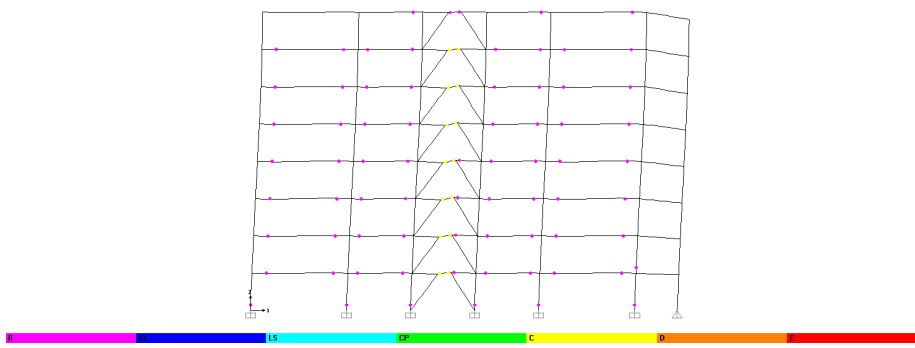
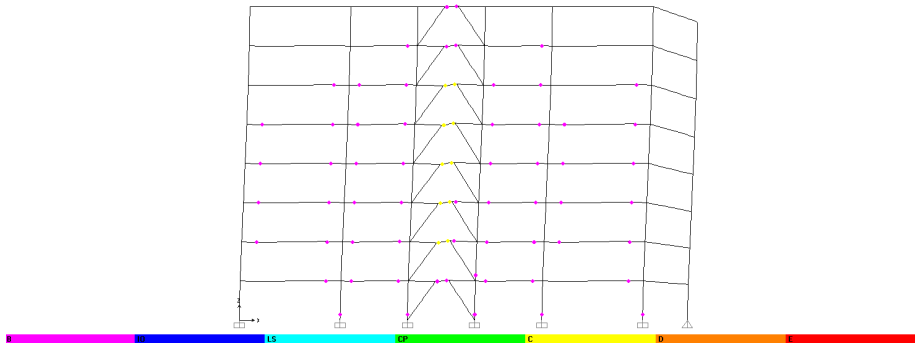
**6 STOREY INV. Y-SCHEME EC8 – NORTHRIDGE  $S_a(T_1)=0.80g$**



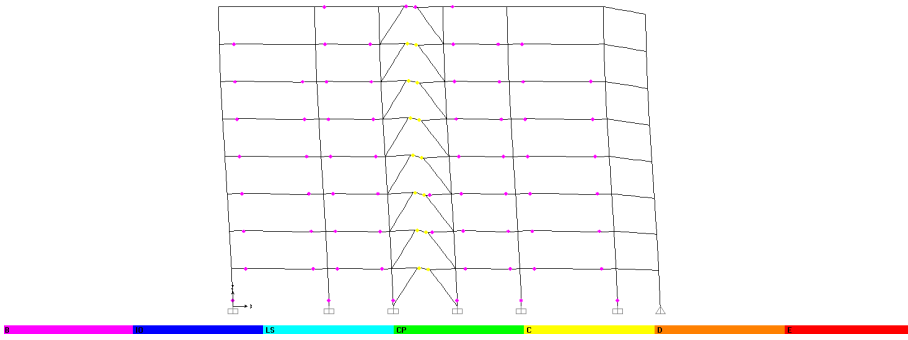
**6 STOREY INV. Y-SCHEME TPMC – PALM SPRINGS  $S_a(T_1)=0.40g$** **6 STOREY INV. Y-SCHEME EC8 – SANTA BARBARA  $S_a(T_1)=0.90g$** **6 STOREY INV. Y-SCHEME EC8 – SPITAK ARMENIA  $S_a(T_1)=0.80g$** 

**6 STOREY INV. Y-SCHEME EC8 – VICTORIA MEXICO  $S_a(T_1)=0.80g$** 

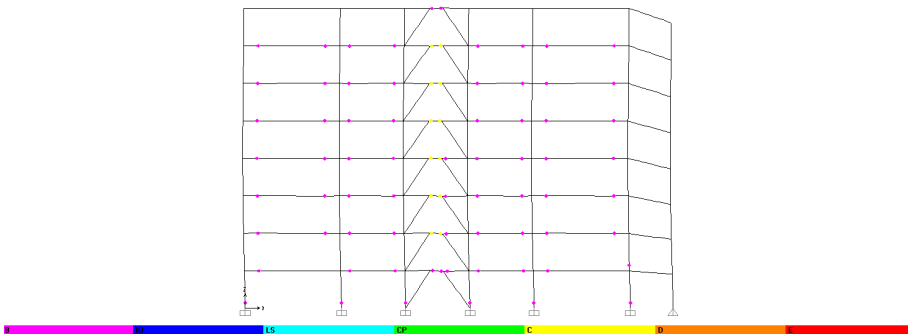
---

**8 STOREY K-SCHEME TPMC – COALINGA  $S_a(T_1)=1.10g$** **8 STOREY K-SCHEME TPMC – FRIULI BUIA  $S_a(T_1)=1.25g$** **8 STOREY K-SCHEME TPMC – IMPERIAL VALLEY  $S_a(T_1)=0.75g$** 

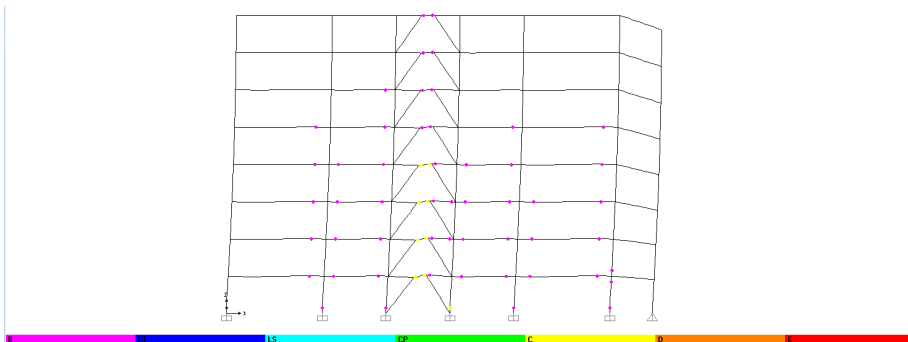
**8 STOREY K-SCHEME TPMC – IRPINIA  $S_a(T_1)=0.90g$**

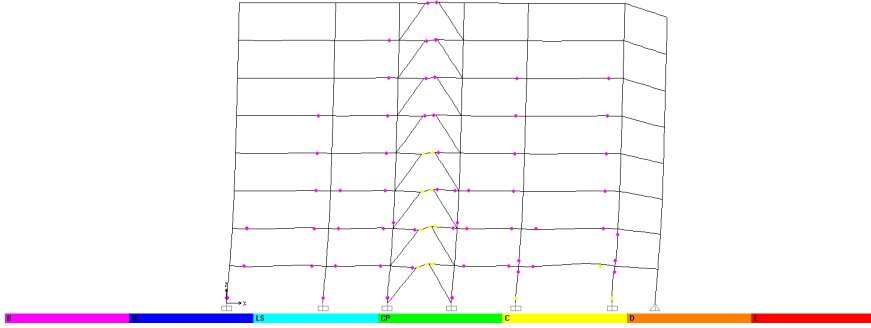
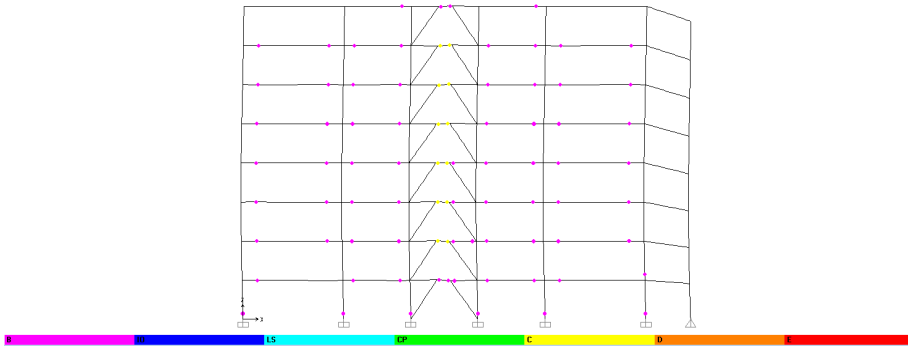
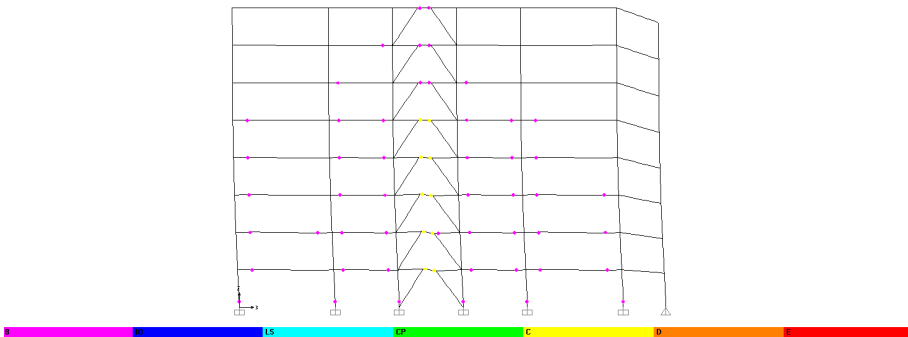


**8 STOREY K-SCHEME TPMC – KOBE  $S_a(T_1)=1.85g$**



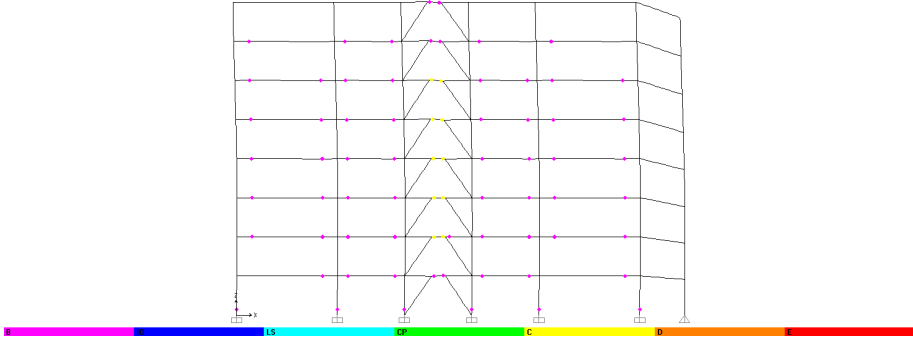
**8 STOREY K-SCHEME TPMC – NORTHRIDGE  $S_a(T_1)=0.75g$**



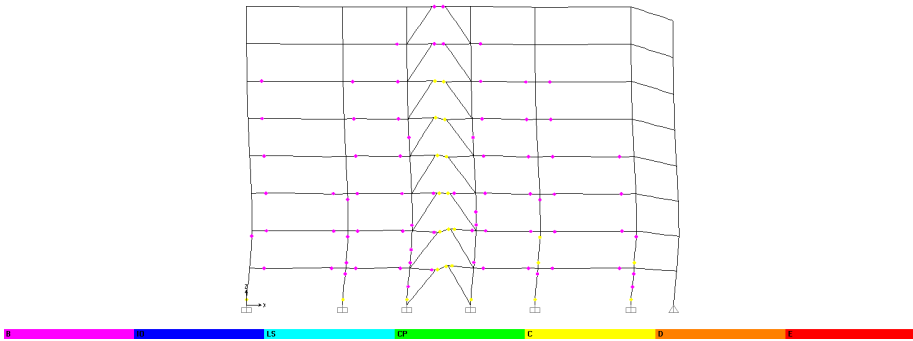
**8 STOREY K-SCHEME TPMC – PALM SPRINGS  $S_a(T_1)=0.40g$** **8 STOREY K-SCHEME TPMC – SANTA BARBARA  $S_a(T_1)=0.65g$** **8 STOREY K-SCHEME TPMC – SPITAK ARMENIA  $S_a(T_1)=0.70g$** 



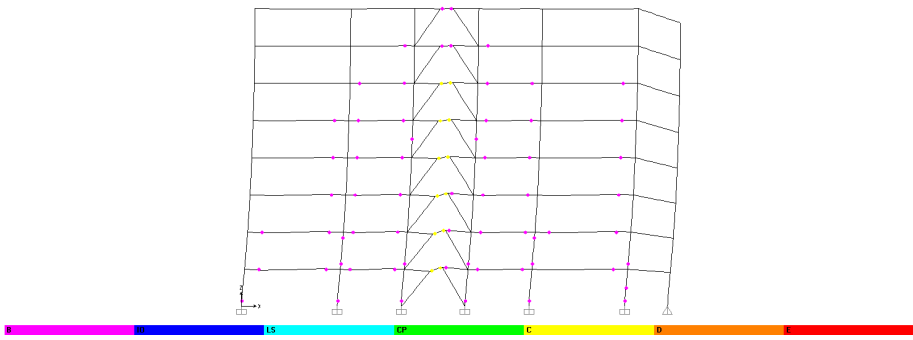
**8 STOREY K-SCHEME TPMC – VICTORIA MEXICO  $S_a(T_1)=1.05g$**

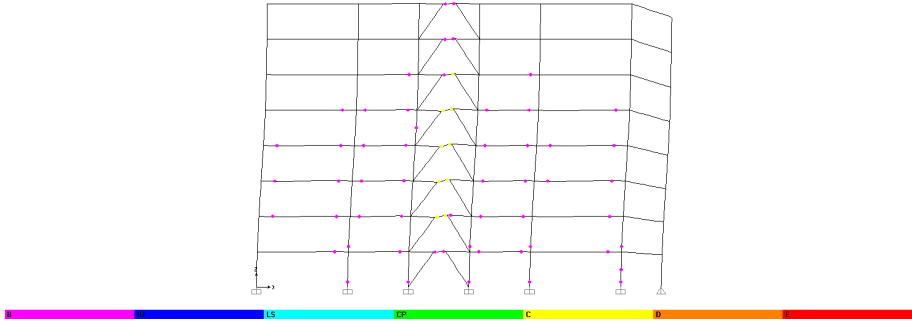
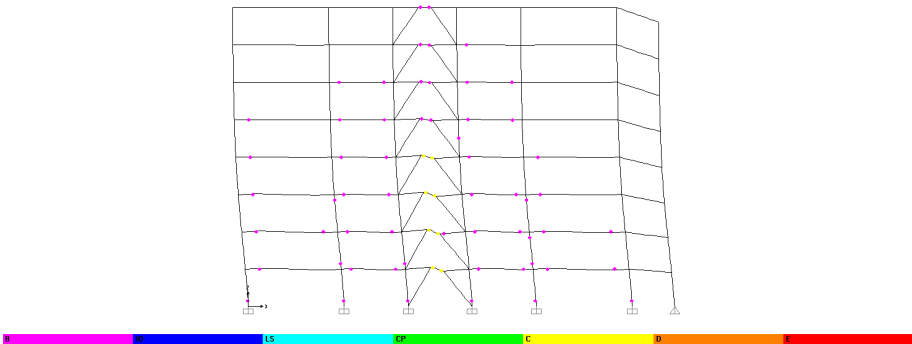
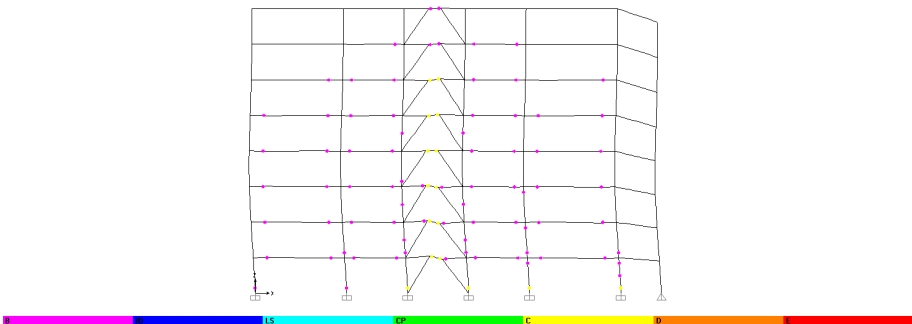


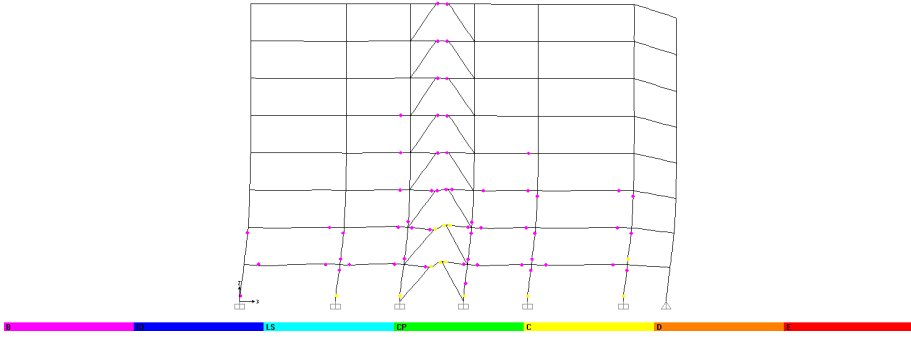
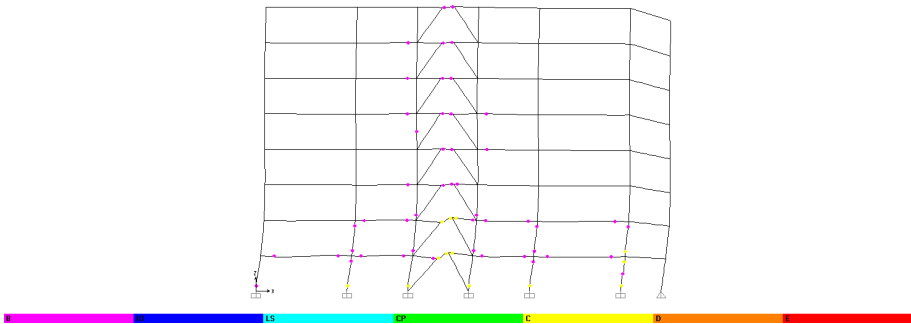
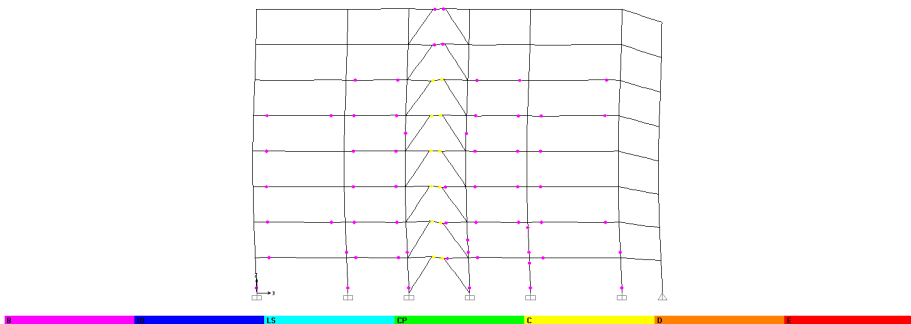
**8 STOREY K-SCHEME EC8 – COALINGA  $S_a(T_1)=0.50g$**

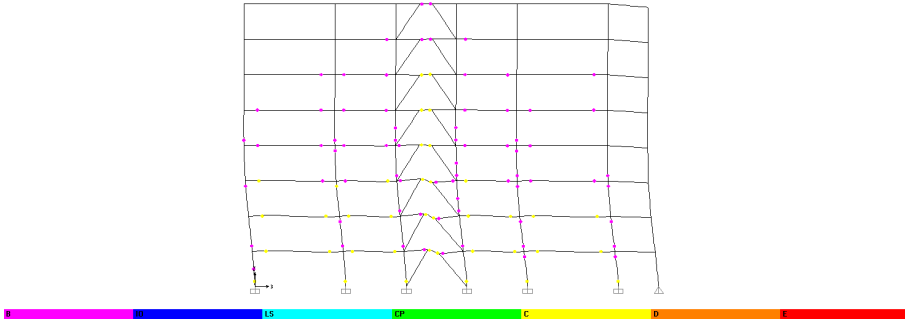
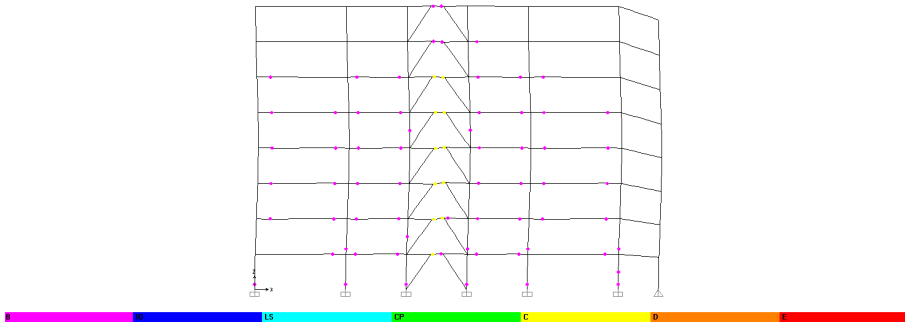
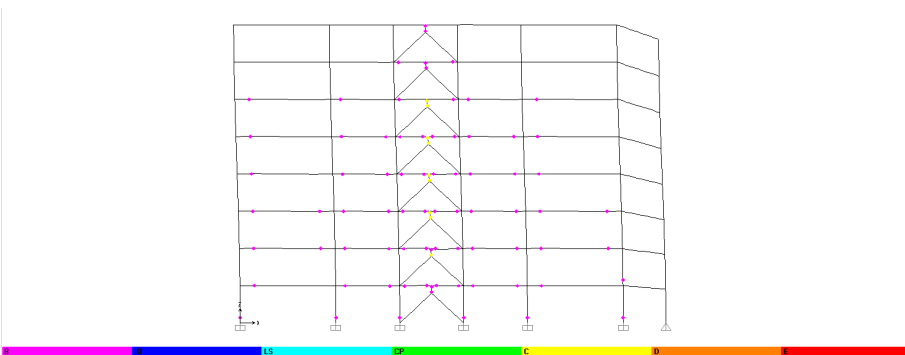


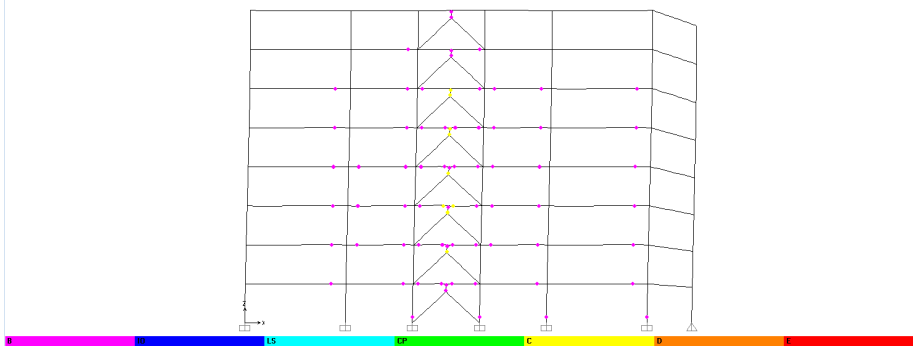
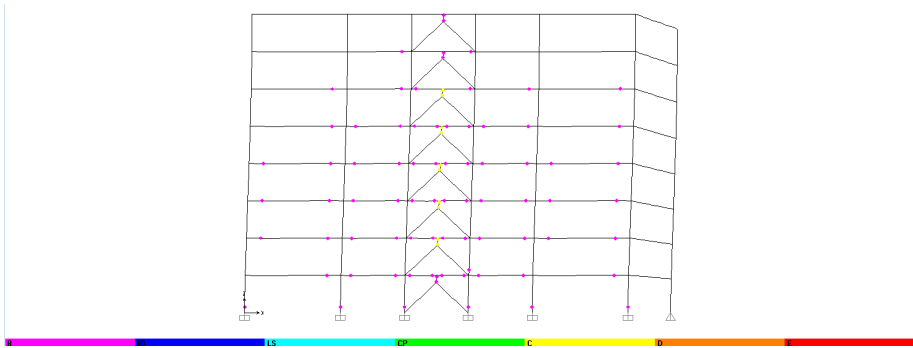
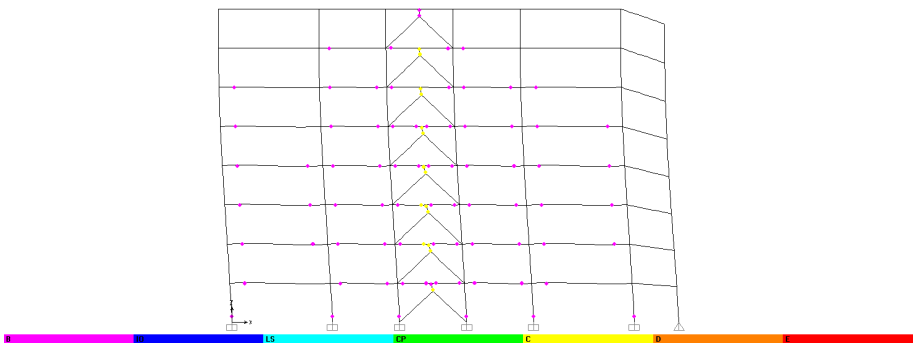
**8 STOREY K-SCHEME EC8 – FRIULI BUIA  $S_a(T_1)=0.80g$**

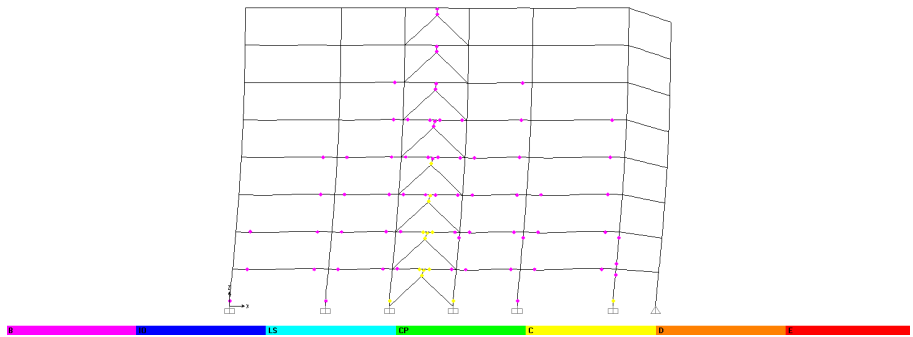
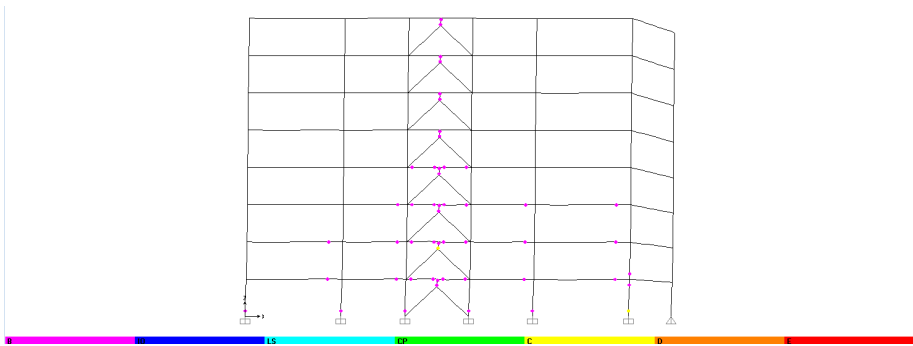


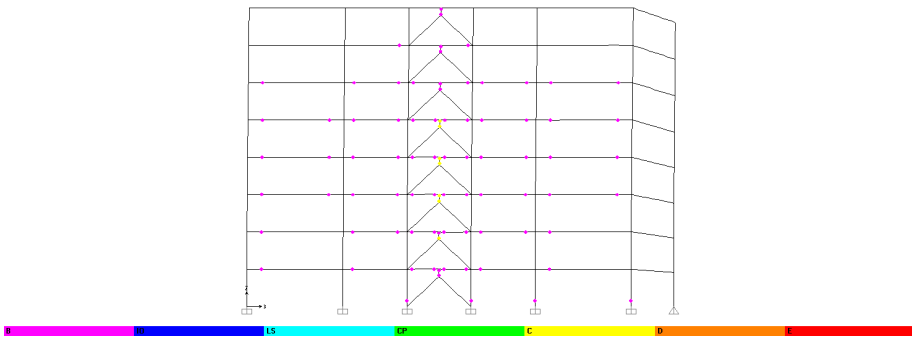
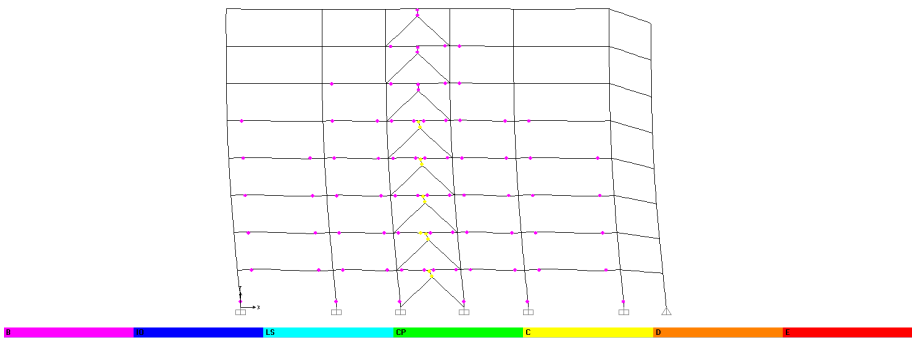
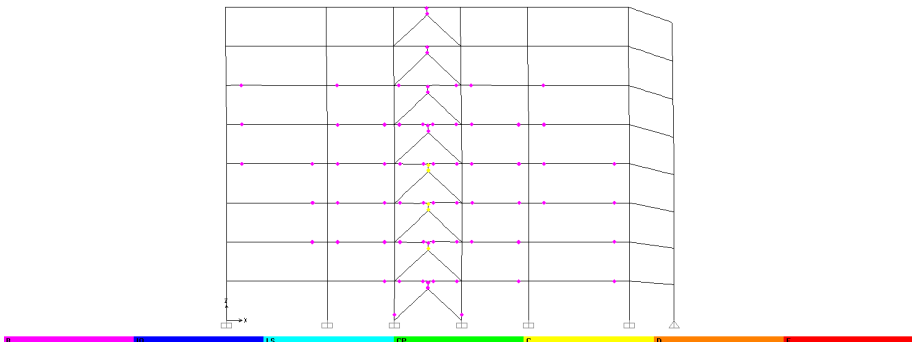
**8 STOREY K-SCHEME EC8 – IMPERIAL VALLEY  $S_a(T_1)=0.60g$** **8 STOREY K-SCHEME EC8 – IRPINIA  $S_a(T_1)=0.60g$** **8 STOREY K-SCHEME EC8 – KOBE  $S_a(T_1)=1.15g$** 

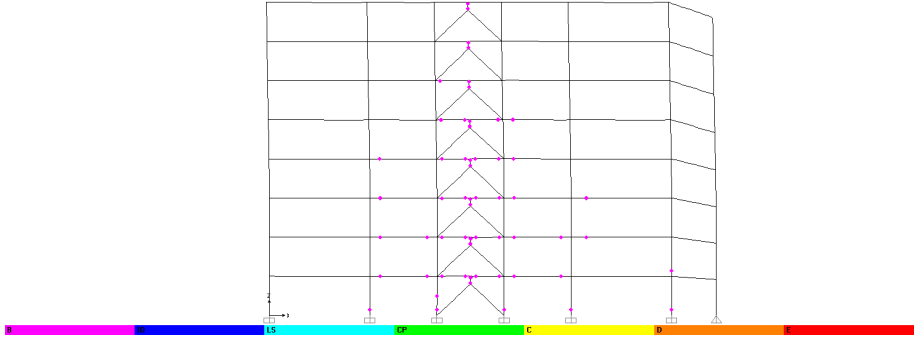
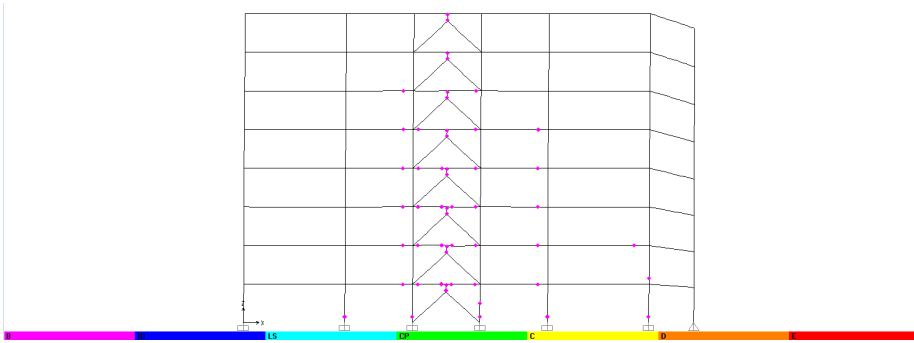
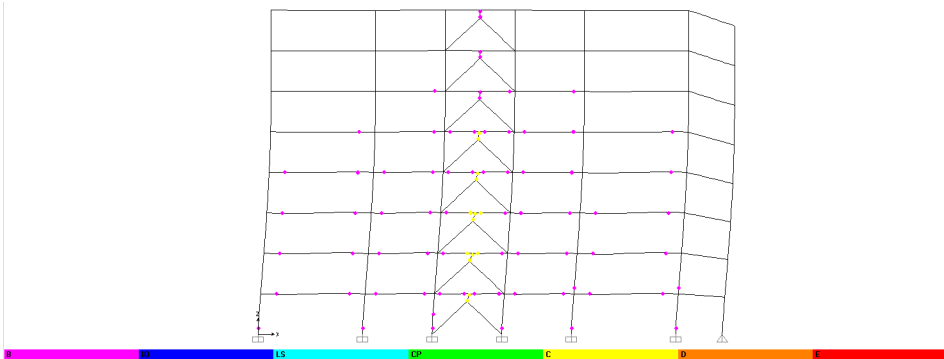
**8 STOREY K-SCHEME EC8 – NORTHRIDGE  $S_a(T_1)=0.40g$** **8 STOREY K-SCHEME EC8 – PALM SPRINGS  $S_a(T_1)=0.30g$** **8 STOREY K-SCHEME EC8 – SANTA BARBARA  $S_a(T_1)=0.40g$** 

**8 STOREY K-SCHEME EC8 – SPITAK ARMENIA  $S_a(T_1)=0.40g$** **8 STOREY K-SCHEME EC8 – VICTORIA MEXICO  $S_a(T_1)=0.70g$** **8 STOREY INV. Y-SCHEME TPMC – COALINGA  $S_a(T_1)=1.10g$** 

**8 STOREY INV. Y-SCHEME TPMC – FRIULI BUIA  $S_a(T_1)=1.30g$** **8 STOREY INV. Y-SCHEME TPMC – IMPERIAL VALLEY  $S_a(T_1)=0.80g$** **8 STOREY INV. Y-SCHEME TPMC – IRPINIA  $S_a(T_1)=1.00g$** 

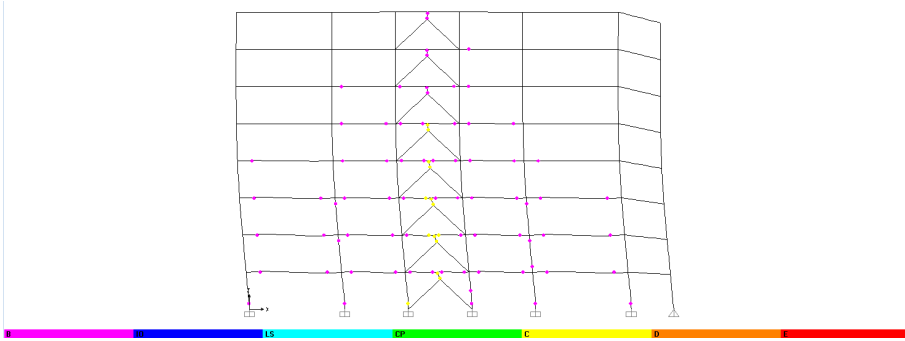
**8 STOREY INV. Y-SCHEME TPMC – KOBE  $S_a(T_1)=1.00g$** **8 STOREY INV. Y-SCHEME TPMC – NORTHRIDGE  $S_a(T_1)=0.90g$** **8 STOREY INV. Y-SCHEME TPMC – PALM SPRINGS  $S_a(T_1)=0.50g$** 

**8 STOREY INV. Y-SCHEME TPMC – SANTA BARBARA  $S_a(T_1)=0.95g$** **8 STOREY INV. Y-SCHEME TPMC – SPITAK ARMENIA  $S_a(T_1)=0.70g$** **8 STOREY INV. Y-SCHEME TPMC – VICTORIA MEXICO  $S_a(T_1)=0.90g$** 

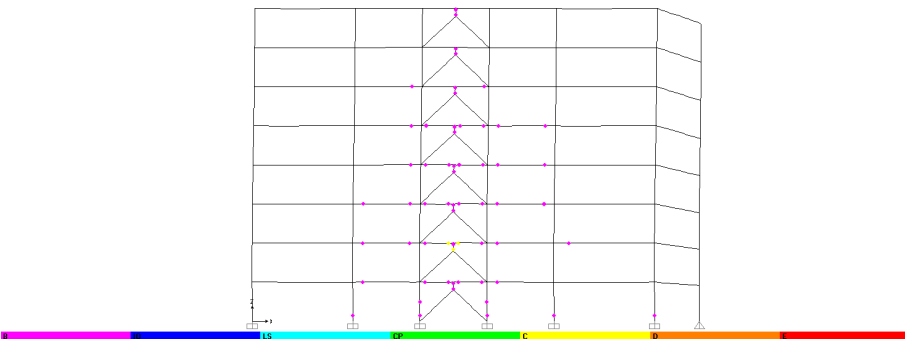
**8 STOREY INV. Y-SCHEME EC8 – COALINGA  $S_a(T_1)=0.70g$** **8 STOREY INV. Y-SCHEME EC8 – FRIULI BUIA  $S_a(T_1)=0.90g$** **8 STOREY INV. Y-SCHEME TPMC – IMPERIAL VALLEY  $S_a(T_1)=0.90g$** 



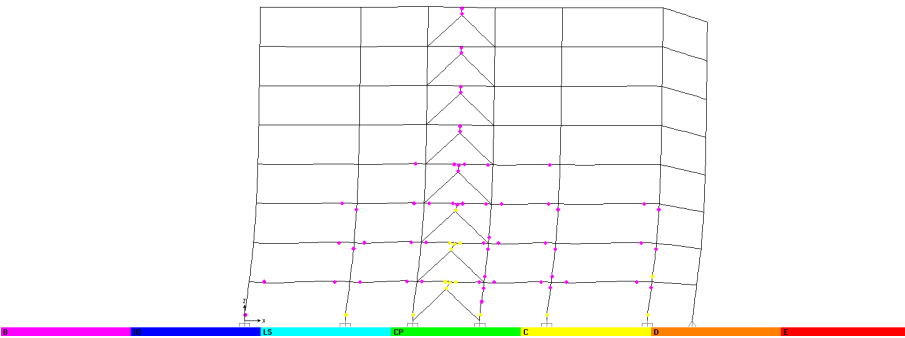
**8 STOREY INV. Y-SCHEME EC8 – IRPINIA  $S_a(T_1)=0.90g$**

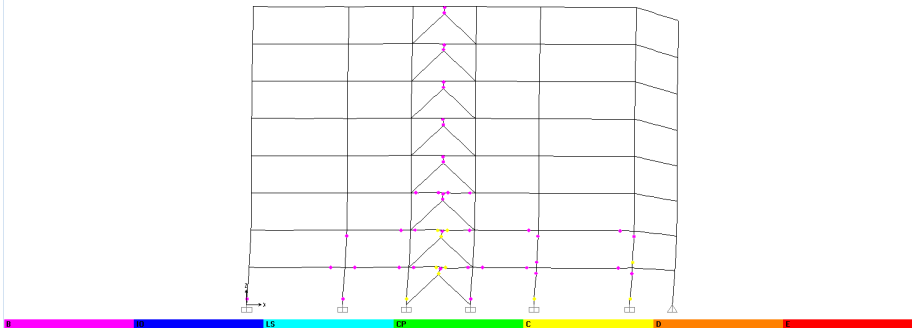
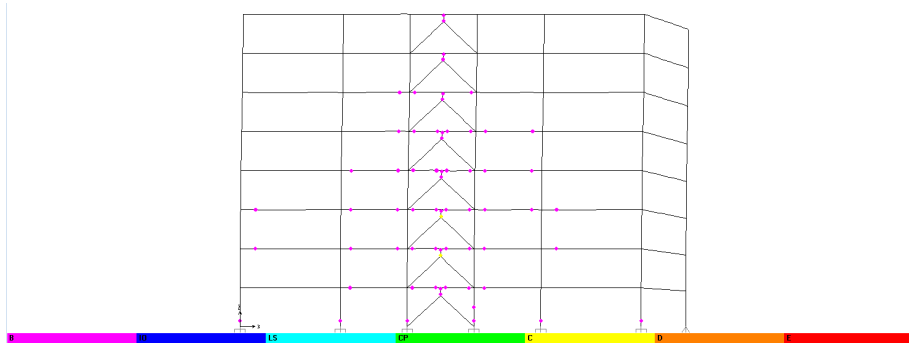
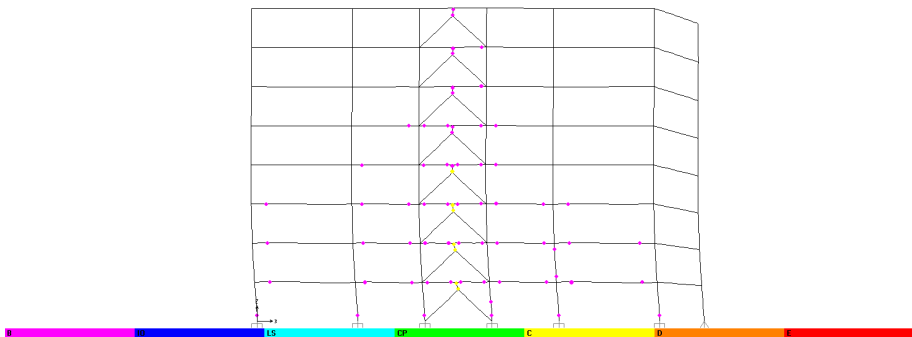


**8 STOREY INV. Y-SCHEME EC8 – KOBE  $S_a(T_1)=0.95g$**



**8 STOREY INV. Y-SCHEME TPMC – NORTHRIDGE  $S_a(T_1)=0.60g$**



**8 STOREY INV. Y-SCHEME EC8 – PALM SPRINGS  $S_a(T_1)=0.30g$** **8 STOREY INV. Y-SCHEME EC8 – SANTA BARBARA  $S_a(T_1)=0.40g$** **8 STOREY INV. Y-SCHEME TPMC – SPITAK ARMENIA  $S_a(T_1)=0.60g$** 

8 STOREY INV. Y-SCHEME EC8 – VICTORIA MEXICO  $S_a(T_1)=0.60g$

